N71-15206
NASA CR-102961

GEOTECHNICAL ENGINEERING

LUNAR SURFACE ENGINEERING PROPERTIES EXPERIMENT DEFINITION

FINAL REPORT: VOLUME III OF IV
BOREHOLE PROBES

by

RICHARD E. GOODMAN
KAREL DROZD
FRANCOIS E. HEUZÉ

PREPARED FOR MARSHALL SPACE FLIGHT CENTER
HUNTSVILLE, ALABAMA UNDER NASA CONTRACT
NAS 8-21432

JANUARY, 1970

SPACE SCIENCES LABORATORY

UNIVERSITY OF CALIFORNIA · BERKELEY

CASE FILE
COPY

University of California
Berkeley
Geotechnical Engineering

LUNAR SURFACE ENGINEERING PROPERTIES EXPERIMENT DEFINITION

FINAL REPORT: VOLUME III OF IV
BOREHOLE PROBES

by

Richard E. Goodman
Karel Drozd
Francois E. Heuzé

Contract Number NAS 8-21432

Control Number DCN 1-8-28-00056(IF)

January 1970

Submitted to
National Aeronautics and Space Administration
George C. Marshall Space Flight Center

Space Sciences Laboratory Series 11 Issue 12

This report was prepared by the University of California, Berkeley, under Contract Number NAS 8-21432, Lunar Surface Engineering Properties Experiment Definition, for the George C. Marshall Space Flight Center of the National Aeronautics and Space Administration. The work was administered under the technical direction of the Space Sciences Laboratory of the George C. Marshall Space Flight Center.

PREFACE

This report presents the results of studies conducted during the period June 20, 1968 - July 19, 1969, under NASA research contract NAS 8-21432, "Lunar Surface Engineering Properties Experiment Definition." This study was sponsored by the Advanced Lunar Missions Directorate, NASA Headquarters, and was under the technical cognizance of Dr. N. C. Costes, Space Science Laboratory, George C. Marshall Space Flight Center.

The report reflects the combined effort of four faculty investigators, a research engineer, a project manager, and six graduate research assistants, representing several engineering and scientific disciplines pertinent to the study of lunar surface material properties. James K. Mitchell, Professor of Civil Engineering, served as Principal Investigator and was responsible for those phases of the work concerned with problems relating to the engineering properties of lunar soils and lunar soil mechanics. Co-investigators were William N. Houston, Assistant Professor of Civil Engineering, who was concerned with problems relating to the engineering properties of lunar soils; Richard E. Goodman, Associate Professor of Geological Engineering, who was concerned with the engineering geology and rock mechanics aspects of the lunar surface; and Paul A. Witherspoon, Professor of Geological Engineering, who conducted studies related to thermal and permeability measurements on the lunar surface. Dr. Karel Drozd, Assistant Research Engineer, performed laboratory tests and analyses pertinent to the development of a borehole probe for determination of the in-situ characteristics of lunar soils and rocks. John Hovland, David Katz, Laith I. Namiq, James B. Thompson, Tran K. Van, and Ted S. Vinson served as Graduate Research Assistants and carried out many of the studies leading to the results presented in this report. Francois Heuzé, Assistant Specialist, served as project manager and contributed to studies concerned with lunar rock mechanics.

Ultimate objectives of this project are:

1) Assessment of lunar soil and rock property data using information obtained from Lunar Orbiter and Surveyor missions.
2) Recommendation of both simple and sophisticated in-situ testing techniques that would allow determination of engineering properties of lunar surface materials.
3) Determination of the influence of variations in lunar surface conditions on the performance parameters of a lunar roving vehicle.
4) Development of simple means for determining the fluid and thermal conductivity properties of lunar surface materials.
5) Development of stabilization techniques for use in loose, unconsolidated lunar surface materials to improve the performance of such materials in lunar engineering application.

The scope of specific studies conducted in satisfaction of these objectives is indicated by the following list of contents from the Detailed Final Report which is presented in four volumes. The names of the investigators associated with each phase of the work are indicated.

VOLUME I

MECHANICS AND STABILIZATION OF LUNAR SOILS

1. Lunar Soil Simulation
(W. N. Houston, L. I. Namiq, and J. K. Mitchell)

2. Lunar Surface Trafficability Studies
(J. B. Thompson and J. K. Mitchell)

3. Foamed Plastic Chemical Systems for Lunar Soil Stabilization Applications
(T. S. Vinson and J. K. Mitchell)

VOLUME II

LUNAR SOIL PROPERTIES FROM PHOTOGRAPHIC RECORDS

1. Soil Property Evaluations From Boulder Tracks on the Lunar Surface
(H. J. Hovland and J. K. Mitchell)

2. Deduction of Lunar Surface Material Strength Parameters from Lunar Slope Failures Caused by Impact Events - Feasibility Study
(T. S. Vinson and J. K. Mitchell)

VOLUME III

BOREHOLE PROBES

1. The Mechanism of Failure in a Borehole in Soils or Rocks by Jack Plate Loading
(T. K. Van and R. E. Goodman)

2. Experimental Work Related to Borehole Jack Probe and Testing
(K. Drozd and R. E. Goodman)

3. Borehole Jack Tests in Jointed Rock - Joint Perturbation and No Tension Finite Element Solution
(F. E. Heuzé, R. E. Goodman, and A. Bornstein)

VOLUME IV

FLUID CONDUCTIVITY OF LUNAR SURFACE MATERIALS

1. Studies on Fluid Conductivity of Lunar Surface Materials
(D. F. Katz, P. A. Witherspoon, and D. R. Willis)

VOLUME III OF FOUR

CONTENTS

		Page
Chapter 1.	*The Mechanism of Failure of a Borehole in Soils or Rocks by Jack Plate Loading* *T. K. Van and R. E. Goodman*	1-1
I.	Introduction	1-1
II.	Mechanisms of Failure of a Circular Borehole Under Different Modes of Loading	1-3
A.	Failure of Rocks by Penetrometer Loading	1-3
B.	Failure of Boreholes in Rocks and Soils by Dilatometer Loading	1-4
C.	Failure of a Circular Borehole in Rocks by Quadrantal Jack Loading	1-12
D.	Failure of a Circular Borehole in Soils and Rocks by Borehole Jack Loading	1-23
III.	General Consideration of the Problem Circular Borehole in a Rock Mass Under Borehole Jack Loading	1-23
A.	Introduction	1-23
B.	Previous Solutions	1-26
C.	The Boundary Conditions for the Borehole Jack in an Elastic Medium	1-31
D.	Some Remarks on Nontensile Mode of Failure and on Nonidealized Materials	1-37
IV.	Tensile Fracturing of an Elastic Medium by Borehole Jack Loading	1-41
A.	Distribution of σ_θ, Induced by Borehole Jack Loading, along a Circular Opening	1-41
B.	Tensile Fracturing of an Elastic Medium by Borehole Jack Loading	1-47

VOLUME III OF FOUR (Cont'd) CONTENTS

		Page
V.	The Mechanism of Failure of a Circular Borehole in Soils by Borehole Jack Loading	1-61
	A. Borehole Jack Loading in Very Dense Soil Masses	1-62
	B. Borehole Jack Loading in Very Loose Soil Masses	1-71
	C. Bearing Plate Against the Wall of a Borehole in a Medium Dense Soil	1-74
	References	1-77
	Appendix A — Solution to a Two-Dimensional Elasticity Problem by Complex Variable Method	1-81
	Appendix B — Solution to the Problem of a Circular Borehole in an Infinite Elastic Medium Under Loading Symmetrical with Respect to Two Perpendicular Axes	1-84
	Appendix C — The General Problem of Unidirectional Boundary Stress Varying Across the Width of the Bearing Plate	1-89
	Appendix D — The General Problem of Unidirectional Principal Boundary Stress Varying Across the Width of the Bearing Plates	1-97
Chapter 2.	*Experimental Work Related to Borehole Jack Probe and Testing* *K. Drozd and R. E. Goodman*	2-1
I.	Introduction	2-1
II.	Model Borehole Loading Tests	2-2
	A. Description of Test Apparatus and Methods	2-2
	B. Materials for Model Studies	2-20
	C. Description of Tests and Results	2-23
	D. Discussion of Test Results	2-44

VOLUME III OF FOUR (Cont'd)

CONTENTS

		Page
III.	Model Bearing Capacity Tests	2-50
	A. Description of Test Apparatus and Methods	2-50
	B. Results	2-51
IV.	Interpretation of Borehole Jack Tests	2-56
	References	2-61
	Appendix A — Description of Model Plate Preparation	2-62
	A-I. Brittle Materials	2-62
	A. Sand-Cement-Water Mixtures	2-62
	B. Plaster-Celite-Water Mixtures	2-62
	A-II. Cohesionless Plates — Monterey Sand No. 20	2-62
	A-III Plastic Plates	2-63
	A-IV. Mica Plate	2-63
	Appendix B — Description of Proposed Lunar Borehole Jack	2-64
Chapter 3.	*Borehole Jack Tests in Jointed Rock — Joint Perturbation and no Tension Finite Element Solutions.* *F. E. Heuzé, R. E. Goodman, and A. Bornstein*	3-1
I.	Introduction	3-1
II.	"Joint Perturbation" Analysis	3-2
	A. Joint Perturbation Program	3-2
	B. Application to Jacking Tests	3-7

VOLUME III OF FOUR (Cont'd) CONTENTS

		Page
III.	"No Tension" Analysis	3-9
	A. Rock as a "No Tension Material"	3-9
	B. Application to Jacking Tests	3-10
IV.	Summary, Conclusions	3-11
	References	3-17
	Appendix A — "Joint Perturbation" Program Listing	3-19
	Appendix B — "No Tension" Program Listing	3-30
	Appendix C — User's Manual for "Joint Perturbation" Program and "No Tension" Programs	3-42

CHAPTER 1

THE MECHANISM OF FAILURE OF A BOREHOLE IN SOILS OR ROCKS BY JACK PLATE LOADING

(T. K. Van and R. E. Goodman)

I. INTRODUCTION

A number of instruments are available for the investigation of the in-situ conditions of rock masses and soil masses by introducing loads against the wall of a borehole. These devices are used to investigate the mechanical properties of soil masses, the deformability of rock masses, the anchorage capacity for rock bolts, the magnitude and direction of the in-situ stress field, and the variation of strength and deformability. The mentioned properties are obtained from the interpretation of the load-deformation relationships.

One group of devices, the borehole penetrometers, apply concentrated forces over small areas on the wall of the borehole in a rock mass. It has been found that the relationships between applied force and indenter penetration are too scattered to give a meaningful interpretation on deformability and strength. The results from such investigations have been used to estimate the anchorage capacity for rock bolts; the interpretation is purely empirical (Stears, 1965).

The second group of devices, the borehole dilatometers or pressuremeters, apply an all-around pressure, over a given length, against the wall of a borehole. These instruments have been used in soils to determine the strength parameters (Menard, 1957, 1966). In rocks they are used to determine the deformability of rock masses, and the magnitude and direction of the in situ

stress field (Kujundzic, 1965, 1966 and Hubbert Willis, 1957). Empirical, semi-empirical, and analytical relations based on simplified assumptions are available (Gibson and Anderson, 1961; Kujundzic, 1965; Menard, 1966; Ladanyi, 1963).

The third group, the borehole jacks, apply forces over two opposed sections of the borehole. These instruments have been used to study the deformability of rock masses and the in-situ stress field. One special type, the "quandrantal jack", applies uniform normal pressure. The solution for the "quandrantal jack" in an elastic medium was derived and some possible applications were presented (Jaeger and Cook, 1963). The more common device, the "borehole jack", forces two rigid plates against the wall of the borehole. It has been used to study the deformability of rock masses. Some simple solutions pertinent to the interpretation of the load-deformation relationship were obtained by a number of investigators (Absi and Seguin, 1967; Wyanecki, 1968; Goodman, Van and Heuzé, 1967). However, none of these solutions is adequate for the interpretation of the deformation response near and at failure, or of the ultimate load.

This research concerns mainly the failure mechanisms associated with the use of the "borehole jack" in rocks. Assumptions are made on the boundary conditions, based on physical considerations. The analytical solutions to the boundary value problems are to be found. The results are used to predict the mode of failure and the ultimate jack load. Experimentation is carried out in the laboratory under controlled conditions. The correlations between analytical and experimental results are to be made. Some theoretical consideration on the behavior of a borehole in soil mass under jack loading is included.

II. MECHANISMS OF FAILURE OF A CIRCULAR BOREHOLE UNDER DIFFERENT MODES OF LOADING

A. Failure of Rocks by Penetrometer Loading

The penetrometers include one or more indenting pins, with hemispherical ends, which are forced against the wall of the borehole by oil-driven pistons. The Bureau of Mines penetrometer has a single indenting pin with a 3/8-inch-diameter head. The movement of the pin is measured by a dial gage or an extensometer connected to a cable. The device was used to estimate the anchorage capacity of rock bolts (Stears, 1965). The Hult penetrometer utilizes an oil-driven piston to deform a proving ring, forcing an 1/8-inch-square indenter into the wall of the borehole. The deformations are measured by strain gages built on the proving ring. The instrument was designed mainly as an active stiff gage for in situ stress measurement (Hult, 1963). The Dryselins penetrometer uses oil pressure to drive three pistons at 60° apart, forcing three cylindrical indenting pins into the wall. Pin displacements are measured by strain gages set on cantilever elements. The instrument was designed as an active stiff gage (Dryselius, 1965).

In general, pin movement or penetration is linearly proportional to applied load at low load levels. As the applied load is increased, the contact stress below the indenting pin's head becomes very large, resulting in local failure. The local failure includes one or more of the three modes of failure: crushing, punching, and lateral chipping. As expected, the failure load varies greatly due to the anisotropy of the material and the small dimensions of the pins.

The scattering of experimental results from the tests made on rocks is too large for establishing a valid empirical relationship between the strength of the material and the test results. However, the range of results have been found to be useful for the estimation of the anchorage capacity of rock bolts installed in the material tests (Stears, 1965).

B. Failure of Boreholes in Rocks and Soils by Dilatometer Loading

The dilatometer exerts a uniform radial pressure all around the circumference of the borehole. It consists simply of a cylindrical cell, which is inflatable by gas or liquid pressure. The deformation of the borehole is measured either from changes in volume or from changes in length of one or more diameters. Dilatometer loading is shown in Figure 1-1.

The problem of a dilatometer in a borehole in an elastic mass is that of a thick-walled cylinder under internal pressure, when the outer radius approaches infinity. Because of load symmetry, in an isotropic, homogeneous, and linearly elastic medium, both the radial stress and the circumferential stress at every point are the principal components. The solution for the stress distribution to this problem was first solved by Lamé (Seeley and Smith, 1959). For an initially non-stressed medium the in situ stress field is zero, the circumferential stress σ_θ is minimum along the edge of the opening, and the ratio $\frac{R}{r}$ of the borehole radius to the radial distance from the center of the borehole is equal to 1. The minimum σ_θ is equal to the applied internal pressure

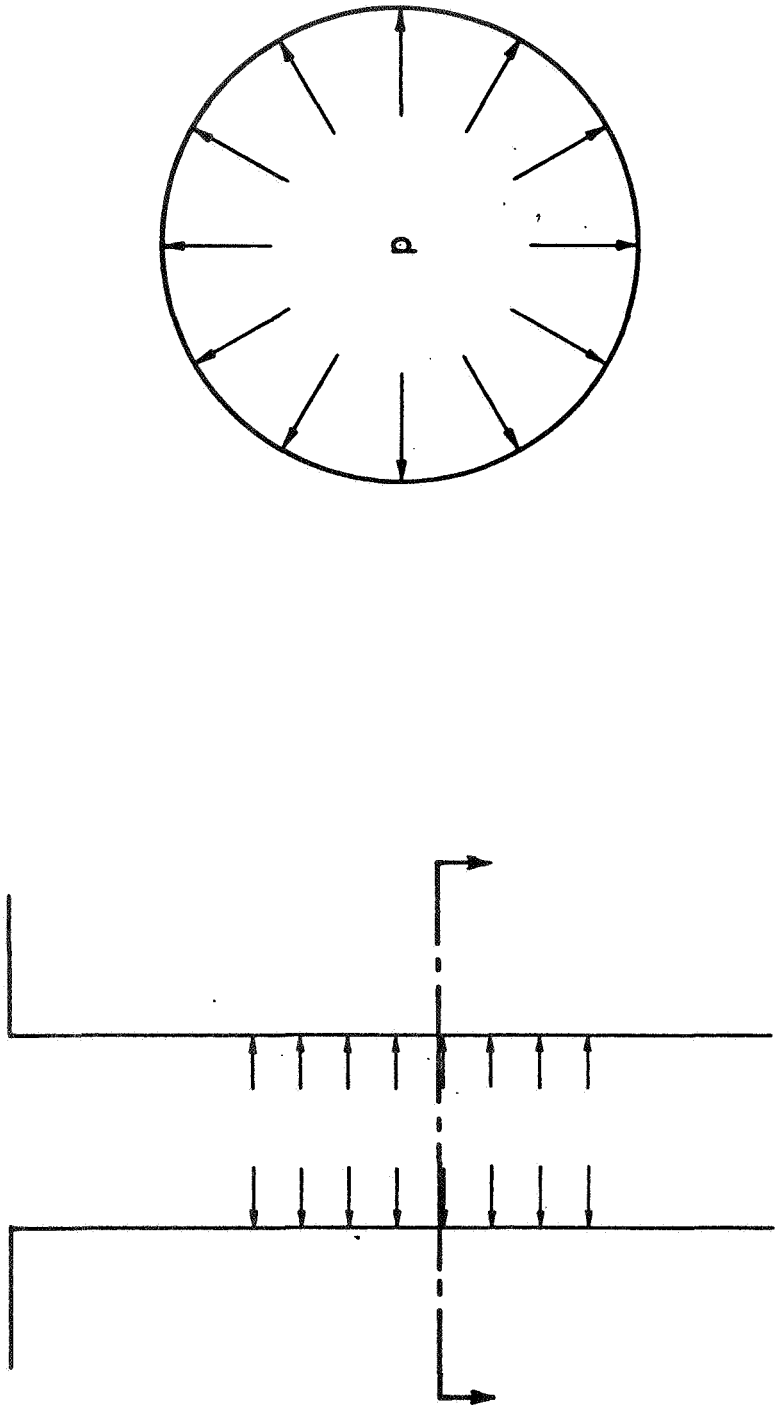

FIGURE 1-1 DILATOMETER LOADING

in magnitude, but has an opposite sign:

$$(\sigma_\theta)_{p=1} = -p \tag{1-1}$$

where p = dilatometer pressure.

Tensional fracturing is initiated when the tensile strength T_s of the medium is reached, $\sigma_\theta = T_s$:

$$P = -T_s \tag{1-2}$$

The circumferential stress σ_θ induced along the edge of a circular opening by an in-situ biaxial stress field (Figure 1-2) is given by:

$$(\sigma_\theta)_{p=1} = p_1 + p_2 - 2\,(p_1 - p_2)\cos 2\theta_1 \tag{1-3}$$

where p_1, p_2 = principal components of the biaxial stress field,

θ_1 = angle measured from p_1-direction.

When the dilatometer loading p is introduced, the net circumferential stress σ_θ which is the minor principal stress for ρ_4 is given by:

$$(\sigma_\theta)_{p=1} = -p + p_1 + p_2 - 2\,(p_1 - p_2)\cos 2\theta_1 \tag{1-4}$$

The minor principal stress σ_θ is minimum at $\theta_1 = 0$;

$$(\sigma_\theta)_{min} = -(p + p_1) + 3p_2 \tag{1-5}$$

Tensile fracturing is initiated at ($\theta_1 = 0$ and π, $\rho = 1$) when T_s is reached, as confirmed by Hubbert and Willis in the study of hydraulic fracturing (Hubbert and Willis, 1957). The dilatometer pressure at the fracture initiation is given by:

$$P_{init} = -(T_s + p_1) + 3p_2 \tag{1-6}$$

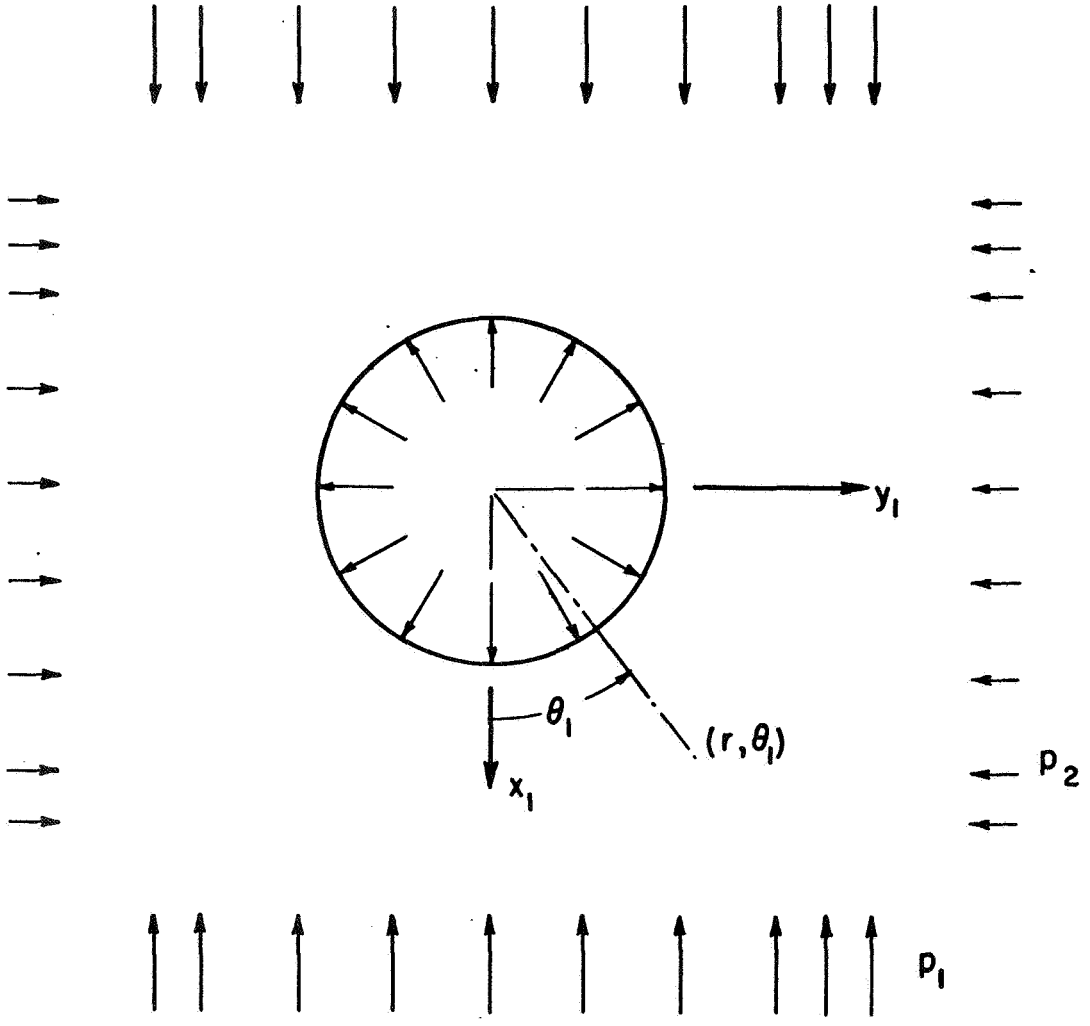

FIGURE 1-2 A BOREHOLE UNDER DILATOMETER, IN A MEDIUM INITIALLY UNDER A BIAXIAL IN SITU STRESS FIELD

When the in situ stress field is isotropic, $p_1 = p_2$, tensile fracturing is initiated at every point along the edge of the opening at the same time:

$$P_{init} = -T_s + 2p_1 \qquad (1\text{-}7)$$

Under dilatometer loading there is a possibility that shear failure could occur before the tensile fracturing could be initiated. If this is the case, then as the applied pressure is further increased, the fracture lines are formed, which should be logarithmic spirals, making a constant angle δ to the radial direction at every point. The appropriate value for δ would be $45° + \phi_{s/2}$, where ϕ_s is the friction angle (Bray, 1967). The radius R_f to which the fracture spirals extend depends on the failure criteria for the intact and fractured materials, the radius of the borehole, and the dilatometer pressure (Figure 1-3).

Ladanyi (1967) solved the problem of the static expansion of a cylindrical cavity in an infinite medium. In his treatment, Ladanyi assumed the medium to be linearly elastic before failure, and to obey the Fairhurst failure criterion. This criterion is more flexible and fits the actual strength behavior of rocks better than the Griffith criterion or its modified form suggested by McLintock and Walsh (Fairhurst, 1964). After failure, the crushed material is assumed to behave according to the Mohr-Coulomb failure criterion. For low absolute values of the ratio n of the in-situ isotropic stress field to the tensile strength of the medium $-\frac{p_1}{T_s}$ ($n = -\frac{p_1}{T_s} \leq 4.82$), at failure, three zones exist simultaneously: crushed; radially cracked; and elastic zones, as shown in Figure 1-4. The material in the radially cracked

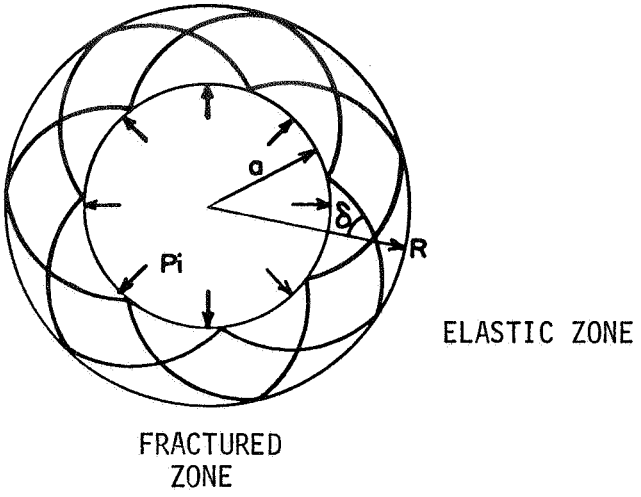

FIGURE 1-3 LOGARITHMIC SPIRAL FRACTURE ZONE AROUND CIRCULAR HOLE UNDER DILATOMETER LOADING (AFTER BRAY, 1967)

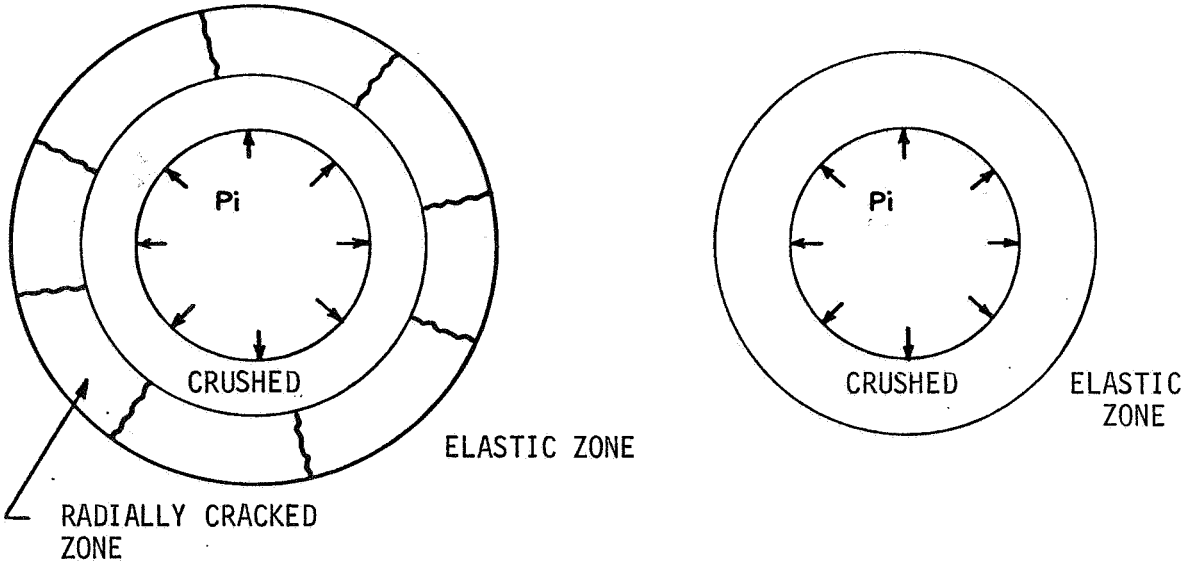

FIGURE 1-4 ROCK FAILURE AROUND A CYLINDRICAL CAVITY (AFTER LADANYI, 1967)

a) $$\left(\frac{p_0}{-T_s}\right) \leq \frac{m(m-2)-1}{2}$$

b) $$\left(\frac{p_0}{-T_s}\right) \geq \frac{m(m-2)-1}{2}$$

zone cannot carry any tension in the circumferential direction. At large in situ stresses ($n \geq 4.82$) the cracked zone does not appear. The ultimate pressure is controlled by the strength parameters of the medium in the intact and broken states, its deformability, the in situ stress field, and the density change due to the change of state (Ladanyi, 1970).

The problems of dilatometer loading and plate jack loading in soils are different from those in rocks, mainly due to the plastic behavior of soils and their inability to carry considerable tension. The interpretation of load-deformation results for dilatometer loading in soils can be based on a number of available solutions. In the study on punching of metals the problem of an expanding cylindrical cavity in a frictionless medium was solved (Bishop, Hill and Mott, 1945). The problem of an expanding cylindrical cavity in a frictionless-medium was solved by some investigators who have also studied the problem of dilatometer loading in clays (Menard, 1957; Kerisel, 1968; Gibson and Anderson, 1961).

The assumptions made by Menard were based on actual deformation-pressure curves for dilatometer loading in clays. Within the initial low pressure range, elasticity applies. In the intermediate pressure range, a plastic zone develops around the opening. The material in this zone is also assumed to be incompressible. Outside this zone, elastic equilibrium continues to exist. The borehole deformation, in terms of radial change, increases exponentially with pressure in this pressure range. There is a stage of loading where deformation increases greatly without any increase in the applied pressure, the deformation-pressure curve has a vertical asymptote $p = p_{ult}$ (Figure 1-5, Menard, 1957).

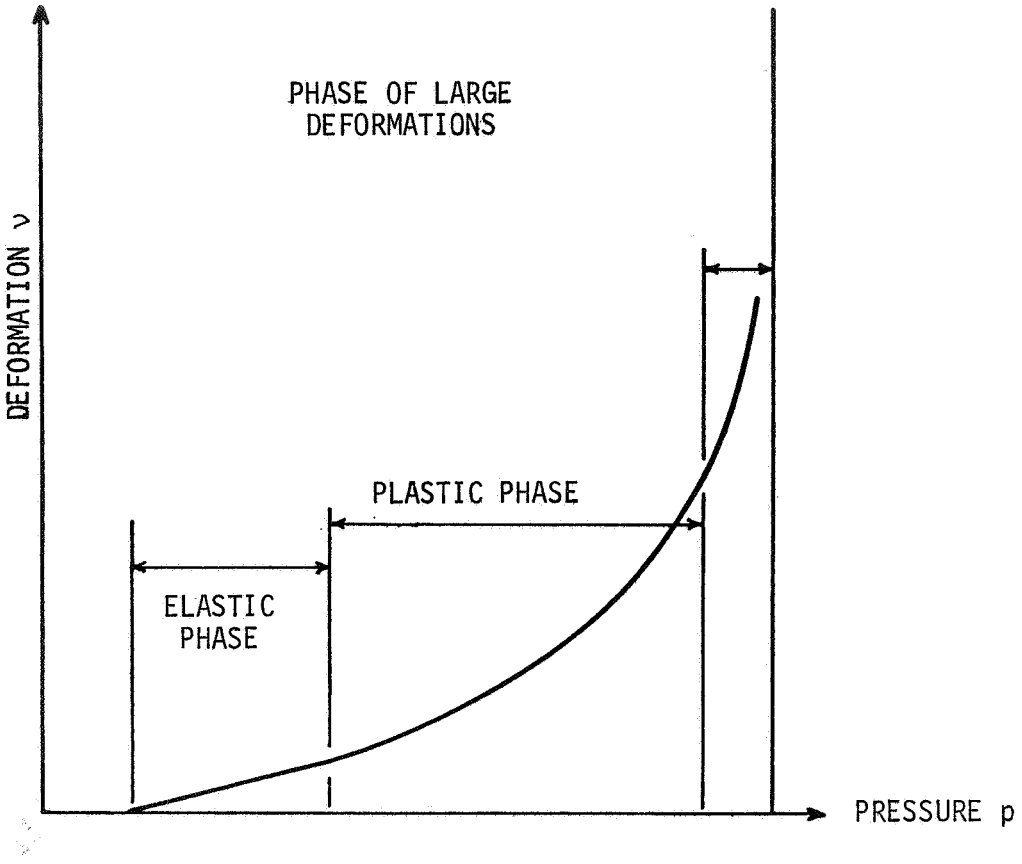

FIGURE 1-5 DEFORMATION-PRESSURE RELATIONSHIP FOR DILATOMETERS IN SOILS (AFTER MENARD, 1957)

To deal with the problem of the expansion of a cavity in a saturated clay under undrained conditions, the problem was treated semi-empirically (Ladanyi, 1963). The solution was based on stress-strain curves and strain-volume change relationships obtained by conventional triaxial tests. The problem was solved by the "step-by-step" numerical integration method.

In the analysis of the cratering caused by a concentrated line charge of explosive, the solution to the problem of an expanding cylindrical cavity with a very small initial radius, in a soil possessing both friction and cohesion, was obtained (Vesić and Barksdale, 1963). At an internal pressure p_{ult}, plastic deformation takes place around the cavity until it becomes large enough to maintain equilibrium. In the plastic zone around the cavity, the material was assumed to be rigid-plastic. The solution for the ultimate cavity pressure p_{ult} was derived. For the special cases of frictionless and cohesionless media, the general solution reduced to those obtained by earlier investigators for these cases.

C. Failure of a Circular Borehole in Rocks by Quadrantal Jack Loading

Jaeger and Cook made an attempt to adapt the flat jack techniques of stress measuring for use in a borehole, by means of thin, elongated flat jacks bent into an arc of a circle, to fit the borehole. The curved jack applies a uniform normal pressure against the wall of the borehole. Two curved jacks are symmetrically placed, each subtending an angle 2β equal to $\frac{\pi}{2}$, and the system was called the quadrantal jack. This name is adopted to all jack systems which apply uniform normal pressure over two symmetrical opposed sections of the borehole. For

small angles β's, a simpler system of loading is used in which the condition of uniform normal boundary pressure is approximate (Figure 1-6b, Jaeger and Cook, 1963).

The elasticity problem pertinent to this system has the boundary stress condition shown in Figure 1-6c. This plane strain problem was first solved by Jaeger and Cook, using complex variable methods. The steps were presented in another work on the use of borehole devices to measure the in-situ deformability of rock masses (Goodman, Van and Heuzé, 1967). This method is very powerful for the solution of boundary-value problems in elasticity with circular boundaries, or with boundaries which can be transformed into circles by conformal mapping. The method is presented briefly in Appendix A.

The stress distribution within the infinite mass, resulting from the boundary loading shown in Figure 1-6c was obtained by the complex variable method (Goodman, Van, Heuzé, 1967):

$$\sigma_\rho \frac{2\pi R \sin\beta}{P} = -2\beta\rho^2 + 2\sum_{m=1}^{\infty} \frac{\rho^{2m}}{m} (m\rho^2 - m + 1) \sin 2m\beta \cos 2m\theta \quad (1\text{-}8a)$$

$$\sigma_\theta \frac{2\pi R \sin\beta}{P} = 2\beta\rho^2 + 2\sum_{m=1}^{\infty} \frac{\rho^{2m}}{m} (m + 1 - m\rho^2) \sin 2m\beta \cos 2m\theta \quad (1\text{-}8b)$$

$$\tau_{r\theta} \frac{2\pi R \sin\beta}{P} = 2(1 - \rho^2)\sum_{m=1}^{\infty} \rho^{2m} \sin 2m\beta \sin 2m\theta \quad (1\text{-}8c)$$

where P = the total applied load against the wall of the borehole in the x-direction; R = radius of the opening; $\rho = \frac{R}{r}$; and r = radial distance.

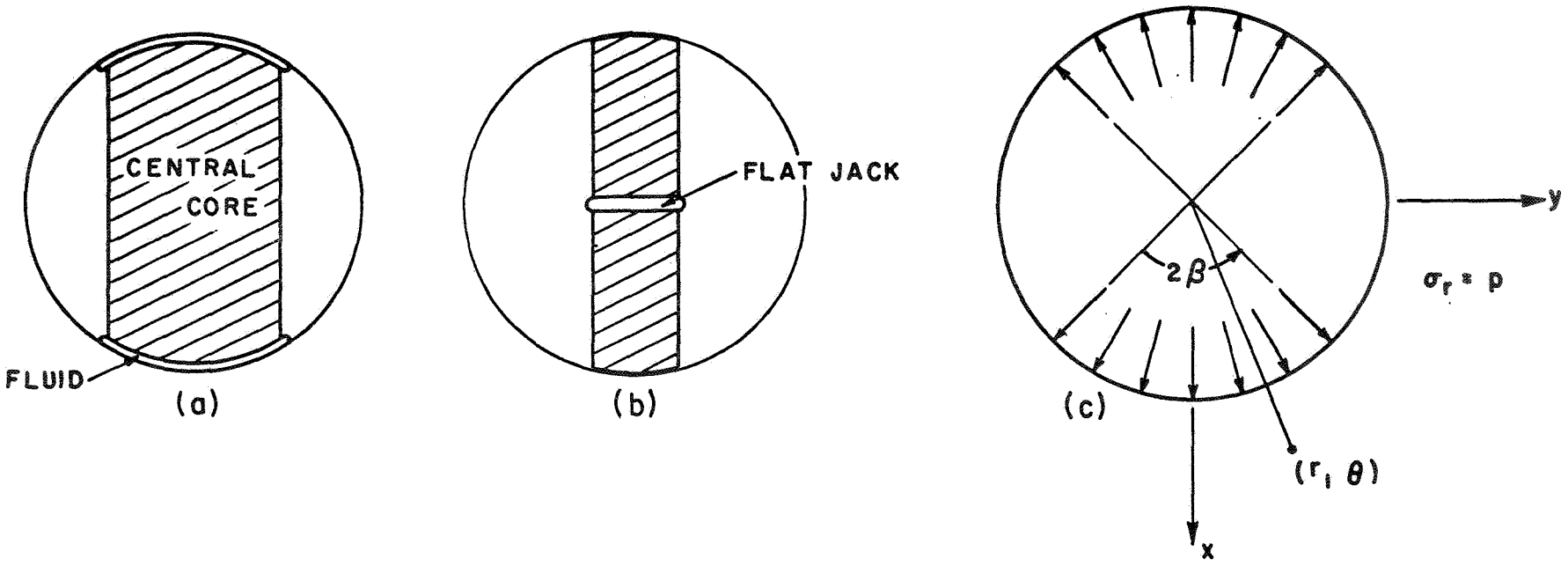

FIGURE 1-6 QUADRANTAL JACK LOADING: (JAEGER AND COOK, 1963)

a. ARRANGEMENT FOR LARGE ANGLE

b. ARRANGEMENT FOR SMALL ANGLE

c. BOUNDARY STRESS CONDITION

Along the edge of the borehole $\rho = 1$, the circumferential stress σ_θ is reduced to:

$$\sigma_\theta \frac{2\pi R \sin \beta}{P} = -2\beta + 2\sum_{m=1}^{\infty} \frac{1}{m} \sin 2m\beta \cos 2m\theta \qquad (1\text{-}9)$$

Along the arcs AB and A'B' (the loaded areas) σ_θ is constant:

$$\sigma_\theta = \frac{(\pi - 4\beta) P}{2\pi R \sin \beta} = \frac{(\pi - 4\beta)}{\pi} p \qquad (1\text{-}10)$$

Along the arcs AB' and A'B (unloaded areas) σ_θ is also constant:

$$\sigma_\theta = - \frac{2\beta P}{\pi R \sin \beta} = - \frac{4\beta}{\pi} .p \qquad (1\text{-}11)$$

It should be noted that along the edge of the opening, due to the absence of the shear stress component, σ_θ is a principal stress component.

Tensile fracturing is initiated when the minor principal stress at one or more points is equal to the tensile strength T_s of the medium. When the medium is initially non-stressed — zero in situ stress field — tensile fracturing is initiated at all points along the arcs AB' and A'B (Figure I-6c) when:

$$\sigma_\theta = T_s = - \frac{2\beta P}{\pi R \sin \beta} \qquad (1\text{-}12a)$$

$$P_{init} = - \frac{\pi R \sin \beta T_s}{2\beta} \qquad (1\text{-}12b)$$

$$P_{ult} = - \frac{\pi T_s}{4\beta} \qquad (1\text{-}12c)$$

An isotropic in situ stress field of magnitude p_1 induces a circumferential stress component along the edge of a circular opening, $\rho = 1$, equal to $2p_1$. When the quadrantal jack loading is introduced, the net circumferential stress for $\rho = 1$ is a principal stress:

Along the arcs AB and A'B' (loaded areas):

$$\sigma_\theta = \frac{(\pi - 4\beta)\ P}{2\pi\ R \sin \beta} + 2p_1 \qquad (1\text{-}13a)$$

Along the arcs AB' and BA' (unloaded areas):

$$\sigma_\theta = - \frac{2\beta\ P}{\pi\ R \sin \beta} + 2p_1 \qquad (1\text{-}13b)$$

As the quadrantal jack pressure increases, tensile fracturing is initiated at all the points in the arc AB' and BA' when T_s is reached:

$$P_{init} = \frac{2p_1 - T_s}{2\beta}\ \pi\ R \sin \beta \qquad (1\text{-}14a)$$

$$P_{init} = \frac{2p_1 - T_s}{4\beta}\ \pi \qquad (1\text{-}14b)$$

A biaxial in situ stress field with principal stress components $p_1 > p_2$ induces a variable circumferential stress along the edge of a circular opening, given by the following expression:

$$\sigma_{\theta_1} = p_1 + p_2 - 2(p_1 - p_2) \cos 2\theta_1 \qquad (1\text{-}15)$$

The x_1-axis, parallel to the direction of p_1, makes an angle α with the x-axis of the quadrantal jack (Figures 1-7). The net σ_θ

resulting from both the in situ biaxial stress field and the quadrantal loading is a principal stress and varies along the edge of the openings:

Along the arcs AB and A'B':

$$\sigma_\theta = \frac{(\pi - 4\beta)\ P}{2\pi\ R \sin \beta} + p_1 + p_2 - 2(p_1 - p_2) \cos 2(\theta - \alpha) \qquad (1\text{-}16)$$

Along the arcs AB' and A'B:

$$\sigma_\theta = -\frac{2\beta\ P}{\pi\ R \sin \beta} + p_1 + p_2 - 2(p_1 - p_2) \cos 2(\theta - \alpha) \qquad (1\text{-}17)$$

As the quadrantal pressure is increased, tensile fracturing is initiated when T_s is reached. Depending on the orientation of the jack relative to the orientation of the biaxial stress field, there are two distinct cases.

When the point $E(\theta = \alpha)$ is on the arc AB' (Figure 1-7a) the minor principal stress σ_θ is minimum at $E(\theta = \alpha)$ and $E'(\theta = \alpha + \pi)$. Tensile fracturing will be initiated first at these two points, E and E':

$$P_{init} = \frac{3p_2 - p_1 - T_s}{2\beta} \cdot \pi\ R \sin \beta \qquad (1\text{-}18a)$$

$$P_{init} = \frac{3p_2 - p_1 - T_s}{4\beta} \cdot \pi \qquad (1\text{-}18b)$$

When the point $E(\theta = \alpha)$ is in the arc AB (Figure 1-7b), the circumferential stress σ_θ along the arc AB' is minimum at $A(\theta = \beta)$:

$$\sigma_{\theta A} = -\frac{2\beta\ P}{\pi\ R \sin \beta} + p_1 + p_2 - 2(p_1 - p_2) \cos 2(\beta - \alpha) \qquad (1\text{-}19)$$

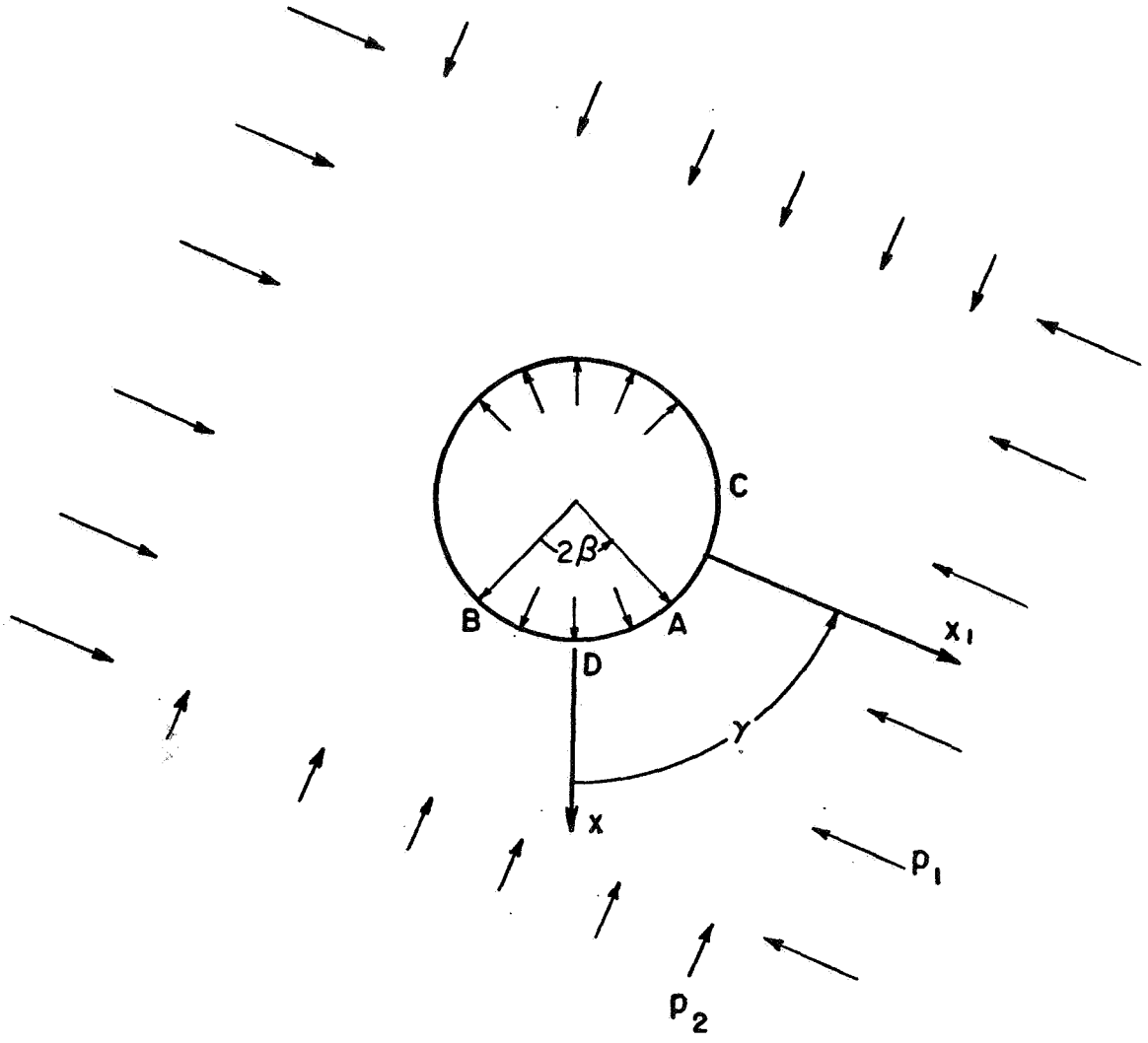

FIGURE 1-7a QUADRANTAL JACK LOADING IN A MEDIUM SUBJECTED TO AN IN SITU BIAXIAL STRESS FIELD; THE CASE OF >β

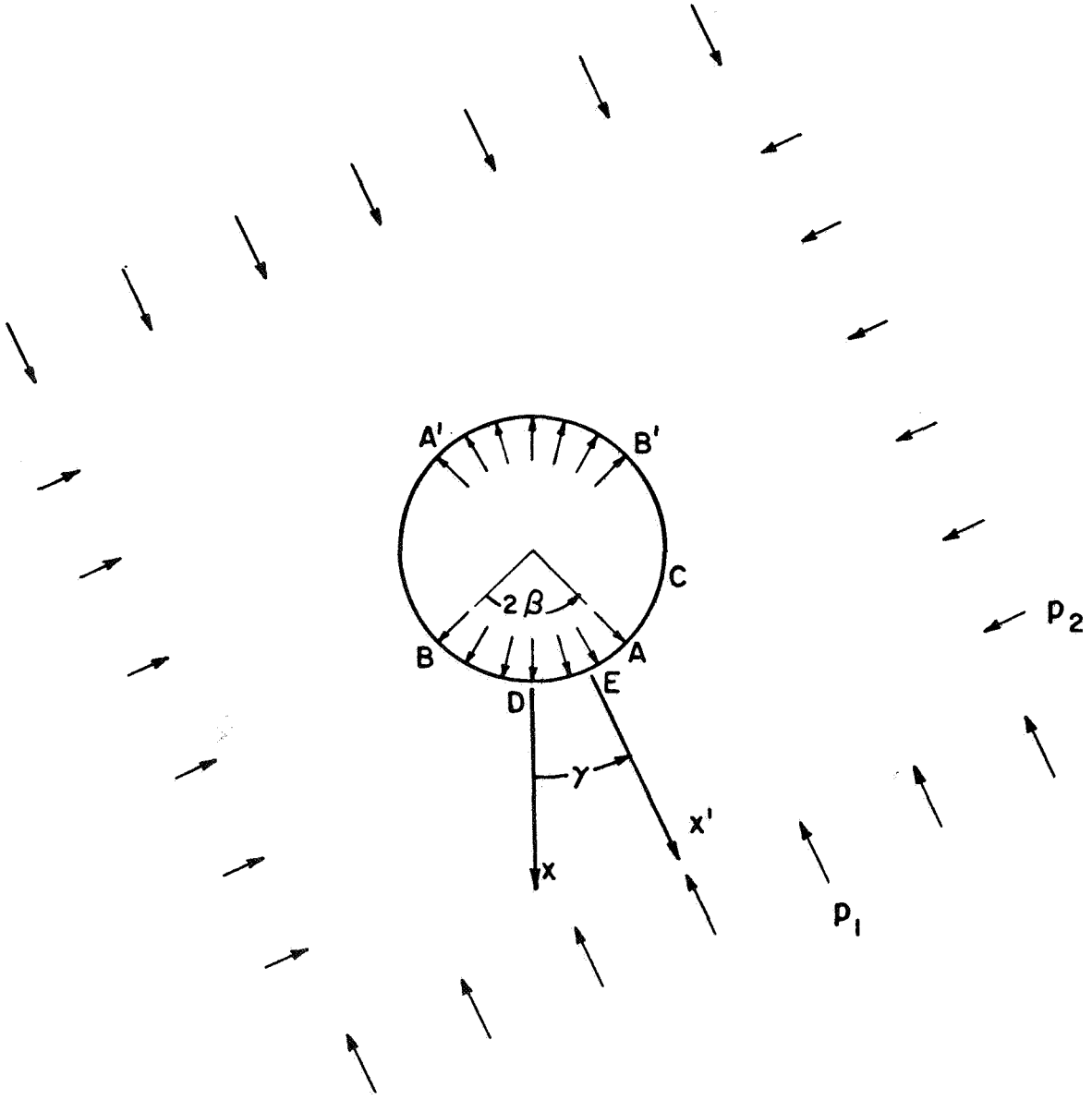

FIGURE 1-7b QUADRANTAL JACK LOADING IN A MEDIUM SUBJECTED TO AN IN SITU BIAXIAL STRESS FIELD; THE CASE OF $<\beta$

Call P_{initA} the load needed to induce a tensile stress T_s at A:

$$P_{initA} = \left\{ p_1 + p_2 - 2(p_1 - p_2) \cos 2(\beta - \alpha) - T_s \right\} \frac{\pi R \sin \beta}{2\beta} \qquad (1\text{-}20a)$$

$$P_{initA} = \left\{ p_1 + p_2 - 2(p_1 - p_2) \cos 2(\beta - \alpha) - T_s \right\} \frac{\pi}{4\beta} \qquad (1\text{-}20b)$$

In the arc AB, $(-\beta<\theta<\beta)$, σ_θ is minimum at the point $E(\theta = \alpha)$:

$$\sigma_{\theta E} = \frac{(\pi - 4\beta) P}{2\pi R \sin \beta} - p_1 + 3p_2 \qquad (1\text{-}21)$$

Call P_{initE} the load needed to induce a stress $\sigma_{\theta E}$ equal to T_s:

$$P_{initE} = (3p_2 - p_1 - T_s) \frac{2\pi R \sin \beta}{4\beta - \pi} \qquad (1\text{-}22a)$$

$$P_{initE} = (3p_2 - p_1 - T_s) \frac{\pi}{4\beta - \pi} \qquad (1\text{-}22b)$$

When the quadrant jack is oriented such that $0 < \alpha < \beta$ (Figure 1-7b), tensile fracturing is initiated first either at A and A' ($\theta = \beta$ and $\beta + \pi$) or at E and E' ($\theta = \alpha$ and $\alpha + \pi$). When $P_{initE} < P_{initA}$, the fracture initiation takes place at E and E' with the jack load $P_{init} = P_{initE}$. When $P_{initA} < P_{initE}$, initiation takes place at A and A' ($\theta = \beta$ and $\beta + \pi$) under the jack load $P_{init} = P_{initA}$. It should be noted that P_{initE} can be negative. In this case, $\sigma_{\theta E}$ is always compressional when quadrantal jack loading is applied. Fracture initiation takes place at A and A' when P_{initE} is negative.

When the angle β approaches $\pi/2$, the quadrantal jack loading approaches the dilatometer loading. Accordingly, to obtain the ultimate quadrantal pressure for the initiation of tensile fracturing when $\beta \to \pi/2$, the angle β is replaced by $\pi/2$ in Equations (1-12c), and (1-14b), and (1-18b), giving the following solutions:

$$\lim_{\beta \to \frac{\pi}{2}} P_{init} = -\frac{T_s}{2} \tag{1-23a}$$

for zero in-situ stress field.

$$\lim_{\beta \to \frac{\pi}{2}} P_{init} = \frac{2p_1 - T_s}{2} \tag{1-23b}$$

for isotropic in-situ stress field.

$$\lim_{\beta \to \frac{\pi}{2}} P_{init} = \frac{3p_2 - p_1 - T_s}{2} \tag{1-23c}$$

for biaxial in-situ stress field.

Comparing these results with the corresponding dilatometer ultimate pressure, Equations (1-2), (1-6), (1-7), it can be concluded that if points of "no-load" (zero contact pressure) are introduced along the edge of a circular opening under dilatometer loading, the crack initiation pressure is reduced by one half. The fracturing initiation takes place at the isolated no-load points instead of at every point along the edge of the opening, when the medium is initially non-stressed or under an isotropic in situ stress field (Figure 1-8).

When the angle β is very small, a large quandrantal jack pressure is needed to initiate tensile fracturing. There is a possibility that the stress distribution in the material along the contact surface

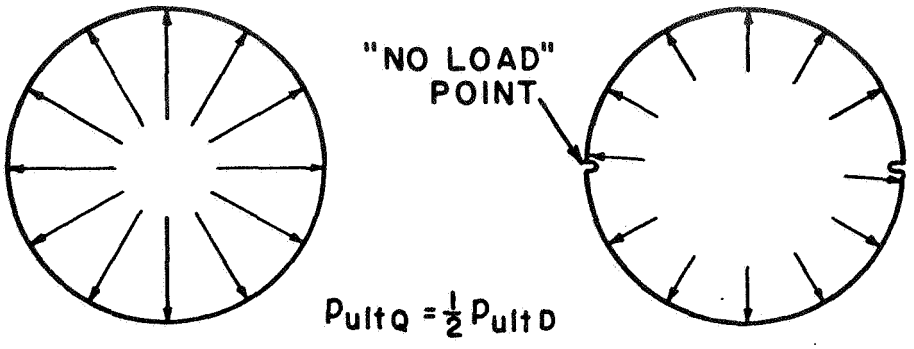

FIGURE 1-8 THE REDUCTION OF p_{ult} FOR DILATOMETER WHEN "NO-LOAD" POINTS ARE INTRODUCED

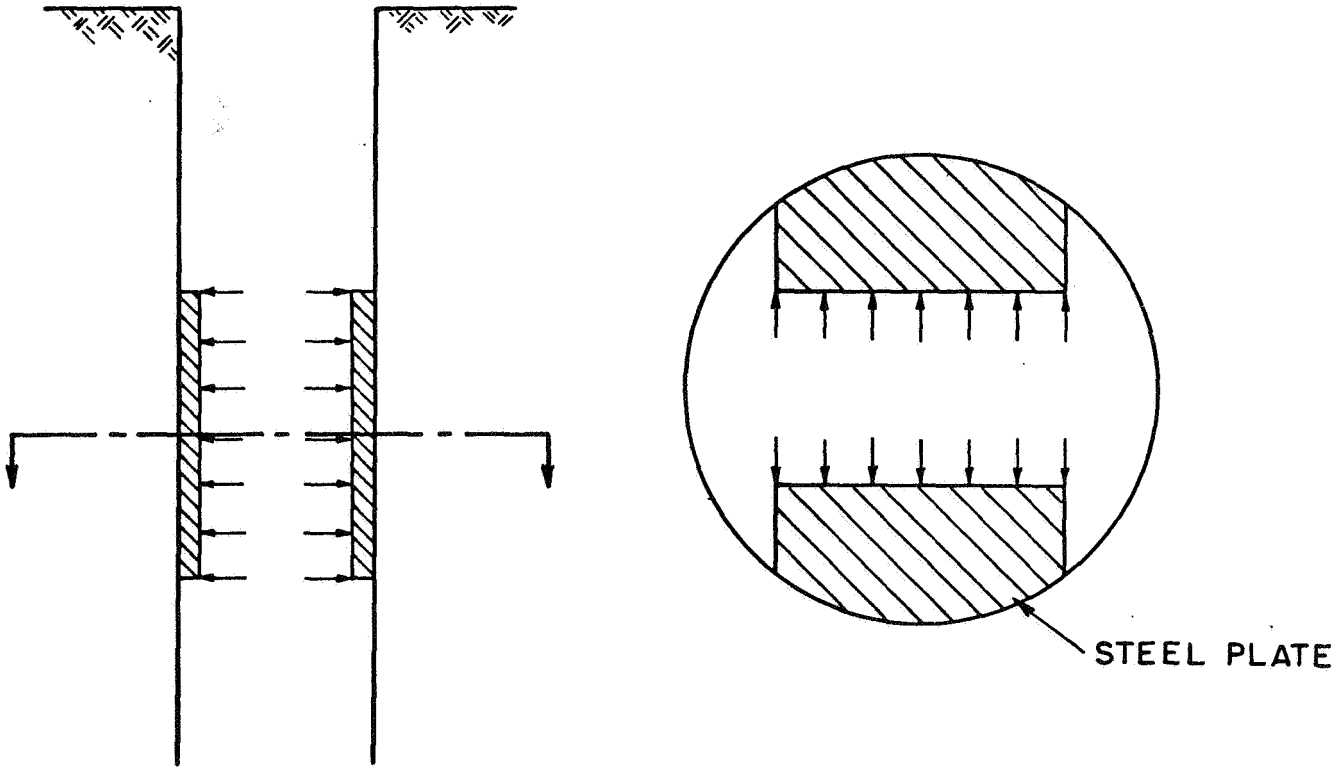

FIGURE 1-10 THE ACTUAL MODE OF BOREHOLE JACK LOADING

satisfies first a non-tensile failure criterion having the form $\tau_{oct} = N + D\sigma_{oct}^{B}$, N, D, and B are material properties (Goodman, 1967). This condition will not be studied. However, the approach to this problem, and the method for the study of the effects of anisotropy of material properties, nonlinearity, and three-dimensional nature of the actual problem on the results will be mentioned later.

D. Failure of a Circular Borehole in Soils and Rocks by Borehole Jack Loading

This problem is complicated due to the lack of understanding of the true boundary condition. The nature and distribution of the contact stress between the rigid bearing plates and the wall of the borehole are not known correctly. Therefore, assumptions must be made on the boundary conditions, based on certain physical considerations and known behavior of the materials. Studies on this problem are presented in the following three sections (III, IV, and V).

III. GENERAL CONSIDERATION ON THE PROBLEM CIRCULAR BOREHOLE IN A ROCK MASS UNDER BOREHOLE JACK LOADING

A. Introduction

There are a number of borehole devices, developed independently, which are very similar in design and in concept of operation. These devices are designated here as borehole jacks; a review is available (Goodman, Van, and Heuzé, 1967). The apparatus* designed by Goodman at the University of California, Berkeley, is described below to demonstrate the design and operation of a borehole jack.

---

*NASA Contract NAS 05-003-189.

The Goodman jack is a hydraulic jack with two curved bearing plates, designed for operation inside a standard NX-size borehole. The jack is operated by twelve, hydraulic, race-track shaped pistons, which force the two curved steel bearing plates against the wall of the borehole. The device is designed to operate at a maximum line pressure of 10,000 psi which produces a force of 158,000 lbs against the 8"-long plates. After the test, the jack is collapsed by means of two reversed pistons to provide 1/4" clearance. The detailed structure of the instrument is shown in Figures 1-9. Under pressure, the borehole deforms. The diametrical deformation at the center of the plates is measured accurately by two self-contained LVDT cells, which are read on calibrated servo-indicators. The actual mode of load application is shown in Figure 1-10. As the applied load increases, failure will eventually take place.

To determine the stress distribution by analytical means, some idealization has to be made and the distribution of contact pressure across the width and along the length of the bearing plates must be known. The problem is three-dimensional. The contact stress distribution is affected by the mechanical properties of the medium, the degree of anisotropy, the evenness of the borehole wall, the length and width of the bearing plates, the relative rigidity between the steel plate and the tested medium, the in situ stress field, and the level of jack loading.

For jacks with the length of the bearing plates in the order of four times the corresponding width, it is reasonable to assume that the length is infinite. The inclusion of the third dimension

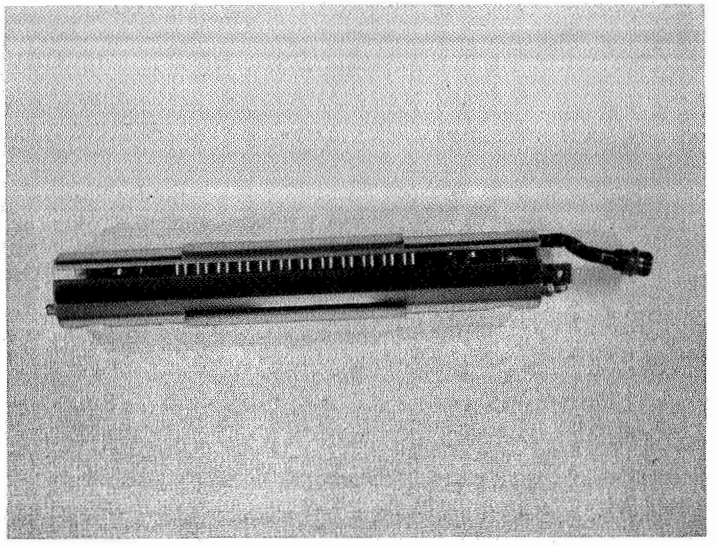

FIGURE 1-9a NX BOREHOLE JACK (GOODMAN JACK)

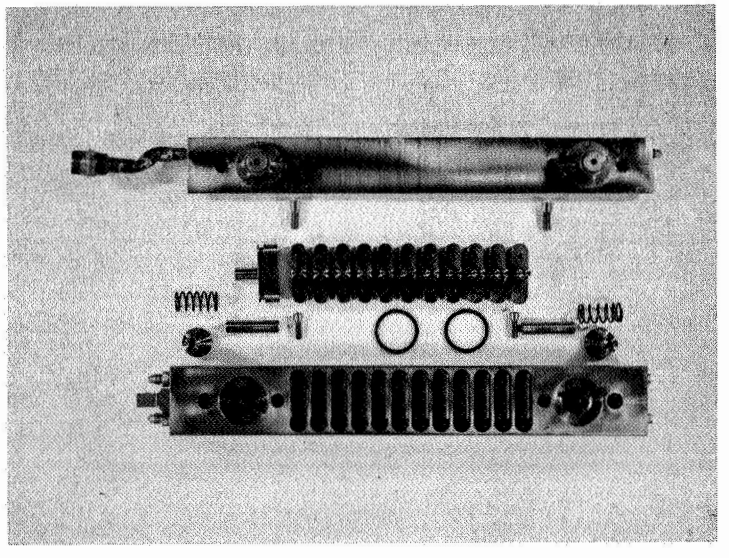

FIGURE 1-9b STRUCTURE OF THE NX BOREHOLE JACK

into the derivation of an analytical solution pertinent to the use of a borehole jack is difficult; however, the effects of the third dimension can be investigated by finite element analysis (Goodman, Van, and Heuzé, 1967). For engineering purposes, it may be reasonable to assume that the problem is essentially two-dimensional, and that the contact stress is uniform along the axial direction-plane strain condition. Other idealized assumptions include homogeneity, isotropy, and linear elasticity of the material.

B. Previous Solutions

Borehole jacks have been used mainly in the in situ determination of the deformability of rock masses. A number of solutions to simplified boundary stress conditions have been derived and used to interpret the load-deformation relationship. (Goodman, Van, and Heuzé, 1968; Absid Seguin, 1967; Wianecki, 1968).

All investigators assumed that the problem is two-dimensional. They have recognized that it is unlikely for the contact stress to be uniform across the width of the bearing plates and have been aware of the existence of the shear component along the contact surface between the plate and the wall of the borehole. However, in their treatments, they have arbitrarily assumed that no such shear component exists. This omission has small effect on the deformability interpretation, but the effect could be large as regards the strength determination. When shear contact stress is omitted, the contact pressure is normal to the contact surface and acts along a radial direction.

Solutions to the problems of sinusoidal and parabolic distributions of contact normal pressure have been derived by two French investigators (Absi and Seguin, 1967). The sinusoidal distribution is given by (p = 1)

$$*\sigma_r = q \cos \frac{\pi\theta}{2\beta} \qquad -\beta \leq \theta \leq \beta \tag{1-24}$$

where q = the normal pressure at the center of the bearing plate and σ_r^* = applied radial stress on the boundary.

The parabolic distribution is given by:

$$\sigma_r^* = q\frac{\beta^2 - \theta^2}{\beta^2} \qquad -\beta \leq \theta \leq \beta \qquad (1\text{-}25)$$

In both cases the normal contact pressure is maximum at the center of the bearing plate ($\theta = 0$) and vanishes at the edges ($\theta = \pm \beta$). Such contact pressure distributions are conceivable for the case of a rigid bearing plate being pushed into a cohesionless soil mass. For this case, the vanishing of contact pressure at the edges is due to the very low confinement at these locations. The same distributions could probably apply to the case of a special jack in an elastic medium with frictionless contact surface edges. The bearing plates of such a jack have the section modulus decreasing rapidly toward their edges (Figure 1-11). These distributions do not represent the actual contact stress distribution on a rigid plate pushed against the wall of a borehole in a more deformable elastic medium. The approximate boundary conditions include rigid uniaxial displacement along the loaded areas and zero boundary stresses along the unloaded areas.

Another French investigator carried out experimentation to determine the distribution of contact stress (Wianicki, 1968). Strain gages were set very close to the edge of the borehole, in the radial and circumferential directions. The radial stresses were calculated from the following stress-strain relationship:

$$\sigma_r = \frac{E}{1 - \nu^2} \qquad (\varepsilon_r + \nu\varepsilon_\theta) \qquad (1\text{-}26)$$

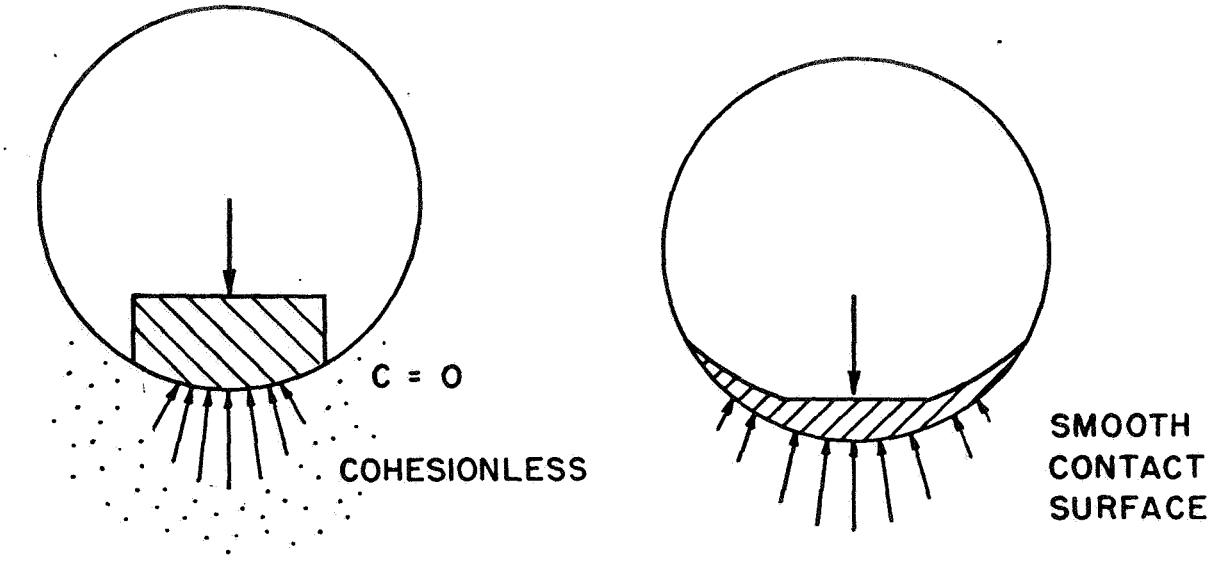

FIGURE 1-11 POSSIBLE SITUATIONS FOR NORMAL CONTACT PRESSURE, MAXIMUM AT CENTER AND VANISHING AT THE EDGES OF THE BEARING PLATES:

a. COHESIONLESS MEDIUM

b. PLATES WITH SECTION MODULUUS VERY SMALL TOWARD ITS EDGES

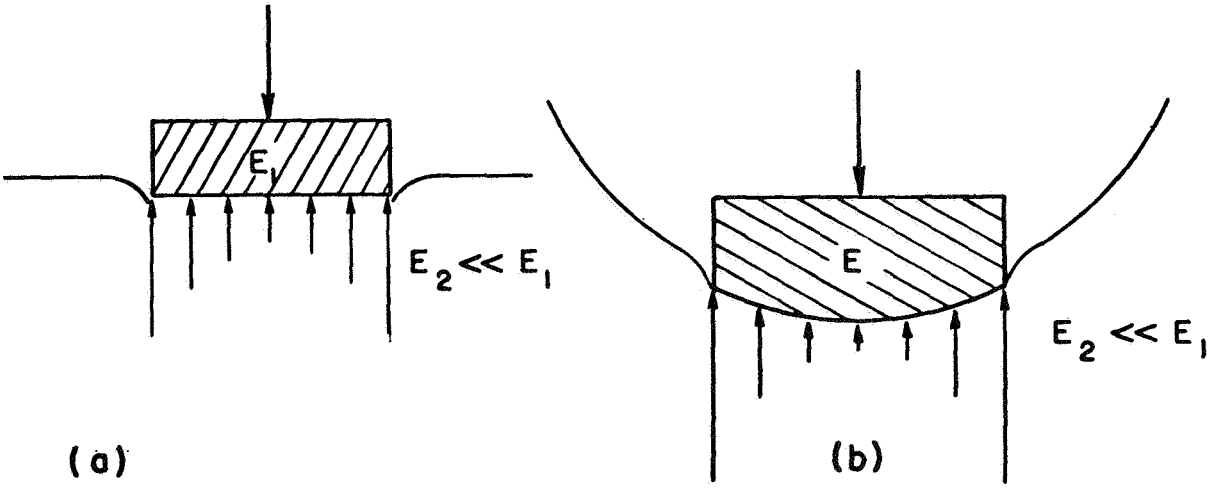

FIGURE 1-12 CONTACT STRESS DISTRIBUTION UNDER A RIGID PLATE WHICH IS FORCED AGAINST THE SURFACE OF A MUCH MORE DEFORMABLE ELASTIC MEDIUM

where ε_r, ε_θ = radial and circumferential strains

and E = modulus of elasticity.

The distribution of the normal contact pressure is assumed to be that of the radial stress, calculated from the strain measurements, for points very close to the edge of the borehole. Experimentation was made for two cases of large relative rigidity

$$\left(\frac{\text{modulus of elasticity of the bearing plate}}{\text{modulus of elasticity of the tested material}} = 28.7 \text{ and } 82\right)$$

and for only one bearing plate width ($2\beta \simeq 70°$). The distribution that best approximates the experimental results is given by (Wianecki, 1968):

$$\sigma_r^* = \frac{P}{R(\beta + \frac{1}{2}\sin 2\beta)} \cos\theta \qquad -\beta \leq \theta \leq \beta \qquad (1\text{-}27)$$

where

P = the total jack load/bearing plate length.

The assumed normal stress distribution given by Equation (1-27) can be very different from the actual distribution of the normal component of the contact stresses. The latter cannot be measured accurately with this experimental approach because it is not possible to set strain gages right on the edge of the opening, especially the gages for radial deformation measurement. The rate of change of the stress components in the radial direction, $\frac{2\sigma_\theta}{\partial r}$ and $\frac{2\sigma_r}{\partial r}$, are functions of both the angle ϕ and the radial distance. The stress components change greatly with respect to θ and r in the region close to the edge of the opening. Therefore, the contact stresses as determined by this experimental approach are only a poor approximation of the actual boundary stresses.

In the study of in situ determination of rock deformability by means of borehole jack, the contact stress was assumed to be uniform, unidirectional, and a principal stress component (Goodman, Van, and Heuzé, 1967):

$$\rho = 1 \qquad -\beta \leq \theta \leq \beta$$

$$\sigma_x = q \tag{1-28}$$

$$\sigma_y = \tau_{xy} = 0$$

This boundary stress assumption leads to the existence of both normal and shear boundary stresses, both variable across the width of the bearing plates:

$$\sigma_r^* = \frac{q}{2}(1 + \cos 2\theta) \tag{1-29a}$$

$$\tau_{r\theta}^* = -\frac{q}{2} \sin 2\theta \tag{1-29b}$$

where

σ_r^*, $\tau_{r\theta}^*$ = Applied normal and shear boundary stresses.

The normal stress component is maximum at the center of the plate ($\theta = 0$) and decreases with the angle θ. The shear component is zero at $\theta = 0$ and increases with θ for $\beta \leq \pi/4$. For large bearing plates, $\beta \geq \pi/4$, the boundary shear component increases with θ up to $\pi/4$, and then decreases with further increase in θ. This boundary stress condition is based on the assumption that the distribution and characteristic of being a principal component of the stress acting on the bearing plates of the hydraulic pistons are transferred unchanged to the contact surface between the plates and the wall of the opening. Finite element analyses of borehole jack

problems, in which the influence of the presence or absence of steel plates has been assessed, have shown that the boundary condition (1-24) is acceptable for the study of deformability, providing that there is no slippage along the contact surface (Goodman, Van, and Heuzé, 1967).

C. The Boundary Conditions for the Borehole Jack in an Elastic Medium

To study the mechanism of failure, the assumed boundary stress distribution must approximate fairly well the actual distribution. The failure initiation takes place on the edge of the opening; therefore, the induced stress concentration along the boundary is to be known accurately to estimate the ultimate jack load and the failure initiation locations correctly. A poor assumption on the applied boundary stresses leads to an incorrect interpretation of the failure mechanism. There is no possible way of estimating the individual effects of the controlling factors on the distribution of boundary stresses. These factors include the mechanical properties of the medium, the relative rigidity of the steel plate and of the medium, $E_R = E_{jack}/E_{med}$, the width of the bearing plates, the evenness and smoothness of the contact surface, and the level of loading.

The boundary stresses include both normal and shear components that vary across the width of the bearing plates. Two probably appropriate assumptions on the distribution of boundary stresses are made in the following sections, based on different considerations.

1. Unidirectional contact stress varying across the width of the bearing plates (Problem I)

When a rigid plate is pressed against the surface of a much more deformable elastic mass, there is a uniform

displacement which induces a contact stress distribution, minimum at the center and maximum along the edge (Figure 1-12a). When the steel plate of the borehole jack is pushed against the wall of the circular opening in a more deformable medium, the displacement below the plate is very close to a uniform and unidirectional condition. For a linearly elastic medium, the contact stress distribution would be as shown in Figure 1-12b.

From finite element analysis of this problem of uniform boundary displacement, the stress distribution that is very close to the edge of the opening below the rigid plates is found to be similar to that shown in Figure 1-12b (Van, 1967). The shape of the distribution curve changes with the applied boundary displacements. The distribution is also influenced by the modulus of elasticity E_m of the medium. For a given material, the difference between the stresses at the center and at the edge of the plate increases with the applied boundary displacement. A given boundary displacement induces a larger stress difference in a medium with higher modulus of elasticity.

This is a mixed boundary-valued problem with uniform unidirectional boundary displacement below the bearing plates, and zero boundary stresses outside the plates, as shown in Figure 1-13a. It is much more convenient to solve this problem when the boundary displacement condition is replaced by an equivalent stress condition. It is reasonable to assume that the distribution of contact stress has the general shape shown in Figure 1-12b. An expression for

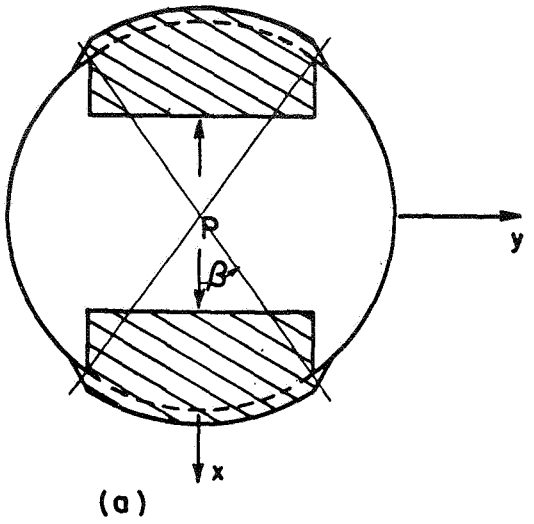

FIGURE 1-13a THE MIXED BOUNDARY CONDITIONS FOR RIGID PLATE DISPLACEMENT PROBLEM

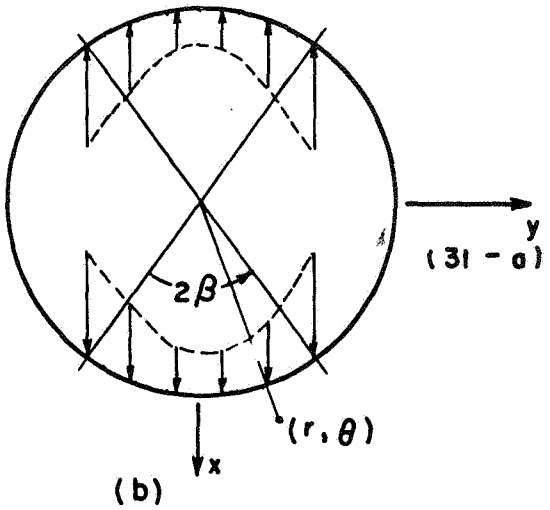

FIGURE 1-13b THE UNIDIRECTIONAL CONTACT STRESS DISTRIBUTION RESULTING FROM RIGID PLATE DISPLACEMENT

this distribution must include a factor k whose different values can accommodate the different shapes of the distribution curves which depend on the modulus of elasticity of the material and the magnitude of the applied boundary displacement.

The boundary stress distribution assumed to be equivalent to the applied uniform unidirectional boundary displacement is shown in Figure 1-13b:

Boundary conditions at $\rho = 1$

$$p_y = 0$$

$$P_x = \begin{cases} q\left\{ k - (k-1)\cos\frac{\pi\theta}{2\beta}\right\} & -\beta \le \theta \le \beta \\ q\left\{ k - (k-1)\cos\frac{\pi(\theta-\pi)}{2\beta}\right\} & \pi \quad -\beta \le \theta \le \pi + \beta \\ 0 & -\beta \le \theta \le \pi - \beta \; ; \quad \pi \quad +\beta \le \theta \le 2\pi - \beta \end{cases} \tag{1-30}$$

Due to the symmetry of the problem, it is convenient to consider the half-plane $x > 0$. From the Equations (1-30) the normal and shear boundary stress distributions are obtained:

$$\sigma_r^* = q\left\{ k - (k-1)\cos\frac{\pi\theta}{2\beta}\right\}\cos\theta \qquad -\beta \le \theta \le \beta \tag{1-31a}$$

$$\tau_{r\theta}^* = q\left\{ k - (k-1)\cos\frac{\pi\theta}{2\beta}\right\}\sin\theta \tag{1-31b}$$

$$\tau_{r\theta}^* = \sigma_r^* = 0 \qquad \beta < \theta < \pi - \beta \; ; \qquad \pi + \beta < \theta < 2\pi - \beta$$

where σ_r^*, $\tau_{r\theta}^*$ = applied normal and shear stress on the boundary

q = normal stress at $\theta = 0$

k = shape factor for the distribution curves.

2. Unidirectional principal boundary stress varying across the bearing plates (Problem II)

The applied stress against the bearing plate is uniform, unidirectional, and principal (Figure 1-14a). The contact stress between the bearing plate and the wall of the borehole is assumed arbitrarily to remain unidirectional and principal, but to vary across the width of the plates (Figure 1-14b). The boundary stress distribution is given by:

$(\rho = 1)$

$$\sigma_y = \tau_{xy} = 0$$

$$\sigma_x = \begin{cases} q\left\{k - (k-1)\cos\dfrac{\pi\theta}{2\beta}\right\} & -\beta \le \theta \le \beta \\ q\left\{k - (k-1)\cos\dfrac{\pi(\theta-\pi)}{2\beta}\right\} & \pi - \beta \le \theta \le \pi + \beta \\ 0 \quad \beta < \theta < \pi - \beta \;;\; \pi + \beta < \theta < 2\pi - \beta & \end{cases} \tag{1-32}$$

The normal and shear boundary stress components are obtained from the Equations (1-32): ($x > 0$ half-plane)

$$\sigma_r^* = \frac{q}{2}\left\{k - (k-1)\cos\frac{\pi\theta}{2\beta}\right\}(1 + \cos 2\theta) \tag{1-33a}$$

$$-\beta \le \theta \le \beta$$

$$\tau_{r\theta}^* = \frac{q}{2}\left\{k - (k-1)\cos\frac{\pi\theta}{2\beta}\right\}\sin 2\theta \tag{1-33b}$$

$$\sigma_r^* = \tau_{r\theta}^* = 0 \qquad \beta < \theta < \pi - \beta \;;\; \pi + \beta < \theta < 2\pi - \beta$$

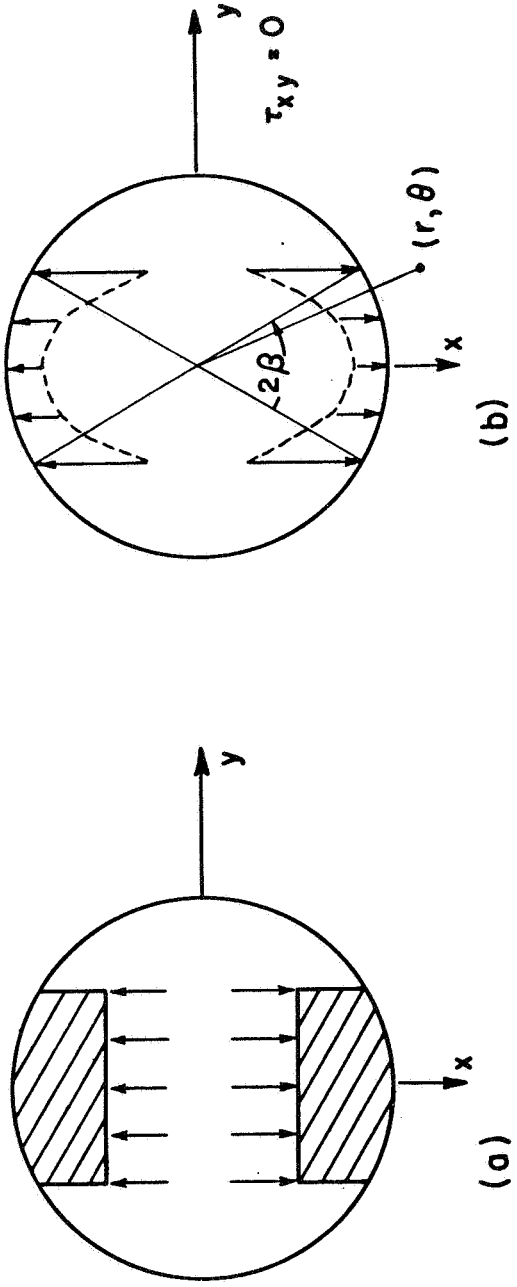

FIGURE 1-14 a. UNIFORM UNIDIRECTIONAL PRINCIPAL STRESS ON JACK PLATES.

b. UNIDIRECTIONAL PRINCIPAL STRESS ALONG THE CONTACT SURFACE BETWEEN THE JACK PLATE AND THE WALL OF THE BOREHOLE.

The boundary shear stress given by the Equation (1-33b) is zero at $\theta = 0$ and $\pi/2$. For $\beta \leq \pi/4$ the shear stress increases with θ. For $\beta > \pi/4$, $\tau^*_{r\theta}$ increases with θ up to $\pi/4$, then decreases with further increase in θ. This variation of the boundary shear stress is in agreement with one physical consideration. When load is applied, the borehole deforms. There is a differential displacement between the bearing plates and the wall along the contact surface in the circumferential direction. Due to symmetry, the four points C, C', D, and D', do not displace in the circumferential direction (Figure 1-15a). When the plate width is small ($\beta < \pi/4$) the differential displacement is zero at D ($\theta = 0$) and maximum at A ($\theta = \beta$). For a large plate width ($\beta > \pi/4$), the differential circumferential movement reaches the maximum at $\theta = \pi/4$, then decreases with further increase in θ (Figure 1-15b). We can reasonably assume that the magnitude of the contact shear stress is proportional to the differential displacement. With this assumption, the boundary conditions (1-33) are appropriate for the differential displacement between the bearing plate and the medium, as shown in Figure 1-15b.

D. Some Remarks on Nontensile Mode of Failure and on Nonidealized Materials

For both quadrantal jack and borehole jack, as the angle becomes small, the applied load needed to initiate tensile fracturing induces large stresses in the regions below the curved jacks or below the bearing plates. When the angle becomes small enough, it

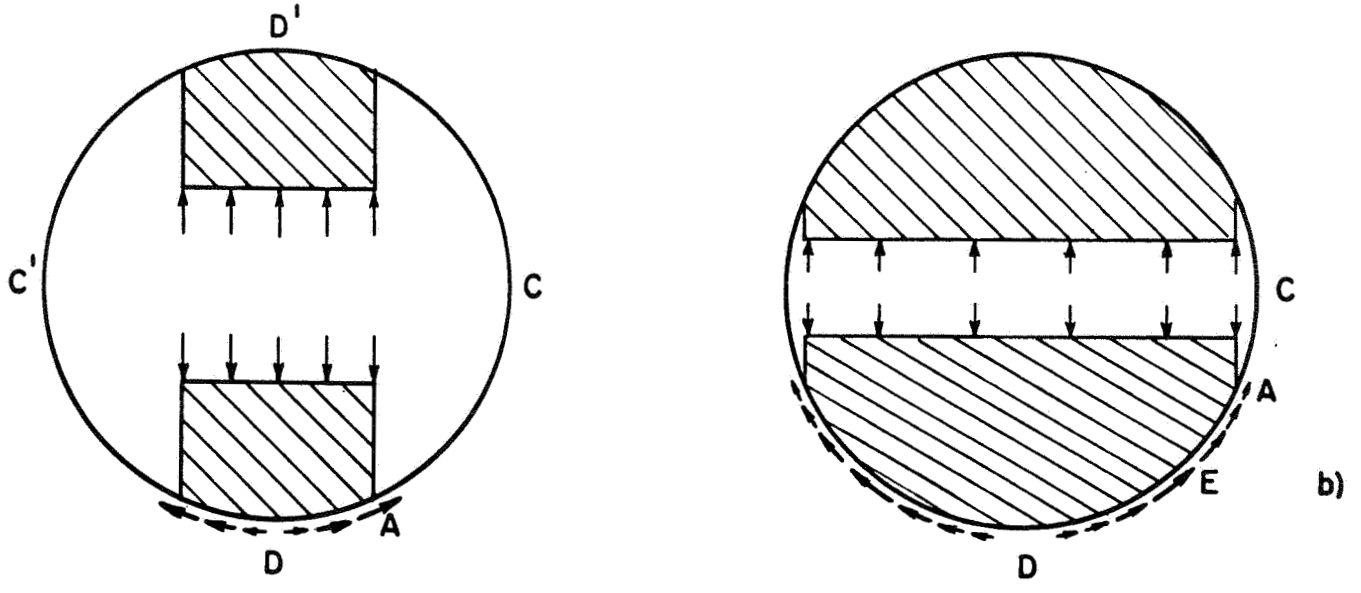

FIGURE 1-15 DIFFERENTIAL DISPLACEMENT BETWEEN THE BEARING PLATES AND THE MEDIUM, ALONG THE CONTACT SURFACE

is possible for the borehole to fail by a nontensile mode of failure, before the initiation of tensile fracturing is reached. When the induced compressive stress below the bearing plates is in order or magnitude of the compressive strength of the material, failure takes place with the following criterion (Goodman, 1967, 1968):

$$\tau_{oct} = N + D\,\sigma_{oct}^{B} \quad \text{for} \quad \sigma_{oct} > 0 \qquad (1\text{-}34)$$

where

τ_{oct}, σ_{oct} = octahedral shear stress and octahedral normal stress

N, D, B = material properties, to be determined experimentally.

For a material with properties N, D, B, and T_s, under an in situ stress field with principal components p_1, p_2, and an orientation angle α, subjected to a borehole jack loading with a contact stress distribution factor k, theoretically there exists a critical bearing plate angle $\beta°$ such that both the failure criterion $\sigma_{minor} = T_s$ and the criterion (1-34) are reached simultaneously as the applied load is increased. The critical angle $\beta°$ can be found when all other parameters are given. For each angle β, the jack load P_{init} for the initiation of tensile fracturing is calculated. The load P_{init} is then used to find the stress distribution, from which the octahedral normal and shear stresses at every point can be calculated. For all angles β's for which the condition $\tau_{oct} < N + D\,\tau_{oct}^{B}$ is satisfied everywhere, the borehole will fail in tension. For all the angle β's, for which there is one or more points where the relation $\tau_{oct} = N + D\,\sigma_{oct}^{B}$ is satisfied, the material fails according to criterion (1-32). The larger the tensile strength T_s and the strength parameters (N, D, and B), the smaller the critical angle $\beta°$.

From experimentation with plaster-celcite mixture, with plate angle $\beta = 10°$, some punching was observed; the mode of failure determined by the criterion (1-34) for a borehole jack test in a rock mass can be achieved only for very small plate angles, probably in the order of a few degrees. A jack with such small bearing plates behaves as a penetrometer. As discussed earlier, for such a penetrometer, the testing results would be too scattered to allow any reasonably meaningful interpretation. Any attempt to make quantitative correlation between the strength of the medium and the untimate load would require a large program of testing; the empirical relations would include large coefficients of uncertainty.

The actual borehole jack problem is three-dimensional. It can be expected that the contact stresses are not uniform along the length of the bearing plates. Rigid plate displacement would result in a larger contact pressure in the regions near the ends of the plates. Rock masses are in general nonhomogeneous and anisotropic; their strength parameters and deformability vary from point to point and are different in different directions. Planes of weakness and joints cannot carry tensile loads; slippage can occur along these planes when a failure criterion in the form $\tau_T = C + \sigma_n \tan \phi$ is met, where C and tan ϕ are joint properties, τ_T and σ_n are tangential and normal stresses to the plane. In general, the stress-strain relationships for rocks are nonlinear, and the modulus of deformability is a function of the stress level. The effects of one or more parameters mentioned on the mechanism of failure can be investigated by finite element analysis (see Chapter 3).

IV. TENSILE FRACTURING OF AN ELASTIC MEDIUM BY BOREHOLE JACK LOADING.

A. Distribution of σ_θ, Induced by Borehole Jack Loading, Along a Circular Opening

The solutions to Problems I and II are presented in Appendices 1-C and 1-D. The boundary stresses for these two problems were given by Equations (1-31) and (1-33).

The total load exerted by the bearing plates against the wall of the borehole in the x-direction is given by the following equation:

$$P = MRq$$

$$= \left\{ 2k \sin \beta - \frac{4(k-1)\,\pi \cos \beta}{\beta \left(\frac{\pi}{\beta} + 2\right)\left(\frac{\pi}{\beta} - 2\right)} \right\} R_q \qquad (1\text{-}35)$$

where P = total jack load/length of the bearing plates

R = radius of the opening

q = normal stress at plate center ($\theta = 0$)

k = boundary stress distribution factor.

The jack load P induces a circumferential stress σ_θ along the circular opening:

$$\sigma_\theta = K\,(k, \beta, \theta)\,\frac{P}{R} \qquad (1\text{-}36)$$

where

$K\,(k, \beta, \theta)$ = stress factor at the location θ on the opening.

Denote $K_I\,(k, \beta, \theta)$ and $K_{II}\,(k, \beta, \theta)$ as the stress factors derived from the solutions to Problems I and II. Along the loaded areas (Figure 1-14) we have (from the Appendices):

$$K_I\ (k, \beta, \theta) = \frac{1}{M}\left[-\left\{ k - (k-1)\cos\frac{\pi\theta}{2\beta}\right\}\cos\theta\right.$$

$$\left. + 8\sum_{m=1}^{\infty}\left\{\frac{k\sin(2m-1)\beta}{(2m-1)\pi} - \frac{2(k-1)\cos(2m-1)\beta}{\beta\,(\frac{\pi}{\beta}+4m-2)\,(\frac{\pi}{\beta}-4m+2)}\right\}\cos 2m\theta\right] \tag{1-37}$$

$$K_{II}\ (k, \beta, \theta) = \frac{1}{M}\left[\frac{k}{2} - \frac{2k\beta}{\pi} + \frac{4(k-1)\beta}{\pi^2} + (\frac{4\beta}{\pi} - \frac{1}{2})\,k\cos 2\theta\right.$$

$$+ \frac{1}{2}(k-1)\cos\frac{\pi\theta}{2\beta}\left\{\cos 2\theta - 1\right\} + \sum_{m=2}^{\infty}\frac{2k}{(m-1)\pi}\sin 2(m-1)\beta\cos 2m\theta$$

$$\left. - \sum_{m=1}^{\infty}\frac{8(k-1)\cos 2(m-1)\beta\cos 2m\theta}{\beta\,(\frac{\pi}{\beta}+4m-4)\,(\frac{\pi}{\beta}-4m+4)}\right] \tag{1-38}$$

Along the unloaded areas, the stress factors K_I and K_{II} are given by:

$$K_I\ (k, \beta, \theta) = \frac{8}{M}\sum_{m=1}^{\infty}\left\{\frac{k\sin(2m-1)\beta}{(2m-1)\pi}\right.$$

$$\left. - \frac{2(k-1)\cos(2m-1)\beta}{\beta\,(\frac{\pi}{\beta}+4m-2)\,(\frac{\pi}{\beta}-4m+2)}\right\}\cos 2m\phi \tag{1-39}$$

$$K_{II}\ (k, \beta, \theta) = \frac{1}{M}\left[-\frac{2k\beta}{\pi} + \frac{4(k-1)\beta}{\pi^2} + \frac{4k\beta}{\pi}\cos 2\theta\right.$$

$$\left. + \sum_{m=2}^{\infty}\frac{2k\sin 2(m-1)\beta}{(m-1)\pi}\cos 2m\theta - \sum_{m=1}\frac{8(k-1)\cos 2(m-1)\beta\cos 2m\theta}{\beta(\frac{\pi}{\beta}+4m-4)\,(\frac{\pi}{\beta}-4m+4)}\right]$$

where

$$M = \left\{2k\sin\beta - \frac{4(k-1)\pi\cos\beta}{\beta\,(\frac{\pi}{\beta}+2)\,(\frac{\pi}{\beta}-2)}\right\} \tag{1-40}$$

The numerical evaluation of the stress factors showed that both K_I and K_{II} are the most tensile (negative) at the edges A, B, A', and B' of the bearing plates ($\theta = -\beta, +\beta, \beta + \pi$, and $\pi - \beta$). The stress factors at those points are denoted as K_{IT} (k_1 β) and K_{IIT} (k_1 β). Their numerical values are given in Tables 1-1a and 1-1b. The variations of the maximum stress factors, K_{IT} and K_{IIT}, with respect to the boundary stress distribution factor k and the bearing plate width angle β are shown in Figures 1-17a and 1-19a

The maximum stress factor K_{IT} (solution I) increases with both k and β. The maximum stress factor K_{IIT} (solution II) increases with k; however, for a given value of k, K_{IIT} has a maximum at the location θ approximately equal to $\pi/4$. For the bearing plates with the angles β's smaller than $\pi/4$, the two solutions I and II give approximately the same tensile stress factors ($K_{IT} \lesssim K_{IIT}$) at the edges of the plates (Figures 1-17a and 1-17b). For bearing plate angles β's larger than $\pi/4$, K_{IT} increases, while K_{IIT} decreases with respect to the angle β.

The two boundary stress conditions I (Equations 1-31) and II (Equations 1-33) induce similar distributions of minor principal stress along the circular opening. For both cases, the minor principal stress is the most tensile at the edges of the bearing plates. Along the unloaded areas, the circumferential stress σ_θ is the minor principal stress. The magnitude of the tensile minor stress σ_θ decreases very rapidly with respect to the angle θ; the stress σ_θ becomes approximately constant a few degrees from the edges of the bearing plates. The variation of the circumferential stress σ_θ along the opening is shown in Figure 1-16. It should be noted that along

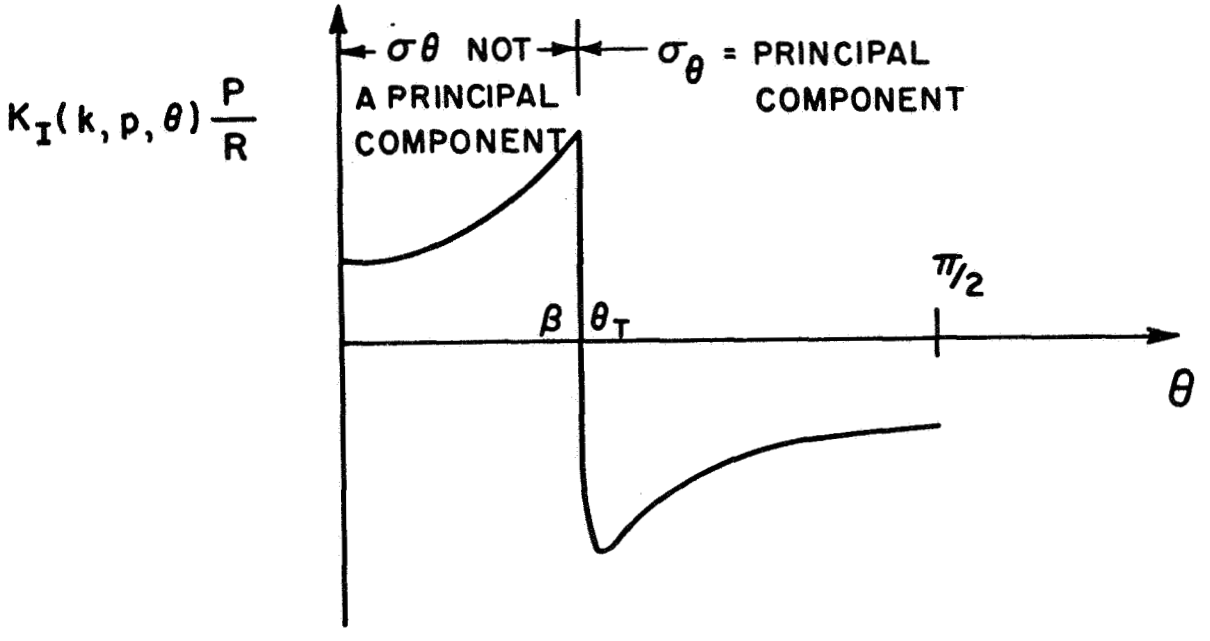

FIGURE 1-16 THE DISTRIBUTION OF CIRCUMFERENTIAL STRESS ALONG THE EDGE OF A CIRCULAR OPENING UNDER BOREHOLE JACK LOADING

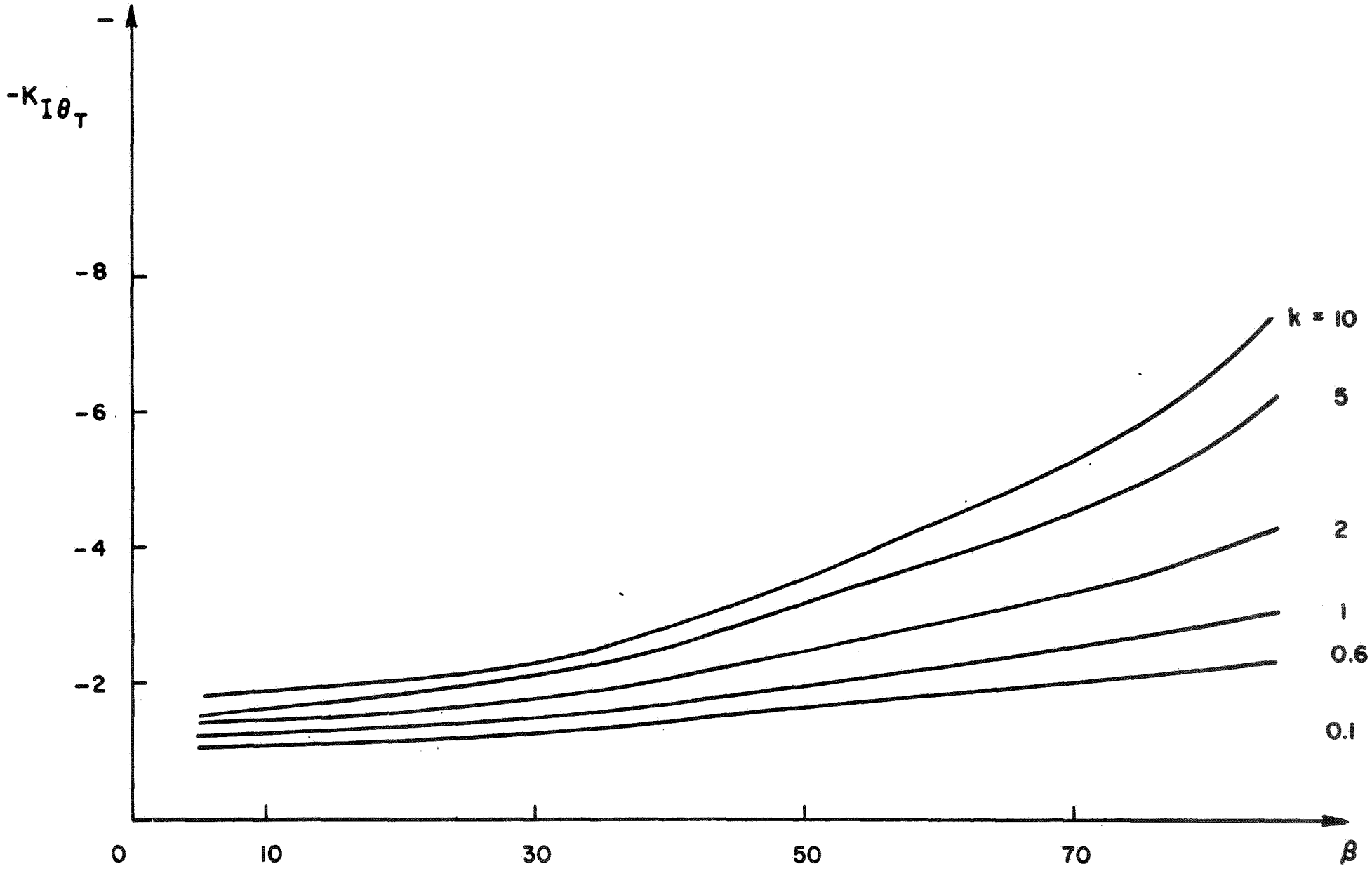

FIGURE 1-17a THE VARIATION OF THE STRESS CONCENTRATION FACTOR K_{IT} (k, β)

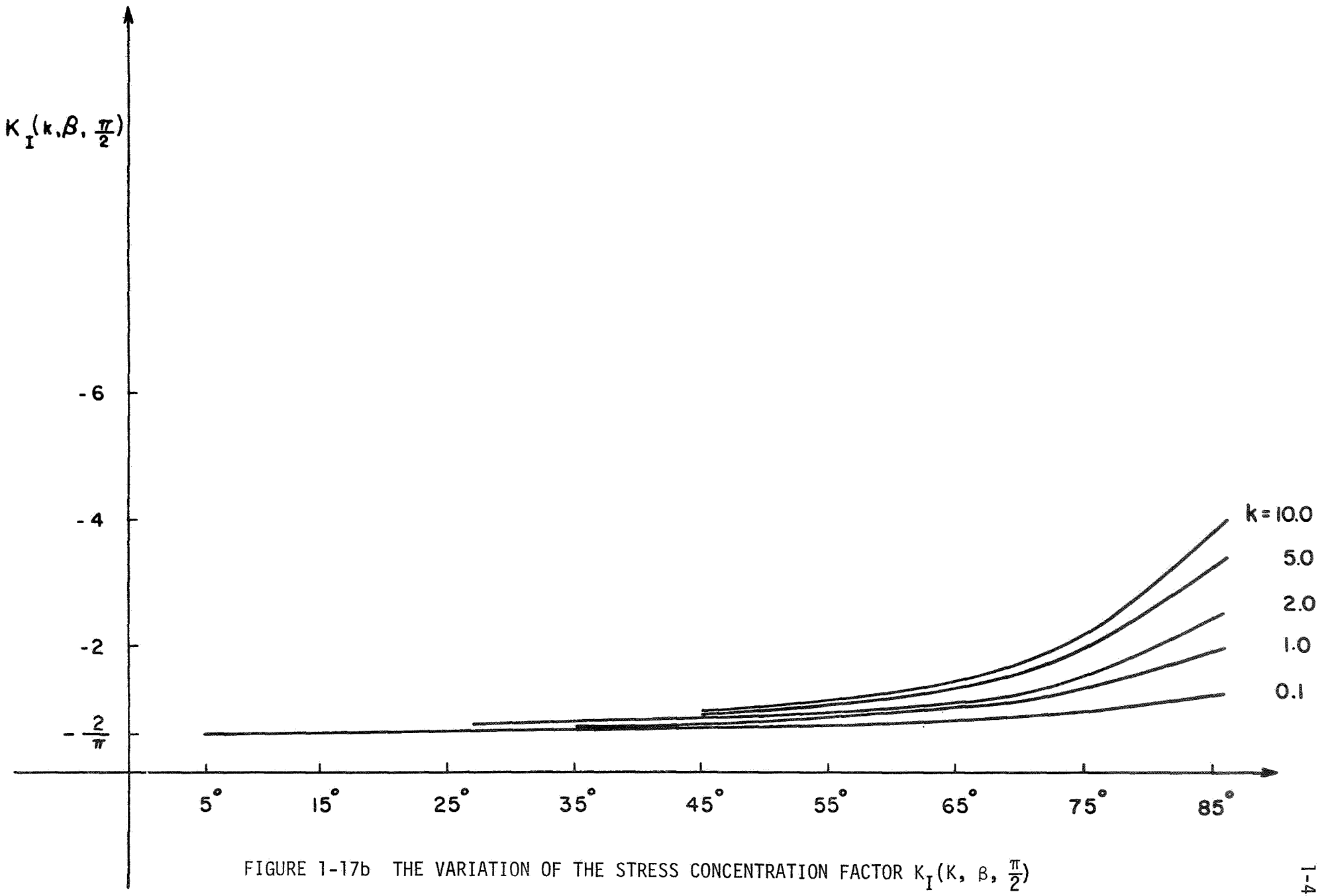

FIGURE 1-17b THE VARIATION OF THE STRESS CONCENTRATION FACTOR $K_I(K, \beta, \frac{\pi}{2})$

the loaded areas, the stress σ_θ is not a principal stress component due to the presence of the applied boundary shear stress $\tau^*_{r\theta}$.

Real materials are not linearly elastic and have the tensile strength varying with the confinement. For these materials, the stress factor at the points C and C' ($\rho = 1$, $\theta = \pi/2$ and $-\pi/2$) is an important controlling factor on the actual fracture initiation loads and the crack locations. The stress factors K_I (k, β, $\pi/2$) and K_{II} (k, β, $\pi/2$) are given in Tables 1-2a and 1-2b. Their variations with respect to k and β are shown in Figures 1-7b and 1-19b.

As the angle β becomes very small ($\beta \to 0$), theoretically, the stress factors K_I (k, β, $\pi/2$) and K_{II} (k, β, $\pi/2$) should approach the same limiting value, independent of k. This limiting value was found to be $-2/\pi$:

$$\lim_{\beta \to 0} K_I \left(k, \beta, \frac{2}{\pi}\right) = -\frac{2}{\pi} \qquad (1\text{-}41a)$$

$$\lim_{\beta \to 0} K_{II} \left(k, \beta, \frac{\pi}{2}\right) = -\frac{2}{\pi} \qquad (1\text{-}41b)$$

The same stress factor was obtained for the quadrantal jack loading when the angle β approaches zero. Two diametrically opposed point loads P's (at $\theta = 0$ and π) induce the same stress factor $-\frac{2}{\pi}$ at the points c and c' ($\theta = \frac{\pi}{2}$ and $-\frac{\pi}{2}$).

B. Tensile Fracturing of an Elastic Medium by Borehole Jack Loading.

A borehole jack with very narrow bearing plates induces local failure in a circular opening in a brittle medium. The local failure includes one or more of the following modes: crushing, punching, and lateral chipping. Such a borehole jack acts as a rock penetrometer.

TABLE 1-1a THE STRESS FACTOR $K_{IT}(k, \beta)$ AS A FUNCTION OF THE BOUNDARY STRESS DISTRIBUTION FACTOR k AND THE BEARING PLATE WIDTH ANGLE β

k	5°	15°	25°	35°	45°	55°	65°	75°	85°
0.1	-.85	-.91	-.95	-1.05	-1.10	-1.15	-1.20	-1.26	-1.39
0.3	-.96	-1.02	-1.08	-1.18	-1.32	-1.43	-1.53	-1.65	-1.85
0.6	-1.09	-1.16	-1.24	-1.37	-1.60	-1.78	-1.95	-2.14	-2.45
1.0	-1.22	-1.30	-1.40	-1.55	-1.88	-2.15	-2.39	-2.66	-3.11
2.0	-1.43	-1.51	-1.66	-1.85	-2.35	-2.75	-3.15	-3.60	-4.33
5.0	-1.68	-1.78	-1.98	-2.23	-2.95	-3.56	-4.18	-4.94	-6.21
10.0	-1.81	-1.92	-2.15	-2.44	-3.28	-4.02	-4.80	-5.77	-7.46

TABLE 1-1b THE STRESS FACTOR $K_{IIT}(k, \beta)$ AS A FUNCTION OF THE BOUNDARY STRESS DISTRIBUTION FACTOR k AND THE BEARING PLATE WIDTH ANGLE β

k	5°	15°	25°	35°	45°	55°	65°	75°	85°
0.1	-0.82	-0.93	-1.01	-1.02	-1.01	-0.98	-0.94	-0.90	-0.87
0.3	-0.89	-0.98	-1.19	-1.26	-1.26	-1.22	-1.16	-1.07	-0.99
0.6	-0.99	-1.03	-1.40	-1.54	-1.57	-1.52	-1.43	-1.29	-1.15
1.0	-1.08	-1.22	-1.61	-1.83	-1.88	-1.83	-1.70	-1.53	-1.33
2.0	-1.22	-1.41	-1.95	-2.29	-2.39	-2.35	-2.19	-1.95	-1.66
5.0	-1.40	-1.63	-2.38	-2.86	-3.04	-3.03	-2.85	-2.55	-2.16
10.0	-1.50	-1.76	-2.16	-3.17	-3.40	-3.41	-3.24	-2.93	-2.50

TABLE 1-2a THE STRESS FACTOR $K_I(k, \beta, \frac{\pi}{2})$, AS A FUNCTION OF THE BOUNDARY STRESS DISTRIBUTION FACTOR k AND THE BEARING PLATE WIDTH ANGLE β.

k	5°	15°	25°	35°	45°	55°	65°	75°	85°
0.1	-0.64	-0.64	-0.65	-0.66	-0.68	-0.70	-0.73	-0.77	-0.81
0.3	-0.64	-0.64	-0.65	-0.67	-0.69	-0.71	-0.75	-0.79	-0.85
0.6	-0.64	-0.65	-0.66	-0.68	-0.70	-0.73	-0.77	-0.83	-0.90
1.0	-0.64	-0.65	-0.66	-0.68	-0.71	-0.75	-0.80	-0.86	-0.95
2.0	-0.64	-0.65	-0.66	-0.69	-0.72	-0.77	-0.84	-0.93	-1.06
5.0	-0.64	-0.65	-0.67	-0.70	-0.74	-0.80	-0.89	-1.02	-1.22
10.0	-0.64	-0.65	-0.67	-0.70	-0.75	-0.82	-0.93	-1.08	-1.32

TABLE 1-2b THE STRESS FACTOR $K_{II}(k, \beta, \frac{\pi}{2})$ AS A FUNCTION OF THE BOUNDARY STRESS DISTRIBUTION FACTOR k AND THE BEARING PLATE WIDTH ANGLE β

k	5°	15°	25°	35°	45°	55°	65°	75°	85°
0.1	-0.64	-0.65	-0.66	-0.69	-0.73	-0.79	-0.87	-0.99	-1.21
0.3	-0.64	-0.65	-0.67	-0.70	-0.76	-0.82	-0.92	-1.08	-1.42
0.6	-0.64	-0.65	-0.68	-0.71	-0.77	-0.86	-0.99	-1.20	-1.69
1.0	-0.64	-0.66	-0.68	-0.73	-0.79	-0.90	-1.05	-1.33	-1.99
2.0	-0.65	-0.66	-0.69	-0.75	-0.83	-0.96	-1.17	-1.56	-2.55
5.0	-0.65	-0.68	-0.71	-0.77	-0.88	-1.05	-1.34	-2.09	-3.98
10.0	-0.65	-0.67	-0.71	-0.79	-0.90	-1.10	-1.43	-2.09	-3.98

When the bearing plates are large enough, the circular opening fails by tensile fracturing under borehole jack loading.

1. Tensile fracture in a medium initially nonstressed.

The in-situ stress field is zero. Under borehole jack loading, the maximum tensile stress is developed at the edges of the bearing plates ($\theta = -\beta$, β, $\pi - \beta$, and $\pi + \beta$) as discussed in part A. Tensile fracturing is initiated when the maximum tensile stress is equal to the tensile strength T_s of the medium. The initiation of the fracturing should take place at the four edges of the two bearing plates when $\sigma_{\theta A} = T_s$ where $\sigma_{\theta A}$ is the circumferential stress at the point A ($\theta = \beta$):

$$T_s = K_T\ (k,\ \beta)\ \frac{P_{init}}{R} \tag{1-42}$$

where

P_{init} = jack load at fracture initiation/length of the bearing plates

R = radius of the opening

$K_T\ (k,\ \beta)$ = maximum stress factor (at the edges of the bearing plates.

= K_{IT} for solution I (Table 1-1a)

= K_{IIT} for solution II (Table 1-2a).

2. Tensile fracture in a medium initially under an isotropic in-situ stress field.

An isotropic in-situ stress field p_1 induces a uniform circumferential stress σ_θ equal to $2p_1$ along a circular opening. When borehole jack loading is introduced, the net stress distribution in

the medium has the minimum minor principal stress at the edges of the bearing plates. Tensile fracturing is initiated when the minor principal stress at the plate edges is equal to the tensile strength of the medium, i.e., $\sigma_{\theta A} = T_s$, where $\sigma_{\theta A}$ is the net circumferential stress at the point A ($\theta = \beta$):

$$T_s = 2p_1 + K_T\,(k,\ \beta)\ \frac{P_{init}}{R} \qquad (1\text{-}43)$$

where

P_1 = magnitude of the in situ stress field, all other terms have been defined above.

It can be seen from the Equation (1-43) that the introduction of an isotropic in situ stress field p_1 requires an extra amount of jack load equal to $-\frac{2R\ p_1}{K_T(k,\ \beta)}$ to cause the fracture initiation.

3. Tensile fracture in a medium initially under an in-situ biaxial stress field.

An in situ biaxial stress field with the principal components $p_1 > p_2$ induces a circumferential stress σ_θ along a circular opening which varies with respect to the angle θ (Figure 1-18):

$$\sigma_\theta = p_1 + p_2 - 2(p_1 - p_2)\cos 2\theta_1 \qquad (1\text{-}44)$$

where

θ_1 = the angle measured from p_1 direction.

When borehole jack loading is applied, the net circumferential stress along the circular opening is obtained by adding the two Equations (1-36) and (1-44).

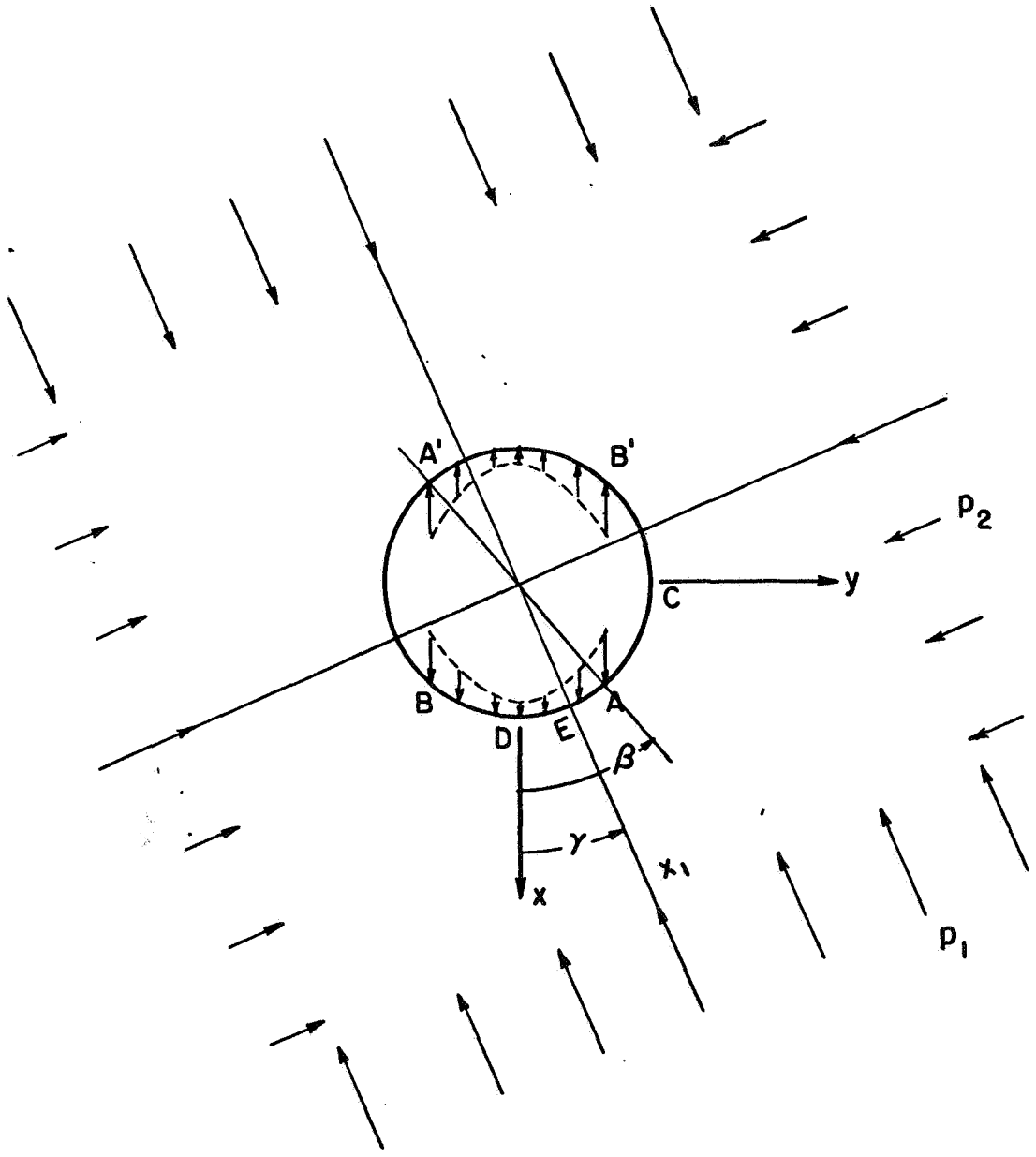

FIGURE 1-18 BOREHOLE JACK LOADING IN A MEDIUM SUBJECTED TO AN IN SITU BIAXIAL STRESS FIELD. CONTACT STRESS IS ASSUMED TO BE UNIDIRECTIONAL.

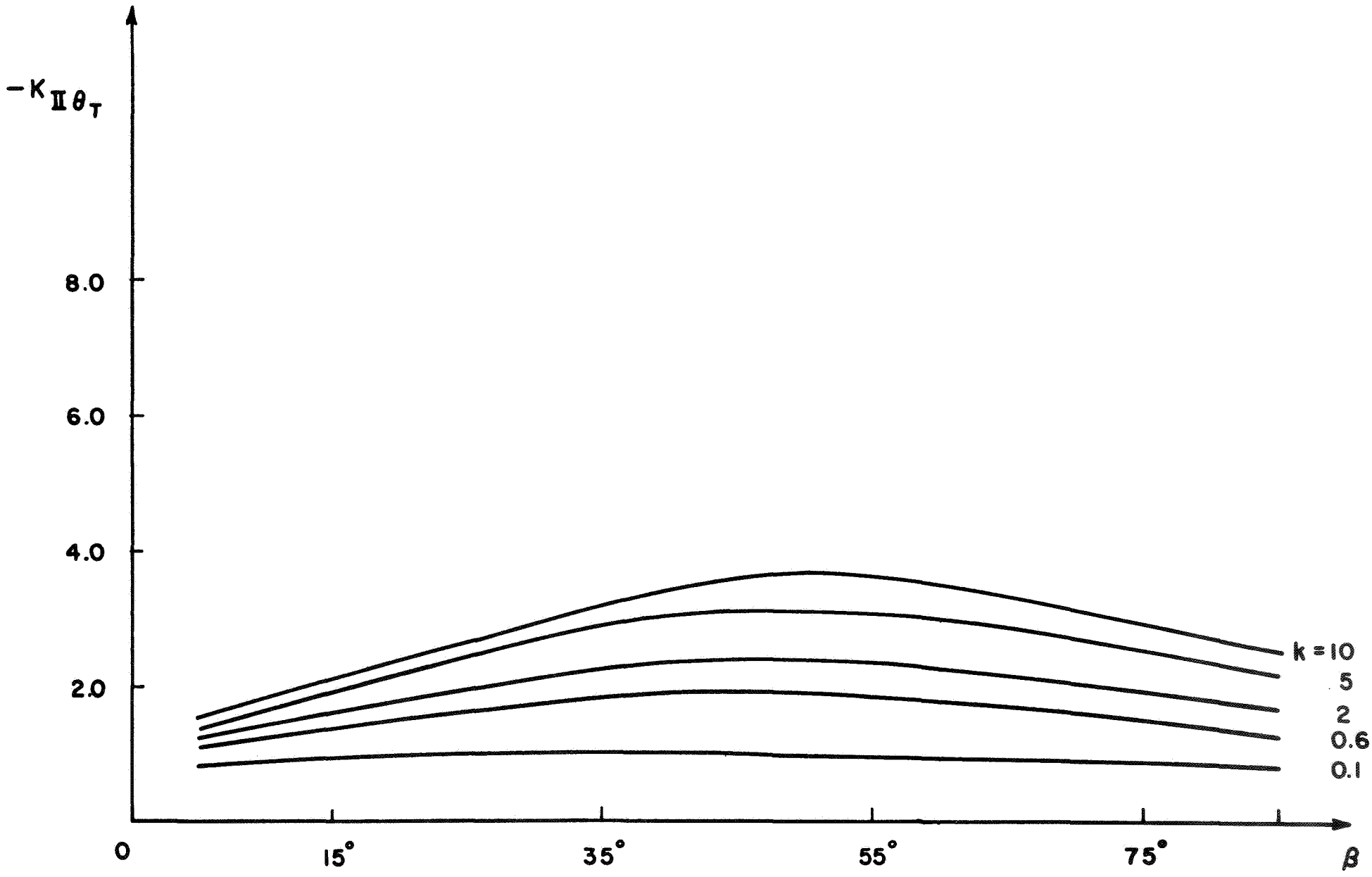

FIGURE 1-19a THE VARIATION OF THE STRESS CONCENTRATION FACTOR K_{IIT} (k, β).

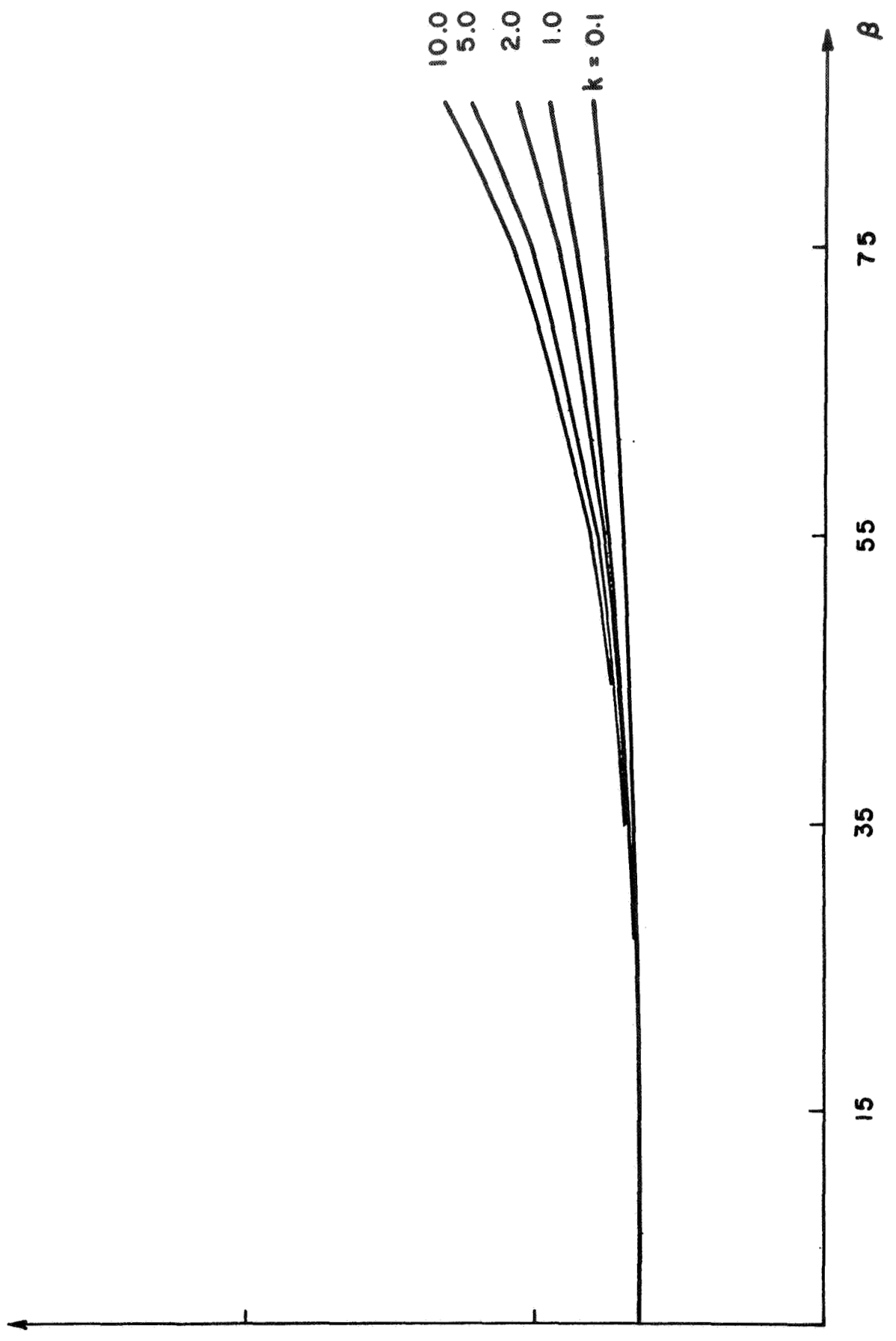

FIGURE 1-19b THE VARIATION OF THE STRESS CONCENTRATION FACTOR K_{II} $(k, \beta, \frac{\pi}{2})$

Along the unloaded arcs (Figure 1-18), the net circumferential stress is a principal stress component:

$$\sigma_\theta = p_1 + p_2 - 2(p_1 - p_2) \cos 2(\theta - \alpha) + K\,(k, \beta, \theta)\,\frac{P}{R} \qquad (1\text{-}45)$$

where

p_1, p_2 = principal components of the in situ stress field.

θ = angle measured from x-direction (Figure 1-18)

α = angle between p_1-direction and x-direction of jack loading.

$$K\,(k, \beta, \theta) = \begin{cases} K_I\,(k, \beta, \theta) \text{ given by the Equation (1-39) for solution I} \\ K_{II}\,(k, \beta, \theta) \text{ given by the Equation (1-40) for solution II.} \end{cases}$$

Along the loaded arcs (below the bearing plates), the net circumferential stress σ_θ is not a principal stress component due to the presence of the applied shear stress $\tau^*_{r\theta}$. The minor principal stress at a point θ on these arcs is calculated from the following equation:

$$\sigma_{minor} = \frac{\sigma^*_r + \sigma_\theta}{2} - \sqrt{\frac{1}{4}\,(\sigma_\theta - \sigma^*_r)^2 + (\tau^*_{r\theta})^2} \qquad (1\text{-}46)$$

where

σ_{minor} = minor principal stress,

σ^*_r , $\tau^*_{r\theta}$ = applied boundary normal and shear stresses.

σ_θ = circumferential stress along the circular opening.

The stress components σ^*_r , $\tau^*_{r\theta}$ and σ_θ to be used in the Equation (1-47) are given by the following expressions:

For the use of solution I:

$$\sigma^*_{rI} = \frac{P}{RM}\left\{k - (k-1)\cos\frac{\pi\theta}{2\beta}\right\}\cos\theta \qquad (1\text{-}47)$$

$$\tau^*_{r\theta I} = -\frac{P}{RM}\left\{k - (k-1)\cos\frac{\pi\theta}{2\beta}\right\}\sin\theta \qquad (1\text{-}48)$$

$$\sigma_{\theta I} = p_1 + p_2 - 2(p_1 - p_2)\cos 2(\theta - \alpha) + K_I\,(k, \beta, \theta)\,\frac{P}{R} \qquad (1\text{-}49)$$

where

$$M = \left\{2k\sin\beta - \frac{4(k-1)\,\pi\cos\beta}{\beta(\frac{\pi}{\beta}+2)\,(\frac{\pi}{\beta}-2)}\right\} \qquad (1\text{-}50)$$

$K_I\,(k, \beta, \theta)$ defined by the Equation (1-37)

For the use of solution II:

$$\sigma^*_{rII} = \frac{P}{2RM}\left\{k - (k-1)\cos\frac{\pi\theta}{2\beta}\right\}(1 + \cos 2\theta) \qquad (1\text{-}51)$$

$$\tau^*_{r\theta II} = -\frac{P}{2RM}\left\{k - (k-1)\cos\frac{\pi\theta}{2\beta}\right\}\sin 2\theta \qquad (1\text{-}52)$$

$$\tau_{\theta II} = p_1 + p_2 - 2(p_1 - p_2)\cos 2(\theta - \alpha) + K_{II}\,(k, \beta, \theta)\,\frac{P}{R} \qquad (1\text{-}53)$$

where

M is defined by the Equation (1-50)

$K_{II}\,(k, \beta, \theta)$ is defined by the Equation (1-38)

The Equation (1-46) can be rearranged into the following form:

$$\sigma_\theta\,\sigma^*_r + \sigma^2_{minor} - (\tau^*_{r\theta})^2 - \sigma_{minor}\,(\sigma_\theta + \sigma^*_r) = 0 \qquad (1\text{-}54)$$

where

P_{init} is defined by the Equations (1-55) and (1-56).

The minimization of P_{init} can be done numerically by first evaluating its values from all the angles θ's. This operation must be handled by computer. An intensive investigation of the influence of all the parameters involved would require a very large amount of computer time to all the possible combinations of the parameter ranges, and this expensive study might find little practical application.

Under normal field conditions, the in situ stresses usually induce a compressive σ_θ along a circular opening ($-p_1 + 3p_2 > 0$). There are possible conditions under which σ_θ could be tensile; however, the maximum tensile stress σ_θ would be much smaller than the tensile strength of the medium ($1 - p_1 + 3p_2\ 1 \ll 1\ T_s 1$). For these cases, under borehole jack loading, tensile fracturing is initiated at two edges (closest to p_1-axis) of the bearing plates, i.e., the two points, A and A' in Figure 1-20:

$$T_s = p_1 + p_2 - 2(p_1 - p_2) \cos 2(\beta - \alpha) + K_T\ (k, \beta) \frac{P_{init}}{R} \qquad (1\text{-}58)$$

where

K_T (k, β) = maximum stress factor, given in Tables 1-1a and 1-2a

P_{init} = jack load to initiate cracks at A and A' (Figure 1-20).

When the jack is oriented such that one edge of a bearing plate is on the p_1-axis ($\alpha = \beta$), the Equation (1-58) becomes:

$$T_s = - p_1 + 3p_2 + K_T\ (k, \beta) \frac{P_{init}}{R} \qquad (1\text{-}59)$$

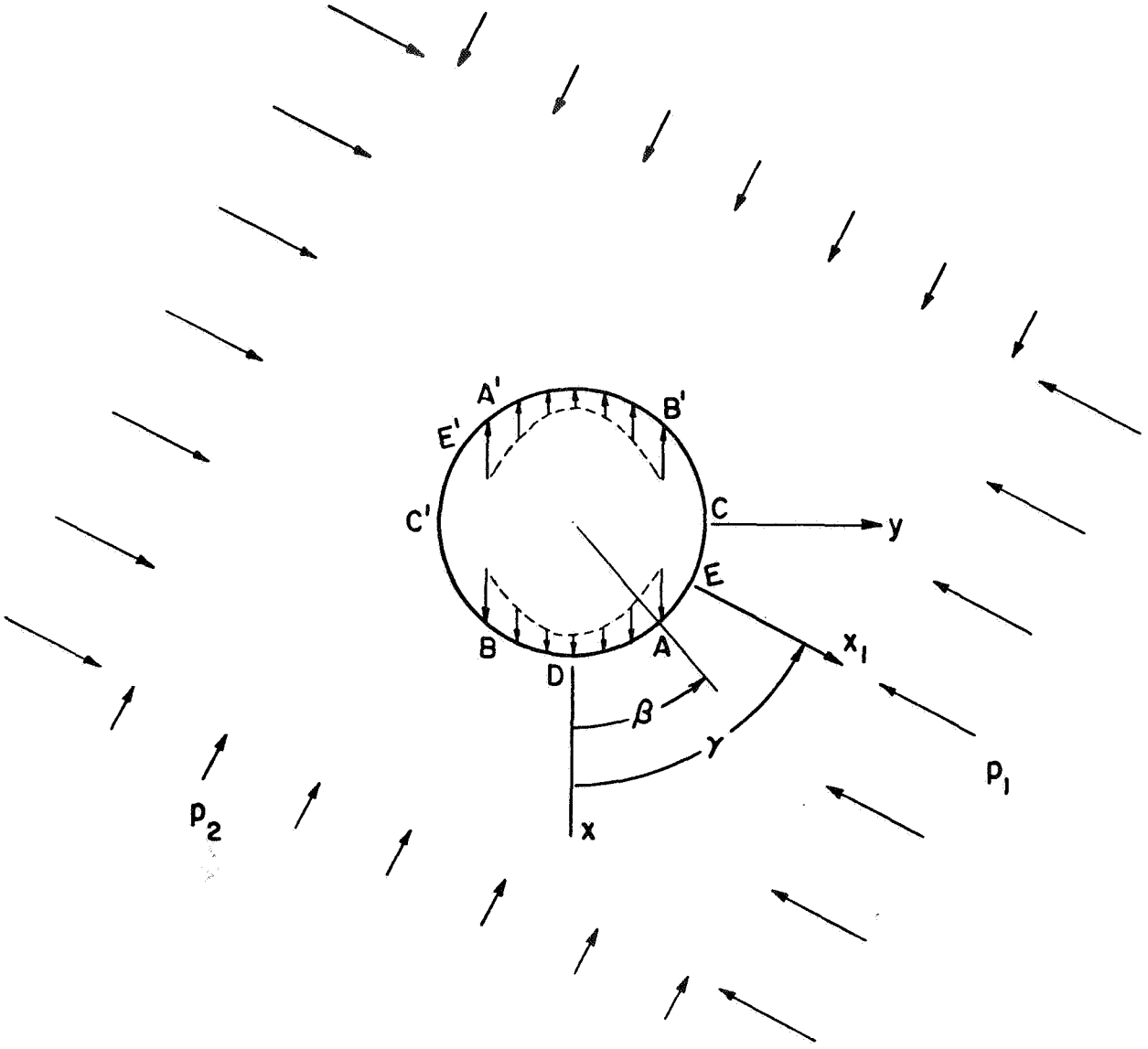

FIGURE 1-20 BOREHOLE JACK LOADING IN A MEDIUM SUBJECTED TO AN IN SITU BIAXIAL STRESS FIELD. CONTACT STRESS IS ASSUMED TO BE UNIDIRECTIONAL AND PRINCIPAL

The rotation of the jack through an 90° angle places one edge of the bearing plate on the p_2-axis ($\alpha = 90 - \beta$). The Equation (1-59) becomes:

$$T_s = 3p_1 - p_2 + K_T\ (k,\ \beta)\ \frac{P_{init}}{R} \qquad (1\text{-}60)$$

For a jack with an angle β is equal to 45° such as the NX-borehole jack (Goodman jack), both the orientations $\alpha = 0$ and π give the same equation:

$$T_s = p_1 + p_2 + K_T\ (k,\ \beta)\ \frac{P_{init}}{R} \qquad (1\text{-}61)$$

V. THE MECHANISM OF FAILURE OF A CIRCULAR BOREHOLE IN SOILS BY BOREHOLE JACK LOADING

The problem of a borehole jack in soils is different from that in rocks due to the plastic behavior of soils and their inability to carry tension of an appreciable magnitude.

With the best precaution and care, the drilling of a borehole in a soil mass still causes disturbance along the wall of the opening, which includes compaction, remolding, and breakage of weak tensional bonds. Natural soil masses are generally not well compacted. When the borehole is under jack load, the material behind the bearing plates is compacted, allowing the bearing plate to be pushed into the soil mass. The resistance to plate movement increases with load due to the increase in the degree of compaction of the material in the region below the plate. A jack designed to be used in soil masses

must provide a very large amount of displacement, in the order of the hole diameter or greater.

One way of analyzing results is to set up a large testing program and then to correlate the resistance to planned movement with the bearing capacity of the material. The relationship between settlement and load can be determined empirically from the experimental results. The testing concept of such a device would be similar to that of the soil penetrometer.

The theoretical consideration of the mechanism of failure of a borehole in soils, subjected to borehole plate loading is presented to provide a background for future development of borehole testing in soils.

A. Borehole Jack Loading in Very Dense Soil Masses

For narrow bearing plates, the problem is that of a strip footing on a curved surface. When the applied load against the plate is large enough, failure takes place along curved surfaces. Either the Prandtl mechanism or the Hill mechanism can be used to interpret the results, but the Hill mechanism was proven to give a more appropriate velocity field (Hill, 1951).

The limit analysis method in plasticity can be used to find the upper and lower bounds to this problem. Usually it is very difficult to find an exact solution, therefore the two bounds are estimated. The solution is within the bounds. If the two bounds coincide, they are the correct solution (Chen, 1966; Finn, 1965).

To find a lower bound, one tries to guess a statically admissible stress field, then to determine the load against the plate which

induces this stress field. Since there is stability for this load, stability is assured for any smaller load. To find an upper bound, a kinematically admissible velocity field is guessed for an assumed failure mechanism which is based on "engineering experience and intuition".

An upper bound is the load needed to induce such a velocity field. The choice of the stress field and the velocity field is completely arbitrary, and the bounds can be very far apart. Theoretically, all possible fields should be considered. In practice, only a number of stress fields are considered; the smallest upper bound and the largest lower bound constitute a bracket. The bracket is narrowed by repeated trials until the range is small enough for the desired purpose, or until no further improvement could be made (Chen, 1966; Shield, 1954; Finn, 1965).

1. Upper bound solution

The small bearing plates are assumed to be flat (Figure 1-21) The failure surface includes the straight line AC, making an angle $(45 + \phi/2)$ with the base AB where ϕ is the angle of internal friction, a logarithmic spiral CD, and a curve approximated by a number of straight lines DE, EF, FG. Each of the blocks BDE, BEF, and BFG moves as a rigid block. Radial shear exists in the spiral zone BCD. Along each of the discontinuous surfaces the velocity makes an angle ϕ with the surface of discontinuity. Along the spiral the velocity varies according to the relation $V_\theta = V_1 e^{2\theta \tan \phi}$ where V_1 is the velocity at $\theta = 0$ (Finn, 1965; Chen, 1966).

Call V_F the field velocity for the downward movement of the plate, the velocity V_1 - making an angle ϕ with the discontinuous surface AC - can be either calculated, or evaluated graphically. With the angle CBD assumed to be $\pi/2$, the velocity V_2 at D is equal to $V_1 e^{\pi \tan \phi}$. The remaining velocities corresponding to other discontinuous surfaces are determined graphically by a hodograph (Figure 1-22). The curve C'D' on the hodograph is a logarithmic spiral with center 0. The radius of this spiral represents the changing velocity along the curve CD.

The amount of energy dissipated along AC, CD and within the deformable zone of radial shear BCD are readily calculated. The energy dissipated on each straight line is equal to cLV cos ϕ where

c = cohesion of the material

L = length of line

V = velocity

For the area defined by the logarithmic spiral, energy is dissipated along the surface CD, and also within the area CBD - to accomodate the deformation caused by radial shear. The total energy dissipated on CD and BCD is equal to $CV_1 \cot \phi \ (e^{\pi \tan \phi} - 1)$ (Finn, 1965).

The total energy is minimized graphically by using various assumptions of discontinuous surface AE, FG.

2. Lower bound solution

This is the problem of a strip footing at the bottom of a symmetrical valley with curved flanks. A lower bound for a strip

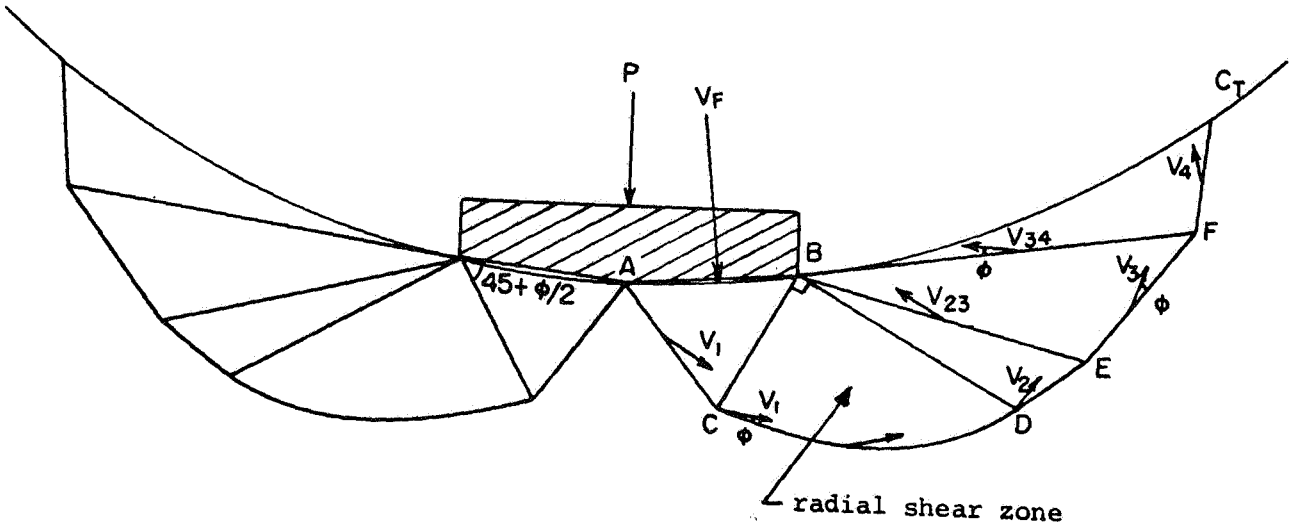

FIGURE 1-21 HILL MECHANISM FOR SMALL BEARING PLATES ON PLASTIC MATERIALS

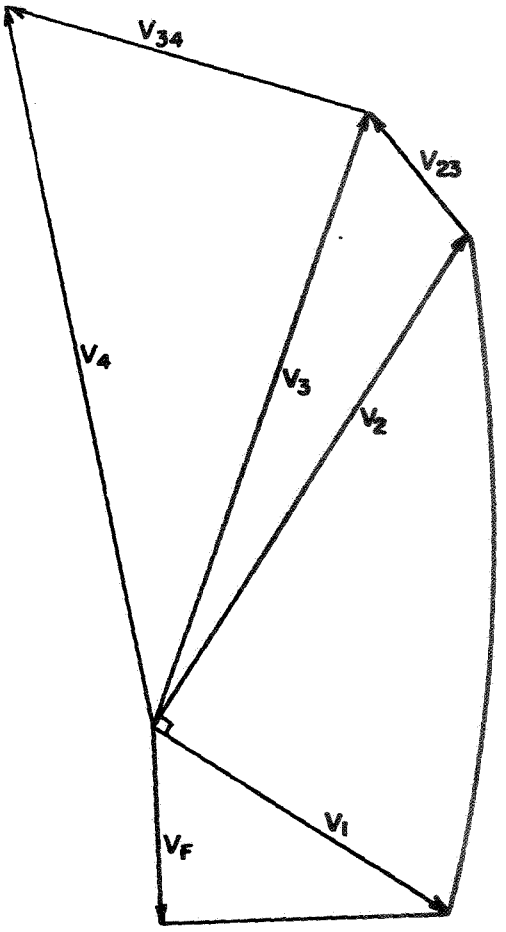

FIGURE 1-22 HODOGRAPH FOR THE VELOCITY FIELD IN FIGURE 1-21

foundation at the bottom of a symmetrical valley with two planar flanks is available (Chen, 1966). This solution can be adopted to the jack problem as shown in Figure 1-23. The stress field for this improved lower bound includes the stress field in the trapezoid FDDF, and the stress field in the wedge CDH - induced the unilateral pressure against CD.

The trapezoid FDDF supports a vertical pressure Q_1 which induces a horizontal pressure q_1 in DDE and a compressional pressure p_1 in each of the two legs of the trapezoid, parallel to the direction DF.

In the vertical region DDCC below the plate, horizontal and vertical compressional pressure Q_2 are arbitrarily added. The arbitrary introduction of stress components does not violate the method of limit analysis in plasticity (Chen, 1966; Finn 1965).

The maximum pressure Q_2 acting on the face CD and inducing a statically admissible state of stress in the wedge CDG is controlled by the material properties ϕ and C, and the angle of inclination α_2 (Figure 1-23) (Chen, 1966):

$$Q_2 = c \cot \phi \left\{ \tan^2 (45^\circ + \phi/2) \frac{\sin (\hat{\nu} + \alpha_2)}{\sin (\hat{\nu} - \alpha_2)} - 1 \right\} \qquad (1\text{-}62)$$

where

$$\cos \nu = \sin \phi \sin_2$$

The same value of Q_2 was obtained earlier by Shield through the application of the general "jump condition" (Shield, 1954).

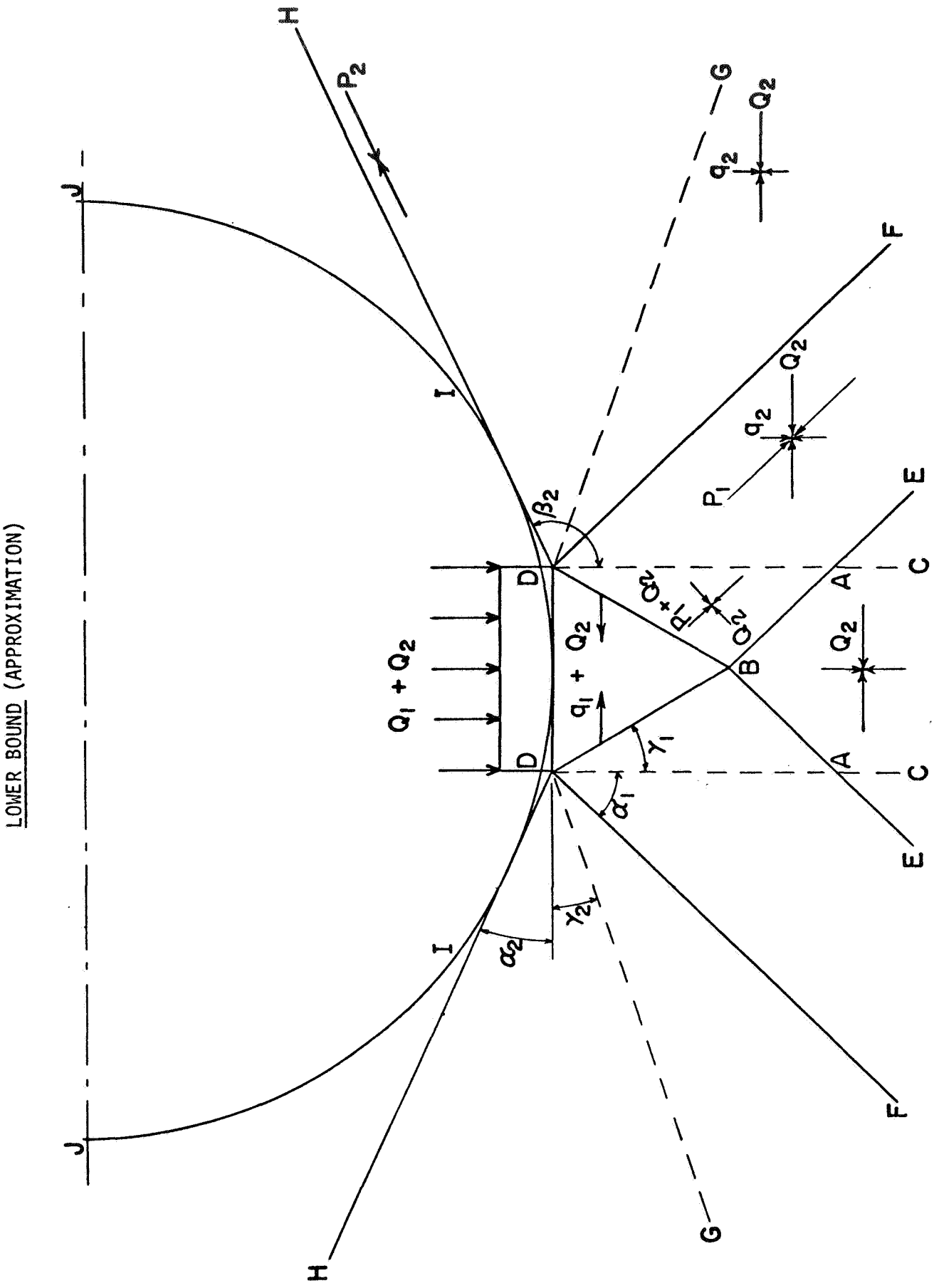

FIGURE 1-23 LOWER BOUND SOLUTION FOR SMALL BEARING PLATES ON PLASTIC MATERIALS (AFTER WAI-FAH CHEN, 1966)

With Q_2 given by Equation (1-62) the yield condition and the angle of inclination α_1, the stress p_1 corresponding to the plastic equilibrium in the legs EBDF is derived (Chen, 1966):

$$p_1 = \frac{4c\ (\sin\phi + \cos 2\alpha_1)}{\cos\phi\ (1 - \sin\phi\ )} \cdot \frac{\sin\ (\beta_2 - \mu_2)}{\sin\ (\beta_2 + \mu_2)} \tag{1-63a}$$

and

$$\sin\alpha_1 = \cos\phi/2 \tag{1-63b}$$

where

$$\begin{cases} \beta_2 = \alpha_2 + \pi/4 \\ \sin\mu_2 = \sin\phi\ \sin\beta_2 \end{cases}$$

The values of p_1 and α_1 given by the Equations (1-63) the condition of equilibrium of forces, and the condition of plastic yield in DDE, are used to calculate Q_1 (Chen, 1966).

$$Q_1 = \frac{c}{2}\tan^3\ (45° + \phi/2)\ \frac{\sin\ (\beta_2 - \mu_2)}{\sin\ (\beta_2 + \mu_2)} \Big\{ 4 + \sin\phi + \sin^2\phi + (1 + \sin\phi)\ (4 + \sin^2\phi)^{1/2} \Big\} \tag{1-64}$$

The load $Q_L = Q_1 + Q_2$ against the bearing plate produces plastic yield in the region EBEFDDF. The state of stress in

the soil mass induced by the lower bound Q_L is everywhere statically admissible:

$$Q_L = c \cot \phi \left\{ \tan^2 (45° + \frac{\phi}{2}) \frac{\sin (\beta_2 - \mu_2)}{\sin (\beta_2 + \mu_2)} - 1 \right\}$$

$$+ \frac{c}{2} \tan^3 (45° + \frac{\phi}{2}) \frac{\sin (\beta_2 - \mu_2)}{\sin (\beta_2 + \mu_2)} \left\{ 4 + \sin \phi \right.$$

$$\left. + \sin^2 \phi + (1 + \sin \phi) (4 + \sin^2 \phi)^{1/2} \right\} \qquad (1\text{-}65)$$

3. Large bearing plates against the borehole in a compacted soil mass.

Initially, as load is applied, the bearing plate is pushed into the dense soil mass causing further compaction in the region below the plate. The rate of plate displacement decreases with load due to higher degree of compaction. In the region MMNN, the weak tensile bonds are broken, creating a "no-stress" zone. The no-stress zones extend deeper into the soil mass as applied load is increased forming two "halves-space". The material below the plates finally failed along curved surfaces (Figure 1-24). The failure surface is assumed to be that of the Prandtl mechanism. The upper bound for a c-ϕ medium is given by (Finn, 1965):

$$Q_U = c \cot \phi \left\{ e^{\pi \tan \phi} \tan^2 (45° + \frac{\phi}{2}) - 1 \right\} \qquad (1\text{-}66)$$

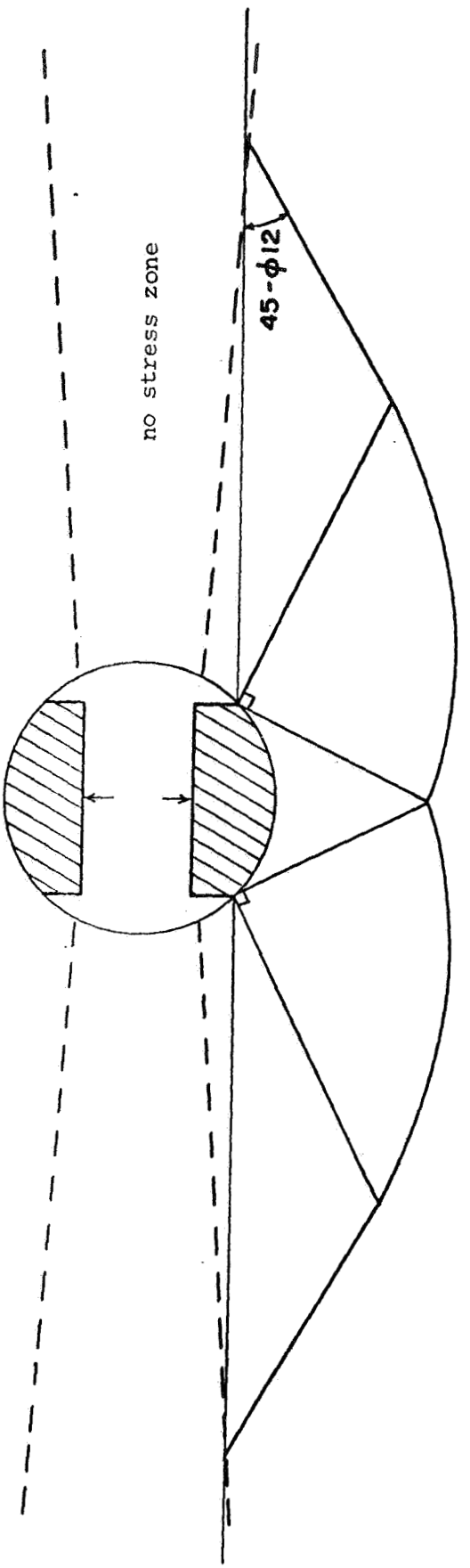

FIGURE 1-24 FAILURE MECHANISM FOR LARGE BEARING PLATE IN EXPANDING SOIL

The lower bound is given by the Equation (1-65) with $\beta_2 = \pi/2$:

$$Q_L = c \cot \phi \left\{\tan^2 (45° + \phi/2) - 1\right\} + \frac{c}{2} \tan^3 (45° + \phi/2)$$

$$\times \left\{4 + \sin \phi + \sin^2 \phi + (1 + \sin \phi)\ (4 + \sin \phi^2)^{1/2}\right\} \qquad (1\text{-}67)$$

B. Borehole Jack Loading in Very Loose Soil Masses

When load is applied, the bearing plate is pushed into the soil mass, compacting the soil below the plate forming a rectangular trench. There would be a slight increase in the degree of compaction of the material along the wall of the trench. The plate displacement and the thickness of the compacted zone below the plate increase with load. Because of the high void ratio, the compacted zone is a rectangular prism, similar to the case of a very porous material subjected to plate load, experiences a structural collapse (Figure 1-25).

For porous solids, the structural collapse takes place when the average pressure below the bearing plate is slightly larger than the compressive strength of the materials (Chercasov, 1967). For loose soils, there should be considerable plate movement when the applied pressure is equal to the unconfined compressive strength of the material which is very small.

For a given applied load, plate movement ceases when the total resisting force, including the normal force exerted against the compacted mass and the shear resistance along its sides, equals the applied load (Figure 1-26). It would be expected that the rate of plate displacement with respect to load ($\frac{\Delta U}{\Delta P}$ = displacement change/load

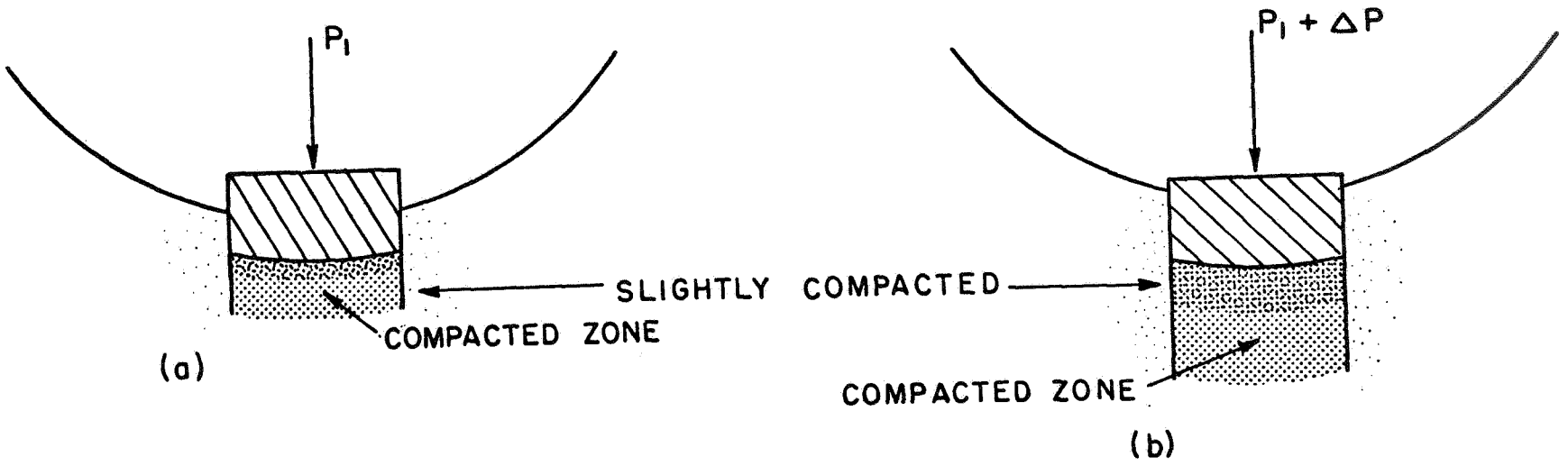

FIGURE 1-25 THE FORMATION OF A COMPACTED ZONE WHEN A BEARING PLATE IS PUSHED AGAINST THE WALL OF A BOREHOLE IN A VERY LOOSE SOIL MASS

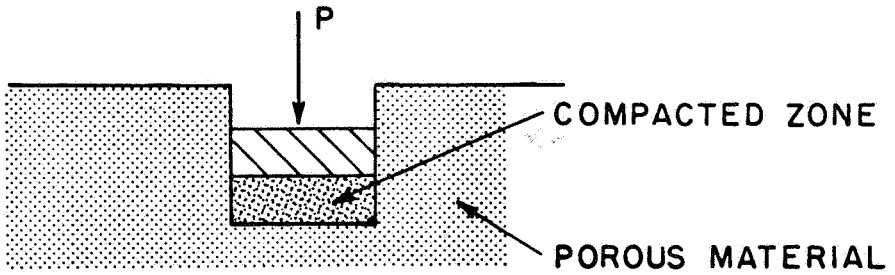

(C)

FIGURE 1-25c THE FORMATION OF A COMPACTED ZONE RESULTING FROM THE STRUCTURAL COLLAPSE OF A POROUS BRITTLE MEDIUM UNDER PLATE LOADING.

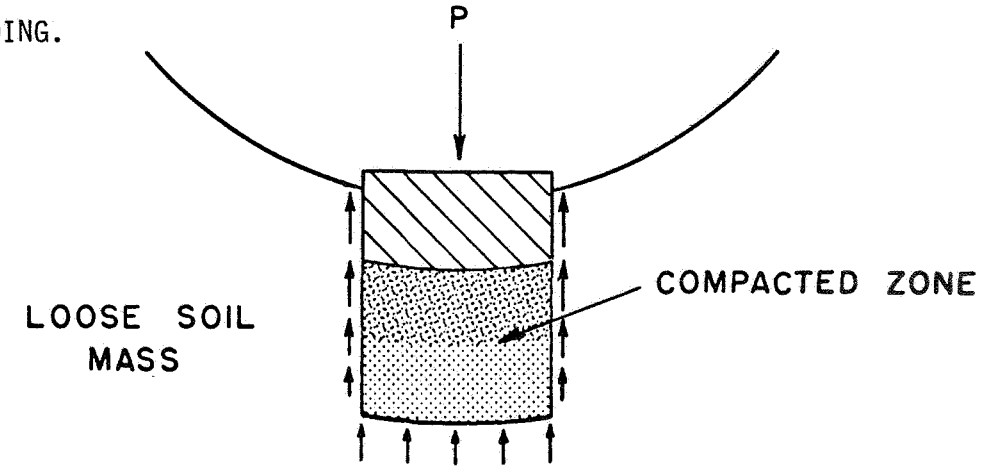

FIGURE 1-26 APPLIED JACK LOAD IS RESISTED BY THE NORMAL PRESSURE AGAINST THE BOTTOM OF THE COMPACTED ZONE, AND THE SHEAR RESISTANCE ALONG ITS SIDES

change) be constant since extra resistance to displacement can be mobilized only from the increase in the shear along the sides of the compacted prism due to the increase of the prism's thickness.

C. Bearing Plate Against the Wall of a Borehole in a Medium Dense Soil

Usually, a natural in situ soil mass is medium dense, somewhere between the two extreme cases of very dense and very loose conditions discussed above. When a small amount of load is applied, the plate is pushed into the soil mass, forming a rectangular trench. A compacted bulb is formed with the highest degree of compaction in the region immediately below the plate. As extra load is added, the compacted bulb increases in size, until the resisting force exerted against it by the surrounding soil mass equals the total applied force (Figure 1-27). It would be expected that the rate of plate displacement with respect to the load be decreasing due to the size increase of the compacted bulb, $[\frac{\partial}{\partial P} (\Delta U/\Delta P) < 0]$. When the total applied load is large enough, any further increase in load causes insignificant plate movement and increase in bulb size. However, the increase in applied load increases the magnitude of the stress field in the region below the plate; and eventually, curved failure surfaces are formed in the compacted bulb - shear failure (Figure 1-28).

Therefore, medium dense soil under jack plate test behaves as a very loose soil when the applied load is very small; at medium load range a compacted bulb is formed, having larger size with increasing loading, and finally, when the applied load and the compacted bulb are large enough, the material below the plate behaves as a compacted dense soil.

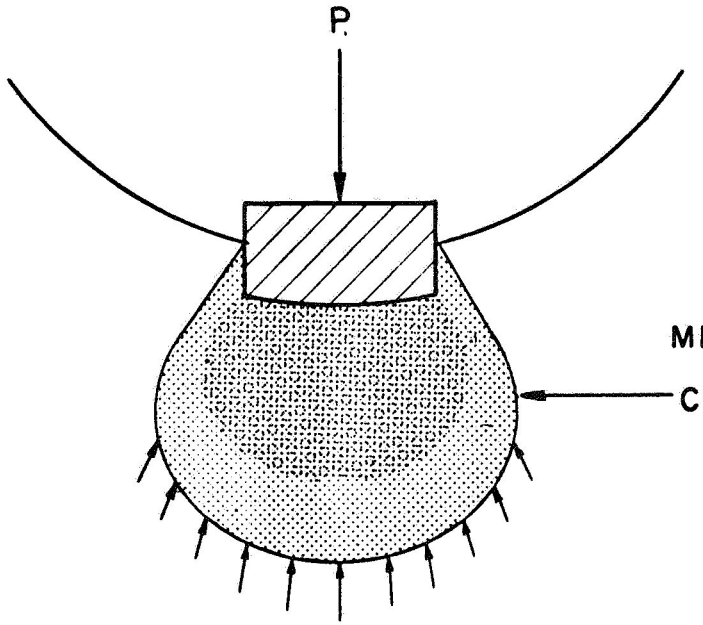

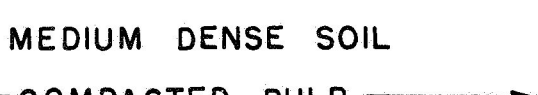

FIGURE 1-27 A COMPACTED BULB IS FORMED WHEN A MEDIUM DENSE SOIL IS SUBJECTED TO BOREHOLE JACK LOADING.

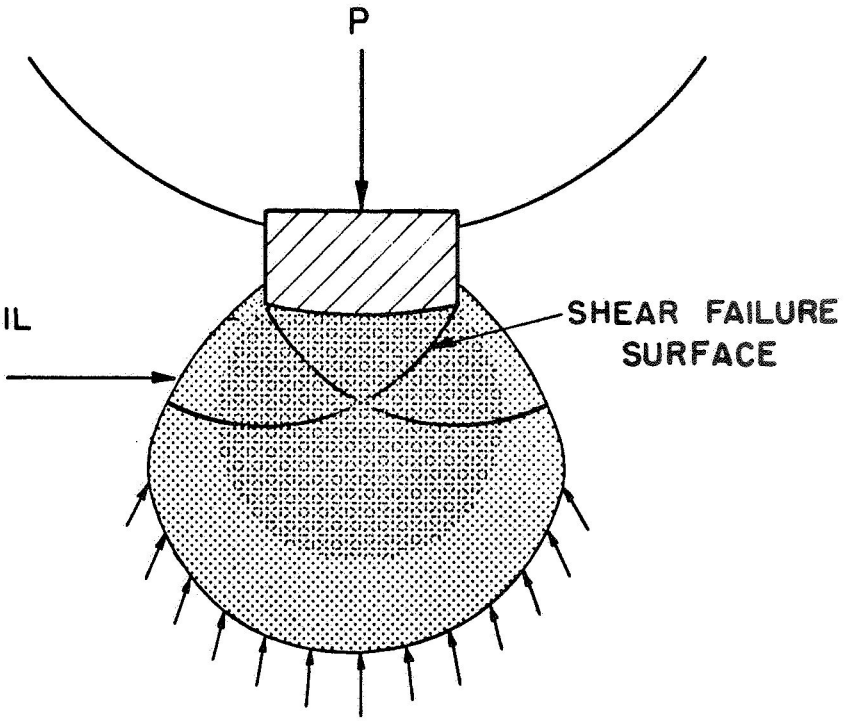

FIGURE 1-28 POSSIBLE SHEAR FAILURE WHEN THE COMPACTED BULB BECOMES VERY LARGE

This is a problem of a penetrometer in soils. The relationships between the parameters such as initial relative density, cohesion, angle of internal friction of the soil mass, the length and width of the bearing plates; and the rate of plate penetration with respect to load, the size and shape of the compacted bulb, the plate penetration and applied load at shear failure can only be studied empirically by a large experimental program (See Chapter 2).

REFERENCES

1. Absi, E. and Seguin, M., "Le Nouveau Geoextensometre," Supplement to *Annales de L'Institut Technique du Batiment et des Travaux Publics.*, No. 235-236, pp. 1151-1158, July-August 1967.

2. Bishop, R. F., Hill, R., and Mott, N. F., "The Theory of Indentation and Hardness Tests," *Proc. Phys. Soc. London*, 57/3, pp. 147-159, 1945.

3. Bray, J. W., "A Study of Jointed and Fractured Rocks, Part II, Theory of Limiting Equilibrium," *Rock Mech. and Engineering Geology*, Vol. 4, 1967.

4. Chen, W. F., *On Solving Plasticity Problems of Relevance to Soil Mechanics. The Bearing Capacity of Concrete*, Ph.D. Thesis, Brown University (1966).

5. Dryselius, G., "Konstricktion au Matcel for Beigtrycks-studier" (Design of a Measuring Cell for the Study of Rock Pressure), *IVA Ingeniorsvetenskapsakademiens Meddelande*, 142, Stockholm, pp. 135-144 (1965).

6. Fairhurst, C., "On the Validity of the Brazilian Test for Brittle Materials," *Int. J. Rock Mechanics and Mining Sciences*, 1, pp. 535-546 (1964).

7. Finn, W. D. L., "Application of Plasticity in Soil Mechanics", Soil Mechanics and Bituminous Materials Research Laboratory, University of California, Berkeley, August 1965.

8. Gibson, R. E. and Anderson, W. F., "In-situ Measurement of Soil Properties with the Pressuremeter," *Civil Engineering and Public Works Review 56*, pp. 615-618 (1961).

9. Goodman, R. E., Van, T. K., and Heuzé, F., "The Measurement of Rock Deformability in Boreholes," *Proc. 10th Symposium on Rock Mechanics, AIME* (1968).

10. Goodman, R. E., "Effects of Joints on the Strength of Tunnels, Analysis of Piledriver Drifts," *Report of Investigation for U. S. Army Engineering District, Omaha* (August 1968).

11. Goodman, R. E., "Analysis of Structures in Jointed Rocks," U. S. Army Engineering District, Omaha, Nebraska (July 1967).

12. Hill, R., *The Mathematical Theory of Plasticity*, Oxford University Press (1951).

13. Hubbert, M. K. and Willis, D. G., "Mechanics of Hydraulic Fracturing," *Trans. American Institute of Mining, Metallurgical, and Petroleum Engineers*, 210 (1957).

14. Hult, K., "On the Measurement of Stresses in Solids," *Trans. Chalmers University of Technology*, Gothenburg, Sweden, N. 280 1963).

15. Jaeger, J. C. and Cook, N. G. W., "Theory and Application of Curved Jacks for Measurement of Stresses," *Intern. Conference on State of Stress in the Earth's Crust, Santa Monica, California*, ed. Judd, pp. 12-3 through 12-23 (Elsevier Press) May 1963.

16. Kerisel, J., "La Mecanique des Sols: recherches et investigations recentes," *Travaux* 42, pp. 874-878 (1968).

17 Ladanyi, B., "Expansion of a Cavity in Saturated Clay Medium," *Proc. ASCE, J. of Soil Mechanics and Foundation Division*, 89, No. SM-4 pp. 127-161 (1963).

18. Ladanyi, B., "Expansion of Cavities in Brittle Media," *Intern. J. Rock Mechanics and Mining Sciences*, V. 4, pp. 301-328 (1967).

19. Ladanyi, B., "Rock Failure under Concentrated Loading," *Proc. 10th Symposium on Rock Mechanics, Texas* (1968).

20. Menard, L., "Measures In-situ des Proprietes Physiques des Sols," *Annales des Ponts et Chaussees*, 127, pp. 357-377 (1957).

21. Menard, L.,"Rules for the Calculation and Design of Foundation Elements on the Basis of Pressuremeter Investigations of the Ground," Translated by B. E. Hartmann, adjusted by J. B. Francq (Distributed by Terremetrics) (April 1966).

22. Muskhelishvili, N. I., *Some Basic Problems of the Mathematical Theory of Elasticity*, translated from the Russian by J. R. Radok (P. Noordhoff Ltd., Groningen, The Netherlands, 1963).

23. Seeley, F. B., and Smith, J. O., *Advanced Mechanics of Materials* (John Wiley and Sons, Inc., New York, 1959) pp. 295-341.

24. Shield, R. T., "Stress and Velocity Field in Soil Mechanics", *J. Mathematical Phys.*, V. 33, No. 2 pp. 144-156 (1954).

25. Skempton, A. W., Yassin, A. A., and Gibson, R. E., "Theorie de la Force Portante des Pieux dans le Sable," *Annales de l'Inst. Tech. Batiment*, No. 63-64, p. 285 (1953).

26. Sokolnifoff, I. S. "Mathematical Theory of Elasticity" (McGraw-Hill Book Company, Inc., New York, 1951).

27. Stears, J. H., "Evaluation of Pentrometer for Estimating Roof Bolt Anchorage," *USBM Report of Investigation 6646*, U. S. Bureau of Mines (1965).

28. Timoshenko, S., and Goodier, J. N., "Theory of Elasticity" (McGraw-Hill Book Company, Inc., New York, 1951).

29. Van, Tran K., "In-situ Determination of Rock Deformability by Borehole Jack Tests," unpublished M. S. Thesis, University of California, Berkeley, California (1967).

30. Vesić, A. B., and Barksdale, R. D., "Theoretical Studies of Cratering Mechanisms Affecting the Stability of Cratered Slopes," Project No. A-655, Eng. Exper. Station, Georgia Inst. of Tech. (1963).

31. Wyanecki, J., "Les Geoextensometres du Centre Experimental de Recherches et d'Etudes du Batiment et des Travaux Publics, Etude Experimentale sur Modeles Reduits", *Laboratoire du Batiment et Travaux Publics*, Supplement aux Annales, No. 246 (June 1968).

32. Kujundzic, B. and Stojakovic, M., "A Contribution of the Experimental Investigation of Changes of Mechanical Characteristics of Rock Massives as a Function of Depth," *in Trans. 8th Congress on Large Dams* (Edinburgh, Great Britain, May 1964) pp. 1051-1067.

33. Kujundzic, B., "Experimental Research into Mechanical Characteristics of Rock Masses in Yugoslavia," *Intern. J. Rock Mechanics and Mining Sciences, England*, vol. 2, pp. 75-91 (1965).

34. Chercasov, I. I. "The Residual Deformations Caused by the Deep Penetration of a Rigid Plate into a Brittle Porous Material," in *Proc. Geotech. Conf.* (Oslo 1967), vol. 1., pp. 179-180.

APPENDIX A

SOLUTION TO A TWO-DIMENSIONAL ELASTICITY PROBLEM BY COMPLEX VARIABLE METHOD

The solution of a two-dimensional problem in elasticity involves the integration of the differential equations of equilibrium, satisfying both the compatibility equations and the boundary conditions (Muskhelisvili, 1963; Sokolnikoff, 1956; Timoshenko and Goodier, 1951). To solve this system of equations more effectively, a function $\Psi(x,y)$, called the Airy stress function, is introduced. In the absence of body forces, the equilibrium condition is satisfied when the following assumption is made:

$$\sigma_x = \frac{\partial^2 \Psi(x,y)}{\partial y^2}$$

$$\sigma_y = \frac{\partial^2 \Psi(x,y)}{\partial x^2}$$

$$\tau_{xy} = - \frac{\partial^2 \Psi(x,y)}{\partial x \, \partial y} \qquad (1\text{-A-}1)$$

To satisfy the condition of displacement compatibility, a solution must satisfy the following equation:

$$\nabla^2 (\sigma_x + \sigma_y) = 0 \qquad (1\text{-A-}2)$$

where

$$\nabla^2 = \frac{\partial^2}{\partial x^2} + \frac{\partial^2}{\partial y^2} = \text{Laplacian operator.}$$

To satisfy both the equations of equilibrum and the compatibility condition, the Airy stress function must satisfy a biharmonic equation:

$$\nabla^4 \Psi(x,y) = \nabla^2 \left(\nabla^2 \Psi(x,y) \right) = 0 \qquad (1\text{-A-}3)$$

The solution of a two-dimensional elasticity problem reduces to finding a solution to the biharmonic Equation (1-A-3) which satisfies the given boundary condition. The uniqueness of the solution to this boundary-value problem is assured (Sokolnikoff, 1956). When the stress function $\Psi(x,y)$ is determined, the stress components at every point in the body are obtained from Equations (1-A-1).

In the Cartesian coordinates, $\Psi(x,y)$ includes a combination of polynomials of various degrees with suitable coefficients determined by the boundary conditions. In polar coordinates, $\Psi(r,\theta)$ consists of an infinite combination of harmonic functions. The function Ψ can be more conveniently presented in terms of two functions of the complex variable $z = x + iy$ as $\phi(z)$ and $X(z)$. These two functions are to be found, in terms of which the suitable stress function can be formed (Sokolnikoff, 1956; Timeshenko and Goodier, 1951).

Corresponding displacements are obtained using Hooke's law. The stress-strain relationship in plane strain or plane stress condition and the biharmonic Equation (1-A-3) lead to the following relations:

$$\sigma_\theta + \sigma_r = 4 \text{ Real} \left\{ \phi'(z) \right\} \qquad \text{(1-A-4a)}$$

$$\sigma_\theta - \sigma_r + 2i\,\tau_{r\theta} = 2 \left\{ \bar{z}\,\phi''(z) + X''(z) \right\} e^{2i\theta} \qquad \text{(1-A-4b)}$$

$$2G(u + iv) = \left\{ n\phi(z) - z\phi(z) - X'(z) \right\} e^{-i\theta} \qquad \text{(1-A-5)}$$

where

$G = \dfrac{E}{2(1 + v)}$; E = modulus of elasticity, and v = Poisson's ratio

u, v = radial and circumferential displacements

$\bar{z}$ = x - iy, complex conjugate of z

$$\phi'(z) = \frac{\partial \phi}{\partial z}$$

$$n = \begin{cases} 3 - 4\nu & \text{for plane strain conditions} \\ \dfrac{3 - \nu}{1 + \nu} & \text{for plane strain conditions} \end{cases}$$

The functions $\phi(z)$ and $X(z)$ are related to the boundary condition of loading by the following relation:

$$\rho = 1$$

$$\sigma_r^* - i\,\tau_{r\theta}^* = \phi'(z) + \overline{\phi'(z)} - \left\{ \bar{z}\,\phi''(z) + X''(z) \right\} e^{2i\theta} \qquad (1\text{-A-6})$$

where σ_r^*, $\tau_{r\theta}^*$ = applied normal and shear stresses on the boundary.

The functions $\phi(z)$, $X(z)$, and the boundary stress quantity $\left(\sigma_r^* - i\,\tau_{r\theta}^*\right)$ are expressed as series:

$$\phi'(z) = \sum_{m=o}^{\infty} a_m z^{-m} \qquad (1\text{-A-7})$$

$$X''(z) = \sum_{m=o}^{\infty} b_m z^{-m} \qquad (1\text{-A-8})$$

$$\sigma_r^* - i\,\tau_{r\theta}^* = \sum_{m=-\infty}^{\infty} A_m e^{mi\theta} \qquad (1\text{-A-9})$$

The boundary stress condition permits the evaluation of the coefficients A_m's. Equations (1-A-6) through (1-A-9) are used to evaluate a_m's and b_m's which are used to form the harmonic functions $\phi(z)$ and $X(z)$.

APPENDIX B

SOLUTION TO THE PROBLEM OF A CIRCULAR BOREHOLE IN AN INFINITE ELASTIC MEDIUM UNDER LOADING SYMMETRICAL WITH RESPECT TO TWO PERPENDICULAR AXES

Earlier, the method of complex variables in elasticity was presented. In engineering, there are many two-dimensional boundary-value problems in elasticity that involve circular openings subject to loadings which are symmetrical with respect to two perpendicular axes. For these problems, the solution to the biharmonic equation can be found without using the complex variable method. The polar coordinate system will be used.

The biharmonic equation is rewritten as:

$$\nabla^4 \Psi(r,\theta) = 0 \qquad \text{(1-A-10)}$$

where ∇^2 is the Laplacian operator:

$$\nabla^2 = \left(\frac{\partial^2}{\partial r^2} + \frac{1}{r}\frac{\partial}{\partial r} + \frac{1}{r^2}\frac{\partial^2}{\partial \theta^2}\right), \text{ and } \nabla^4 = \nabla^2\left(\nabla^2\right)$$

The expressions for the stress components (1-A-1) in polar coordinates are rewritten as:

$$\sigma_r = \frac{1}{r}\frac{\partial \Psi}{\partial r} + \frac{1}{r^2}\frac{\partial^2 \Psi}{\partial \theta^2}$$

$$\sigma_\theta = \frac{\partial^2 \Psi}{\partial r^2}$$

$$\tau_{r\theta} = -\frac{\partial}{\partial r}\left(\frac{1}{r}\frac{\partial \Psi}{\partial \theta}\right) \qquad \text{(1-A-11)}$$

For problems with two perpendicular axes of symmetry, the solutions include only terms of even multiples of the angle θ. The stress function $\Psi(r, \theta)$ for a problem with a circular boundary has the term log r/R. The stress function $\Psi(r, \theta)$ has the following general form (Wianecki, 1968):

$$\Psi(r, \theta) = a_o \log \frac{r}{R} + \sum_{m=1}^{\infty} f_m(r) \cos 2m\theta \qquad (1\text{-A-12})$$

where

a_o = a suitable coefficient

$f_m(r)$ = a function of r only

Applying the biharmonic operator ∇^4 on $\Psi(r, \theta)$ which is defined by the Equation (1-A-12), one obtains:

$$\nabla^4\Psi(r, \theta) = \sum_{m=1}^{\infty} \left(\frac{d^2}{dr^2} + \frac{1}{r}\frac{d}{dr} - \frac{1}{r^2} 4m^2 \right) f_m(r) \cos 2m\theta = 0 \qquad (1\text{-A-13})$$

From the Equation (1-A-13), the solution for $f_m(r)$ is obtained:

$$f_m(r) = a_{2m} r^{-2m} + b_{2m} r^{-2m+2} + C_{2m} r^{2m} + d_{2m} r^{2m+2} \qquad (1\text{-A-14})$$

The assumption of "no-stress" at infinity, i.e., zero in situ stress field, requires $C_{2m} = d_{2m} = 0$. The Equation (1-A-12) becomes:

$$\Psi(r, \theta) = a_o \log \frac{r}{R} + \sum_{m=1}^{\infty} \left(a_{2m} r^{-2m} + b_{2m} r^{-2m+2} \right) \cos 2m\theta \qquad (1\text{-A-15})$$

The constants a_o, a_{2m}, and b_{2m} are uniquely determined by the given boundary conditions, either as the condition of boundary stresses or as the condition of boundary displacements. The stress distribution is obtained by

substituting stress function $\Psi(r, \theta)$ given by the Equation (1-A-15) into the Equation (1-A-11) (Wianecki, 1968):

$$\sigma_r = \frac{a_o}{r^2} - 2\sum_{m=1}^{\infty} \left\{ m(2m+1)\, a_{2m} r^{-2m+2} + (m+1)(2m-1)\, b_{2m} r^{-2m} \right\} \cos 2m\theta \qquad (1\text{-A-16a})$$

$$\sigma_\theta = \frac{a_o}{r^2} + 2\sum_{m=1}^{\infty} \left\{ m(2m+1)\, a_{2m} r^{-2m-2} + (m-1)(2m-1)\, b_{2m} r^{-2m} \right\} \cos 2m\theta \qquad (1\text{-A-16b})$$

$$\tau_{r\theta} = -2\sum_{m=1}^{\infty} \left\{ m(2m+1)\, a_{2m} r^{-2m-2} + m(2m-1)\, b_{2m} r^{-2m} \right\} \sin 2m\theta \qquad (1\text{-A-16c})$$

The strains are obtained from the stresses, using Hooke's law:

$$\varepsilon_r = \frac{\partial u}{\partial r} = \frac{1}{E}(\sigma_r - \nu\sigma_\theta)$$

$$\varepsilon_\theta = \frac{u}{r} + \frac{1}{r}\frac{\partial v}{\partial \theta} = \frac{1}{E}(\sigma_\theta - \nu\sigma_r)$$

$$\gamma_{r\theta} = \frac{1}{r}\frac{\partial v}{\partial r} - \frac{v}{r} = \frac{2(1+\nu)}{E}\tau_{r\theta} \qquad (1\text{-A-17})$$

where

ε_r, ε_θ, $r_{r\theta}$ = radial, circumferential, and shear strains

u, ν = radial and circumferential displacements.

When the displacements are needed, they can be computed from the Equations (1-A-17).

Along the boundary, $\rho = \frac{R}{r} = 1$, the stress distribution given by the Equations (1-A-16) is equal to the applied boundary stresses:

$$\sigma_r^* = \frac{a_o}{R^2} - 2\sum_{m-1}^{\infty} \left\{ m(2m+1)\, a_{2m} R^{-2m-2} + (m+1) b_{2m} R^{-2m} \right\} \cos 2m\theta \qquad (1\text{-A-18a})$$

$$\tau_{r\theta}^* = -2\sum_{m-1}^{\infty} \left\{ m(2m+1)\, a_{2m} R^{-2m-2} + m(2m-1)\, b_{2m} R^{-2m} \right\} \sin 2m\theta \qquad (1\text{-A-18b})$$

The applied boundary stresses can be expressed as Fourier series:

$$\sigma_r^*(\theta) = A_o + \sum_{m-1}^{\infty} A_{2m} \cos 2m\theta \qquad (1\text{-A-19a})$$

$$\tau_{r\theta}^*(\theta) = \sum_{m-1}^{\infty} B_{2m} \sin 2m\theta \qquad (1\text{-A-19b})$$

where

$$A_o = \frac{1}{2\pi} \int_{-\pi}^{\pi} \sigma_r^*(\theta)\, d\theta$$

$$A_{2m} = \frac{1}{\pi} \int_{-\pi}^{\pi} \sigma_{r\theta}^*(\theta) \cos 2m\theta\, d\theta \qquad (1\text{-A-20})$$

$$B_{2m} = \frac{1}{\pi} \int_{-\pi}^{\pi} \tau_{r\theta}^*(\theta) \sin 2m\theta\, d\theta$$

Comparing the Equations (1-A-18) to the Equations (1-A-19), one obtains:

$$a_o = A_o R^2$$

$$a_{2m} = \frac{mA_{2m} - (m + 1) B_{2m}}{2m(2m + 1)} R^{2m+2}$$

$$b_{2m} = \frac{B_{2m} - A_{2m}}{2(2m - 1)} R^{2m} \qquad \text{(1-A-21)}$$

Adding the Equations (1-A-16a) and (1-A-16b) a useful relationship is derived:

$$\sigma_r + \sigma_\theta = - \sum_{m-1}^{\infty} 4(2m - 1) b_{2m} r^{-2m} \cos 2m\theta$$

$$= - \sum_{m-1}^{\infty} 2(B_{2m} - A_{2m}) \rho^{2m} \cos 2m\theta \qquad \text{(1-A-22)}$$

APPENDIX C

THE GENERAL PROBLEM OF UNIDIRECTIONAL BOUNDARY STRESS VARYING ACROSS THE WIDTH OF THE BEARING PLATE

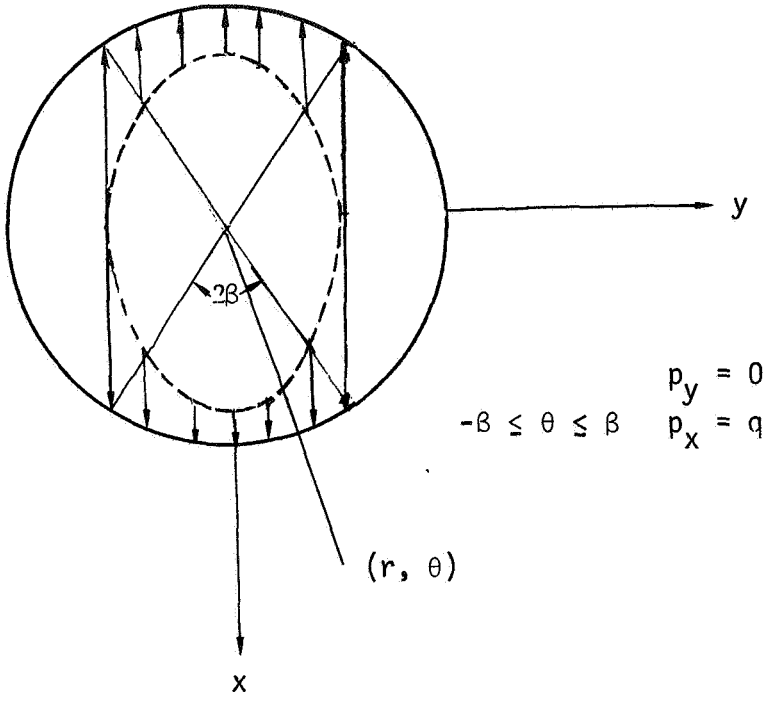

$$-\beta \le \theta \le \beta \qquad p_y = 0, \quad p_x = q\left\{k-(k-1)\cos\frac{\pi\theta}{2\beta}\right\}$$

Boundary condition at $\rho = 1$

$$-\beta \le \theta \le \beta \begin{cases} \sigma_r^* = q\left\{k-(k-1)\cos\dfrac{\pi\theta}{2\beta}\right\}\cos\theta \\ \tau_{r\theta}^* = q\left\{k-(k-1)\cos\dfrac{\pi\theta}{2\beta}\right\}\sin\theta \end{cases} \qquad (1\text{-A-}23)$$

1. The Solution

The problem can be divided into two simpler problems, with the boundary stress distribution ($-\beta < \theta < \beta$) given by:

$$A \begin{cases} \sigma_r^* = kq\cos\theta \\ \tau_{r\theta}^* = -kq\sin\theta \end{cases} \qquad (1\text{-A-}24)$$

where σ_r^*, $\tau_{r\theta}^*$ = applied normal and shear stresses on the boundary.

$$B \begin{cases} \sigma_r^* = -(k+1)\, q \cos \frac{\pi\theta}{2\beta} \cos\theta \\ \tau_{r\theta}^* = (k-1)\, q \cos \frac{\pi\theta}{2\beta} \sin\theta \end{cases} \qquad (1\text{-A-}25)$$

a. Solution to Problem A

The Fourier series representation of the boundary stresses has the following coefficients:

$$A_o = \frac{1}{2\pi} \int_{-\pi}^{\pi} \sigma_r^*(\theta)\, d\theta$$

$$= \frac{2kq}{\pi} \sin\beta \qquad (1\text{-A-}26a)$$

$$A_{2m} = \frac{1}{\pi} \int_{-\pi}^{\pi} \sigma_r^*(\theta) \cos 2m\theta\, d\theta$$

$$= \frac{2kq}{\pi} \left\{ \frac{\sin(2m-1)\beta}{2m-1} + \frac{\sin(2m+1)\beta}{2m+1} \right\} \qquad (1\text{-A-}26b)$$

$$B_{2m} = \frac{1}{\pi} \int_{-\pi}^{\pi} \tau_{r\theta}^*(\theta) \sin 2m\theta\, d\theta$$

$$= \frac{2kq}{\pi} \left\{ \frac{\sin(2m+1)\beta}{2m+1} - \frac{\sin(2m-1)\beta}{2m-1} \right\} \qquad (1\text{-A-}26c)$$

Using the Equations (1-A-21) and (1-A-26), one obtains:

$$a_o = \frac{2kq}{\pi} R^2 \sin \beta$$

$$a_{2m} = \frac{kqR^{2m+2}}{m\pi} \left\{ \frac{\sin (2m - 1) \beta}{2m - 1} - \frac{\sin (2m + 1) \beta}{(2m + 1)^2} \right\}$$

$$b_{2m} = - \frac{2kq R^{2m}}{(2m - 1)^2} \sin (2m - 1) \beta \qquad \text{(1-A-27)}$$

The stress distribution is obtained by substituting Equations (1-A-27) into Equations (1-A-16):

$$\sigma_{rA} \frac{\pi}{2kq} = \rho^2 \sin \beta + \sum_{m=1}^{\infty} \rho^{2m} \left\{ \frac{[-(2m + 1) \rho^2 + 2m + 2]}{2m - 1} \sin (2m - 1) \beta \right.$$

$$\left. + \frac{\rho^2}{2m + 1} \sin (2m + 1) \beta \right\} \cos 2m\theta \qquad \text{(1-A-28a)}$$

$$\sigma_{\theta A} \frac{\pi}{2kq} = -\rho^2 \sin \beta + \sum_{m=1}^{\infty} \rho^{2m} \left\{ \frac{[-(2m + 1) \rho^2 - 2m + 2]}{2m - 1} \sin (2m - 1) \beta \right.$$

$$\left. - \frac{\rho^2}{2m + 1} \sin (2m + 1) \beta \right\} \cos 2m\theta \qquad \text{(1-A-28b)}$$

$$\tau_{r\theta A} \frac{\pi}{2kq} = \sum_{m=1}^{\infty} \rho^{2m} \left\{ \frac{[1-(2m + 1) \rho^2]}{2m + 1} \sin (2m - 1) \beta \right.$$

$$\left. + \frac{\rho^2}{2m + 1} \sin (2m + 1) \beta \right\} \sin 2m\theta \qquad \text{(1-A-28c)}$$

where $\rho = \frac{R}{r}$, radius/radial distance.

b. Solution to Problem B

Steps similar to those for Problem A are taken and the results are presented without repeating the explanation:

For $\frac{\pi}{\beta} - 2 \neq 0$,

$$A_o = - \frac{4(k - 1)\, q \cos \beta}{\beta (\frac{\pi}{\beta} + 2)\ (\frac{\pi}{\beta} - 2)} \qquad \text{(1-A-29a)}$$

For $\frac{\pi}{\beta} - 2 = 0$,

$$A_o = - \frac{(k - 1)\, q\, \beta}{\pi} \qquad \text{(1-A-29b)}$$

For $(\frac{\pi}{\beta} - 4m - 2)\ (\frac{\pi}{\beta} - 4m + 2) \neq 0$,

$$A_{2m} = - \frac{4(k - 1)\, q}{\pi} \left\{ \frac{\cos\ (2m + 1)\, \beta}{(\frac{\pi}{\beta} + 4m + 2)\ (\frac{\pi}{\beta} - 4m - 2)} \right.$$

$$\left. + \frac{\cos\ (2m - 1)\, \beta}{(\frac{\pi}{\beta} + 4m - 2)\ (\frac{\pi}{\beta} - 4m + 2)} \right\} \qquad \text{(1-A-29c)}$$

$$B_{2m} = - \frac{4(k - 1)q}{\beta} \left\{ \frac{\cos\ (2m - 1)\, \beta}{(\frac{\pi}{\beta} + 4m + 2)\ (\frac{\pi}{\beta} - 4m - 2)} - \frac{\cos\ (2m - 1)\, \beta}{(\frac{\pi}{\beta} + 4m - 2)\ (\frac{\pi}{\beta} - 4m + 2)} \right\}$$

(1-A-29d)

$$a_o = - \frac{4(k - 1)\, R^2 \cos \beta}{\beta (\frac{\pi}{\beta} + 2)\ (\frac{\pi}{\beta} - 2)} \qquad \text{(1-A-30a)}$$

$$a_{2m} = \frac{2(k-1)\, q\, R^{2m+2}}{m(2m+1)} \left\{ \frac{\cos\,(2m+1)\,\beta}{(\frac{\pi}{\beta} + 4m + 2)\,(\frac{\pi}{\beta} - 4m - 2)} \right.$$

$$\left. - \frac{(2m+1)\,\cos\,(2m-1)\,\beta}{(\frac{\pi}{\beta} + 4m - 2)\,(\frac{\pi}{\beta} - 4m + 2)} \right\} \qquad \text{(1-A-30b)}$$

$$b_{2m} = \frac{4(k-1)\, q\, R^{2m} \cos\,(2m-1)\,\beta}{(2m-1)\,\beta(\frac{\pi}{\beta} + 4m - 2)\,(\frac{\pi}{\beta} - 4m + 2)} \qquad \text{(1-A-30c)}$$

The stress distribution is given by:*

$$\sigma_{rB} \frac{\beta}{4(k-1)\, q} = -\frac{\rho^2 \cos\,\beta}{(\frac{\pi}{\beta} + 2)\,(\frac{\pi}{\beta} - 2)} + \sum_{m=1}^{\infty} \rho^{2m} \left\{ \frac{[(2m+1)\,\rho^2 - 2m - 2]}{(\frac{\pi}{\beta} + 4m - 2)\,(\frac{\pi}{\beta} - 4m + 2)} \right.$$

$$\left. \cos\,(2m-1)\,\beta - \frac{\rho^2 \cos\,(2m+1)\,\beta}{(\frac{\pi}{\beta} + 4m + 2)\,(\frac{\pi}{\beta} - 4m - 2)} \right\} \cos\,2m\theta$$

(1-A-31a)

---

*For all the expressions in Problem B:

When $(\frac{\pi}{\beta} - 4m - 2) = 0$, replaces the expression

$$\frac{\cos\,(2m+1)\,\beta}{(\frac{\pi}{\beta} + 4m + 2)\,(\frac{\pi}{\beta} - 4m - 2)} \text{ by } \frac{\beta}{4\pi}$$

When $(\frac{\pi}{\beta} - 4m + 2) = 0$ replaces the expression

$$\frac{\cos\,(2m-1)\,\beta}{(\frac{\pi}{\beta} + 4m - 2)\,(\frac{\pi}{\beta} - 4m + 2)} \text{ by } \frac{\beta}{4\pi}$$

$$\sigma_{\theta B}\,\frac{\beta}{4(k-1)\,q} = \frac{\rho^2\cos\beta}{(\frac{\pi}{\beta}+2)\,(\frac{\pi}{\beta}-2)} + \sum_{m=1}^{\infty}\rho^{2m}\left\{\frac{[2m-2-(2m+1)\,\rho^2]}{(\frac{\pi}{\beta}+4m-2)\,(\frac{\pi}{\beta}-4m+2)}\right.$$

$$\left.\cos\,(2m-1)\,\beta + \frac{\rho^2\cos\,(2m+1)\,\beta}{(\frac{\pi}{\beta}+4m+2)\,(\frac{\pi}{\beta}-4m-2)}\right\}\cos\,2m\theta$$

(1-A-31b)

$$\tau_{r\theta B}\,\frac{\beta}{4(k-1)\,q} = \sum_{m=1}^{\infty} m\rho^{2m}\left\{\frac{[(2m+1)\,\rho^2-2m]}{(\frac{\pi}{\beta}+4m-2)\,(\frac{\pi}{\beta}-4m+2)}\cos\,(2m-1)\,\beta\right.$$

$$\left.-\frac{\rho^2\cos\,(2m+1)\,\beta}{(\frac{\pi}{\beta}+4m+2)\,(\frac{\pi}{\beta}-4m-2)}\right\}\sin\,2m\theta \qquad \text{(1-A-31c)}$$

The net stress distribution is obtained by adding Equations (1-A-28) and (1-A-31):

$$\sigma_r = \sigma_{rA} + \sigma_{rB}$$

$$\sigma_\theta = \sigma_{\theta A} + \sigma_{\theta B}$$

$$\tau_{r\theta} = \tau_{r\theta A} + \tau_{r\theta B} \qquad \text{(1-A-32)}$$

Along the edge of the opening, $\rho = 1$, the circumferential stress σ_θ is given by:

Inside the arc AB (along the loaded area):

$$\sigma_\theta = -\left\{k-(k-1)\cos\frac{\pi\theta}{2\beta}\right\}q\cos\theta + \sum_{m=1}^{\infty}8q\left\{\frac{k\sin\,(2m-1)\,\beta}{(2m-1)\,\pi}\right.$$

$$\left.-\frac{2(k-1)\cos\,(2m-1)\beta}{\beta(\frac{\pi}{\beta}+4m-2)\,(\frac{\pi}{\beta}-4m+2)}\right\}\cos\,2m\theta \qquad \text{(1-A-33a)}$$

Along the unloaded areas:

$$\sigma_\theta = \sum_{m=1}^{\infty} 8q \left\{ \frac{k \sin (2m - 1)\beta}{(2m - \nu \pi} \right.$$

$$\left. - \frac{2(k - 1) \cos (2m - 1)\beta}{\beta(\frac{\pi}{\beta} + 4m - 2)(\frac{\pi}{\beta} - 4m + 2)} \right\} \cos 2m\theta \qquad (1\text{-A-33b})$$

Due to the presence of the boundary shear stress $\tau^*_{r\theta}$ along the arc AB, the circumferential stress σ_θ given by Equation (1-A-33a) is not a principal stress component; σ_θ given by Equation (1-A-33b) is a principal stress component.

The total load P exerted by the bearing plate against the wall of the borehole in the x-direction is given by (Figure 1-13b):

$$P = \int_{-\beta}^{\beta} p_x R \cos\theta \, d\theta$$

$$= \left\{ 2k \sin\beta - \frac{4(k - 1) \pi \cos\beta}{\beta(\frac{\pi}{\beta} + 2)(\frac{\pi}{\beta} - 2)} \right\} Rq = MRq \qquad (1\text{-A-34})$$

The circumferential stress $(\sigma_\theta)_{p=1}$ can be more conveniently expressed in terms of the total load P:

$$(\sigma_\theta)_{p=1} = K_I (k, \beta, \theta) \frac{P}{R} \qquad (1\text{-A-35})$$

where in the arc AB (the loaded area):

$$K_I\ (k,\beta,\theta) = \frac{1}{M}\left[-\left\{ k - (k-1)\cos\frac{\pi\theta}{2\beta}\ \cos\theta + \sum_{m=1}^{\infty} 8\left\{ \frac{k \sin (2m-1)\beta}{(2m-1)\pi} - \frac{2(k-1)\cos(2m-1)\beta}{\beta(\frac{\pi}{\beta}+4m-2)\ (\frac{\pi}{\beta}-4m+2)} \right\} \cos 2m\theta \right] \right. \qquad \text{(1-A-36a)}$$

and outside the arcs AB and A'B' (the unloaded areas):

$$K_I\ (k,\beta,\theta) = \frac{1}{M} \sum_{m=1}^{\infty} \left\{ \frac{k \sin (2m-1)\beta}{(2m-1)\pi} - \frac{2(k-1)\cos(2m-1)\beta}{\beta(\frac{\pi}{\beta}+4m-2)\ (\frac{\pi}{\beta}-4m+2)} \right\} \cos 2m\theta \qquad \text{(1-A-36b)}$$

where $$M = \left\{ 2k \sin\beta - \frac{4(k-1)\pi\cos\beta}{\beta(\frac{\pi}{\beta}+2)\ (\frac{\pi}{\beta}-2)} \right\}$$

APPENDIX D

THE GENERAL PROBLEM OF UNIDIRECTIONAL PRINCIPAL BOUNDARY STRESS VARYING ACROSS THE WIDTH OF THE BEARING PLATES

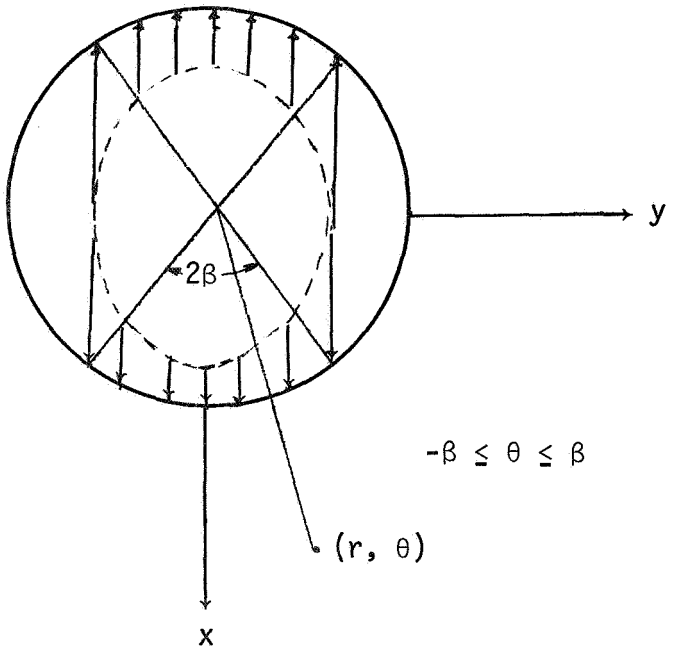

$$\sigma_y = 0$$

$$-\beta \le \theta \le \beta \qquad \sigma_x = q\left\{k - (k-1)\cos\frac{\pi\theta}{2\beta}\right\}$$

Boundary Condition at $\rho = 1$

$$\tau_{xy} = 0$$

$$-\beta \le \theta \le \beta \begin{cases} \sigma_r^* = \frac{q}{2}\left\{k - (k-1)\cos\frac{\pi\theta}{2\beta}\right\}(1 + \cos 2\theta) \\ \tau_{re}^* = -\frac{q}{2}\left\{k - (k-1)\cos\frac{\pi\theta}{2\beta}\right\}\sin 2\theta \end{cases} \qquad (1\text{-A-}37)$$

The Solutions

The problem can be divided into four simpler problems (C, D, E, F), with the boundary stress distribution ($-\beta < \theta < \beta$) given by:

$$\left.\begin{aligned} \sigma_r^* &= \frac{kq}{2} \\ \tau_{re}^* &= 0 \end{aligned}\right\} \text{ Problem C} \qquad (1\text{-A-}38)$$

$$\left.\begin{aligned} \sigma_r^* &= -\frac{(k-1)}{2} q \cos\frac{\pi\theta}{2\beta} \\ \tau_{r\theta}^* &= 0 \end{aligned}\right\} \text{ Problem D} \qquad \text{(1-A-39)}$$

$$\left.\begin{aligned} \sigma_r^* &= \frac{kq}{2}\cos 2\theta \\ \tau_{r\theta}^* &= \frac{kq}{2}\sin 2\theta \end{aligned}\right\} \text{ Problem E} \qquad \text{(1-A-40)}$$

$$\left.\begin{aligned} \sigma_r^* &= \frac{-(k-1)}{2} q \cos\frac{\pi\theta}{2\beta}\cos 2\theta \\ \tau_{r\theta} &= \frac{(k-1)}{2} q \cos\frac{\pi\theta}{2\beta}\sin 2\theta \end{aligned}\right\} \text{ Problem F} \qquad \text{(1-A-41)}$$

Solution to Problem C.

Problem C has been solved by the complex variable method (Van, 1967). The stress distribution is given by:

$$\sigma_\theta \frac{2\pi}{kq} = -2\beta\rho^2 + \sum_{m=1}^{\infty} \frac{\rho^{2m}}{m} (m\rho^2 - m + 1) \sin 2m\beta \cos 2m\theta \qquad \text{(1-A-42a)}$$

$$\sigma_r \frac{2\pi}{kq} = 2\beta\rho^2 + \sum_{m=1}^{\infty} \frac{\rho^2}{m} (m + 1 - mm\rho^2) \sin 2m\beta \cos 2m\theta \qquad \text{(1-A-42b)}$$

$$\tau_{r\theta} \frac{2\pi}{kq} = 2(1-\rho^2) \sum_{m=1}^{\infty} \rho^2 \text{ sim } 2m\beta \sin 2m\theta \qquad \text{(1-A-42c)}$$

Solution to Problem D.

All the steps used to solve Problems A and B are repeated here without repeated explanation:**

$$A_o = - \frac{2(k - 1)\ \beta q}{\pi^2}$$

$$A_{2m} = - \frac{4(k - 1)\ q}{\beta(\frac{\pi}{\beta} + 4m)\ (\frac{\pi}{\beta} - 4m)} \cos 2m\ \beta$$

$$B_{2m} = 0 \qquad \text{(1-A-43}$$

$$a_o = - \frac{2(k - 1)\ \beta q\ R^2}{\pi^2}$$

$$a_{2m} = - \frac{2(k - 1)\ q \cos 2m\ \beta}{(2m - 1)\ \ \beta(\frac{\pi}{\beta} + 4m)\ (\frac{\pi}{\beta} - 4m)} R^{2m+2}$$

$$b_{2m} = \frac{2(k - 1)\ q \cos 2m\ \beta}{(2m - 1)\ \ \beta(\frac{\pi}{\beta} + 4m)\ (\frac{\pi}{\beta} - 4m)} R^{2m} \qquad \text{(1-A-44)}$$

** When $(\frac{\pi}{\beta} - 4m) = 0$, replace $\frac{\cos 2m\ \beta}{(\frac{\pi}{\beta} + 4m)\ (\frac{\pi}{\beta} - 4m)}$ by $\frac{\beta}{4\pi}$

When $(\frac{\pi}{\beta} - 4m + 4) = 0$, replace $\frac{\cos 2(m - 1)\ \beta}{(\frac{\pi}{\beta} + 4m - 4)\ (\frac{\pi}{\beta} - 4m + 4)}$ by $\frac{\beta}{4\pi}$

When $(\frac{\pi}{\beta} - 4m - 4) = 0$, replace $\frac{\cos 2(m + 1)\ \beta}{(\frac{\pi}{\beta} + 4m + 4)\ (\frac{\pi}{\beta} - 4m - 4)}$ by $\frac{\beta}{4\pi}$

The stress distribution is given by:

$$\sigma_{rD} = -\frac{2(k-1)\,\beta q\,\rho^2}{\pi^2} + \sum_{m=1}^{\infty} -\frac{8(k-1)\,q\rho^{2m}\,[-m\rho^2 + m + 1]}{\beta(\frac{\pi}{\beta} + 4m)\,(\frac{\pi}{\beta} - 4m)}$$

$$\times \cos 2m\beta \cos 2m\theta \qquad \text{(1-A-45a)}$$

$$\sigma_{\theta D} = \frac{2(k-1)\,\beta\, q\,\rho^2}{\pi^2} + \sum_{m=1}^{\infty} -\frac{8(k-1)\,q\,\rho^{2m}\,(m\rho^2 - m + 1)}{\beta(\frac{\pi}{\beta} + 4m)\,(\frac{\pi}{\beta} - 4m)}$$

$$\times \cos 2m\beta \cos 2m\theta \qquad \text{(1-A-45b)}$$

$$\tau_{r\theta D} = \sum_{m=1}^{\infty} -\frac{8m\,\rho^{2m}\,(k-1)\,(1-\rho^2)\,q}{\beta(\frac{\pi}{\beta} + 4m)\,(\frac{\pi}{\beta} - 4m)} \cos 2m\,\beta \sin 2m\theta \qquad \text{(1-A-45c)}$$

Solution to Problem E.

$$A_o = \frac{kq}{2\beta} \sin 2\beta$$

$$A_2 = \frac{kq}{2\pi} \left\{ 2\beta + \frac{1}{2} \sin 4\beta \right\}$$

$$B_2 = -\frac{kq}{2\pi} \left\{ 2\beta - \frac{1}{2} \sin 4\beta \right\} \qquad \text{(1-A-46a)}$$

$m \geq 2$

$$A_{2m} = \frac{kq}{2\pi} \left\{ \frac{\sin 2(m+1)\,\beta}{m+1} + \frac{\sin 2(m-1)\,\beta}{m-1} \right\}$$

$$B_{2m} = \frac{kq}{2\pi} \left\{ \frac{\sin 2(m+1)\,\beta}{m+1} - \frac{\sin 2(m-1)\,\beta}{m-1} \right\} \qquad \text{(1-A-46b)}$$

$$a_o = \frac{kq}{2\beta} R_2 \sin 2\beta$$

$$a_2 = \left\{ \frac{3kq}{\pi} \beta - \frac{kq}{4\pi} \sin 4\beta \right\} R^4$$

$$b_2 = - \frac{kq\beta}{\pi} R^2 \qquad \text{(1-A-47a)}$$

$\underline{m \geq 2}$

$$a_{2m} = - \frac{kq\ R^{2(m+1)}}{4m\ \pi\ (2m+1)} \left\{ \frac{\sin 2(m+1)\ \beta}{m+1} - \frac{2m+1}{m-1} \sin 2(m-1)\ \beta \right\}$$

$$b_{2m} = - \frac{k\ q\ R^{2m}}{2\pi\ (m-1)\ (2m-1)} \sin 2(m-1)\ \beta \qquad \text{(1-A-47b)}$$

The stress distribution is given by:

$$\sigma_{rE} = \frac{kq\ \rho^2}{2\beta} \sin 2\beta + \frac{kq}{\pi} \left\{ -18\beta\rho^2 + 4\beta\ \rho^2 + \frac{3\rho^4}{2} \sin 4\beta \right\}$$

$$\cos 2\theta + \sum \frac{kq\ \rho^{2m}}{2\pi} \left\{ \frac{\rho^2}{m+1} \sin 2(m+1)\ \beta \right.$$

$$\left. + \frac{[2m + 2 - (2m+1)\ \rho^2]}{m-1} \sin 2(m-1)\ \beta \right\} \cos 2m\theta \qquad \text{(1-A-48a)}$$

$$\sigma_{\theta E} = - \frac{kq\ \rho^2}{2\beta} \sin 2\beta + \frac{kq\ \rho^4}{\pi} \left(18\beta - \frac{3}{2} \sin 4\beta\right) \cos 2\theta$$

$$+ \sum_{m=2}^{\infty} \frac{kq\rho^{2m}}{2\pi} \left\{ - \frac{\rho^2}{m+1} \sin 2(m+1)\ \beta + \frac{[-2m + 2 + (2m+1)\ \rho^2]}{m-1} \right.$$

$$\left. \times \sin 2(m-1)\ \beta \right\} \cos 2m\theta \qquad \text{(1-A-48b)}$$

$$\tau_{r\theta E} = \frac{kq}{\pi}\left\{-18\beta\,\rho^4 + \frac{3}{2}\rho^4 \sin 4\beta + 2\beta\,\rho^2\right\}\sin 2\theta$$

$$+\sum_{m=2}^{\infty}\frac{kq\rho^{2m}}{2\pi}\left\{\frac{\rho^2}{m+1}\sin 2(m+1)\,\beta\right.$$

$$\left.+\frac{[m-(2m+1)\,\rho^2]}{m-1}\sin 2(m-1)\,\beta\right\}\sin 2m\theta \qquad (1\text{-A-48c})$$

Solution to Problem F.

$$A_o = -\frac{2(k-1)\,q}{\beta(\frac{\pi}{\beta}+4)\,(\frac{\pi}{\beta}-4)}\cos 2\beta$$

$$A_{2m} = -\frac{2(k-1)\,q}{\beta}\left\{\frac{\cos 2(m+1)\,\beta}{(\frac{\pi}{\beta}+4m+4)\,(\frac{\pi}{\beta}-4m-4)}+\frac{\cos 2(m+1)\,\beta}{(\frac{\pi}{\beta}+4m-4)\,(\frac{\pi}{\beta}-4m+4)}\right\}$$

$$B_{2m} = \frac{2(k-1)\,q}{\beta}\left\{\frac{\cos 2(m-1)\,\beta}{(\frac{\pi}{\beta}+4m-4)\,(\frac{\pi}{\beta}-4m+4)}-\frac{\cos 2(m+1)\,\beta}{(\frac{\pi}{\beta}+4m+4)\,(\frac{\pi}{\beta}-4m-4)}\right\}$$

$$a_o = -\frac{2(k-1)\,q\,R^2\cos 2\beta}{\beta(\frac{\pi}{\beta}+4)\,(\frac{\pi}{\beta}-4} \qquad (1\text{-A-49})$$

$$a_{2m} = \frac{(k-1)\,q\,R^{2m+2}}{m\beta}\left\{\frac{\cos 2(m+1)\,\beta}{(2m+1)\,(\frac{\pi}{\beta}+4m+4)\,(\frac{\pi}{\beta}-4m-4)}\right.$$

$$\left.-\frac{\cos 2(m-1)\,\beta}{(\frac{\pi}{\beta}+4m-4)\,(\frac{\pi}{\beta}-4m+4)}\right\}$$

$$b_{2m} = \frac{2(k-1)\,q\,R^{2m}\cos 2(m-1)\,\beta}{(2m-1)\,\beta\,(\frac{\pi}{\beta}+4m-4)\,(\frac{\pi}{\beta}-4m+4)} \qquad (1\text{-A-50})$$

The stress distribution is given by:

$$\sigma_{rF} = -\frac{2(k-1)\, q\rho^2 \cos 2\beta}{\beta(\frac{\pi}{\beta}+4)(\frac{\pi}{\beta}-4)} + \sum_{m=1}^{\infty} \frac{2(k-1)\, q\rho^{2m}}{\beta} \times$$

$$\left\{ \frac{-\rho^2 \cos 2(m+1)\beta}{(\frac{\pi}{\beta}+4m+4)(\frac{\pi}{\beta}-4m-4)} + \frac{[(2m+1)\rho^2 - 2m - 2]\cos 2(m-1)\beta}{(\frac{\pi}{\beta}+4m-4)(\frac{\pi}{\beta}-4m+4)} \right\}$$

$$\times \cos 2m\theta \qquad \text{(1-A-51a)}$$

$$\sigma_{\theta F} = \frac{2(k-1)\, q\rho^2 \cos 2\beta}{\beta(\frac{\pi}{\beta}+4)(\frac{\pi}{\beta}-4)} + \sum_{m=1}^{\infty} \frac{2(k-1)\, q\rho^{2m}}{\beta} \times$$

$$\left\{ \frac{\rho^2 \cos 2(m+1)\beta}{(\frac{\pi}{\beta}+4m+4)(\frac{\pi}{\beta}-4m-4)} + \frac{[2m - 2 - (2m+1)\rho^2]\cos 2(m-1)\beta}{(\frac{\pi}{\beta}+4m-4)(\frac{\pi}{\beta}-4m+4)} \right\}$$

$$\times \cos 2m\theta \qquad \text{(1-A-51b)}$$

$$\tau_{r\theta F} = \sum_{m=1}^{\infty} \frac{2(k-1)\, q\rho^{2m}}{\beta} \left\{ -\frac{\rho^2 \cos 2(m+1)\beta}{(\frac{\pi}{\beta}+4m+4)(\frac{\pi}{\beta}-4m-4)} \right.$$

$$\left. + \frac{[(2m+1)\rho^2 - 2m]\cos 2(m-1)\beta}{(\frac{\pi}{\beta}+4m-4)(\frac{\pi}{\beta}-4m+4)} \right\} \sin 2m\theta \qquad \text{(1-A-51c)}$$

The net stress distribution is obtained by summing the results of the four elemental problems, (C, D, E, and F):

$$\sigma_r = \sigma_{rC} + \sigma_{rD} + \sigma_{rE} + \sigma_{rF}$$

$$\sigma_\theta = \sigma_{\theta C} + \sigma_{\theta D} + \sigma_{\theta E} + \sigma_{\theta F}$$

$$\tau_{r\theta} = \tau_{r\theta C} + \tau_{r\theta D} + \tau_{r\theta E} + \tau_{r\theta F} \qquad (1\text{-A-}52)$$

Along the edge of the borehole, $\rho = 1$, in the arc AB ($-\beta < \theta < \beta$) the circumferential stress σ_θ is not a principal stress, due to the presence of the shear component $\tau^*_{r\theta}$. Its distribution is given by:

$$\sigma_\theta = \left(\frac{1}{2} - \frac{2\beta}{\pi}\right) kq + \frac{4(k-1)\,\beta q}{\pi 2} + \left(\frac{4k\,\beta}{\pi} - \frac{k}{2}\right) q \cos 2\theta$$

$$- \frac{(k-1)}{2} q \cos \frac{\pi\theta}{2\beta} + \frac{(k-1)}{2} q \cos \frac{\pi\theta}{2\beta} \cos 2\theta$$

$$+ \sum_{m=2}^{\infty} \frac{2kq}{(m-1)\,\pi} \sin 2(m-1)\,\beta \cos 2m\theta$$

$$- \sum_{m=1}^{\infty} \frac{8(k-1)\,q \cos 2(m-1)\,\beta}{\beta\left(\frac{\pi}{\beta} + 4m - 4\right)\left(\frac{\pi}{\beta} - 4m + 4\right)} \cos 2m\theta \qquad (1\text{-A-}53a)$$

Along the unloaded areas, σ_θ is the principal stress:

$$\sigma_\theta = -\frac{2\,kq\,\beta}{\pi} + \frac{4(k-1)\,\beta q}{\pi 2} + \frac{4\,kq\,\beta}{\pi}\cos 2\theta$$

$$+\sum_{m=2}^{\infty}\frac{2\,kq}{(m-1)\,\pi}\sin 2(m-1)\,\beta\cos 2m\theta$$

$$-\sum_{m=1}^{\infty}\frac{8(k-1)\,q\cos 2(m-1)\,\beta}{\beta\left(\frac{\pi}{\beta}+4m-4\right)\left(\frac{\pi}{\beta}-4m+4\right)}\cos 2m\theta \qquad \text{(1-A-53b)}$$

The total load exerted by the bearing plate against the wall of the borehole is given by:

$$P = \int_{-\beta}^{\beta}\sigma_x R\cos\theta d\theta$$

$$= \left\{2k\sin\beta - \frac{4(k-1)\,\pi\cos\beta}{\beta\left(\frac{\pi}{\beta}+2\right)\left(\frac{\pi}{\beta}-2\right)}\right\} Rq$$

$$= MRq \qquad \text{(1-A-54)}$$

The circumferential stress given by Equation (1-A-52) can more conveniently be expressed in terms of the total load P:

$$(\sigma_\theta)_{\rho=1} = K_{II}\,(k,\,\beta,\,\theta)\,\frac{P}{R} \qquad \text{(1-A-55)}$$

where:

In the arc AB (loaded area):

$$K_{II}(k, \beta, \theta) = \frac{1}{M}\left[\frac{k}{2} - \frac{2k\beta}{\pi} + \frac{4(k-1)\beta}{\pi 2}\right.$$

$$+ \left(\frac{4\beta}{\pi} - \frac{1}{2}\right) k \cos 2\theta - \frac{(k-1)}{2} \cos \frac{\pi\theta}{2\beta}$$

$$+ \frac{(k-1)}{2} \cos \frac{\pi\theta}{2\beta} \cos 2\theta + \sum_{m=2}^{\infty} \frac{2k}{(m-1)\pi}$$

$$\times \sin 2(m-1)\beta \cos 2m\theta$$

$$\left. - \sum_{m=1}^{\infty} \frac{8(k-1) \cos 2(m-1)\beta \cos 2m\theta}{\beta\left(\frac{\pi}{\beta} + 4m - 4\right)\left(\frac{\pi}{\beta} + 4m + 4\right)}\right] \qquad (1\text{-A-}56a)$$

In the arcs A'B and AB' (unloaded areas):

$$K_{II}(k, \beta, \theta) = \frac{1}{M}\left[-\frac{2k\beta}{\pi} + \frac{4(k-1)\beta}{\pi^2} + \frac{4k\beta}{\pi} \cos 2\theta\right.$$

$$\left. + \sum_{m=2}^{\infty} \frac{2k \sin 2(m-1)\beta \cos 2m\theta}{(m-1)\pi} - \sum_{m=1}^{\infty} \frac{8(k-1) \cos 2(m-1)\beta \cos 2m\theta}{\beta\left(\frac{\pi}{\beta} + 4m - 4\right)\left(\frac{\pi}{\beta} - 4m + 4\right)}\right]$$

where

$$M = \left\{2k \sin \beta - \frac{4(k-1)\pi \cos \beta}{\beta\left(\frac{\pi}{\beta} + 2\right)\left(\frac{\pi}{\beta} - 2\right)}\right\} \qquad (1\text{-A-}56b)$$

CHAPTER 2

EXPERIMENTAL WORK RELATED TO BOREHOLE JACK PROBE AND TESTING

(K. Drozd and R. E. Goodman)

I. INTRODUCTION

This report describes model studies performed for the purpose of obtaining an independent, empirical determination of the load-deformation-strength relationship of a jack in a borehole. The model studies were performed to allow appropriate assumptions to be made in the mathematical solutions presented in Chapter 1 of this volume. Also, the tests clarified the actual mode of failure of rocks and soils under plate loading in a borehole. Three failure modes were postulated: (1) cracking in a tension zone created by the jack load, (2) shearing along a curved surface, and (3) indentation as a progressive shearing failure (punching). The relationship between observed load-deformation behavior during jack loading and basic deformation and failure parameters for soils and rocks was another object of the studies. Finally, we hoped through the experience of model testing to be in a better position to select a suitable method of testing for lunar expoloration and to propose a testing system.

This chapter is divided into three sections. The first section describes model borehole loading tests and reports the results. The second section describes model bearing capacity tests on the same materials used for the borehole loading tests. Finally, the third section compares the borehole jack results with the known bearing capacities to resolve the applicability of such test methods to bearing capacity design problems. A proposal for a new field prototype borehole jack is also given.

II. MODEL BOREHOLE LOADING TESTS

A. Description of Test Apparatus and Methods

The model studies attempted to reproduce the action of rigid plates forced against opposite walls of a borehole by pistons. In the laboratory the boreholes were three inches (7.6 cm) in diameter and arranged in a plate to represent a slice through the ground, as described subsequently. Figure 2-1 shows the test arrangement details, including the position of the jack-loaded rock plate on a rigid steel-base with a thick stiffened plexiglass sheet above. Figure 2-2 is a general view of the set-up. To reduce shearing stresses on the plane, a thin sheet of teflon was introduced between the steel base and the model plate. In some tests, a frame was circumscribed about the model plate to prevent prevent premature tensile failure. Also, in some cases a loading frame was introduced to superimpose a uniaxial stress of up to 4 kg/cm^2 in the plate (Figure 2-3).

The model borehole jack is a cylindrical hydraulic cylinder 5.1 cm long and 2.5 cm in diameter containing a circular piston 1.65 cm in diameter. The maximum piston stroke is 13 mm (0.5 inch). The jack delivers a load of up to 570 kg to the bearing plates. Four different sets of bearing plates were used (Figure 2-4). All had a radius of curvature of 38 mm (1-1/2 inches) to fit exactly against the borehole wall, but the plates had different angular widths and therefore different contact areas as follows:

Bearing Plate No.	Height (cm)	Projected Width (cm)	Contact Area (cm^2)	Projected Contact Area (cm^2)
I	3.8	1.27	4.85	4.85
II	3.8	2.54	9.90	9.70
III	3.8	5.23	21.70	19.90
IV	3.8	7.50	41.20	28.70

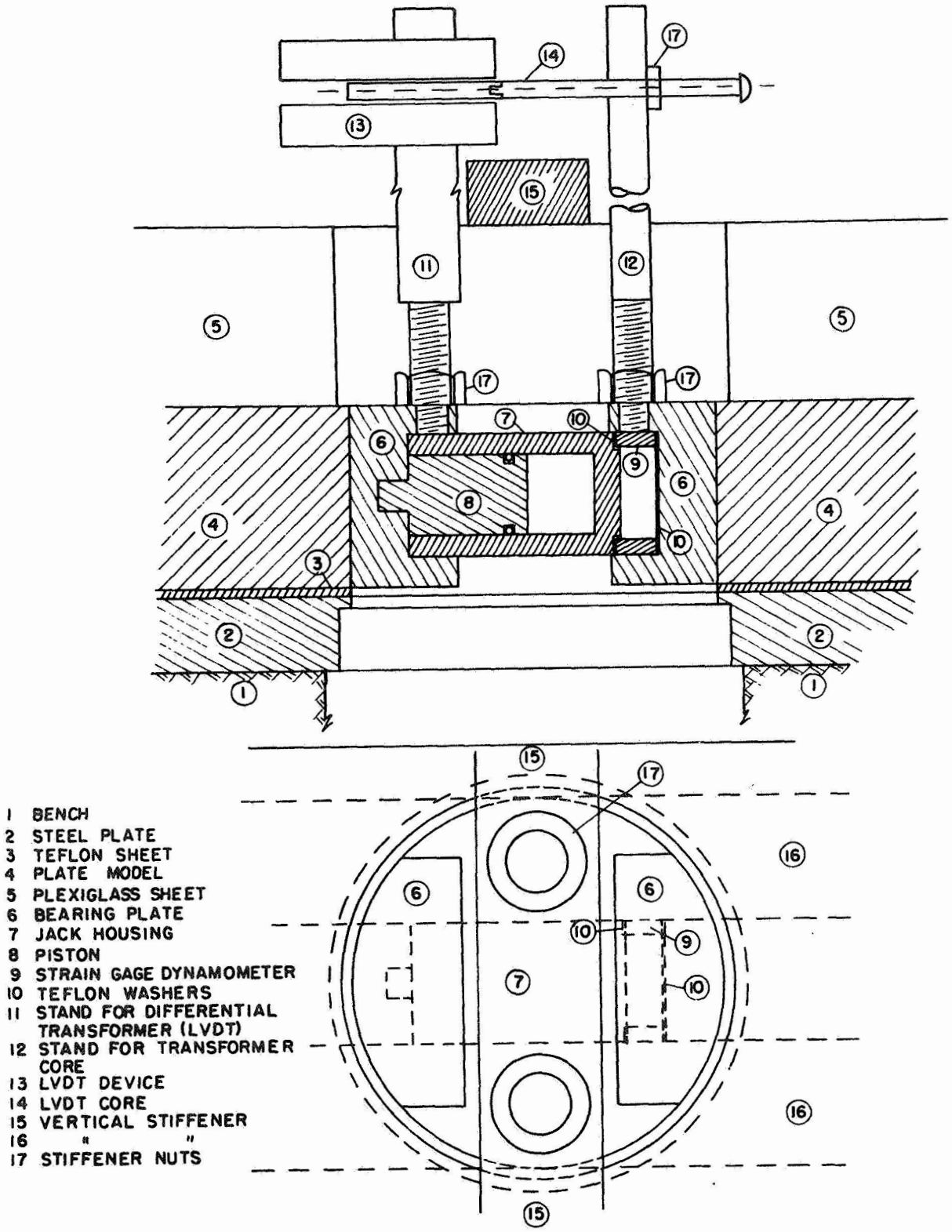

FIGURE 2-1 DETAILED DESCRIPTION OF MODEL TEST SET-UP

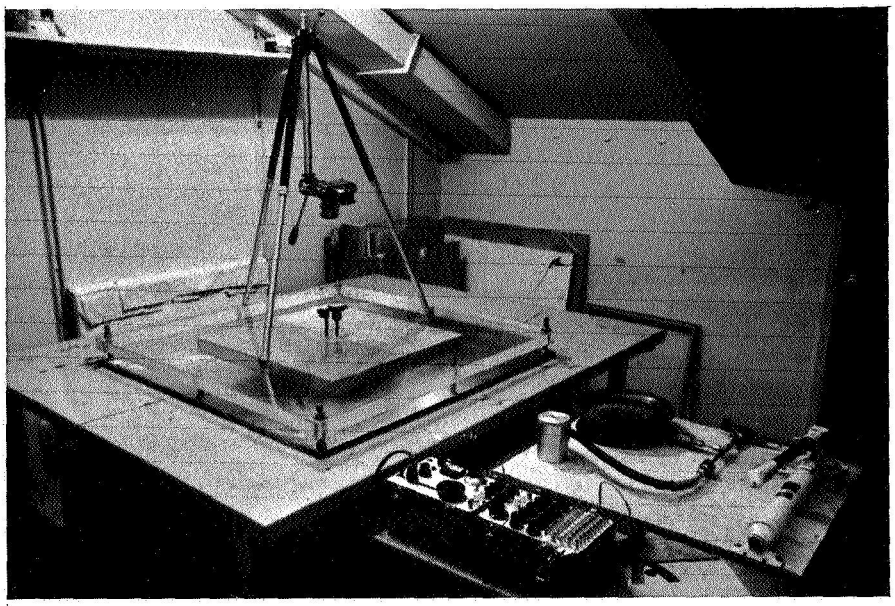

FIGURE 2-2 MODEL TESTS ON A TESTING BENCH

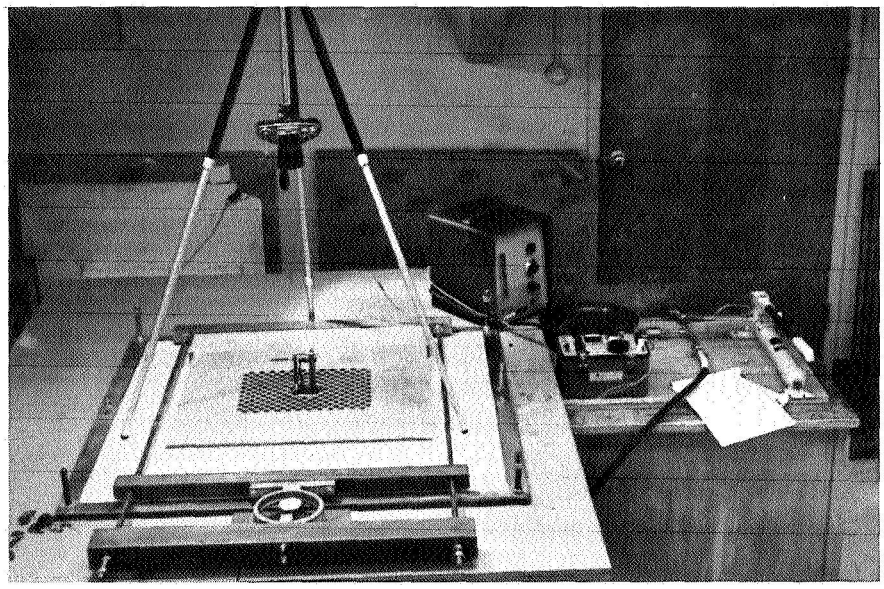

FIGURE 2-3 MODEL TEST — UNIAXIAL LOAD

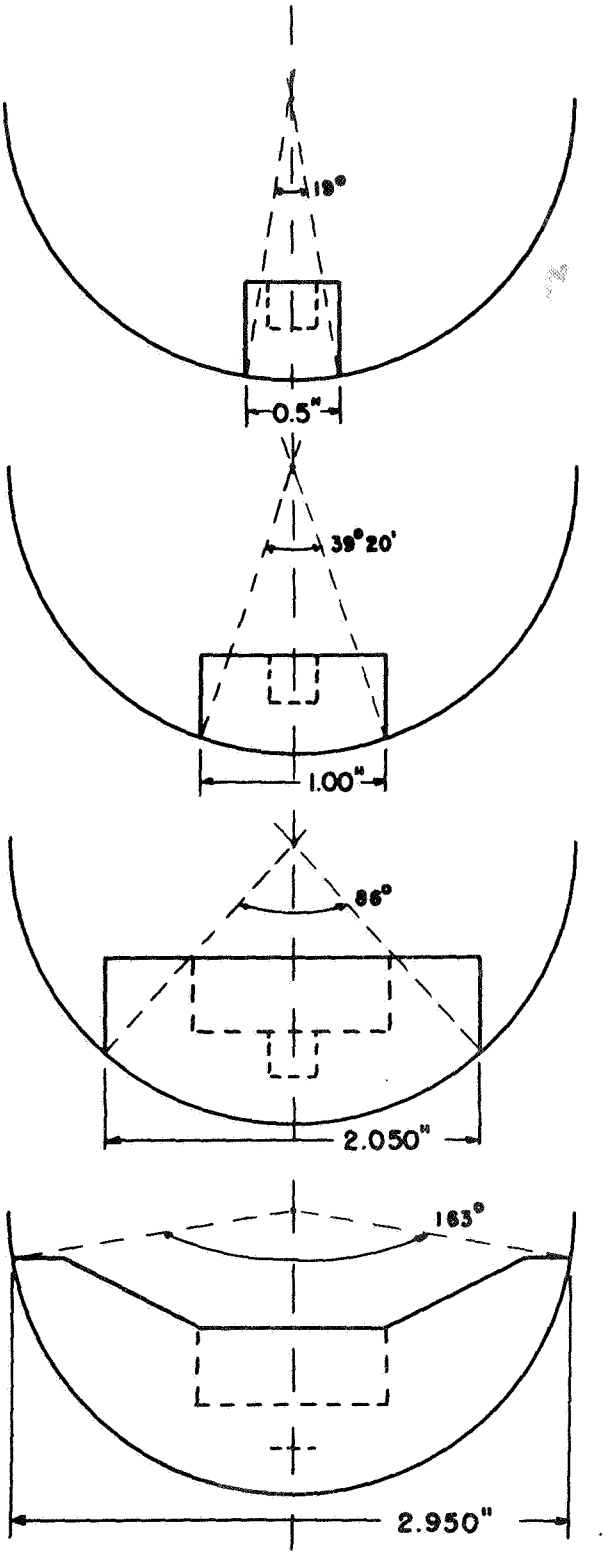

FIGURE 2-4 DESCRIPTION OF THE DIFFERENT BEARING PLATES USED

It was necessary to develop techniques to measure (1) the actual loads developed by the jack, (2) the displacements of the bearing plates, and (3) the internal deformations of the model. The jack load was developed by an internal fluid pressure which was measured by an accurate manometer (smallest division 50 psi) with a total capacity of 4000 psi. The jack was calibrated to relate the internal jack pressure to the jack force (50 psi = 7.2 kg). However, greater precision was needed. A strain gauge load cell was installed in series with the jack. The load cell consisted of a 2.54 cm diameter steel ring with 2 two-legged strain gauge bridge circuits wired on the inside of its 0.3 cm thick walls. The system yielded a least reading of 1.2 kg. Figures 2-5a and 2-5b show the jack under calibration.

During the testing program three methods were employed to measure displacements of the bearing plates when forced against the borehole walls. First a jewelled dial gauge was mounted in parallel with the jack between the bearing plates. With this arrangement the stiffness of the gauge proved to be so great as to interfere with the model test. Second, a micro-caliper was used, but the accuracy was not acceptable. Finally, a linear variable differential transformer (LVDT) was installed in parallel with the jack. In general this proved to be satisfactory, but unknown rotations of the support arms (No. 11 on Figure 2-1) interfered with some of the measurements as will be explained later. The best approach for measuring displacements would incorporate measurements on both sides of the borehole. Unfortunately, this was not technically possible.

Internal deformations of the model were measured by a variety of techniques. Because different materials were studied, no single method could be adapted to all tests. The Moiré fringe method (Figure 2-6)

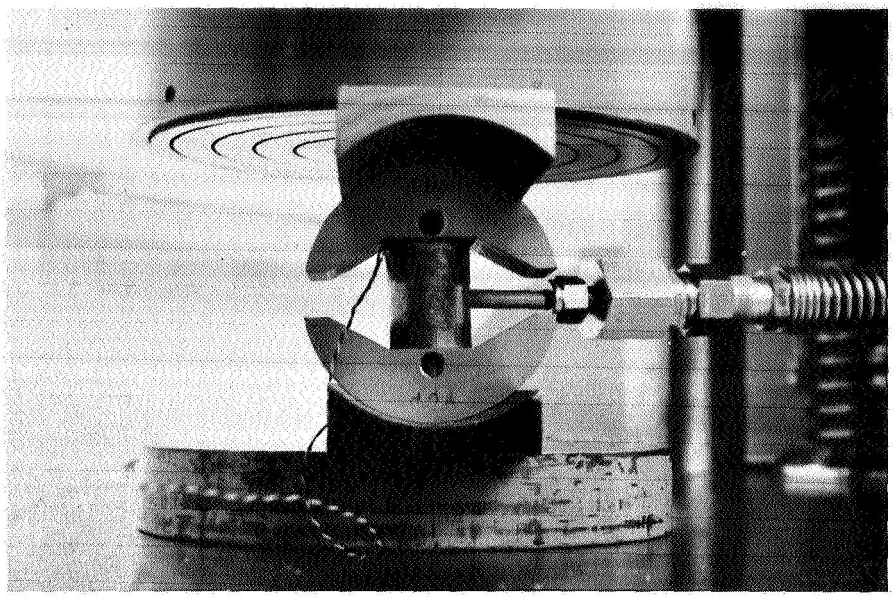

FIGURE 2-5a CALIBRATION TEST

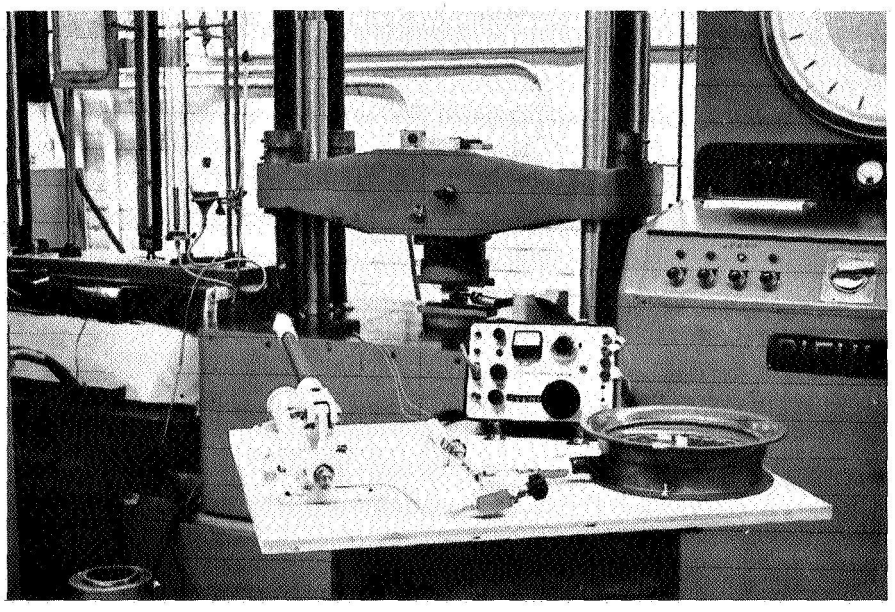

FIGURE 2-5b CALIBRATION TEST

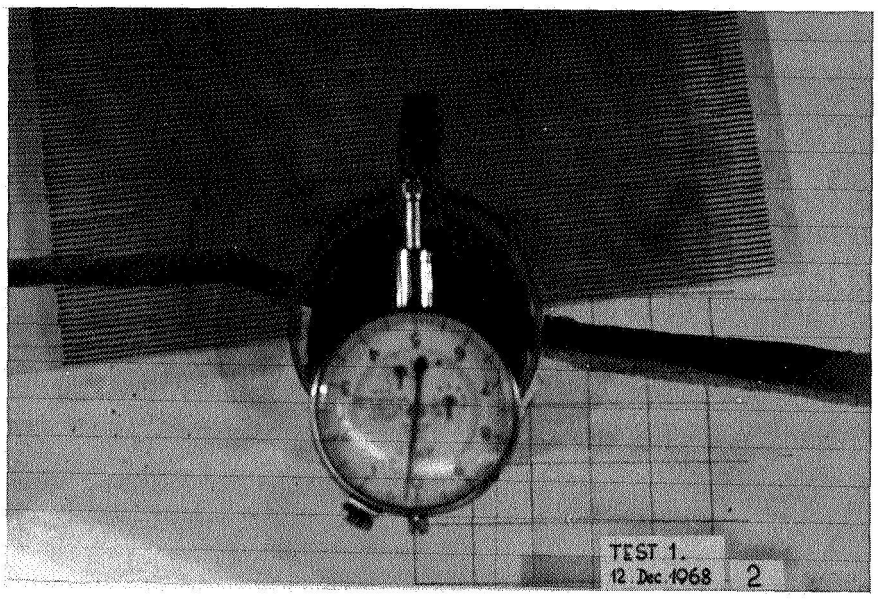

FIGURE 2-6 MOIRÉ FRINGE METHOD, MODEL TEST NO. 1

was too insensitive in the only materials for which it is an applicable method (brittle materials). A grid of small dots sprayed on a thin plaster coating on the surface of some materials (Figures 2-7 and 2-8) which indicated internal deformations by the straining of the grid lines proved to be a sensitive indicator of strain in regions of extension. However, this method was unsuccessful in regions of compressive strain owing to interference by the stiff coating between the plexiglass cover and model plate. When the brittle coating was omitted, the grid of dots sprayed directly on the model plate surface proved a sensitive indicator of compressive strains but was not satisfactory in the regions of extension. When large circular dots were used, the strain of the individual dots themselves increased the sensitivity of this method. Another method attempted was to record the displacement vectors of individual grains by holding a camera lens open during deformation (Figure 2-9). This was abandoned as it required an extremely rapid loading rate. Displacement vectors of individual grains were successfully recorded by placing a soft transparent sheet between the surface of the model and the plexiglass cover. During loading by the jack, the grain movements scratched the sheet (Figures 2-10, 2-11, and 2-12). Finally, a stereoscopical method proved to faithfully detail the internal deformations. In this method the camera position was fixed while the model was undergoing deformation. Successive exposures contained a strain induced parallax so that there was apparent relief when any two exposures were viewed stereoscopically (Figures 2-13 through 2-16). (A stereo viewer should be used to observe these figures.) By contouring the apparent relief, using stereo plotting instruments, displacement contours are obtained. The displacement represents the component of total displacement in the direction parallel to the viewer's eye base.

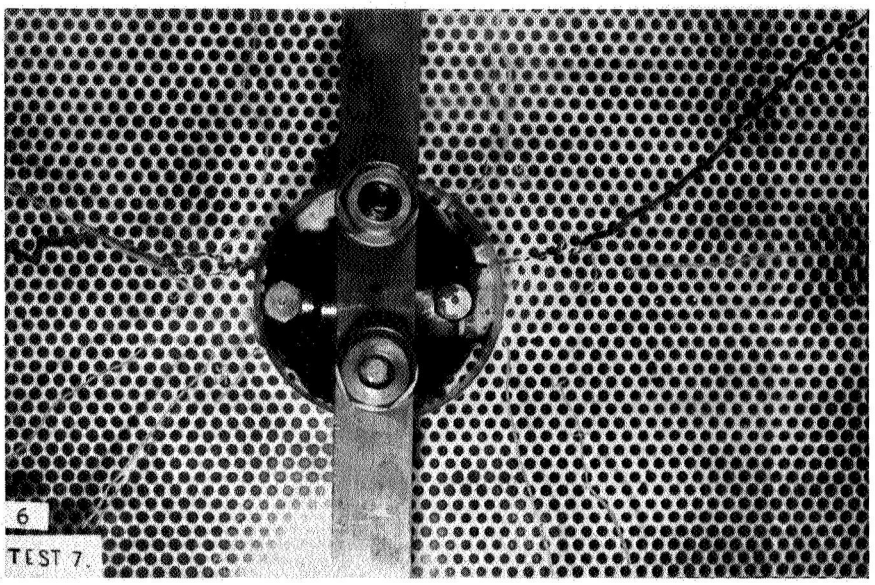

FIGURE 2-7 GRID METHOD, MODEL TEST NO. 7

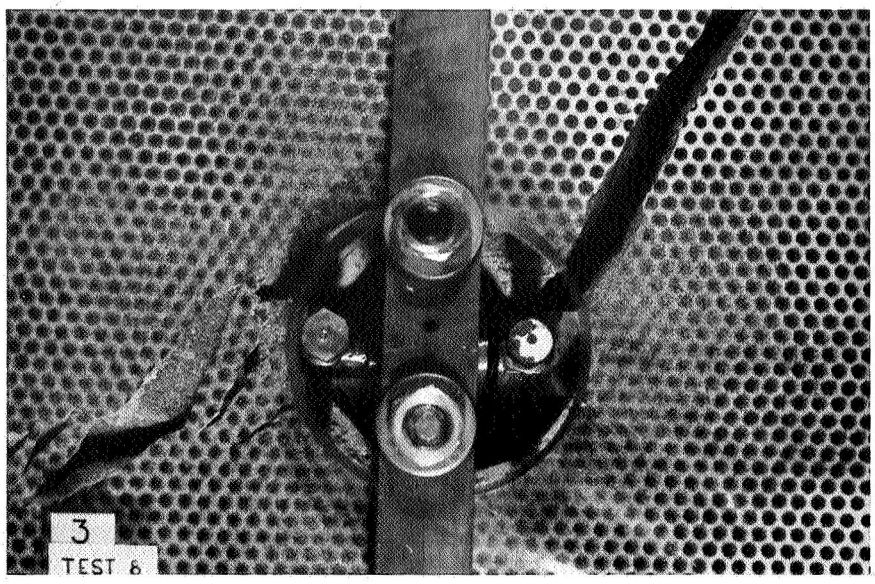

FIGURE 2-8 GRID METHOD, MODEL TEST NO. 8

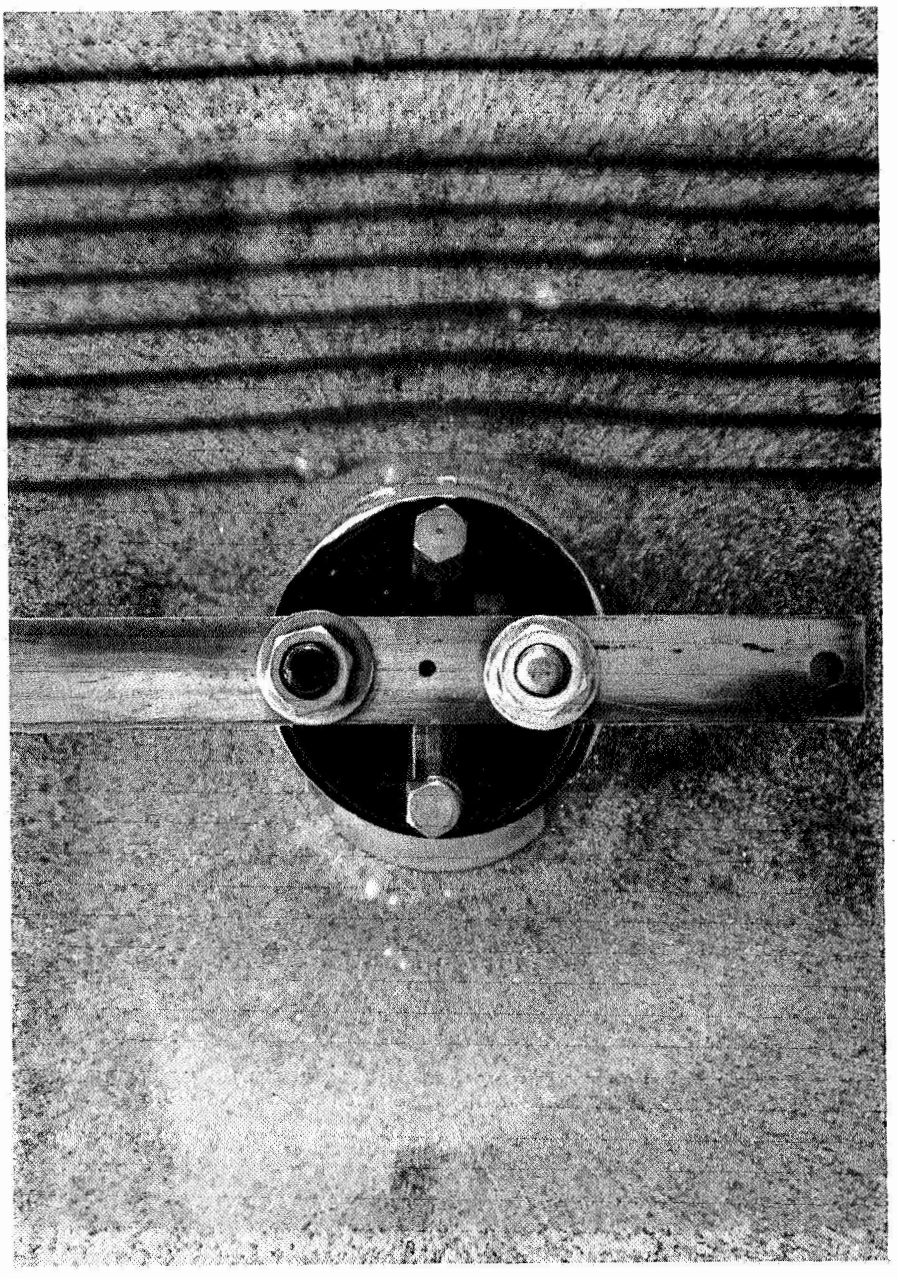

FIGURE 2-9 TEST NO. 19 — TIME EXPOSURE

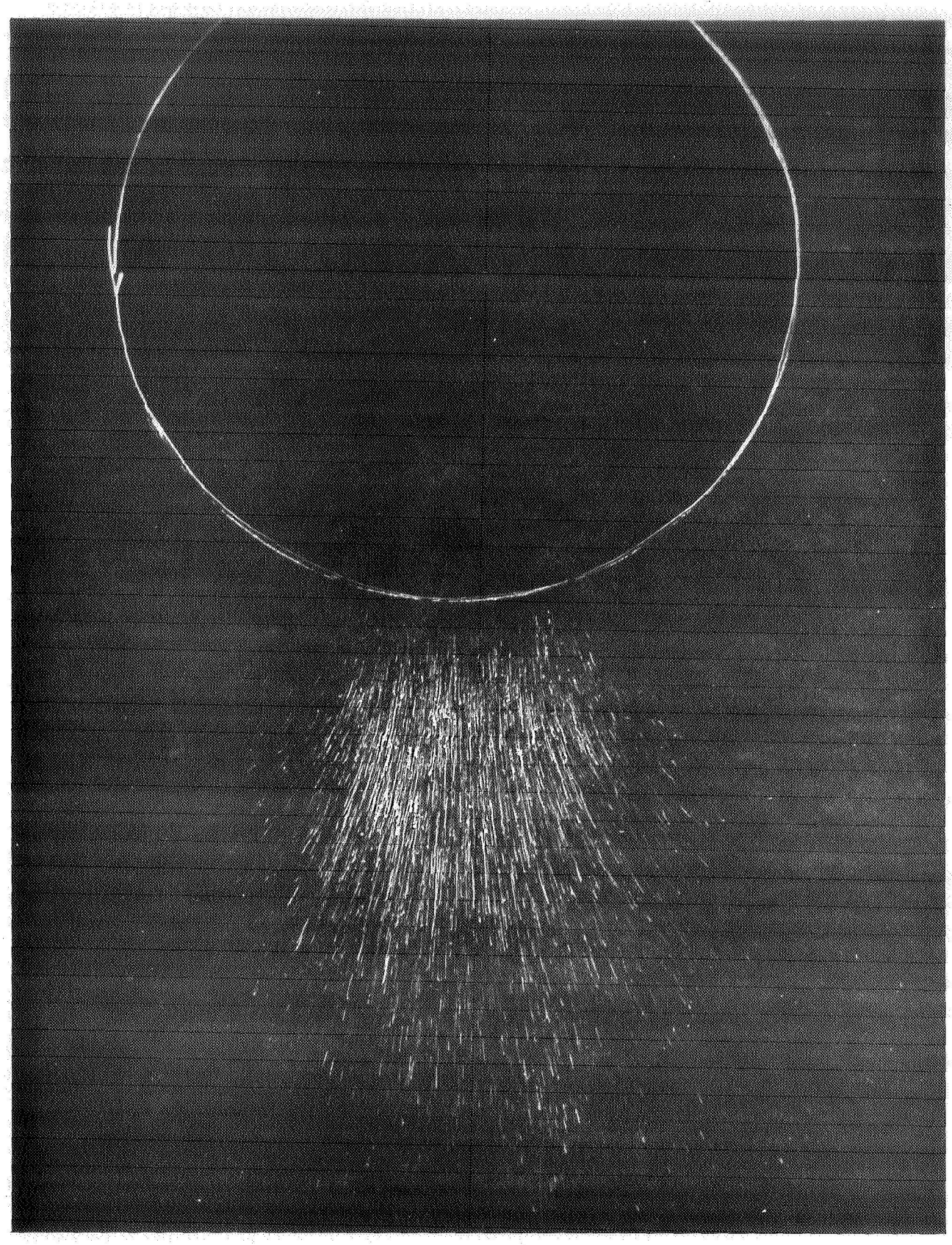

FIGURE 2-10 SCRATCHING METHOD

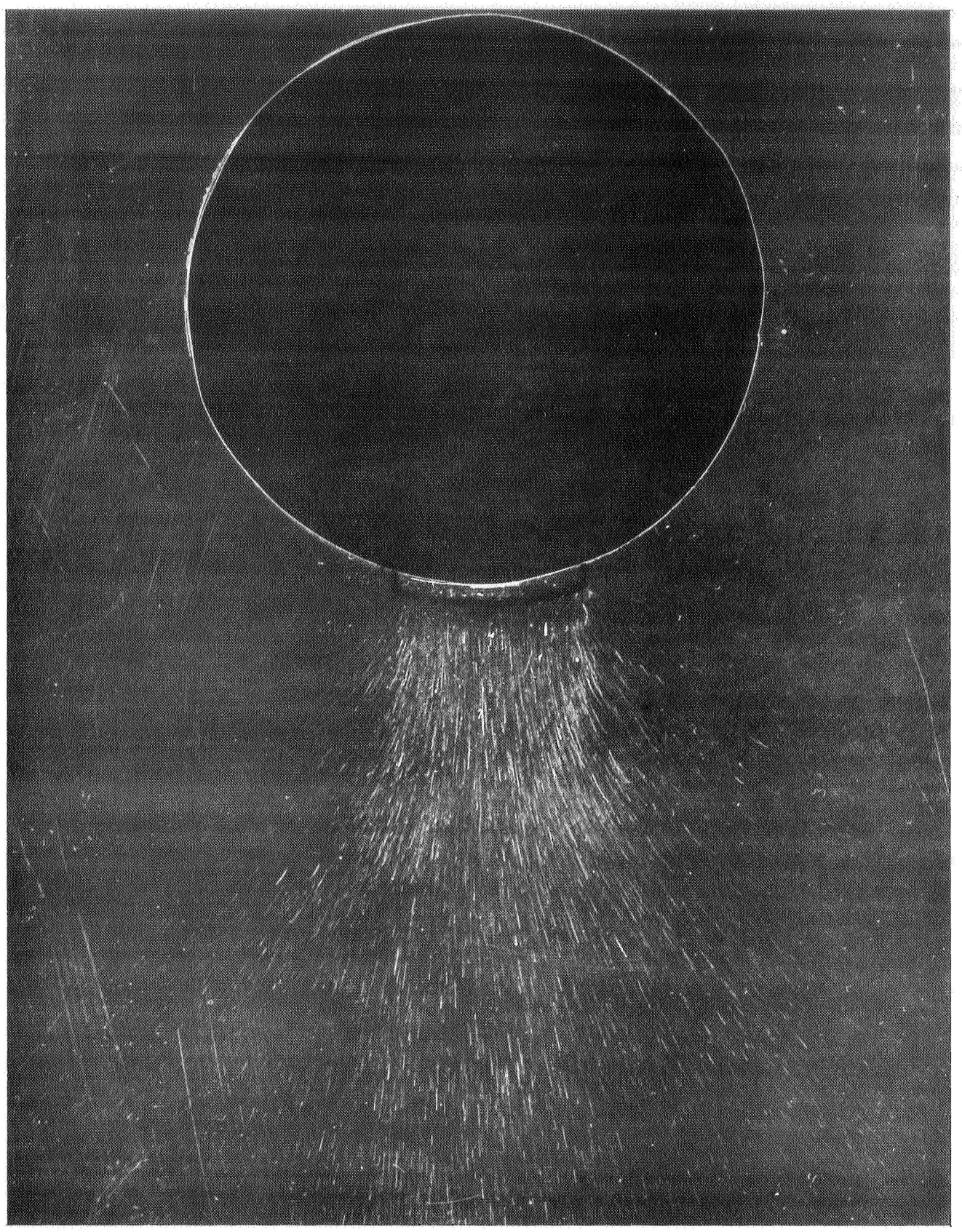

FIGURE 2-11 SCRATCHING METHOD

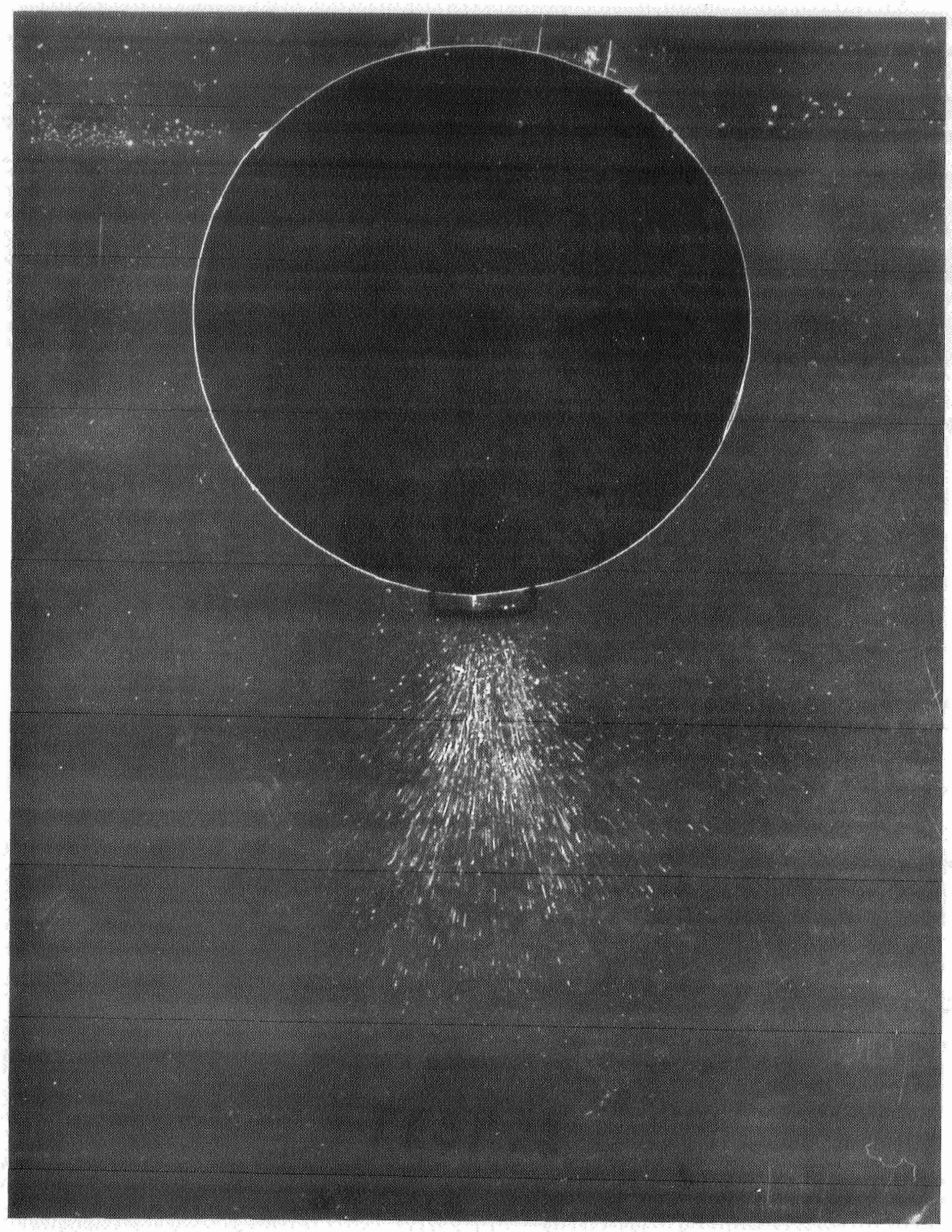

FIGURE 2-12 SCRATCHING METHOD

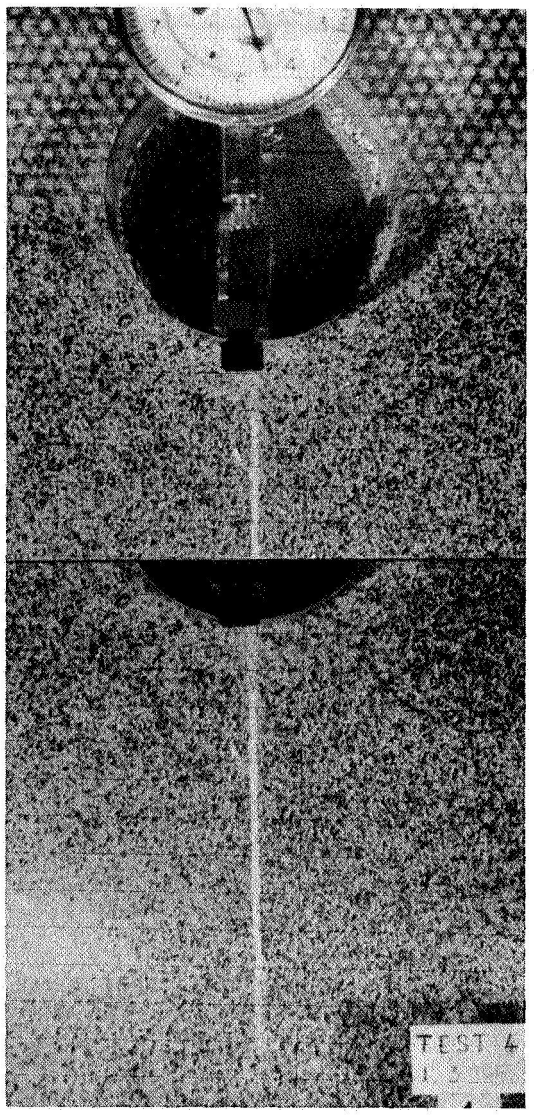

FIGURE 2-13 STEROSCOPIC VIEW - MODEL TEST NO. 4

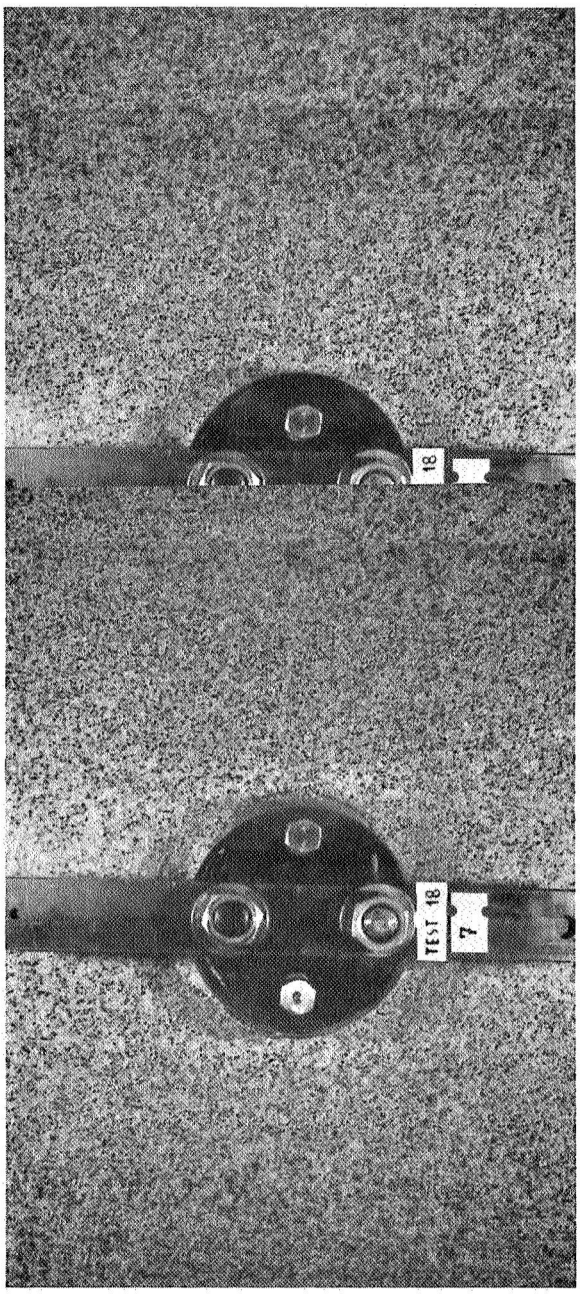

FIGURE 2-14 STEREOSCOPIC VIEW — MODEL TEST 18

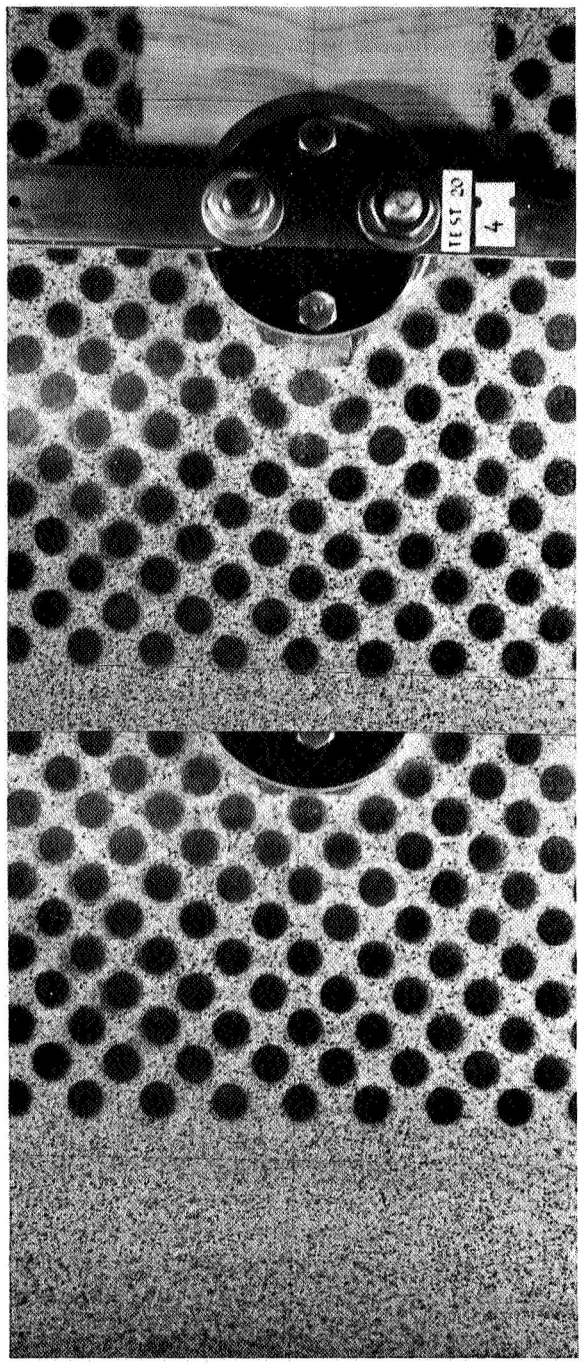

FIGURE 2-15 STEREOSCOPIC VIEW — MODEL TEST 20

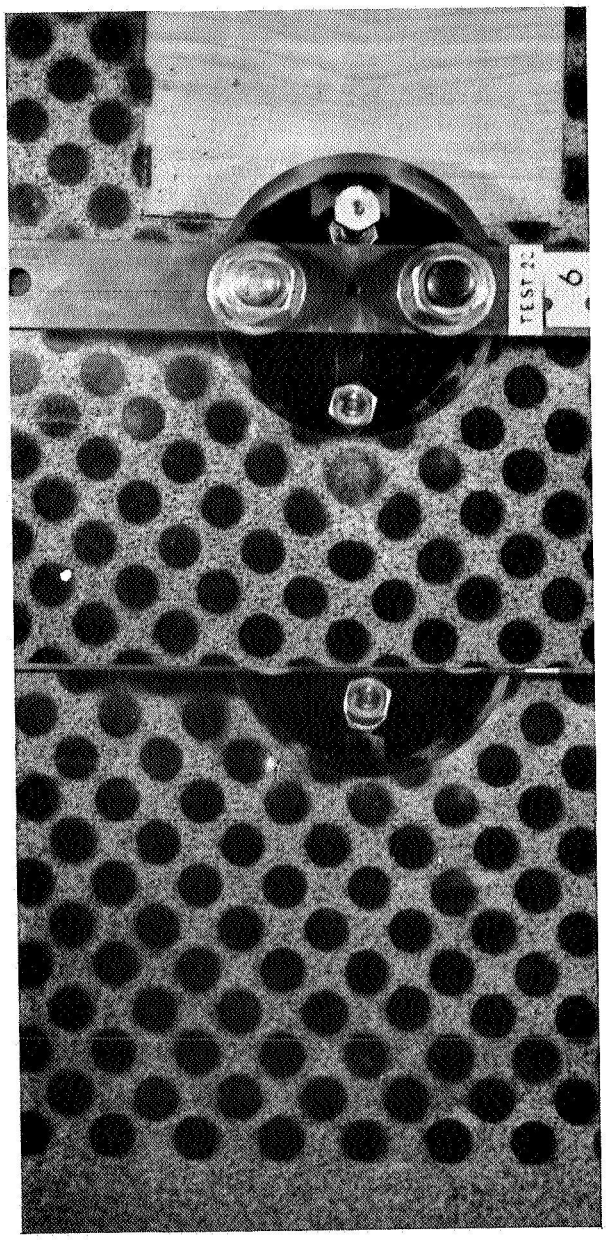

FIGURE 2-16 STEREOSCOPIC VIEW — MODEL TEST 22

Tests were performed by incremental loading. The load steps were either 14.3, 28.6, or 57.2 kg (conforming to even steps of the hydraulic pressures). Each load increment was maintained until deformations ceased or 30 minutes time elapsed, whichever was shorter. Three to seven photographs were taken at intermediate stages of each test.

B. Materials for Model Studies

The materials used for the model studies were chosen to allow a range of behaviors to be examined. The studies were performed at prototype dimensions, thus no scale factor was necessary. The basic components of the model materials were as follows:

1. medium sand (PCA "lapis lustre" No. 20)
2. fine sand (PCA "lapis lustre" No. 00)
3. crushed mica (Van Waters C3000)
4. Portland cement (PCA type 1)
5. gypsum plaster (U. S. gypsum "red top")
6. powdered diatomite (Johns Mansville "celite")
7. paraffin (American Oil Company household wax "parowax")

The grain size distribution of the filler materials (1, 2, and 3) are presented in Figure 2-17. The materials were mixed according to varying formulas as described in Table 2-1. A description of model plate preparation is given in Appendix A2. To simulate brittle materials, two basic mixes were used. The first consisted of medium sand, cement, and water. The second consisted of plaster, celite, and water. In both mixes the proportions of the materials were varied to achieve slightly different properties. Cohesionless models (models with low cohesion) were obtained by using medium sand alone, or densified mica. Plastic material was simulated by mixing sand, mica, and paraffin.

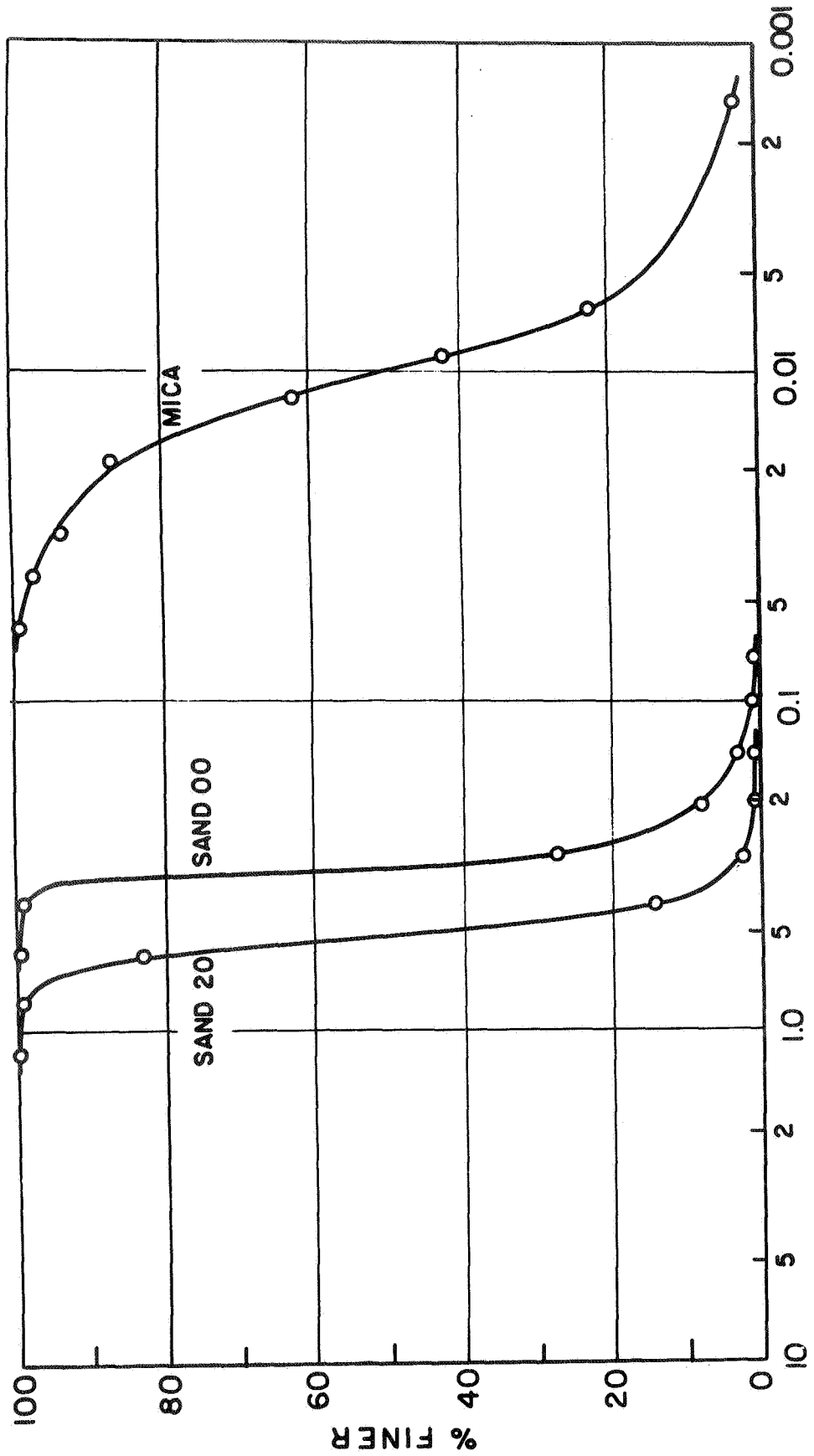

FIGURE 2-17 DISTRIBUTIONS OF COMPONENT FILLER MATERIALS

TABLE 2-1 DESCRIPTION OF MODEL MATERIALS

Material number	Type	Components	Proportions by weight
I	brittle	plaster-celite-water	100:40:160
II	brittle	sand No. 20-cement-water	100:5:5
III	plastic	sand-parowax	100:4
IV	plastic	sand-mica-parowax	100:2:3,5
V	plastic	sand-mica-parowax	100:5:2
VI	cohesionless	sand No. 20	—
VII	plastic	sand No. 20 and sand No. 00-mica-parowax	(50 + 50):5:3
VIII	plastic	sand No. 20-parowax	100:3
IX	brittle	sand No. 20-cement-water	100:20:12
X	brittle	sand No. 20-cement-water	100:10:6
XI	slightly cohesive	mica	—

The properties of the mixes were determined in direct shear (Karol Warner machine), unconfined compression, and indirect tension. In the direct shear tests the shortening of the specimens (6.35 cm in diameter and 5.1 cm high) under a constant normal load alone was first measured. Then, the shear stress was applied (under the constant normal load) yielding the shear strength data presented in Figures 2-18, 2-19, and 2-20. Figure 2-18 presents the shear strength of the basic components, while Figures 2-19 and 2-20 present the shear strength data for plastic and brittle mixtures, respectively. In addition, the tensile strength was determined by Brasilian tests on 2.5 inch diameter cylinders.

From the normal loading of the direct shear specimens, the modulus of deformation, M, was determined as the tangent to the deformation curves between 4.0 and 8.0 kg/cm^2 (Figure 2-21). The modulus of deformation, E, was determined from unconfined compression tests as the initial tangent to the curves.

Table 2-2 presents the results from all tests performed. Also given are the mixture formulas and physical properties for all materials tested.

C. Description of Tests and Results

The first model tests were directed toward developing testing techniques and improving equipment. An effort was made to approach plane strain conditions and, as previously noted, to find suitable methods for measuring internal deformations. By the completion of test No. 10, only tensile or punching failures had been observed. Of greatest concern, however, is the measurement of shear strength parameters of soils and rocks with borehole tests. To achieve this end an effort was launched to produce materials and conditions yielding bearing capacity

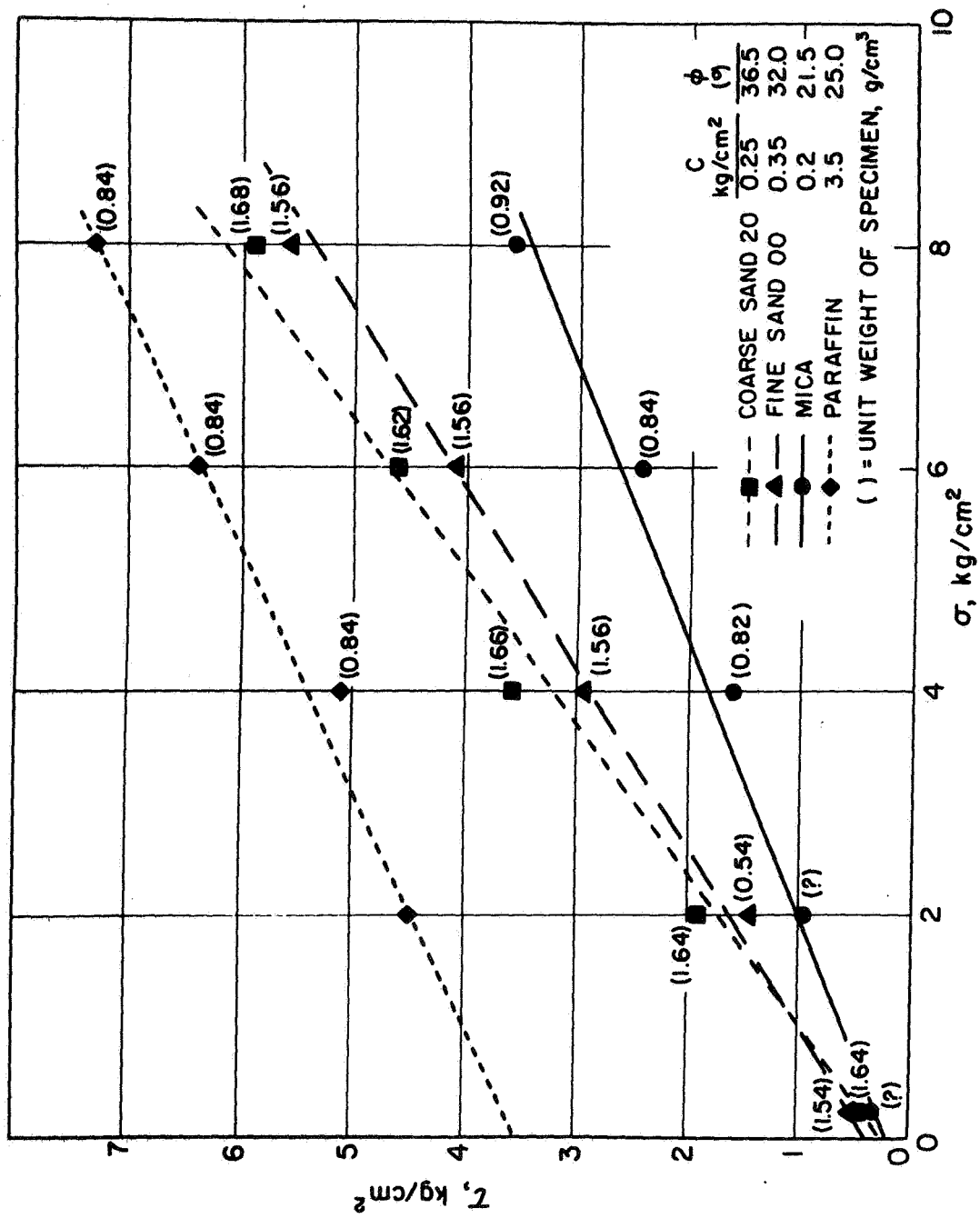

FIGURE 2-18 SHEARING RESISTANCE OF BASIC MATERIAL

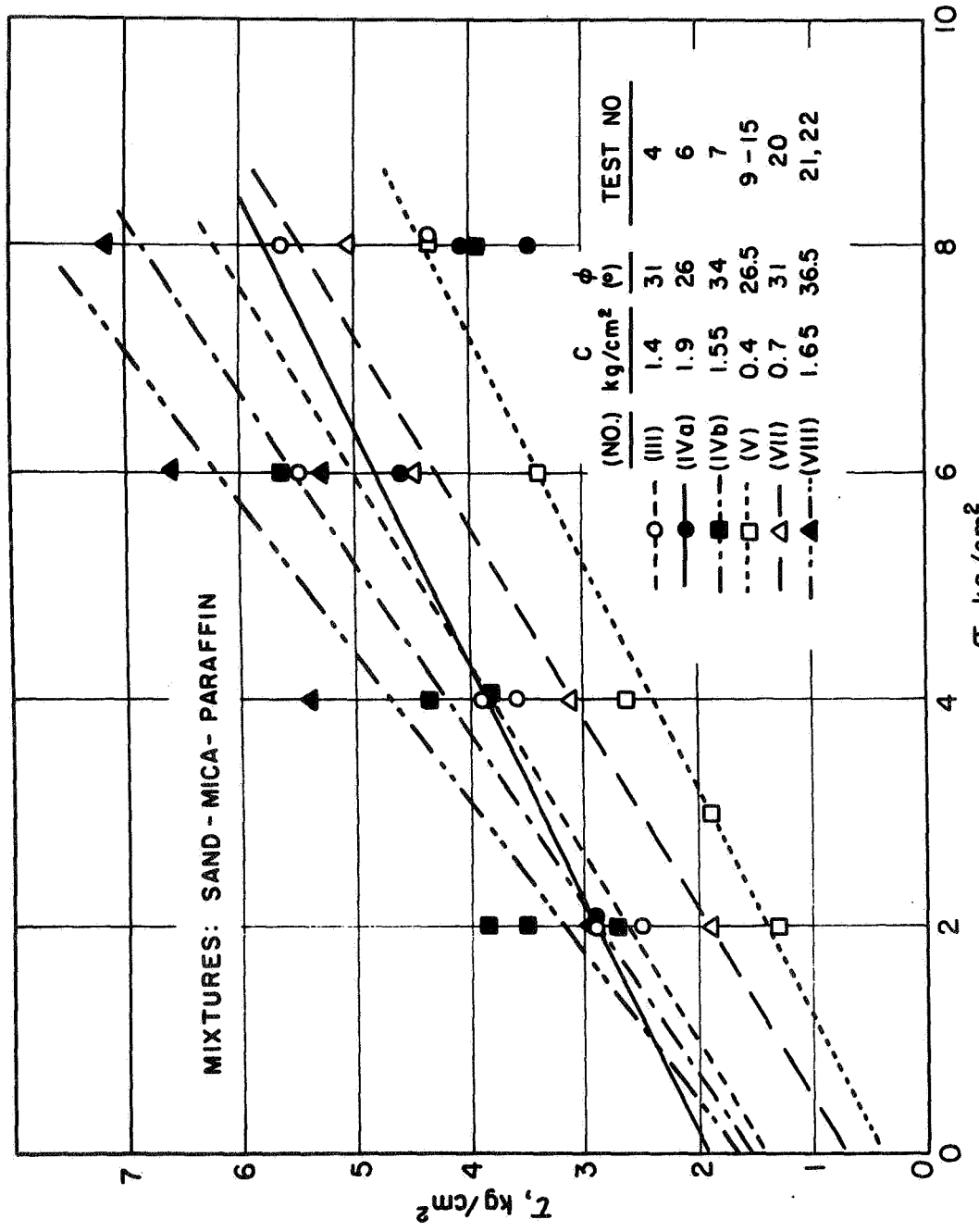

FIGURE 2-19 SHEARING RESISTANCE OF MIXTURES

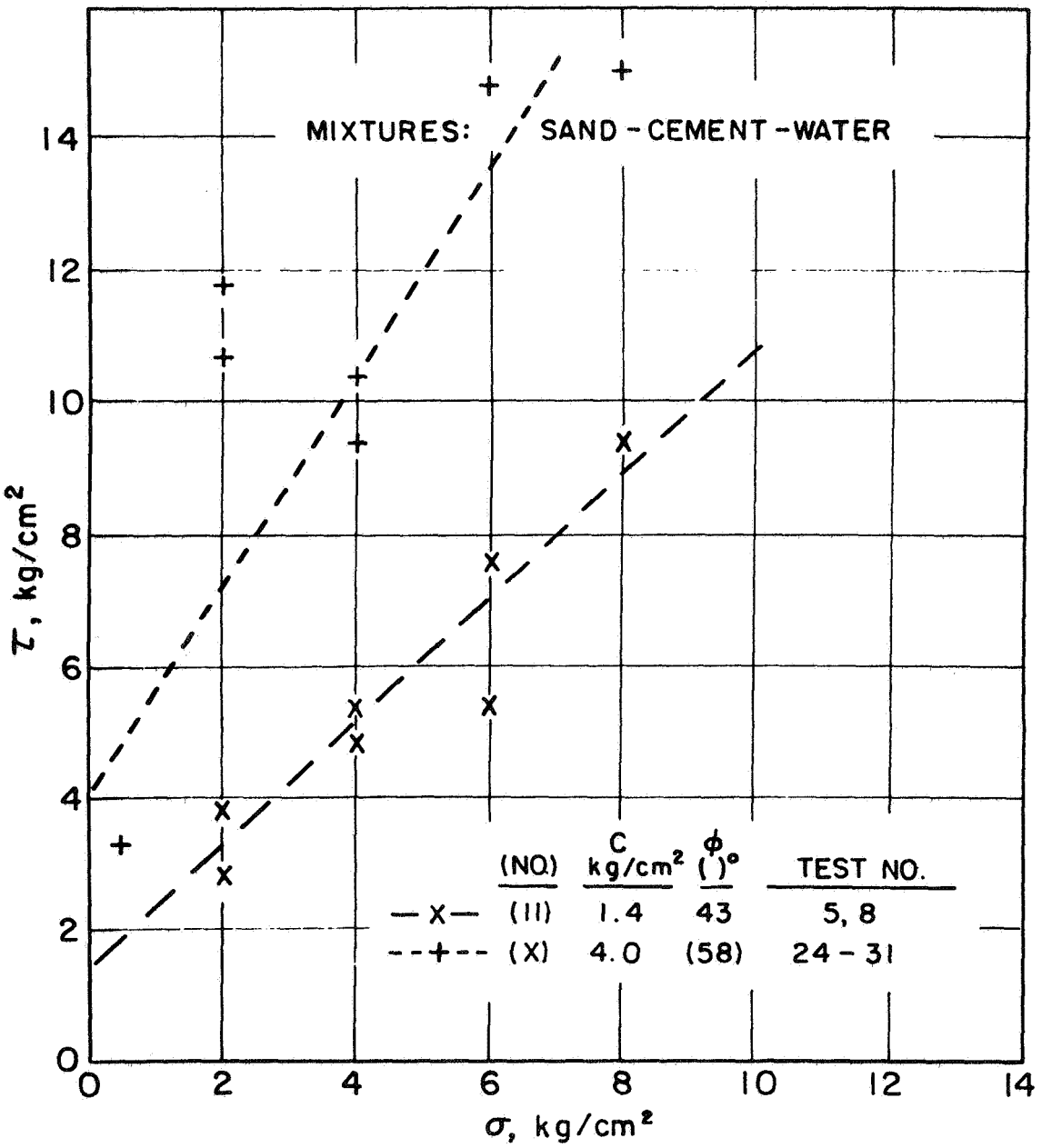

FIGURE 2-20 SHEARING RESISTANCE OF MIXTURES

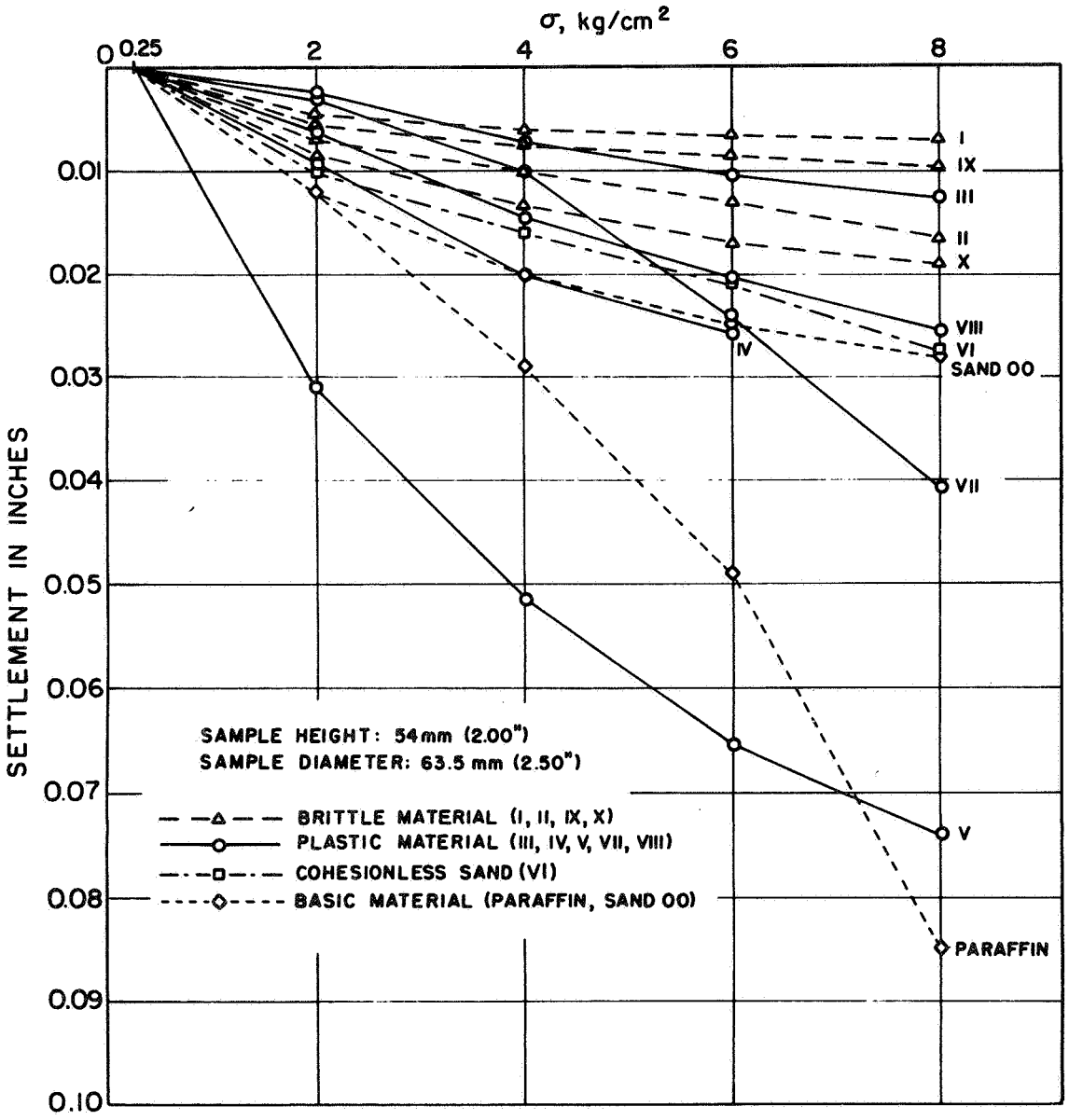

FIGURE 2-21 DEFORMATION CURVES

TABLE 2-2 PROPERTIES OF MODEL MATERIALS

Tested Material	Number of the material	Components	Mixing ratio in % of weight	Unit weight g/cm^3	Tensile strength kg/cm^2	Unconfined compression strength kg/cm^2	Modulus of deformation kg/cm^2	Modulus of deformation (uniaxial test) kg/cm^2	Cohesion kg/cm^2	Angle of internal friction ( )°
Brittle	I	plaster:celite:water	100:40:160	0.78	8.5	45.0	134×10^3	19.7×10^3	9.8	43
	IX	sand No. 20:cement: water	100:20:12	1.89-1.93	11.3	63.5	41×10^3	80.0×10^3	not determined	
	X	sand No. 20:cement: water	100:10:6	1.63-1.75	4.5	33.0	15.5×10^3	$58. \times 10^3$	4.0	58
	II	sand No. 20:cement: water	100:5:5	1.49-1.54	1.45	12.3	13.2×10^3	2.4×10^3	1.4	43
Cohesionless and slightly cohesive	VI	sand No. 20	100	1.64-1.68	-	-	7.3×10^3	-	0.25	36.5
	XI	densified mica	100	0.77	-	-	-	-	0.2	26.5
Plastic sand and paraffin	III	sand No. 20:paraffin	100:4	1.54-1.66	1.42	7.4	13.8×10^3	5.8×10^3	1.4	31.0
	VIII	sand No. 00:paraffin	100:3	1.57-1.59	1.35	8.2	7.7×10^3	3.2×10^3	1.65	36.5
Plastic sand and mica and paraffin	IV	sand No. 20:mica: paraffin	100:2:3.5	1.56-1.60	1.15	3.32	8.3×10^3	0.65×10^3	1.9	26
	VII	sand No 20	50:	1.65-1.74	0.24	2.25	2.8×10^3	0.7×10^3	0.7	31
		sand No 00:mica:paraffin	50: 5:3							
	V	sand No 20:mica:paraffin	100:5:2	1.55-1.59	0.1	0.29	2.5×10^3	0.09×10^3	0.4	26.5

failures. Four techniques were used in this effort: (1) a steel frame was circumscribed about the model plate to prevent premature tension failure of the whole plate, (2) the maximum displacement of the bearing plates was doubled by using a rigid base on one side of the jack. The displacement was further increased by introducing washers to compensate for permanent deformation on cycles of loading and unloading, (3) a higher density and lower strength model material was developed (materials V and VII) to decrease the likelihood of punching and discourage tension cracking, and (4) the narrowest bearing plate was used to increase contact pressures. Tests 15 and 20 combine all of these techniques. They can be considered to have the greatest probability of shearing failure.

A description of all tests is presented in Table 2-3 and the modes of failure are presented in Figure 2-6 through 2-9, 2-13 through 2-16, and 2-22 through 2-43. The conclusions from these tests can be summarized briefly as follows:

1. Complete, classical shearing failure was not obtained in any borehole jack test, even where intense effort was made to increase shearing stresses and reduce shearing strength.

2. Punching was the predominant failure mode in the plastic materials. The displacement vectors are radial under the center line of the bearing plate and curve away from the radius symmetrically under the edges of the bearing plate (Figures 2-10, 2-11, and 2-12). Complete recurving of the displacement lines to intersect either the free walls of the borehole or the half plane bisecting the borehole normal to the jack was not observed, even though it is postulated by theoretical plasticity solutions. In fact when a special brittle surface coating was used, the zone of punching was seen to be separated from the rest of the region by a symmetrical system of cracks (Figures 2-27 and 2-43).

TABLE 2-3 DESCRIPTION OF MODEL TESTS

Number of test	Material type	External steel frame used	Stiff base used in one direction	Type of bearing plate	Type of surface coating	Unit weight g/cm^3	Remarks
1	I	no	no	IV	without coating	not determined	failure by cracks in tensile zone
2	I	no	no	II	Moire fringe pattern, without coating,	not determined	miscarried test
3	I	no	no	II	Moire fringe pattern, without coating,	not determined	failure by cracks in tensile zone
4	III	no	no	II	Moir fringe pattern, without any coating,	not determined	failure by punching
5	II	no	no	II	without coating, small plaster dots	not determined	failure by cracks in tensile zone
6	IV	no	no	II	without coating, small plaster dots	not determined	miscarried test
7	IV	no	no	II	plaster coating, small black dots	not determined	failure by cracks in tensile zone
8	II	no	no	II	plaster coating, small black dots	not determined	failure by cracks in tensile zone
9	V	yes	no	II	plaster coating, small black dots	not determined	failure by cracks in tensile zone
10	V	yes	no	II	lacquer coating, small black dots	1.64	failure by punching
11	V	yes	no	II	lacquer coating, small black dots	1.62	failure by punching
12	V	yes	no	III	lacquer coating, small black dots	1.63	failure by cracks and punching
13	V	yes	yes	III	lacquer coating, large black dots	1.64	failure by cracks and punching
14	V	yes	yes	IV	lacquer coating, large black dots	1.65	failure by cracks and punching
15	V	yes	yes	I	lacquer coating, large black dots	1.65	failure by punching
16	I	yes	no	II	without coating, large black dots	not determined	first cracks at 480 lbs. load; slow propagation of cracks to the boundary of the plate; no other kind of failure even at 1050-lb load

TABLE 2-3 (Cont'd)

Number of test	Material type	External steel frame used	Stiff base used in one direction	Type of bearing plate	Type of surface coating	Unit weight g/cm^3	Remarks
17	VI	yes	no	III	without any coating	1.61	failure by punching; deformation of bore-hole let sand fall out
18	VI	yes	no	III	without any coating	1.68	failure by punching; deformation of bore-hole let sand fall out
19	VI	yes	no	III	lacquer coating, black lines	not determined	failure by punching; deformation of bore-hole let sand fall out
20	VII	yes	yes	II	surface coating, large black dots	1.72	only punching failure
21	VIII	yes	yes	II	surface coating, large black dots	1.51	only punching failure
22	VIII	yes	yes	I	surface coating, large black dots	1.50	only punching failure
23	IX	no	no	IV	no surface coating, large black dots	not determined	no failure even at highest available load (1260 lbs.)
24*	IX	no	no	IV	no surface coating, large black dots	not determined	failure of tensile cracks at the load 960 lbs.
25*	X	no	no	III	no surface coating, large black dots	not determined	failure by tensile cracks at the load 1260 lbs.
26*	X	no	no	II	no surface coating, large black dots	not determined	failure by tensile cracks at the load 1260 lbs.
27*	X	no	no	I	no surface coating, large black dots	not determined	failure by tensile cracks at the load 1260 lbs.
28**	X	no	no	II	no surface coating, large black dots,	not determined	failure by tensile cracks at the load 960 lbs.
29**	X	no	no	III	no surface coating, large black dots,	not determined	failure by tensile cracks at the load 1030 lbs.
30**	X	no	no	IV	no surface coating, large black dots,	not determined	failure by tensile cracks at the load 1100 lbs.
31**	X	no	no	I	no surface coating, large black dots,	not determined	failure by tensile cracks at the load 1140 lbs.
32**	IX	no	no	II	no surface coating, large black dots,	not determined	no failure even at maximum load (1260 lbs).
33	XI	yes	no	II	no surface coating, small black dots	not determined	failure by punching and local tensile cracks

* plane stress tests (without stiffened plexiglass cover)

** plane stress tests with horizontal applied pressure in the nodal plate directed perpendicular to the axis of the jack load

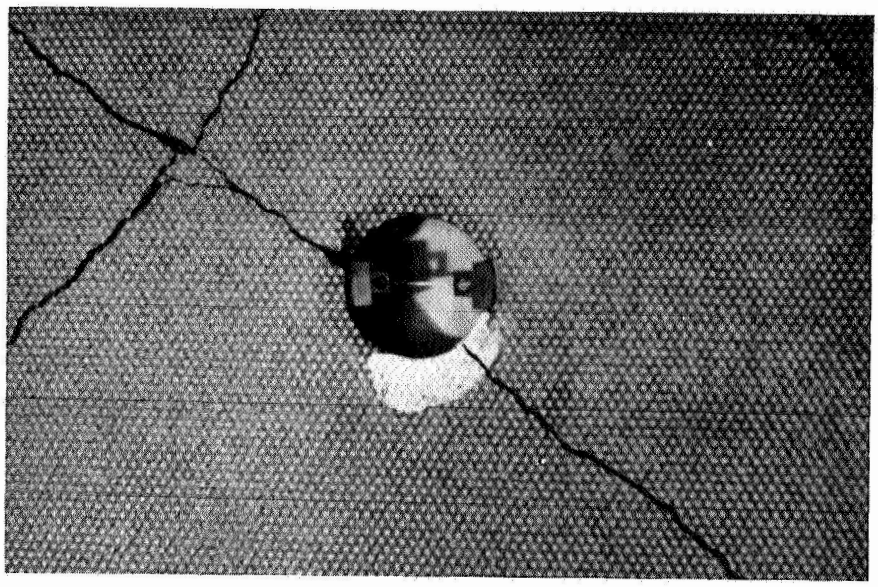

FIGURE 2-22 MODEL TEST NO. 5

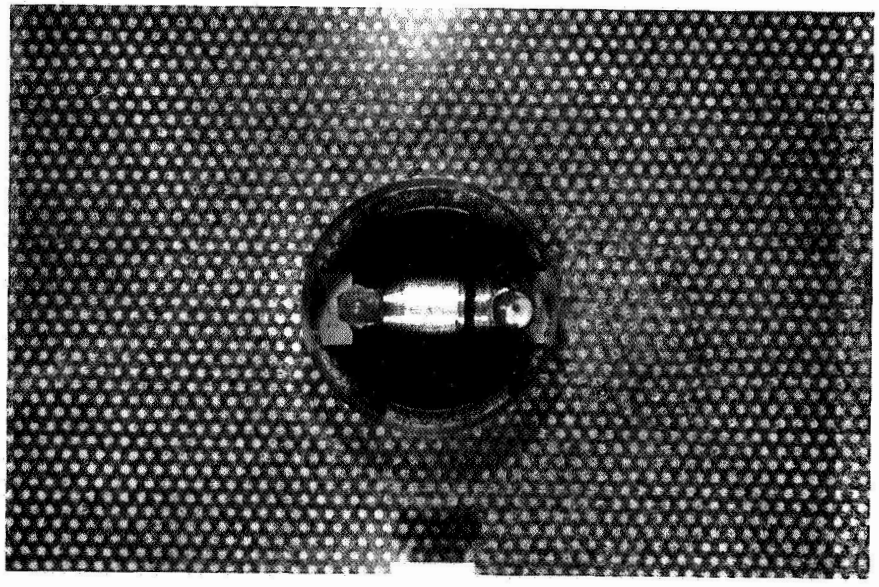

FIGURE 2-23 MODEL TEST NO. 6

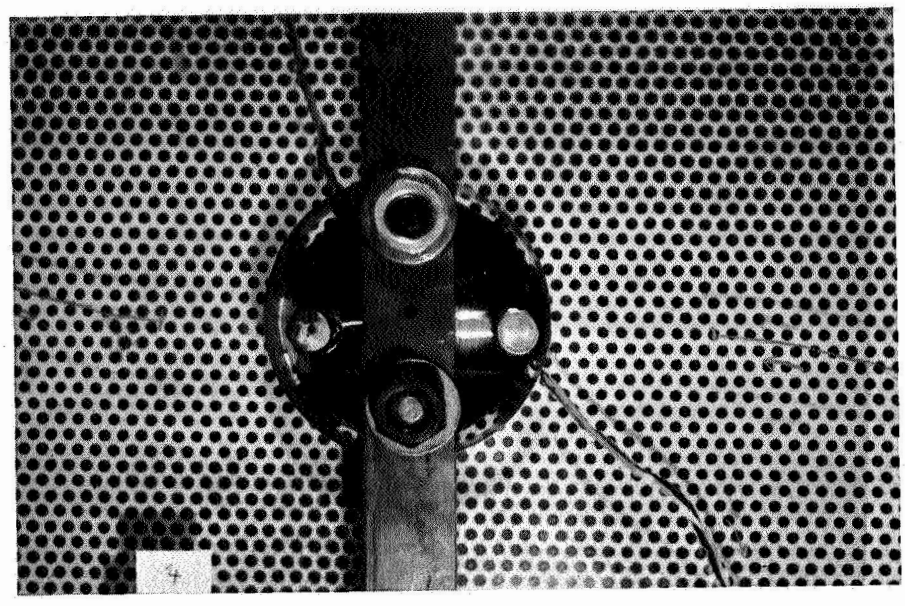

FIGURE 2-24 MODEL TEST NO. 9

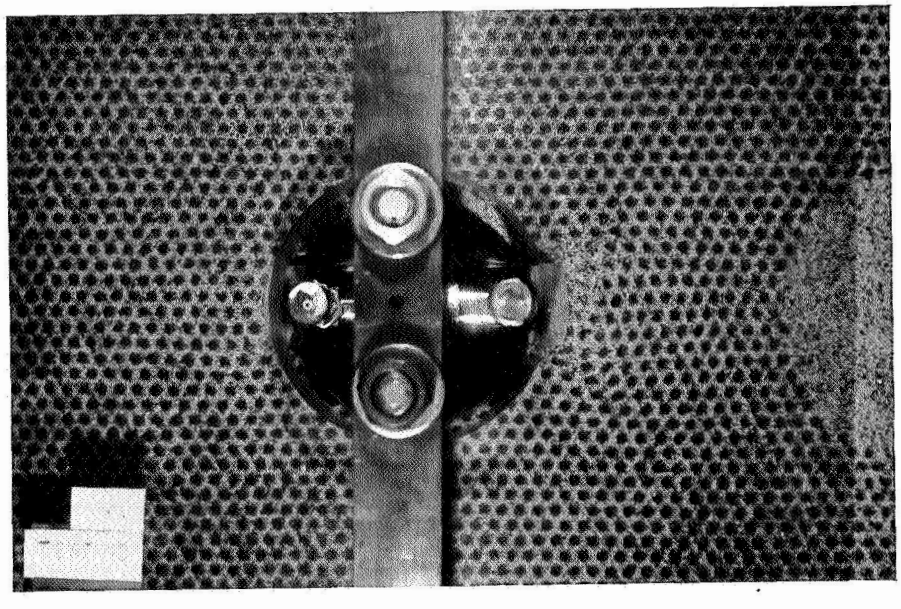

FIGURE 2-25 MODEL TEST NO. 10

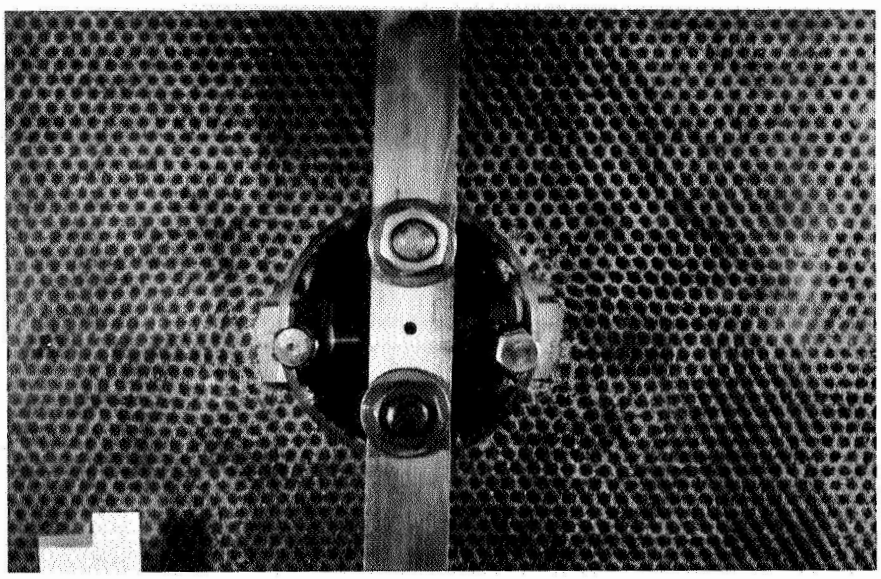

FIGURE 2-26 MODEL TEST NO. 11

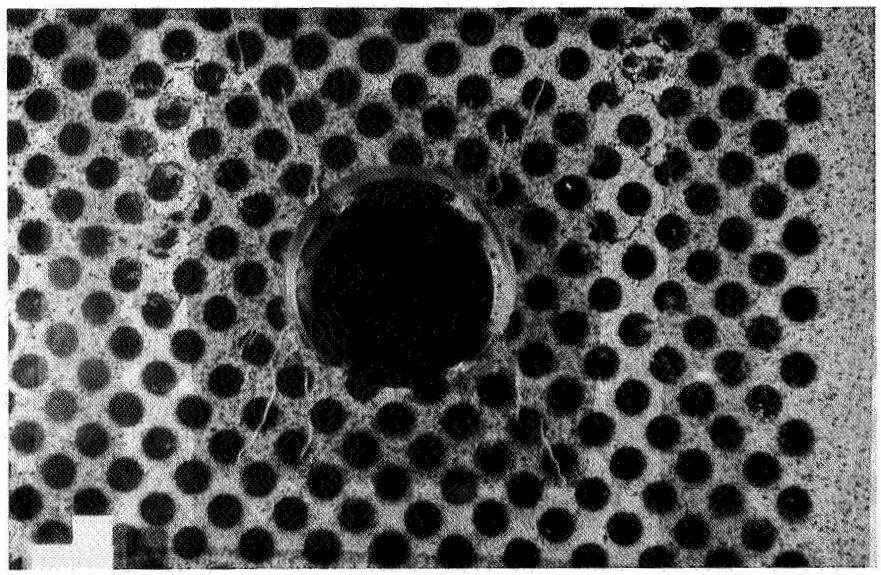

FIGURE 2-27 MODEL TEST NO. 12

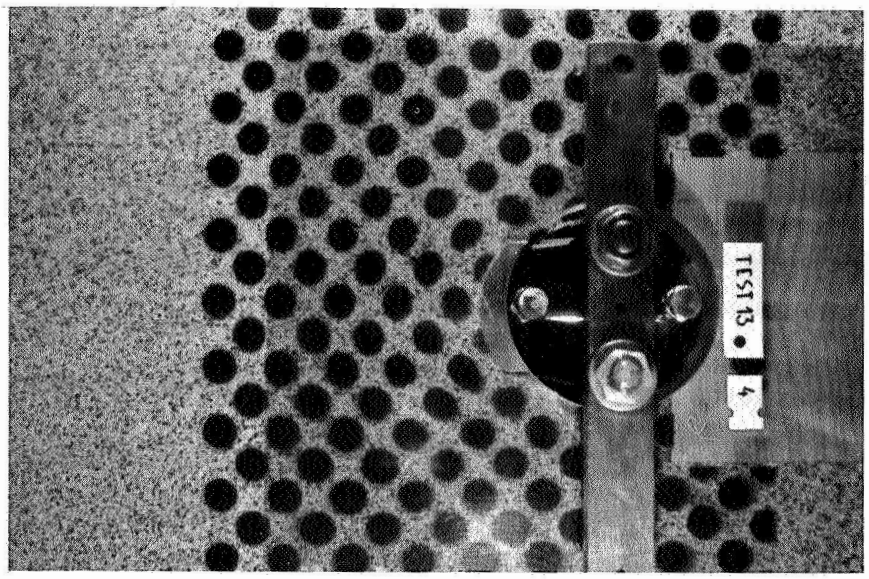

FIGURE 2-28 MODEL TEST NO. 13

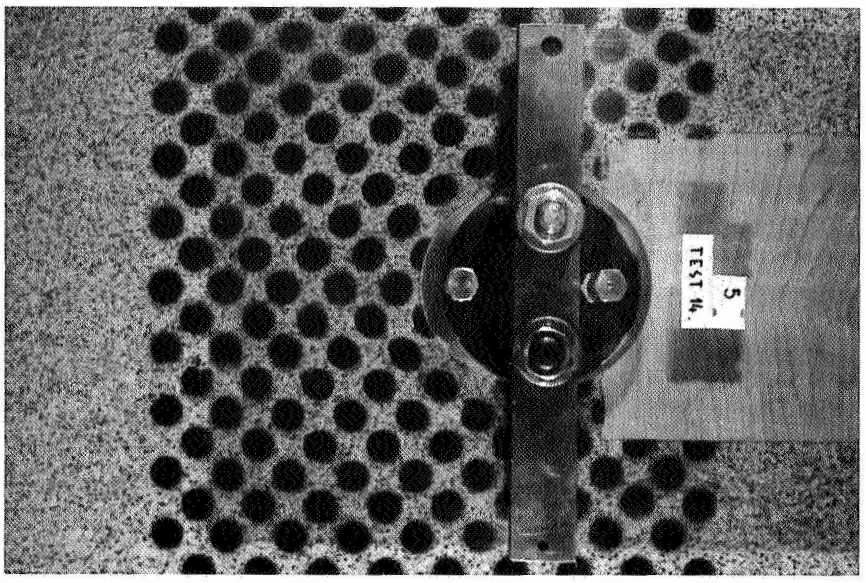

FIGURE 2-29 MODEL TEST NO. 14

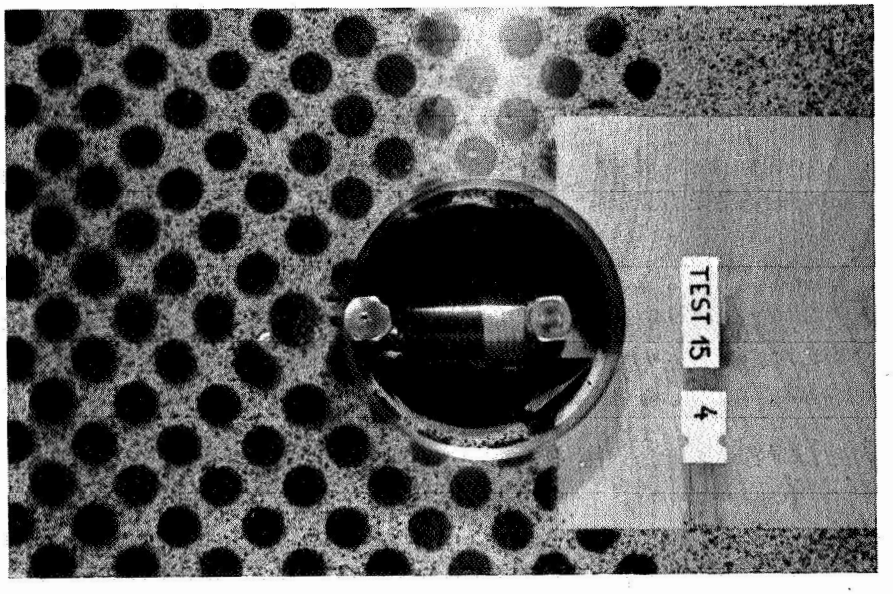

FIGURE 2-30 MODEL TEST NO. 15

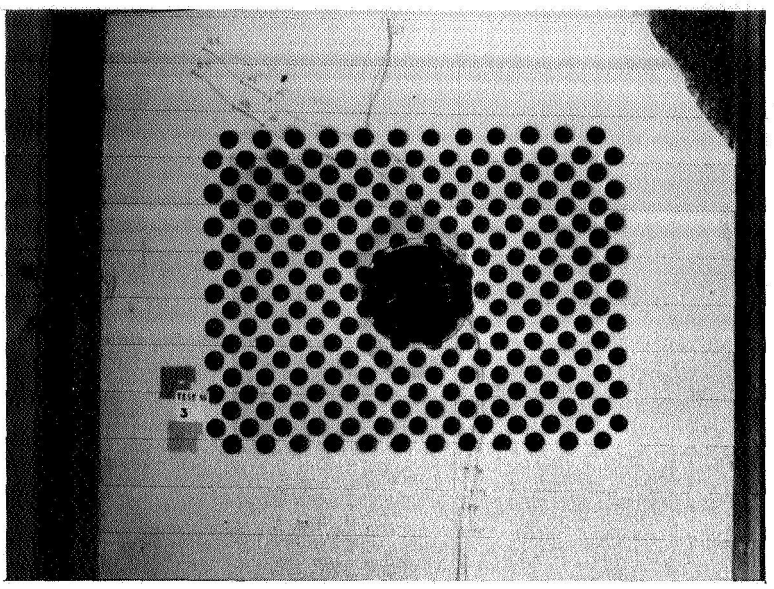

FIGURE 2-31 MODEL TEST NO. 16

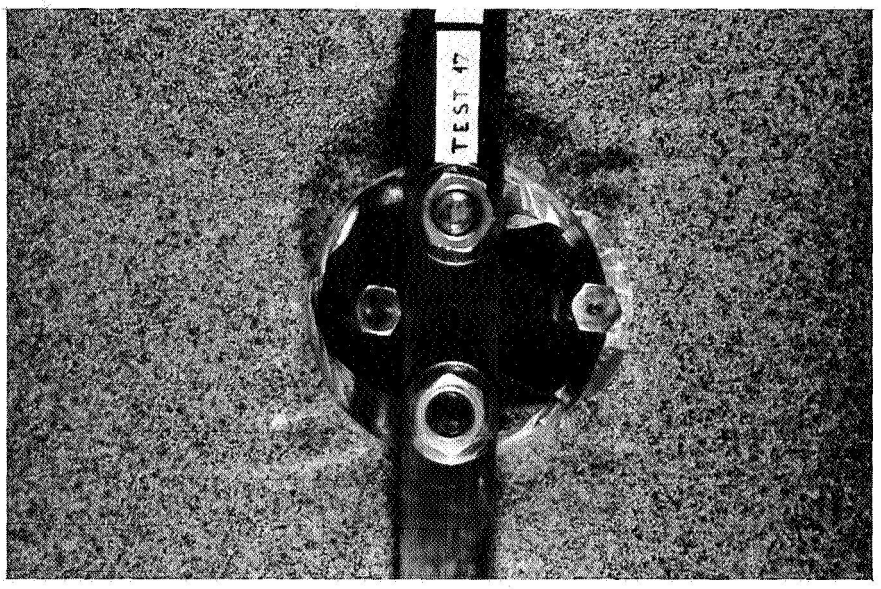

FIGURE 2-32 MODEL TEST NO. 17

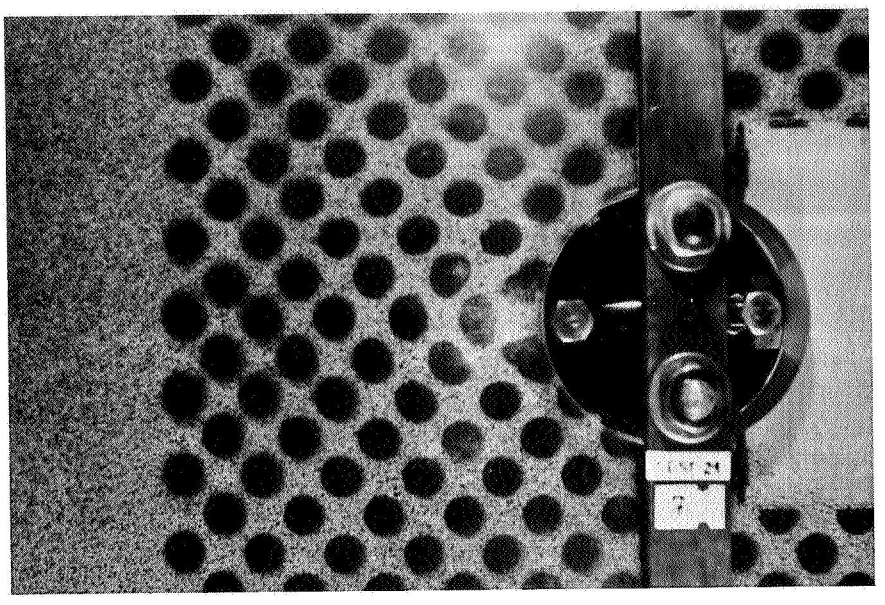

FIGURE 2-33 MODEL TEST NO. 21

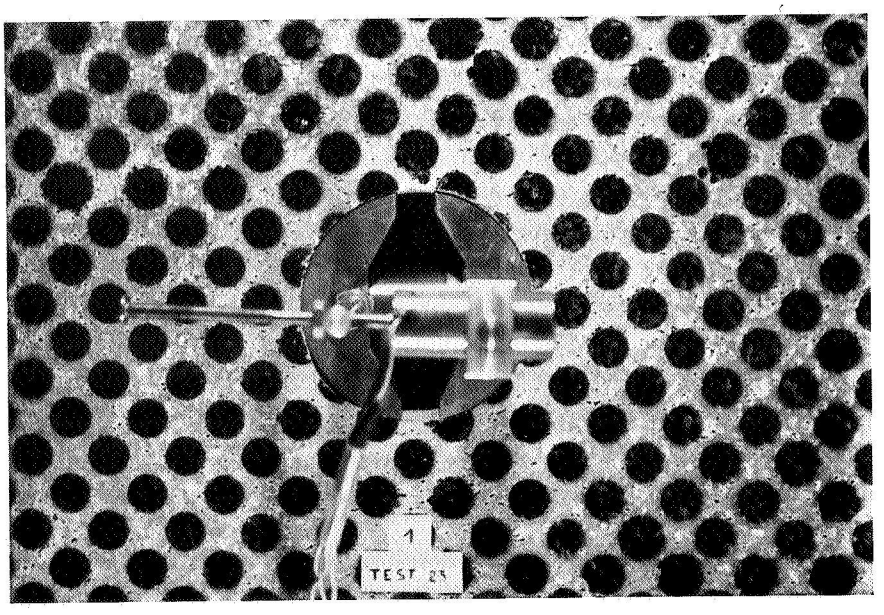

FIGURE 2-34 MODEL TEST NO. 23

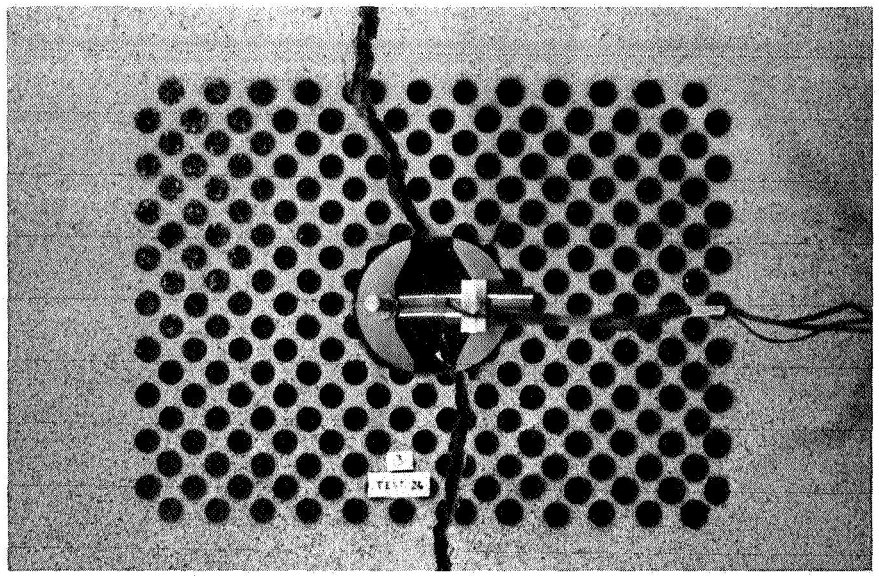

FIGURE 2-35 MODEL TEST NO. 24

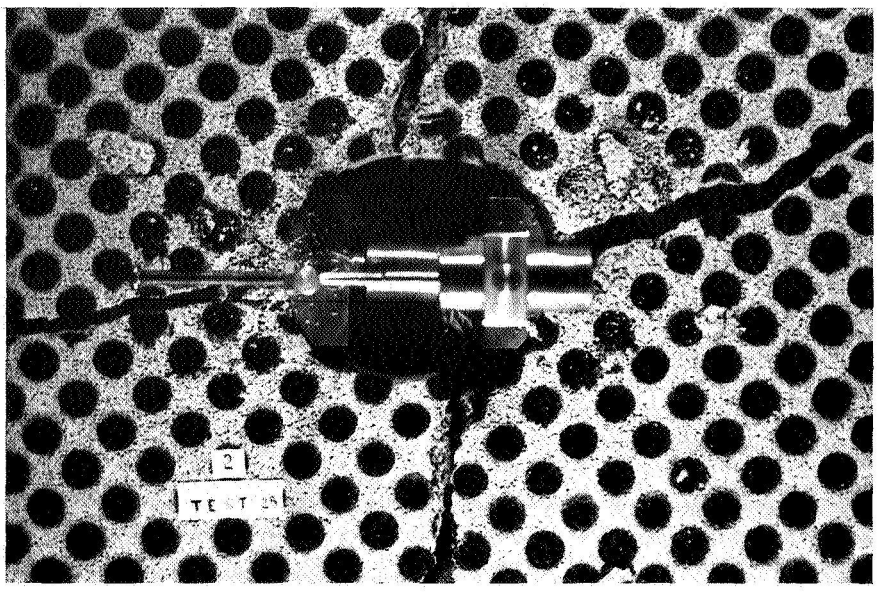

FIGURE 2-36 MODEL TEST NO. 25

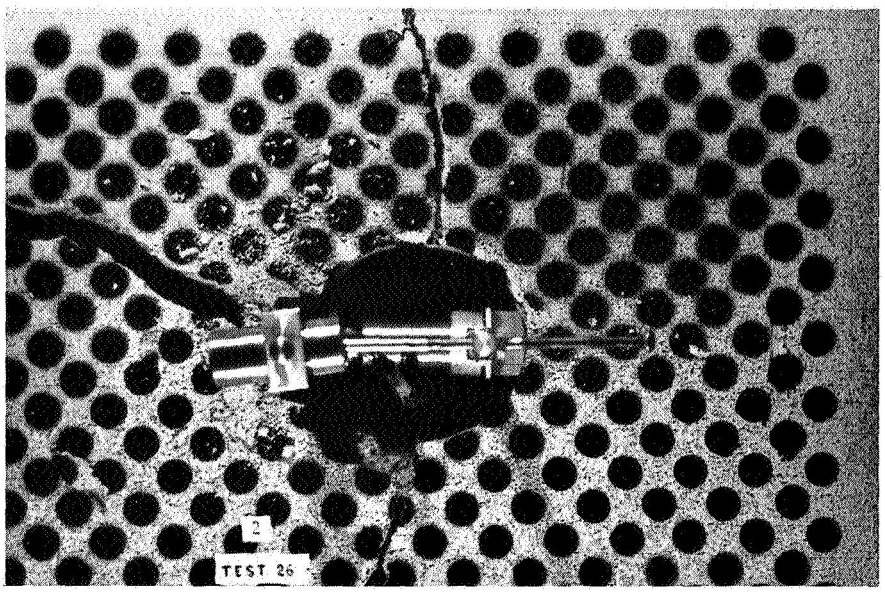

FIGURE 2-37 MODEL TEST NO. 26

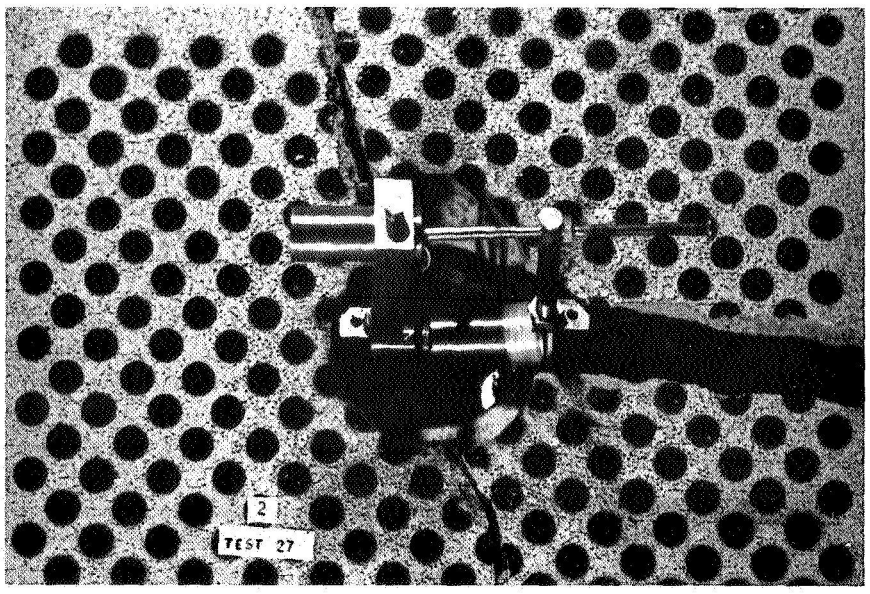

FIGURE 2-38 MODEL TEST NO. 27

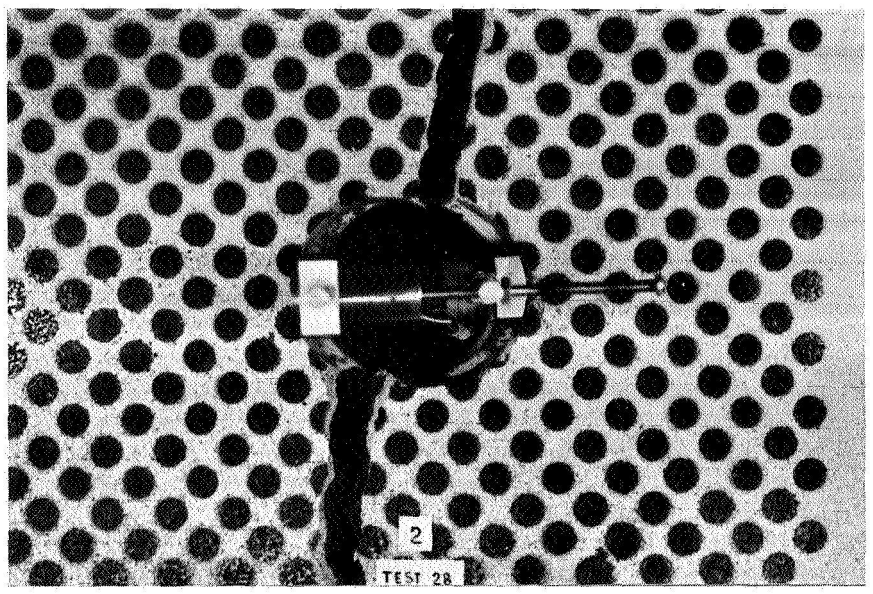

FIGURE 2-39 MODEL TEST NO. 28

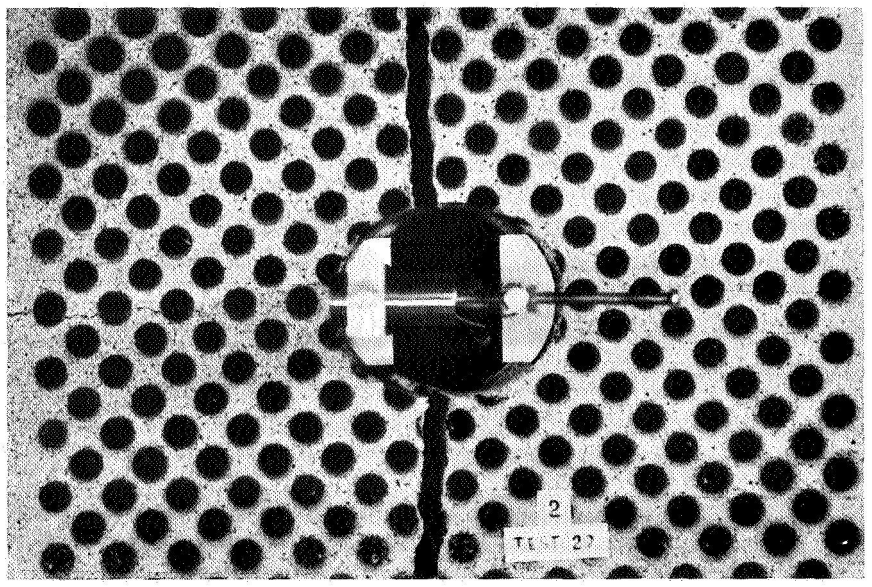

FIGURE 2-40 MODEL TEST NO. 29

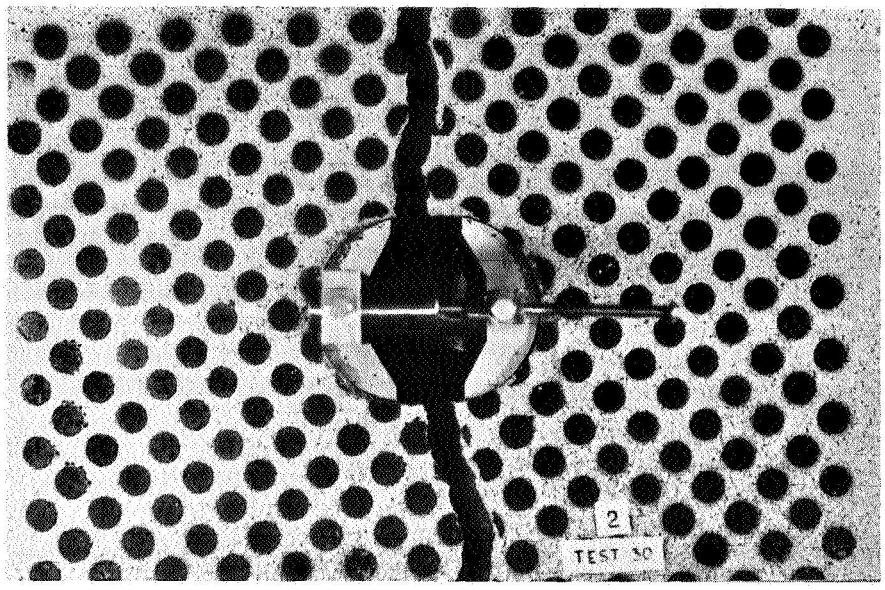

FIGURE 2-41 MODEL TEST NO. 30

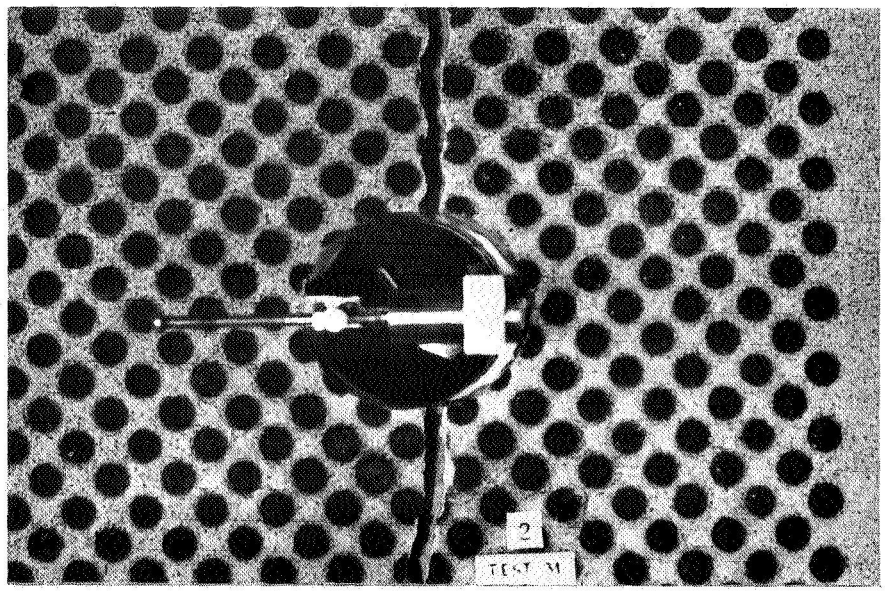

FIGURE 2-42 MODEL TEST NO. 31

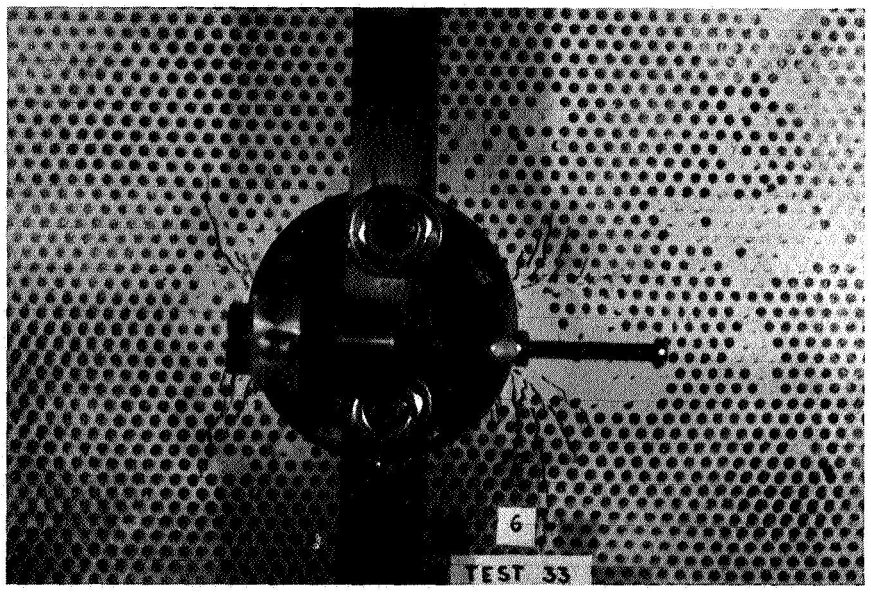

FIGURE 2-43 MODEL TEST NO. 33

3. Tensile cracks initiated at the edge of the borehole. In brittle (and some plastic materials) cracks usually started at one of the edges of the bearing plate (e.g., Figure 2-35). When these cracks propagated outward under increased loading, secondary cracks sometimes propagated from the outside inward. This resulted from the fact that the model plate, being finite, became eccentrically loaded after initial cracking (e.g., Figures 2-36, 2-37, and 2-38). When a uniaxial external load is superimposed on the internal jack load in a direction transverse to the jack axis, the point of cracking moves to the center of the wall between the bearing plates and failure occurs at a lower load (Figures 2-39, 2-40, 2-41, and 2-42).

4. Load-deformation curves are presented in Figures 2-44 and 2-45, the former for tests without and the latter for tests with an external steel frame. The relationships are of three types. In brittle materials, the load-deformation curve is linear ending in rupture. In cohesionless materials, the curve also is linear but was not terminated in the test series as only punching had occurred at maximum load. In plastic materials the rate of displacement increases with load and approaches a constant terminal value.

D. Discussion of Test Results

It is desirable to measure two properties of in situ geologic materials relative to predicting their performance in engineering applications. The first is the deformability. This is useful for making settlement calculations. The second is the shear strength. This is useful in computing the bearing capacity of the material.

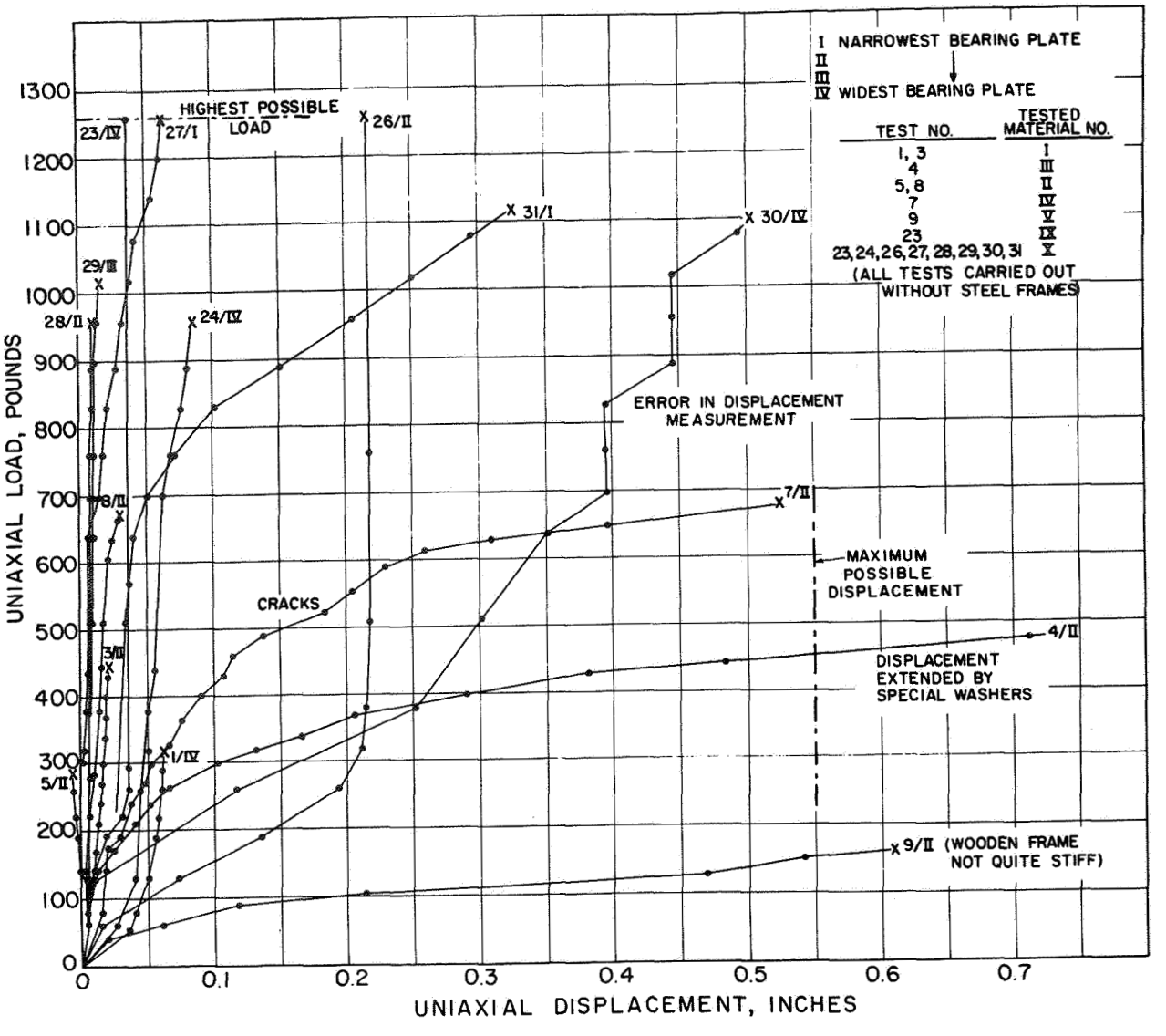

FIGURE 2-44 BOREHOLE JACK TESTS, LOAD-DEFORMATION CURVES

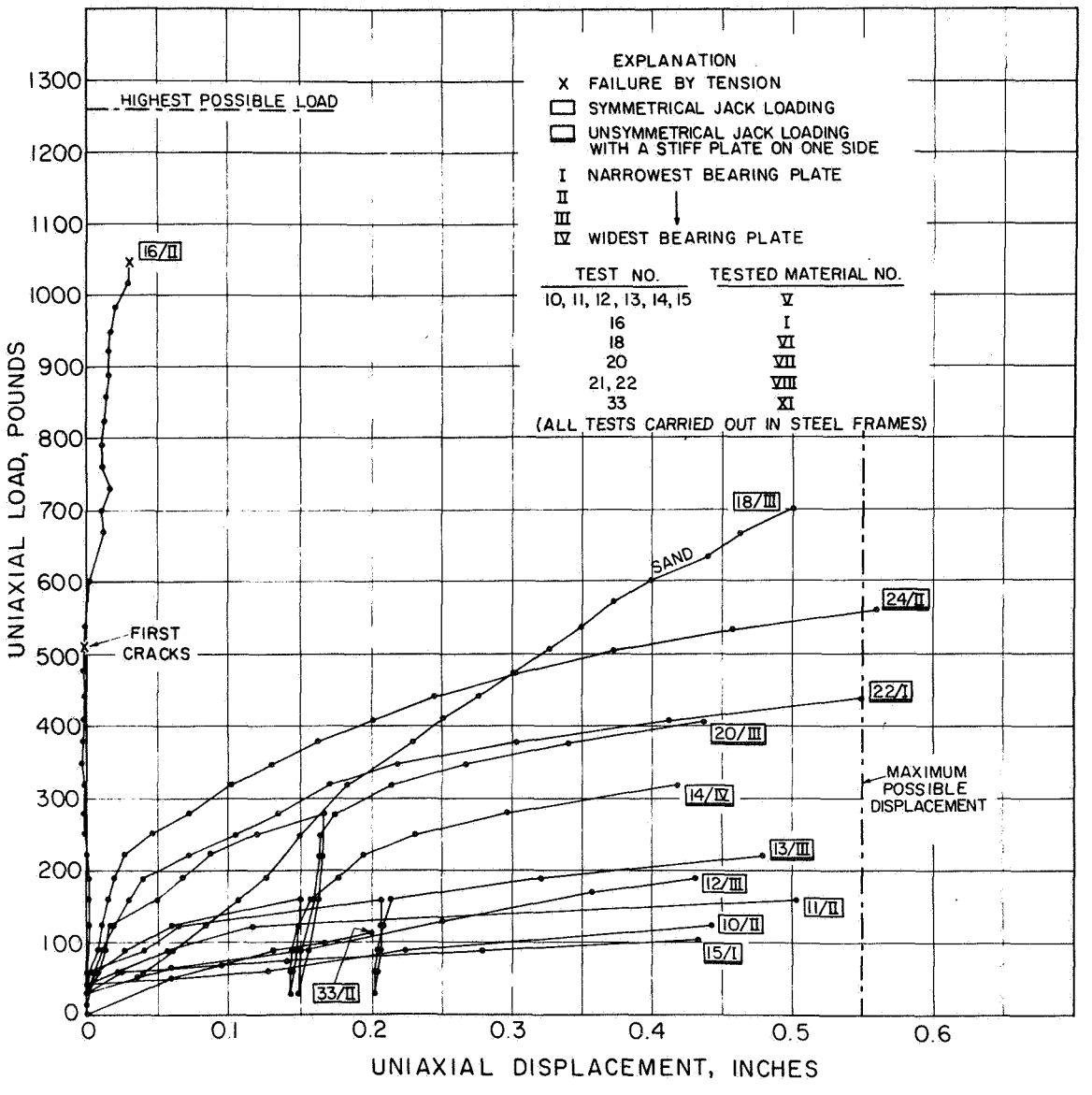

FIGURE 2-45 BOREHOLE JACK TESTS, LOAD-DEFORMATION CURVES

The results of this program reinforce the previous conclusion (Goodman and Heuzé, 1969) that it is practical to determine deformability properties of soils and rocks with a borehole jack but demonstrate that strength properties are difficult to obtain. Rupture parameters for design of foundations against shear failure can not be based, rationally, on empirical rules derived from experiments in which punching was the sole failure mechanism. On the other hand, it is reasonable to determine the strength properties on the basis of a limiting settlement (Tchebotarioff, 1953, and Akroyd, 1957). In this case design parameters can be obtained, in principle, from the results of borehole jack tests.

In each model test, the load corresponding to a certain limiting deformation was reported and the average stress, σ_p, under the loading plate was calculated. σ_p was related to the shearing characteristics of the model materials as determined by direct shear tests. The empirical relationship between σ_p and the shearing parameters, with much scatter, is shown in Figure 2-46. The scatter is due to two factors: (1) the limited number of tests performed to determine shearing resistance, and (2) the large number of variables which were introduced to increase the possibility of shearing failure. As given in Table 2-4, the variables of the model tests are: (1) the dimensions of the tested region, (2) the width of bearing plates, (3) the symmetry of loading, (4) the boundary conditions affecting the shear stresses on the plates, (5) bearing plate friction, (6) methods of measuring displacement, and (7) the smoothness of the borehole.

In this experimental program, the principle objective was to define the behavior patterns of rock and soil in borehole loading configurations so that an appropriate field prototype can be designed. Enough has

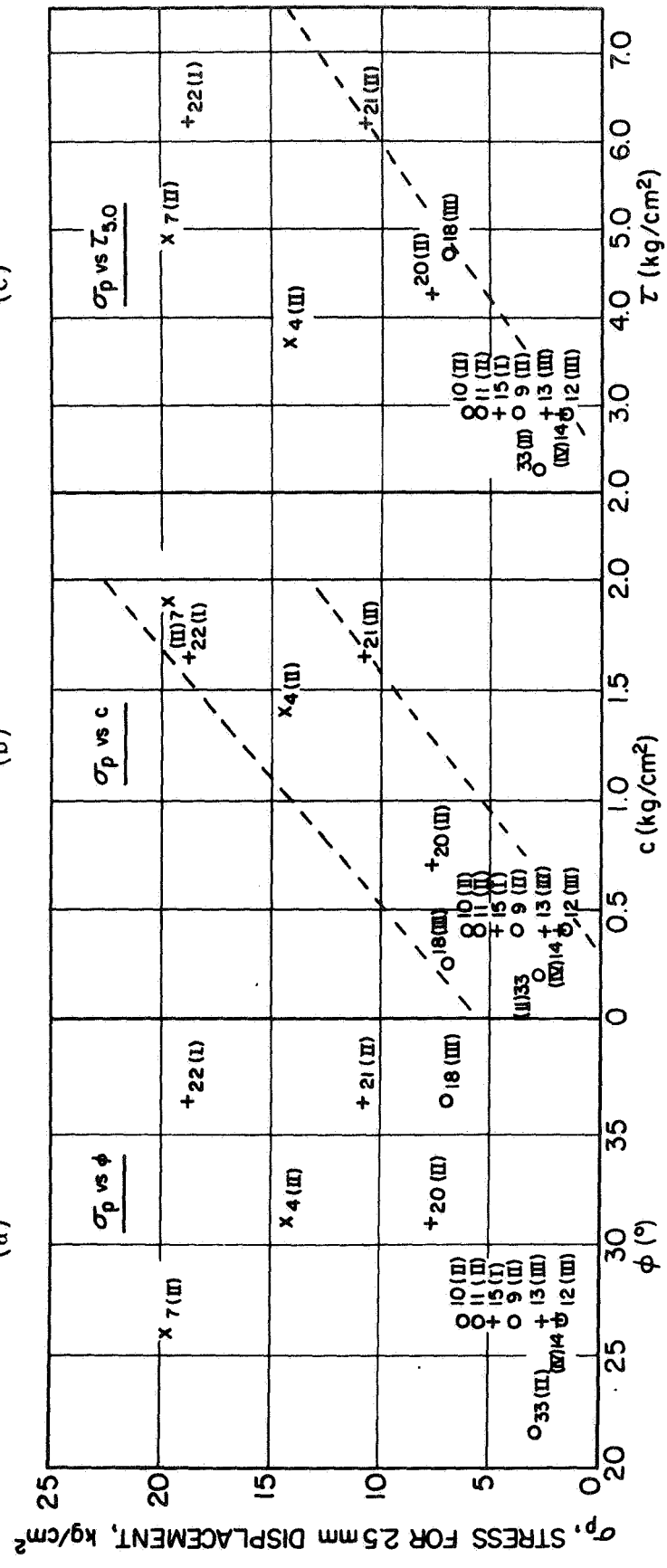

FIGURE 2-46 SHEARING PARAMETER VERSUS STRESS, CORRESPONDING TO 2.5-mm DISPLACEMENT

TABLE 2-4 DESCRIPTION OF SYSTEM VARIABLES

Variable		Test Number																																
		1	2	3	4	5	6	7	8	9	10	11	12	13	14	15	16	17	18	19	20	21	22	23	24	25	26	27	28	29	30	31	32	33
Width of bearing plate	a. plate no. I															X							X					X						
	b. plate no. II		X	X	X	X	X	X	X	X	X	X					X				X	X					X		X			X	X
	c. plate no. III												X	X				X	X	X						X				X				
	d. plate no. IV	X													X									X	X						X			
Dimensions of tested region	a. 36" x 36"	X	X	X																														
	b. 24" x 22.5"				X	X	X	X	X	X														X	X	X	X	X	X	X	X	X	X	
	c. 19" x 19"										X	X	X	X	X	X	X	X	X	X	X	X	X											X
External boundary	a. free	X	X	X	X	X	X	X	X															X	X	X	X	X						
	b. enclosed in a frame									X	X	X	X	X	X	X	X	X	X	X	X	X	X						X	X	X	X	X	X
	c. uniaxially loaded																																	
Symmetry of internal loading	a. in one direction													X	X	X					X	X	X											
	b. in opposite direction	X	X	X	X	X	X	X	X	X	X	X	X				X	X	X	X				X	X	X	X	X	X	X	X	X	X	X
Upper boundary condition affecting normal stresses parallel to borehole	a. free (plane stress)																							X	X	X	X	X	X	X	X	X	X	
	b. plexiglass cover (interm. between plane stress and plane strain)	X	X	X	X	X	X																											
	c. restrained (plexiglass cover, approaching plane strain)							X	X	X	X	X	X	X	X	X	X	X	X	X	X	X	X											X
Boundary conditions affecting shear stresses on lower surface of plate (friction)	a. steel	X	X		X	X	X	X					X							X	X	X	X										
	b. teflon									X	X	X		X	X	X	X	X	X					X	X	X	X	X	X	X	X	X	X	X
	c. paper			X					X																									
Boundary conditions affecting shear stresses on upper surface of plate (friction)	a. free																							X	X	X	X	X	X	X	X	X	X	
	b. plexiglass	X	X	X	X													X																
	c. teflon sheet					X	X		X	X	X	X	X	X	X	X	X		X	X	X	X	X											X
	d. plaster coating							X																										
Bearing plate friction	a. steel against borehole	X	X	X	X	X	X	X					X		X				X	X		X	X	X	X	X	X	X	X	X	X	X	X	X
	b. teflon between steel and borehole								X	X	X	X		X		X	X	X			X													
Method of measuring displacement	a. dial gauge	X	X	X	X	X	X																											
	b. microcaliper							X	X	X	X	X	X	X	X	X	X	X	X	X	X	X	X											
	c. differential transformer																							X	X	X	X	X	X	X	X	X	X	X
Smoothness of borehole (infinitely variable without measurement)	a. very smooth (plaster, mica)	X	X	X													X																	X
	b. moderate smoothness (sand, paraffin)				X		X	X		X	X	X	X	X	X	X		X	X	X	X	X	X											
	c. moderately rough (concrete, mortar)					X			X															X	X	X	X	X	X	X	X	X	X	

been learned that this goal can be considered to have been achieved, as discussed in the next section. When the field instrument is built, all of the system variables will have been defined and calibration tests will then be performed to more clearly evaluate the function relating test material properties.

III. MODEL BEARING CAPACITY TESTS

A. Description of Test Apparatus and Methods

The bearing capacity model tests were conducted to determine the failure mode of the model materials previously described when tested by a load applied perpendicular to the surface. The same four bearing plates (I-IV) were pressed against the upper surface of the model plates, constructed as before. In all tests, the plates were confined by a steel frame to prevent failure by tension cracks. The plates were 40-70 mm thick, which is of the same order as the width of the widest plate. The tests were conducted by driving the plates at a constant deformation rate with a compression testing machine. The load and deformation were recorded.

Three types of tests were run. In Type 1, "unidirectional sinkage," the motion of the plate was constrained to be always normal to the surface. This is the type of test condition of a borehole loading device. The second type of test had no such constraint and is termed "free displacement." In this type a ball bearing allowed the bearing plate to rotate with the deforming foundation. In Type 3 tests friction was reduced at the base of the loading plate by inserting a teflon sheet between the bearing plate base and the surface to be loaded. Again, as in Type 1 tests, the motion of the plate was constrained to be always normal to the surface.

B. Results

The results of the model bearing capacity tests are presented in Tables 2-5, 2-6, and 2-7. Table 2-5 presents ultimate loads and displacements for all unidirectional sinkage tests. The twenty-four tests comprise 6 different materials with four different bearing plates. In Table 2-6, for five materials, results are compared for the three test types: unidirectional displacement, free displacement, and reduced friction. All 15 tests were conducted with the same bearing plate (No. II).

The results presented in Table 2-6 show clearly the decrease of bearing capacity when the method of free displacement and reduced friction is used. The ultimate bearing capacity loads (kg) and the corresponding displacement (mm) are compared and the bearing capacity is expressed as a percentage of the ultimate load in unidirectional tests.

In Table 2-7, results of calculated bearing capacity for plate No. II are given. The bearing capacity was calculated from the well-known Meyerhof equation (Meyerhof, 1951)

$$q_{max} = \gamma D N_q + \gamma \frac{1}{2} B N_\gamma + c N_c \qquad (2\text{-}1)$$

where,

D = the depth of the footing plane below the surface

B = the width of the bearing plate

γ = unit weight of material

N_q, N_γ, N_c = Meyerhof coefficients which depend on the angle of internal friction

c = the cohesion of the material

TABLE 2-5 MODEL BEARING TESTS WITH PLATES I - IV

Testing Mixtures		Bearing Plates							
		I		II		III		IV	
		Ultimate load (kg)	Maximum displacement (mm)	Ultimate load (kg)	Maximum displacement (mm)	Ultimate load (kg)	Maximum displacement (mm)	Ultimate load (kg)	Maximum displacement (mm)
Densified mica	mat. No. XI	20	8.7	36	12.7	45	16.0	51	16.5
Medium sand	mat. No. VI	1.4	11.9	2.7	10.7	6.8	9.7	12.5	18.6
Mixtures (sand, paraffin, mica	mat. No. III	275	7.4	490	7.9	795	10.4	785	10.4
	mat. No. V	18	4.1	39	8.1	56	16.1	59	11.2
	mat. No. VII	55[1]	3.3	151	5.1	189[1]	10.9	232[1]	11.4
	mat. No. VIII	325	5.1	770	8.8	950	not determined	860	9.9

[1] Failure by tensile cracks first, then shearing failure

TABLE 2-6 BEARING CAPACITY TESTS

Type of Material	Mica No. XI		Mixture No. III		Mixture No. V		Mixture No. VII		Mixture No. VIII	
	Ultimate load (kg)	Maximum displacement (mm)	Ultimate load (kg)	Maximum displacement (mm)	Ultimate load (kg)	Maximum displacement (mm)	Ultimate load (kg)	Maximum displacement (mm)	Ultimate load (kg)	Maximum displacement (mm)
Unidirectional Test	36	12.7	490	7.9	39	8.1	151	5.1	770	8.8
Free Displacement	28	10.9	470	5.9	32	6.4	147	5.1	570	5.3
Percentage of Ultimate Load of Unidirectional Test	78%		96%		82%		97%		74%	
Directed Displacement Test with Teflon on the Contact Area	29.5	12.0	380	7.9	37	6.9	141	4.4	525	7.9
Percentage of Ultimate Load of Unidirectional Test	82%		78%		95%		93%		68%	

TABLE 2-7 COMPARISON OF BEARING CAPACITY: CALCULATED - MEASURED

Tested Material (according to Table I)	Shearing Strength		Calculated Values			Model Bearing Capacity Tests		Model Borehole Jack Tests		Ratio Column 8/6
	ϕ ( )°	c kg/cm^2	Coefficient* N_c	Bearing Capacity cN_c kg/cm^2	Bearing Load for Plate II kg	Measured Bearing Load kg	Maximum Displacement mm	Highest Load kg	Maximum Displacement mm	
Column	1	2	3	4	5	6	7	8	9	10
Mica, No. XI	21.5	0.2	16.5	3.3	32	36[1]	12.7	127	12.7[5]	3.5
Medium Sand, No. VI	36.5	0.25	50	12.5	122	2.7[1]	10.7	330[3]	12.7[5]	122.0
Mixtures No. III	31	1.4	34	47	455	490	7.9	245[3]	26.0[3]	0.52
No. IV	26	1.9	23	44	425	not determined		310	10.0[5]	
No. V	26.5	0.4	24	3.6	35	39[2]	8.1	75-87[4]	15[4]	2.2
No. VII	31	0.7	34	24	230	151[2]	5.1	200[4]	12.7[4]	1.3
No. VIII	36.5	1.65	50	83	800	770	8.8	265[4]	12.7[4]	0.35

*Coefficients determined by V. Mencl (Reference 8), corresponding very closely to the values given by G. G. Meyerhof.

1 Lower measured value was influenced by lower cohesion initial strength in the model box in comparison with that determined from the shearing tests.

2 Lower measured value was influenced by tensile cracking.

3 Test carried out with plate No. III.

4 Test carried out with stiff base on one side — the displacement represents deformation only in one direction.

5 Test carried out with displacement measurement across the diameter; to compare column 9 with column 7, it is necessary to divide the displacements in column 9 by a factor of 2.

In Equation (2-1) the shape factor was not introduced as it is felt that this term is insignificant (Feda, 1960, 1961). As the first terms in Equation (2-1) are zero and the second terms are very small, the bearing capacity (column 4, Table 2-7) depends mainly on the coefficient N_c and the cohesion c. For calculations, the angle of internal friction (column 1) and cohesion c (column 2) determined from laboratory shearing tests are introduced (see Table 2-2). The bearing load for the size of contact area of plate No. II is given in column 5. Columns 6 and 7 give the bearing load and corresponding displacement from the model bearing tests. In column 8 and 9, the highest load and corresponding displacement from the uniaxial borehole model tests are given. Column 10 represents the ratio between the highest load from uniaxial borehole model tests (column 8) and the bearing load from model unidirectional tests (column 6).

In the bearing capacity tests, the failures observed were by shearing. The load deformation curve displayed a peak with a classical development of shearing failure as the material below the model plate was thrust out. In harder model materials (mixtures No. VII and VIII), the shearing failure was influenced by tension cracks spreading from the corners of the bearing plate.

Good agreement between the bearing capacity calculated by Equation (2-1) and the measured bearing capacity was obtained in model materials Nos. III, V, VIII, and XI. Owing to the development of tensile cracks in material No. VII, the measured bearing capacity load was lower than the calculated one. There was a large difference between the measured and the calculated capacities in medium sand (material No. VI)

which was attributed to the presence of a slight amount of cohesion in the physical model that was not considered in the calculations. According to the results presented in Table 2-6, bearing capacities were observed to be 4-26% lower for free displacement tests and 5-32% lower for reduced friction tests than for unidirectional sinkage tests.

IV. INTERPRETATION OF BOREHOLE JACK TESTS

Model borehole loading test failures were characterized by cracking in a tension zone created by the jack load or by indentation as a progressive shearing failure (punching). Bearing capacity failure with a classical thrust of material from below the plate was not observed.

In contrast, bearing capacity tests conducted on model plates with flat surfaces displayed classical bearing capacity failures. Occasionally, these failures were accompanied by tension cracks expanding diagonally from the corners of the bearing plates in harder material. Bearing capacity failures were always preceded by significant punching, with sinkage of the order of 6-19 mm.

It might be postulated that punching is a progressive shearing failure culminating in bearing capacity failure at high deformations, and that for one reason or another, deformations sufficiently high to produce bearing capacity failure were not achieved in the model borehole loading tests.

The results presented in Table 2-7 indicate that in two cases (material No. VI, medium sand, and material No. XI, densified mica) the stroke of the model piston might not have been sufficient to completely develope a bearing capacity failure. However, other tests indicated that even when high displacement of the bearing plates was achieved, no ultimate load was reached. This behavior may be attributed to

additional forces involved in the model borehole loading tests, especially forces caused by friction and constraint conditions, raised threshold loads and displacements for bearing capacity failure.

Model bearing capacity tests have shown the influence of constraining the displacement, and the influence of friction on the contact area between the model plate and the borehole wall. These factors can raise the measured bearing capacity by as much as 50%.

In brittle and some plastic materials, another failure mechanism occurs. The ultimate load rapidly decreased after full development of tensile cracks. These cracks propagate outward from the edges of the bearing plates. The rate of spreading depends on the constraint condition. In borehole tests under plane stress condition, the creation of tensile cracks and the spreading was abrupt. The cracks initiated mostly from the edges of the bearing plates. In some cases, especially when uniaxial external load was applied perpendicularly to the direction of uniaxial load in the borehole, the point of cracking moved to the center of the wall between bearing plates. The creation of tensile cracks confirmed the theoretical solutions presented in the previous part.

Let us consider the behavior of rocks and soils in field tests when a borehole jack test is performed on rocks and soils in situ. A curve relating load and displacement can be obtained. These curves can have a peak load which demonstrates either tensile failure, a steadily growing load indicative of punching, or, rarely, a bearing capacity failure.

If it is assumed that punching is usually followed by a bearing capacity failure, then, the shearing characteristics of the tested material are involved in plastic behavior of material below the bearing plates. Therefore, it should be possible to estimate the shearing resistance from the load corresponding to a certain deformation. The problem of evaluating strength in the absence of a peak load occurs occasionally when evaluating shear strength from unconfined compression tests. In those tests where an ultimate load is not reached, the load at 20% strain is used in determining the shearing resistance (Tchebotarioff, 1953, and Akroyd, 1957). The same method can be used for interpretation of borehole jack tests.

Even though many factors influenced model borehole jack test results, Figure 2-46 shows that an evaluation of shearing resistance is possible. A relationship exists (Figure 2-46b) between the cohesion c and average pressure, σ_p, for a certain displacement. Also, a relationship exists between the shear strength mobilized at a constant normal load (5 kg/cm^2) with a given displacement (2.5 mm) (Figure 2-46c).

The accuracy of a working relationship that would allow interpretation of borehole jack data, would, of course, be increased by restricting the system variables to one set. Therefore, to refine the relationship between strength and limiting load, it will be necessary to carry out calibration tests in different materials with the actual borehole jack prototype.

A schematic drawing of a borehole jack for a 3-inch-diameter lunar borehole is shown on Figure 2-47. If a 2-inch diameter lunar borehole jack is selected all dimensions shown on Figure 2-47 should be decreased proportionately. A set of 10 pistons working in

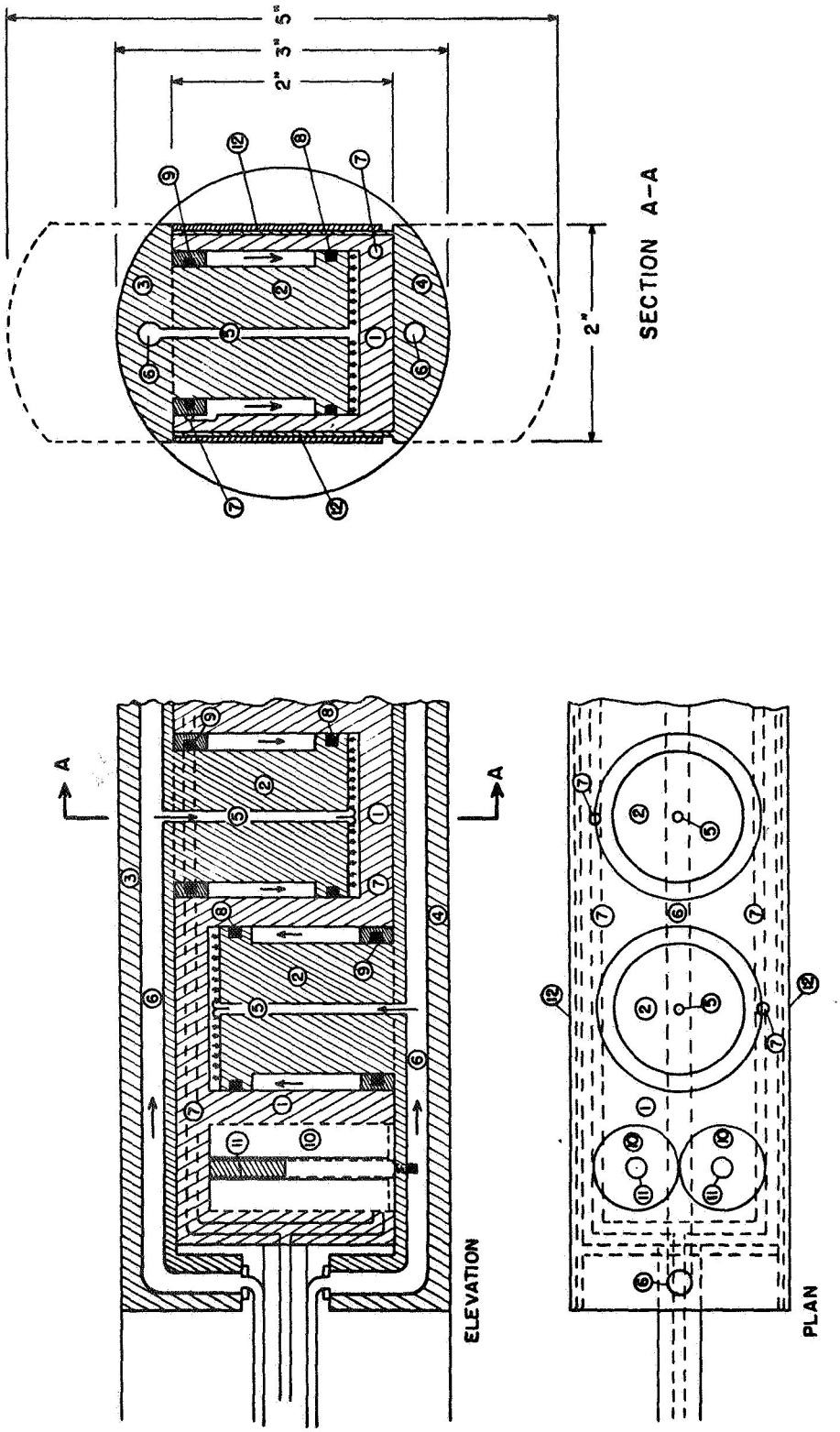

FIGURE 2-47 SKETCH OF PROPOSED LUNAR JACK (SEE APPENDIX B)

opposite directions from a stationary central member is proposed so that a large stroke of 2.0 inches can be achieved. The hydraulic fluid below the pistons is introduced by pipes leading through the movable bearing plates. Two pipes in the center core enable the pistons to contract after the test. On both ends of the borehole equipment, there are four linear variable differential transducers (LVDT). The LVDT's are held by the center member, while the LVDT cores move with the bearing plates. A two inch width of bearing plates corresponding to model bearing plate No. III was found to be most satisfactory. The equipment is to be protected by two telescoping side plates.

The total load created by 10 jacks was calculated to be 81,000 kg. This implies a maximum contact pressure of 260 kg/cm^2 on the bearing plate. This pressure is about 3-5 times higher than the highest pressure of model borehole jack.

The model borehole jack tests have shown the importance of the stress acting parallel to the borehole axis. Therefore, when calibration tests are made with a borehole jack prototype, they should be carried out under stress conditions varying in a direction parallel to the borehole. These calibration tests simulating the different depth of testing in a borehole below the surface should be performed in the same way as the cone penetrometer calibrations that underlie that method.

REFERENCES

1. J. Horeni, M. Petrik, J. Olmer (1958), "Modely z ekvivalentnich materialu (Models of Equivalent Materials)." Research work UTAM-2, Prague.

2. Gregory P. Tchebotarioff (1953), Soil Mechanics, Foundations, and Earth Structures, McGraw-Hill Book Company, London.

3. T. M. W. Akroyd (1957), Laboratory Testing in Soil Engineering, G. T. Foulis and Co. Ltd., London.

4. Richard E. Goodman, Francois E. Heuzé (1969), "The Measurement of Rock Deformability in Boreholes. Material Studies Related to Lunar Surface Exploration." Final Report: Volume II, Space Sciences Laboratory, Series 10, Issue 28, University of California, Berkeley. NASA Contract NSR 05-003-189.

5. G. G. Meyerhof (1951), "Bearing Capacity of Foundations", II, c, 4.

6. J. Feda (1960), "Bearing Capacity and Deformation of Loose Medium." Research report of UTAM. Czechoslovak Academy of Sciences, Prague.

7. J. Feda (1961), "Research on the Bearing Capacity of Loose Soil." Proceedings of the 5th ICSMFE. Paris.

8. Vojtech Mencl (1966): Mechanika zemin a skalnich hornin (Soil and rock mechanics) ACADEMIA, Prague.

APPENDIX A

DESCRIPTION OF MODEL PLATE PREPARATION

A-1. BRITTLE MATERIALS

A. Sand-Cement-Water Mixtures

The proper portions of the basic components were weighed and put into a baker's mixer for several minutes. The mixture was poured into a wooden frame 24 × 22.5 inches lying in a horizontal position. To prevent sticking to the aluminum sheet either Krylon's Silicon Spray No. 1325 or a plastic sheet was used. The plates were water-cured a week and used in tests after 1-2 months air-dry curing.

B. Plaster-Celite-Water Mixtures

The proper portions of the basic components were determined before mixing in the baker's mixer. A retarder was used to prevent the mixture from hardening too fast. The mixture was poured into a steel frame in a vertical position. Krylon's Silicon Spray was used to prevent the mixture from sticking to the casting plates. The mixture was cured in the laboratory with an electric heater before testing.

A-II. COHESIONLESS PLATES — MONTEREY SAND NO. 20

The test plate was separated from the environment by a steel frame and by a rubber sleeve inserted into the center hole. Scotch filament tape was used to seal the frame to the plexiglass sheet and to the teflon base. The same tape was used to seal the rubber sleeve to the walls of the center hole in the plexiglass sheet and the sheet plate beneath the teflon. Special bracing rings of thin steel were used to assure the cylindrical shape of the rubber sheet. After sealing in this manner a vacuum was applied to the sand to produce a slight confinement and thereby maintain the borehole walls.

A-III. PLASTIC PLATES

Plastic plates consisting of mixtures of sand, mica, and parawax were used in an attempt to produce shearing failure. The objectives were: (1) to make plates as weak as possible (to decrease the angle of internal friction and cohesion), and (2) to prepare plates with such a high density that punching failures would be avoided. The first objective was achieved by increasing the proportion of mica and decreasing the paraffin. The second objective was met by increasing the proportion of fine sand.

All weak plates were prepared directly on the testing bench. The corresponding weights of sand, mica, and paraffin were heated up to approximately 80-90°C. All components in the heated state, were mixed in baker's mixer for several minutes. The hot mix was poured in a shell frame 19 × 19 inches or a wooden frame 24 × 22.5 inches. After cooling, the cast plate was prepared for tests. Most tests were performed in a steel or wooden frame in order to avoid a premature tensile failure before punching failure or possible shearing failure.

A-IV. MICA PLATE

The test plate was separated from the environment by a steel frame. Crushed mica powder was confined in the steel frame and subjected to a uniform load up to 40,000 lbs. In order to increase the consolidating process (to press the air out of the powder), a sheet of soft foam plastic was put on the top of the powder below the loading plate. New powder was added so that the total thickness of the densified mica was 1.5 in. The central hole simulating the section of a borehole was carefully cut out. The model borehole test was carried out in plane strain conditions without any protection of the walls in the borehole section.

APPENDIX B

DESCRIPTION OF PROPOSED LUNAR BOREHOLE JACK

The new proposed equipment for uniaxial borehole tests consists of three parts. The center member (1)* is motionless and contains ten cylindrical housings for movable pistons (2).

Five pistons connected to the movable bearing plate (3) move in one direction and five move in the opposite direction (4). Each piston has a total stroke of one inch. This arrangement enables the total expansion of the borehole from 3.0 inches to 5.0 inches.

Hydraulic fluid is brought below the pistons by holes (5) going through the center of each piston, while the main supply is brought through the holes (6) in the movable bearing plates.

The center member has additional holes (7) for the hydraulic fluid used in returning the pistons to their original position. This arrangement needs double sealing rings for each piston. One sealing ring (8) is connected near the base of the piston and moves with the piston. The other one (9) is fixed to the center member and seals on the return stroke.

The displacement of the bearing plates is measured on both ends of the cylindrical equipment by linear variable differential transducers (10). On each end, two transducers are installed. The housings for the transducers are fixed to the center member. The coil cores (11) are fixed to the movable bearing plates (3) and (4).

---

*Numbers refer to points on Figure 2-47.

The bearing plates are two inches wide (projected normal to the piston axis), which corresponds to the size of model bearing plates No. III. The center member is protected on the sides by two telescoping sheets (12) fixed to the bearing plates.

General technical data relating to the proposed jack is as follows:

Total area of 10 piston bases = 113 cm^2

Total contact area of bearing plates = 310 cm^2

Maximum pressure in pistons (10,000 psi) = 710 kg/cm^2

Maximum load = 81,000 kg

Maximum pressure in contact area of bearing plates = 260 kg/cm^2.

CHAPTER 3

BOREHOLE JACK TESTS IN JOINTED ROCK — JOINT PERTURBATION AND NO TENSION FINITE ELEMENT SOLUTIONS

(Francoise E. Heuzé, Richard E. Goodman, and Ann Bornstein)

I. INTRODUCTION

Sound design of structures in or upon rock requires a thorough knowledge of the rock mass deformability. Instruments have been designed to obtain this information from tests in drill holes. The advantages of borehole tests are well established when compared to more cumbersome experiments (plate bearing, pressure chamber) and their easy repetition enables a thorough coverage of a given engineering site (Van 1967, Heuzé 1967).

Of all devices — penetrometers, dilatometers, plate jacks — the borehole jacks have been determined to be best suited to field conditions and data analysis, owing to the high pressure they can apply and the rigid loading boundary conditions they insure.

A closed form, analytical solution, was first obtained by Van (1967) for the problem of uniaxial jack loading of a borehole wall. The medium was assumed to be isotropic and elastic. The influence of a possible tensile crack formation on data reduction was also included in the initial study of the borehole jack problem and review of instruments (Goodman, Van, and Heuzé 1968). This last approach did not modify the medium's properties but rather changed some of its displacement boundary conditions. (It will be referred to here as "joint simulation" technique). It provided a lower bound on the value of the modulus of deformation (half a borehole in a semi-infinite medium). An upper bound is indeed provided by the elastic solution.

The true response to jack loading of a jointed rock mass or of a medium unable to resist tensile forces was not yet satisfactorily modeled. The need was thus underscored for a narrowing of the upper bound-lower bound bracket using improved techniques. They are proposed here as a refined "joint pertrubation" analysis and a "no tension" analysis. An idealization of the problem is given on Figure 3-1 for a single radial joint.

II. "JOINT PERTURBATION" ANALYSIS

A. Joint Perturbation Program

A joint element was developed by Goodman, Taylor, and Brekke (1968) and applied to several rock mechanics problems: sliding of joint with a tooth, behavior of joint intersections, tunnel in a system of staggered rocks. Heuzé and Goodman (1967) also used it to simulate the behavior of mine roofs.

The original version defined normal and shear stiffnesses, K_N and K_S, for joints and assembled the linkage element into the overall structure. Since appreciable movement can take place at the level of the joints and their properties might then change, the procedure has to be an iterative one. Two major refinements were introduced in the original program.

(1) Initial stress field

An initial stress field can now be input (always compressive) in a structure with joints. (See Appendix A - Subroutine JTSTR). The stress and displacement sign convention is illustrated in Figure 3-2. This model satisfies displacement compatibility of the joint elements and solid elements, and joint stresses are computed for each joint from its nodal points displacement.

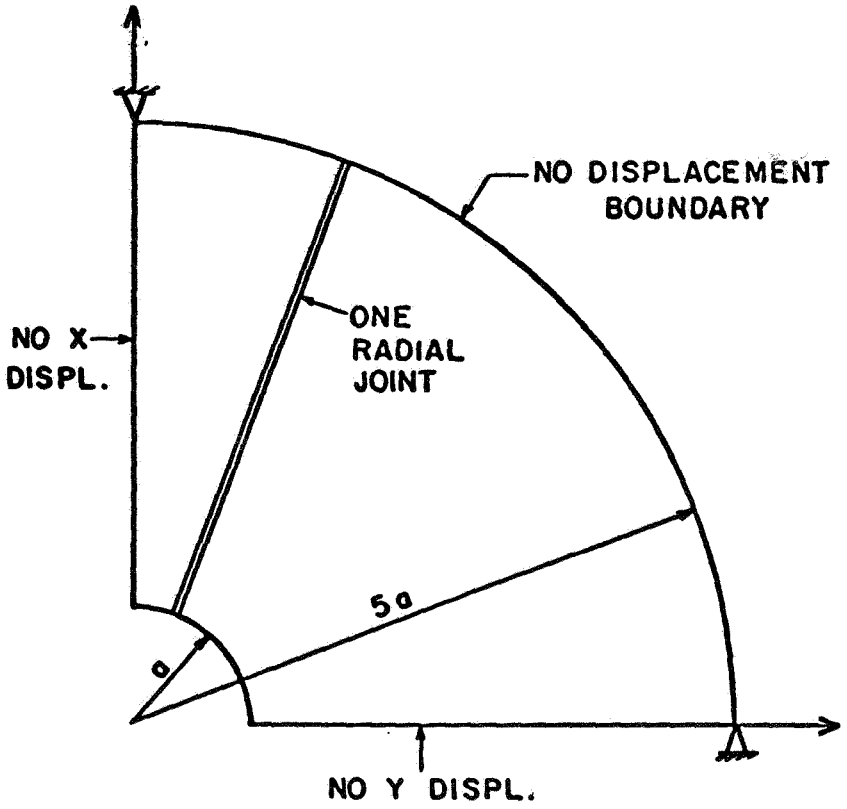

FINITE ELEMENT IDEALIZATION AND
BOUNDARY CONDITIONS ON MESH.
THREE TYPES OF MESHES WERE USED.

NODAL POINTS	ELEMENTS
775	720
380	342
131	110

FIGURE 3-1

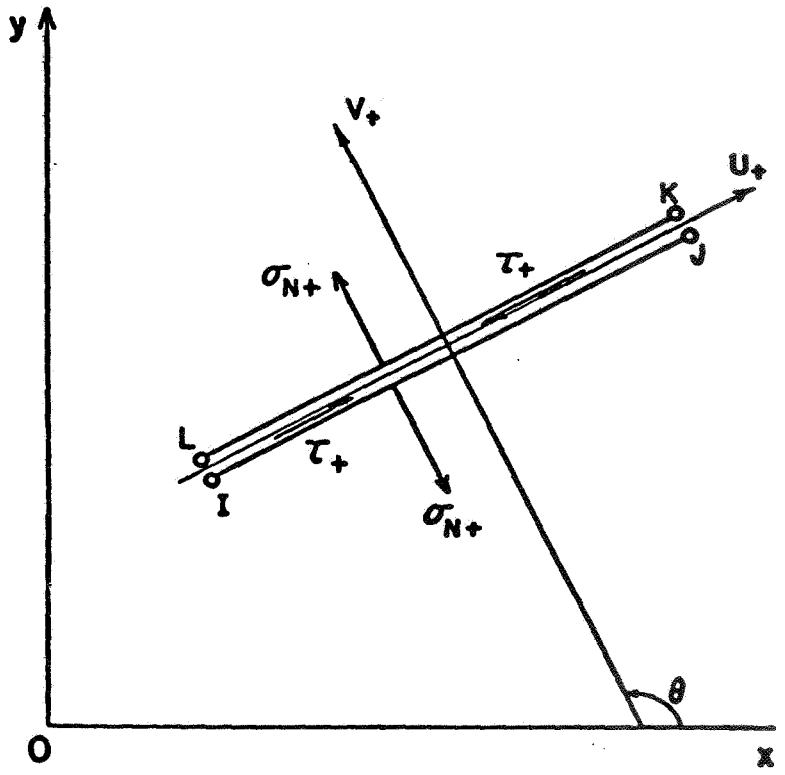

LINKAGE OR "JOINT ELEMENT" WITH ITS
LOCAL COORDINATE SYSTEM.
THE SIGN CONVENTION ON STRESSES
AND DISPLACEMENTS IS INDICATED.

FIGURE 3-2

With the initial stress feature one can truly model excavating in a jointed medium where the discontinuities can all be recognized and mapped.

(2) Shear and normal joint stiffness modifications

As displacements take place at the joints, normal and tangential properties must be modified.

Shear Stiffness: Originally K_S would be set equal to zero if tension developed across the joint and set to a residual predetermined value if the shear stress in the joint exceeded the joint strength. The new approach, as illustrated in Figure 3-3, is more flexible; joint strength depends upon the joint properties and the normal stress acting at any time across it — any change in shear stiffness will be progressive so that the joint will always tend to stay at its peak strength for a given state of the structure. No arbitrary modification of its properties is imposed.

Normal Stiffness: Previous versions would set the normal stiffness to zero upon joint opening and set it to an arbitary high value upon closure. New stiffness modifications as shown on Figure 3-4 are designed to adapt progressively to tendencies of the joint either to open or to undergo excessive closure (this simulates for example the presence of a soft filling material which can be extruded).

Owing to the more flexible response of the modified joint element, convergence is insured in a smooth manner, provided the structure does not fail, and a low number of iterations (typically 4) leads to a stable and realistic solution.

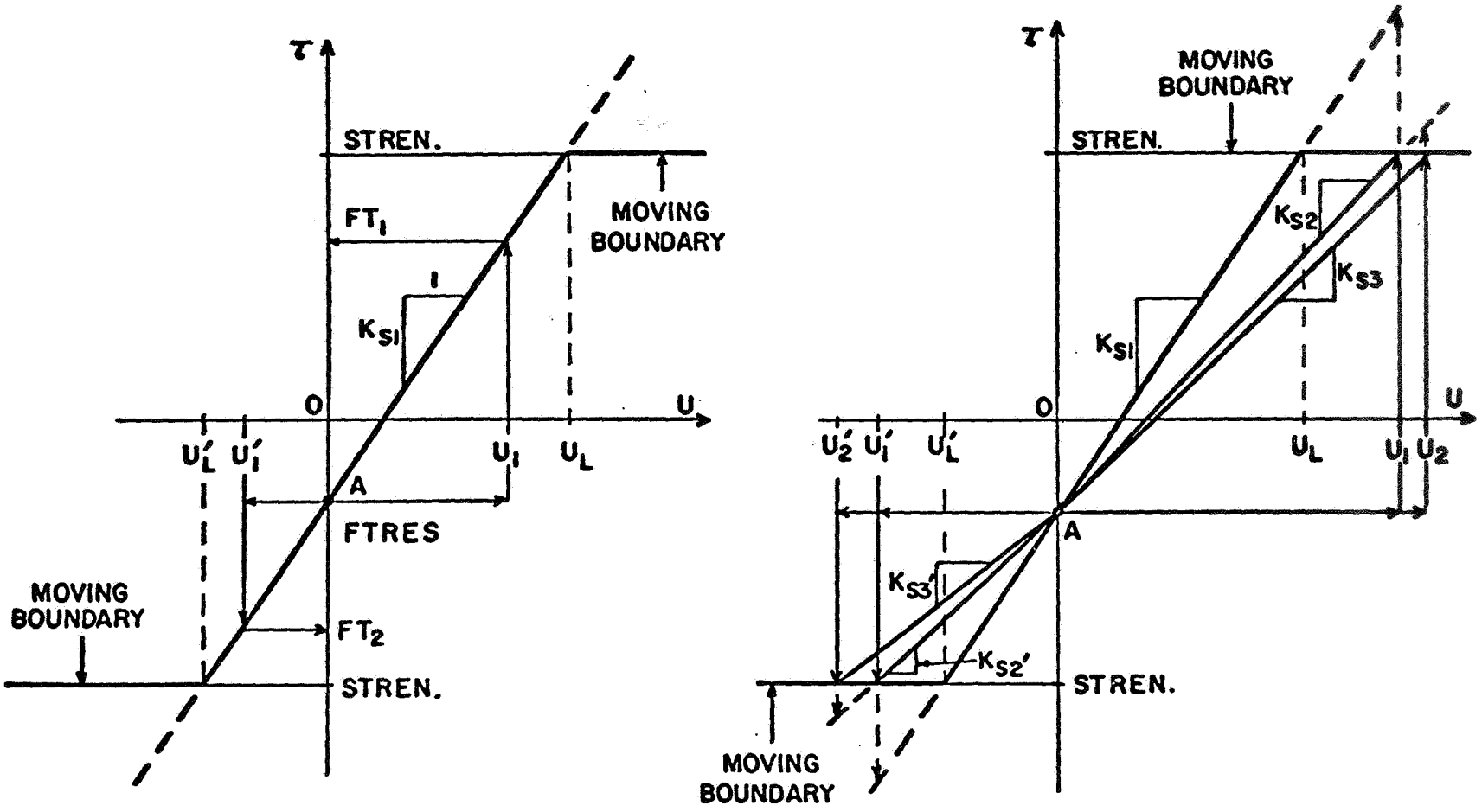

a) DISPLACEMENT STRESS + INITIAL STRESS <STRENGTH — STABLE SOLUTION IN ONE ITERATION.

b) FINAL SHEAR STRESS (FT = FTRES + K_S × U) WOULD EXCEED STRENGTH — NEED TO REDUCE STIFFNESS AND ITERATE.

FIGURE 3-3 SHEAR STRESS (τ) VS. TANGENTIAL DISPLACEMENT (U) FOR "JOINT ELEMENTS". STIFFNESS WILL BE MODIFIED IF STRESS TENDS TO EXCEED ALLOWABLE STRENGTH

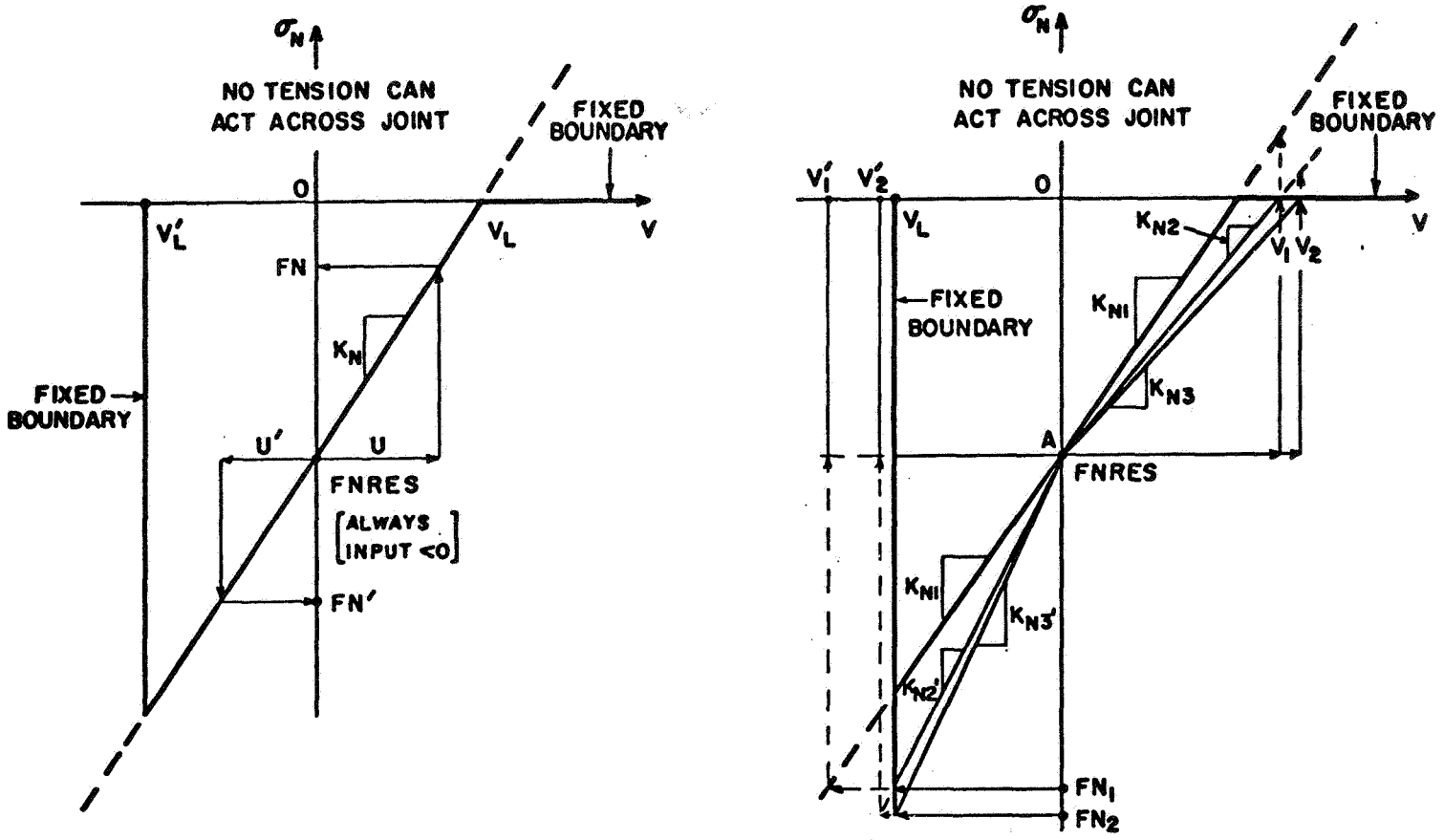

a) NO LIMITS EXCEEDED.
STABLE IN ONE ITERATION.

b) EITHER LIMIT EXCEEDED.
SEVERAL ITERATIONS REQUIRED.

FIGURE 3-4 NORMAL STRESS VS. NORMAL DISPLACEMENT FOR "JOINT ELEMENTS".
STIFFNESS WILL BE MODIFIED IF TENSION TENDS TO DEVELOP (K DECREASED)
OR IF CLOSURE TENDS TO EXCEED MAXIMUM ALLOWABLE (K INCREASED)

B. Application to Jacking Tests

Many types of joints, in various directions, can intersect a borehole where a deformability test is being conducted. Some of them will critically affect the results of the tests by allowing more plate displacement for a given hydraulic pressure than would be expected in an unfractured medium. Since modeling all possible joints is being practical, the approach adopted was to confine oneself to a set of radial fractures of variable inclinations. They represent a means of describing the full change of properties of the medium from semi-infinite (lower bound) to infinite elastic (upper bound).

As shown on Figure 3-5 one notes that these joints fall in either of two categories—intersecting the bearing plate or not. Within each category, results expressed in terms of the average pressure obtained under the jack plate for a given displacement are from fairly uniform (joints not intersecting) to slightly variable (apparent hardening at the medium as the tensile component of jacking across the joint decreases — see Figure 3-8).

Even in a moderately fractured rock which could be considered globally competent, local discontinuities will very probably be found in such a position that they will influence the test results to, or close to, the maximum possible extent. Their influence is to reduce drastically the ability of the medium to sustain tension, thus apparently reducing the stiffness of that rock volume involved in the test.

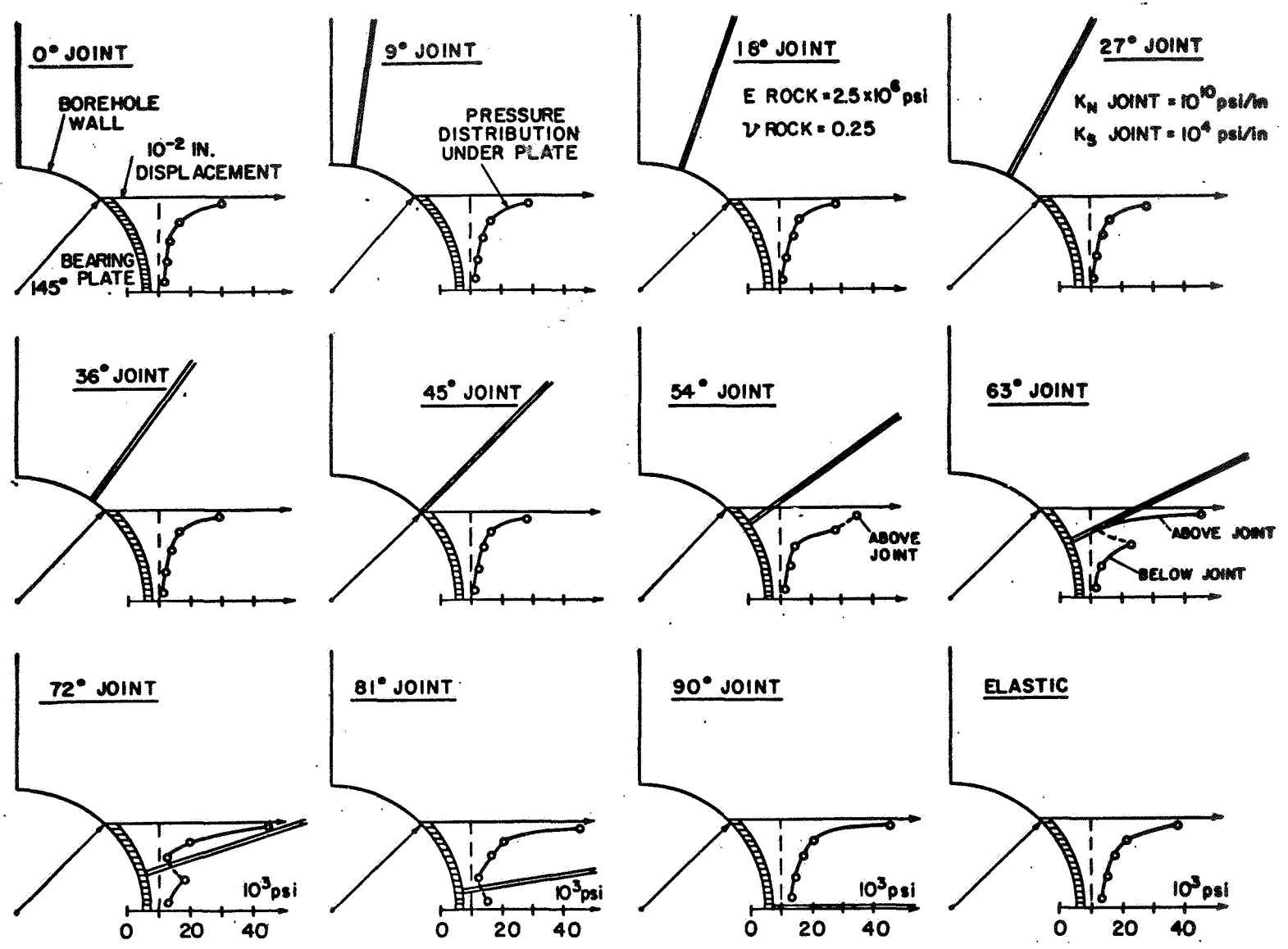

FIGURE 3-5 INFLUENCE OF RADIAL JOINT ON THE DISTRIBUTION OF PRESSURE UNDER A BOREHOLE JACK PLATE SUBJECTED TO A CONSTANT DISPLACEMENT FINITE ELEMENT ANALYSIS — JOINT PROGRAM

If a formula of the type

$$E = K(\nu,\beta)\ \frac{\Delta Q}{\Delta u_d/d}$$

E = modulus of deformation
ΔQ = increase in jack pressure
Δu_d = increase in diametral bore hole deformation
d = borehole
ν = Poisson's ratio
β = bearing plate half-angle

is used (Goodman, Van, and Heuzé 1968), an increase of K (ν,β) from its elastic solution value will be required so that the actual modulus of deformation in compression of the rock will be obtained. From what preceedes this increase can so far be set at 25 to 30%, but further refinement is possible as discussed.

III. "NO TENSION" ANALYSIS

A. Rock as a "No Tension Material"

Knowing that jointed rock masses respond differently to compressive and tensile forces, finite element modeling has taken different forms, each of them subject to shortcomings. Multilinear analysis using incremental loading is very time consuming and joint perturbation techniques are fully satisfactory only if a reasonably thorough mapping of discontinuties is feasible at a given site. Thus a global approach not requiring point-to-point mapping of the medium, but involving reasonable computing time, would be most useful. Such a procedure has been presented by Zienkiewicz et al. (1968, 1969) under the name of "no tension" analysis or "stress transfer" technique.

The procedure is as follows:

(1) Obtain an elastic solution to the problem at hand, giving compressive and tensile stresses, if any, in the structure.

(2) Re-analyze the structure under only those tensile stresses previously developed. Add the new compressive stresses to the previous one and store them, and again analyze the structure with the latest tensile stresses as input.

(3) Repeat step 2, until no appreciable difference in magnitude and distribution of stresses is obtained upon iterating. One can then consider the region of irreducible tensile stresses as a cracked portion of the medium, thus giving a qualitative evaluation of fracture initiation and propagation problems.

B. Application to Jacking Tests

A computer program* (See Appendix B3) was thus developed for no tension analysis from the two-dimensional Finite Element formulation due to Wilson (1963, 1965). Since the global stiffness of the structure is not modified upon iterating, considerable saving of computing time is accomplished (each iteration after the first one requires only 15% of the elastic solution time).

However, in order to get quantitative results for the borehole jack problem, a last step was added to the procedure: the cracked zone was given modified properties (greatly reduced stiffness) and the problem was analyzed elastically once more with the original boundary conditions.

---

*A user's manual for both "Joint Perturbation" and "No Tension" computer programs is included as Appendix C3.

The efficiency of the technique in reducing tensile stresses and delineating a cracked region is apparent in Figure 3-6. Generally 7 to 8 iterations are sufficient to give a satisfactory answer. At convergence, a finite, low percentage of the original highest value of tension is used to determine the actual boundary of that region (5% here) before the last run. Thus complete solution involves about 3 times the computing required for an elastic solution, as opposed to about 4 times for joint solutions and more for multilinear analysis. Figure 3-7 shows the need for delineating the cracked region quite precisely by previous runs rather than arbitrarily trying to model it.

IV. SUMMARY, CONCLUSIONS

The results of all studies are presented in Table 3-1 and can be regrouped as follows:

(1) Elastic solutions. Two different finite elements were used; the original-4-nodal point quadrilateral element (Program 1, Wilson 1963, 1965) and a refined 5 nodal point element (Program 2, Doherty, Wilson & Taylor 1969). Three different mesh sizes were also used (775, 380, and 121 nodal points) requiring, respectively, 220, 80, and 20 seconds of CDC 6400 for an elastic solution. Average plate pressure obtained with the coarsest mesh were only 3% off from those obtained with the finest when a proper concentration of elements was insured in the region of highest stress gradients. The 121 N.P. mesh was thus consistently used thereafter at a considerable saving of computer time.

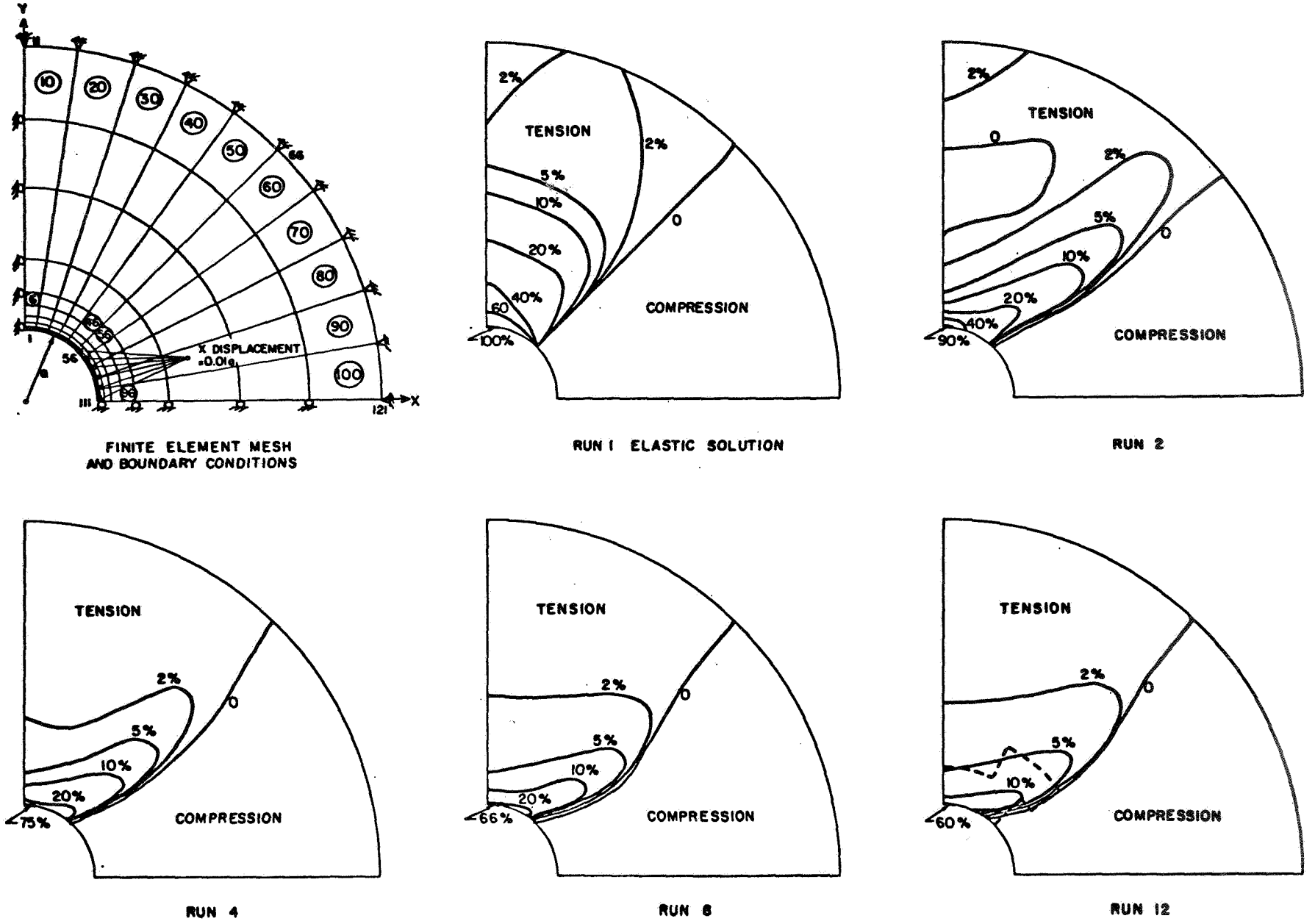

FIGURE 3-6 REDISTRIBUTION OF STRESSES (σ_x) AND DISSIPATION OF TENSION IN UNIAXIAL JACK LOADING
(100% IS THE MAXIMUM TENSILE STRESS OF ALL ELEMENTS IN THE FIRST ITERATION)

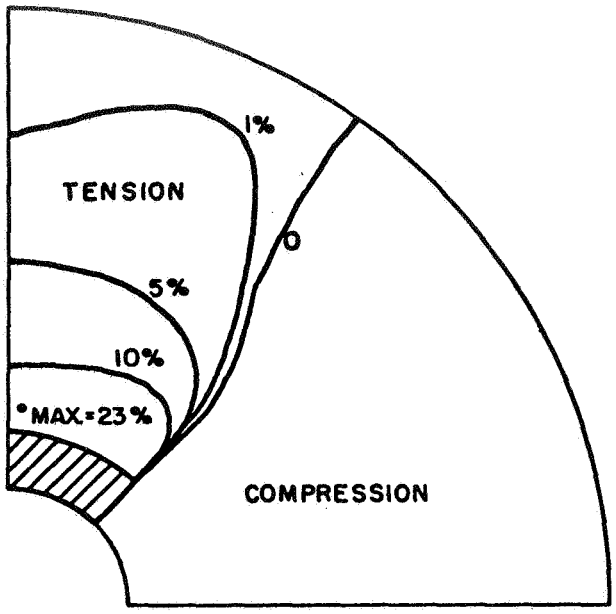

FINAL RUN: OPTION 1

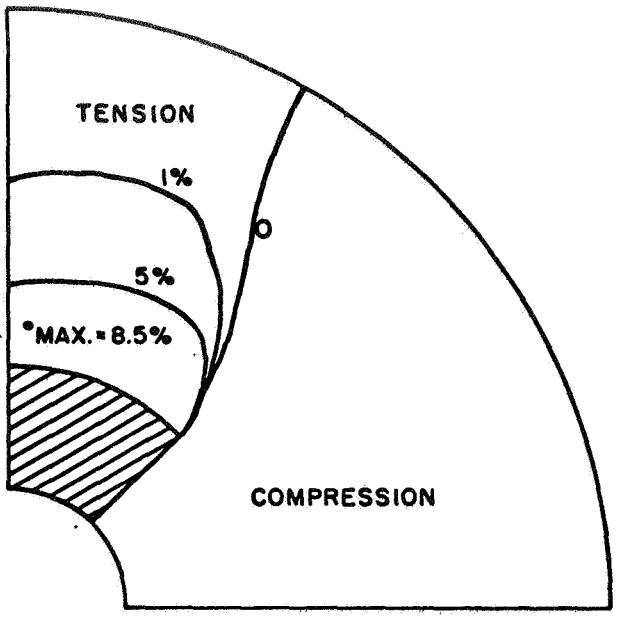

FINAL RUN: OPTION 2

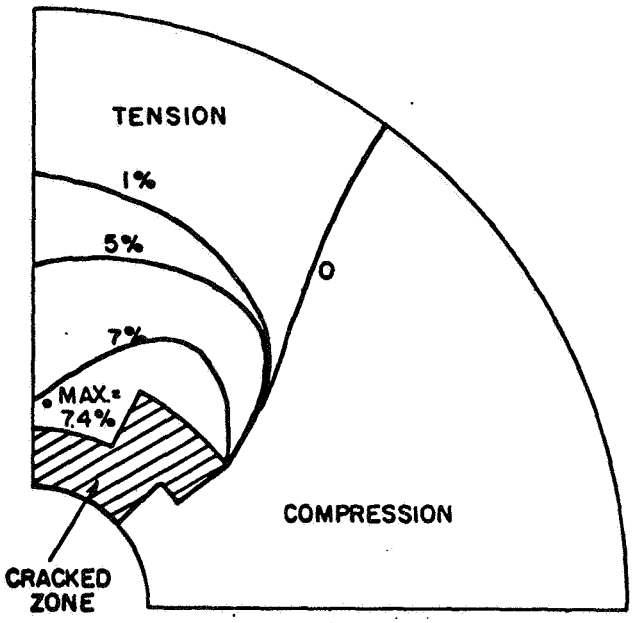

FINAL RUN: OPTION 3

(OPTIMUM - BASED ON 5% CONTOUR, RUN 12)

FIGURE 3-7 CHOICE OF MODIFICATIONS FOR FINAL RUN

TABLE 3-1

SUMMARY OF RESULTS FOR FINITE ELEMENT ANALYSIS OF THE BOREHOLE JACK PROBLEM

$E = 2.5 \times 10^6$ psi d = 1 in $U_x = 10^{-2}$ in

SOLUTION		MESH SIZE	AVERAGE PLATE PRESSURE (psi)	K (ν,β)
ELASTIC	PROGRAM 1	775 N.P.	20920	1.250
ELASTIC	"	380 N.P.	20896	1.254
ELASTIC	"	121 N.P.	20190	1.292
ELASTIC	PROGRAM 2	775 N.P.	20925	1.250
ELASTIC	"	380 N.P.	20913	1.250
ELASTIC	"	121 N.P.	20025	1.309
0° JOINT SIMUL.	PROGRAM 1	121 N.P.	15715	1.664
0° JOINT SIMUL.	PROGRAM 2	121 N.P.	15625	1.672
0° JOINT HARD	JOINT PERTURBATION	121 N.P.	16260	1.607
9° JOINT SOFT	" "	121 N.P.	15905	1.640
9° JOINT HARD	" "	121 N.P.	15905	1.640
18° JOINT HARD	" "	121 N.P.	15725	1.660
27° JOINT HARD	" "	121 N.P.	15810	1.651
36° JOINT HARD	" "	121 N.P.	16085	1.625
45° JOINT HARD	" "	380 N.P.	16609	1.572
45° JOINT HARD	" "	121 N.P.	16015	1.631
45° JOINT SOFT	" "	121 N.P.	16015	1.631
54° JOINT HARD	" "	121 N.P.	20355	1.288
63° JOINT HARD	" "	121 N.P.	20465	1.276
72° JOINT HARD	" "	121 N.P.	20730	1.261
81° JOINT SOFT	" "	121 N.P.	21000	1.244
81° JOINT HARD	" "	121 N.P.	20745	1.260
90° JOINT HARD	" "	121 N.P.	21100	1.240
NO TENSION	OPTION 3	121 N.P.	16100	1.622
NO TENSION	OPTION 2	121 N.P.	17000	1.538
NO TENSION	OPTION 1	121 N.P.	18300	1.428

(2) Joint perturbation solutions. Included were radial joints of different inclinations and surface properties. As expected, Figure 3-8 shows that the properties of joints have little effect on the results as long as these are subjected to predominant tension. As the shear component increases along the joint, the medium seems to harden.

(3) No tension solution. As shown in Figure 3-8 and in Table 3-1, results of no tension analysis using the best final option agree remarkably well with those of joint problem where tension is almost completely eliminated by the presence of a critical discontinuity.

Thus refinements have been made to existing Finite Element programs and new options have been developed. Their results agree, indicating that, given a jointed medium or any rock mass where tensile cracks are likely to develop upon application of high loads, results of elastic solutions have to be appreciably revised. In the case of borehole jack tests, the actual modulus of deformation of the rock in compression shall be taken as 29 to 30% higher than the elastic solution value.

Joint perturbation and no tension programs as presented here remain complementary to each other in most rock mechanics field problems, as the possibility of mapping significant discontinuities of a rock mass and determining their in situ surface properties may or may not exist. A realistic lower bound solution is thus permanently available, to insure meaningful application of rock engineering tools to actual designs.

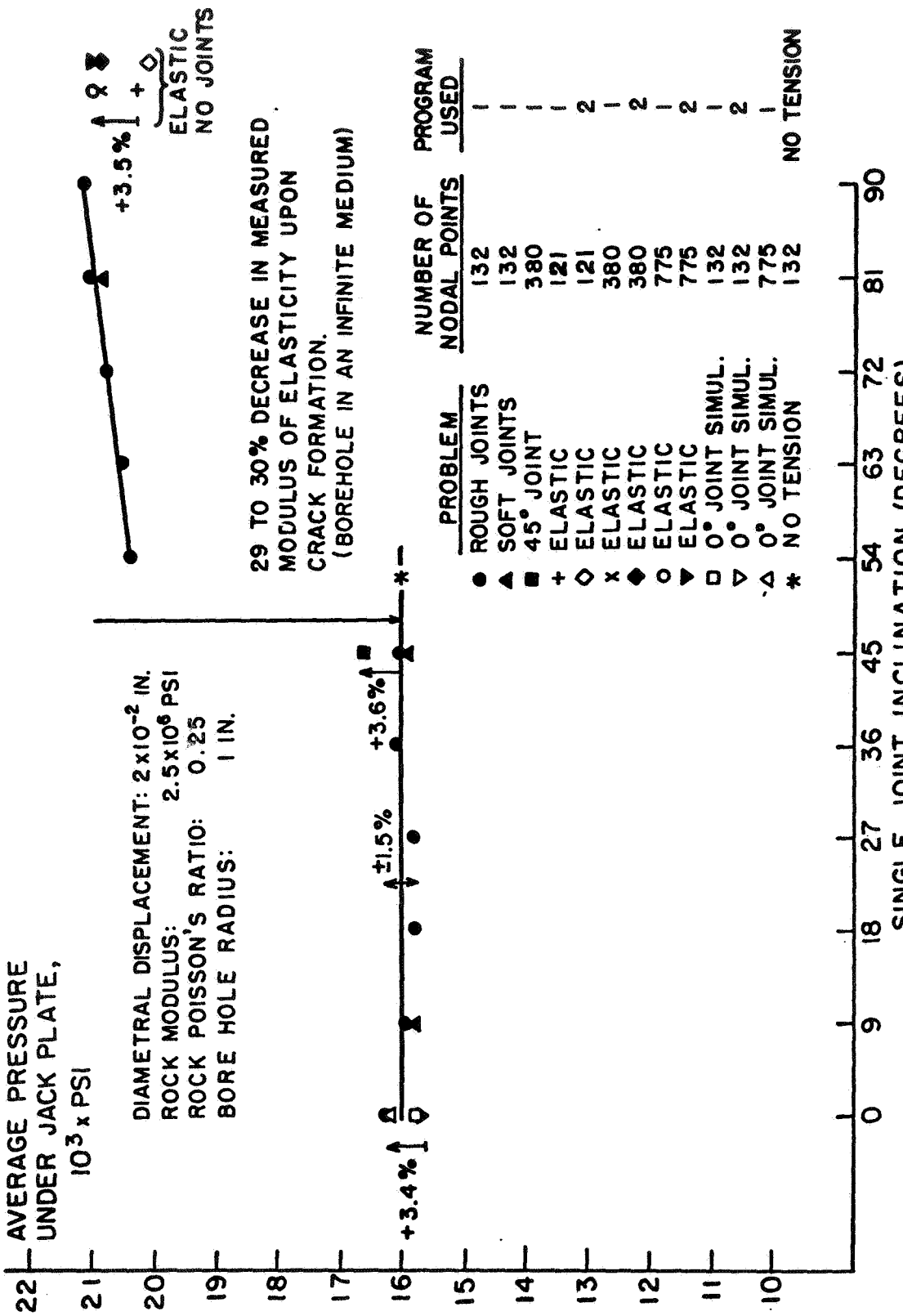

FIGURE 3-8 AVERAGE PRESSURE UNDER BOREHOLE JACK PLATE SUBJECTED TO A CONSTANT DISPLACEMENT

INFLUENCE OF RADIAL JOINT ORIENTATION

INFLUENCE OF RADIAL JOINT STIFFNESS

INFLUENCE OF MESH SIZE

REFERENCES

1. Doherty, W. P., Wilson, E. L., and Taylor, R. L. (1969) "Stress Analysis of Axisymmetric Solids Utilizing Higher Order Quadrilateral Finite Elements" *Rep. No. 69-3* Structural Eng. Lab., University of California, Berkeley, January.

2. Goodman, R. E., Van T. K., and Heuzé, F. E. (1968) "The Measurement of Rock Deformability in Bore Hole-Adaptability to a Lunar Exploration Program" *NASA CR-61202.*

3. Goodman, R. E., Taylor, R. L., and Brekke, T. (1968) "A Model for the Mechanics of Jointed Rock" *J. Soil Mech. & Found. Div. Proc. ASCE*, v. 94, n. SM3.

4. Heuzé, F. (1967) "Mechanical Properties and In Situ Behavior of the Chino Limestone, Riverside, California" M. Sc. Thesis, University of California, Berkeley, March, also (R. E. Goodman co-author) *Proc. 9th Symp. on Rock Mechanics*, Golden, Colorado, April.

5. Stagg, K. G., and Zienkiewicz, O. C. (1968) *Rock Mechanics in Engineering Practice*, J. Wiley & Sons Ed.

6. Van, T. K. (1967) "In Situ Determination of Rock Deformability by Bore Hole Jack Tests" Unpublished M. Sc. Thesis, Dept. of Civ. Eng. University of California, Berkeley, December.

7. Wilson, E. L. (1963) "Finite Element Analysis of Two Dimensional Structures" Doctor of Engineering Dissertation, University of California, Berkeley, June.

8. Wilson, E. L. (1965) "Structural Analysis of Axisymmetric Solids" *AIAA Journal*, v. 3.

9. Zienkiewicz, O. C., Valliappan, S., and King, I. P., (1968) "Stress Analysis of Rock as a 'No Tension' Material" *Geotechnique*, v. 18, n. 1.

10. Zienkiewicz, O. C., Valliappan, S., and King, I. P. (1969) "Elasto Plastic Solutions of Engineering Problems 'Initial Stress', Finite Element Approach," *Int. Journ. for Numeric. Meth. in Engineering*, v. 1.

APPENDIX A — "JOINT PERTURBATION" PROGRAM LISTING

```
      PROGRAM MAIN(INPUT,OUTPUT,TAPE8,TAPE9,PUNCH)
C*****************************************************************
C
C PLANE STRAIN STRUCTURES.PERTURBATION SOLUTION WITH JOINT ELEMENTS.
C INITIAL STRESS OPTION.GRAVITY OPTION.
C
C*****************************************************************

000003       COMMON // B(160), A(80,160), MBAND, ND2, NUMBLK, MBMAX, NB
000003       COMMON /STF/ NUMNP, NUMPC, IBC(200), JBC(200), PR(200),
            1            UR(900), UZ(900)
000003       COMMON /OTHER/ N, IX(800,5), EPS(3),   MTAG(900), RESID(800,3),
            1               NUMEL, NRES, NSHELL, R(900), Z(900), CODE(900),
            2               RSTRS(4), LBAD, NEC, ACELX, ACELY, VOL, E(8,12),
            3               RO(12), S(10,10), P(10), NP, NNN
000003       COMMON /SCRATCH/ HED(8), MTYPE, XTRA(147)
000003       DATA  END/3HEND/
000003       DIMENSION PRNSTR(800,3)
      C
C*****************************************************************
C     READ AND PRINT OF CONTROL INFORMATION AND MATERIAL PROPERTIES
C*****************************************************************
000003       LBAD = 0
000004       MBMAX = 80
000005       ND2 = 160
000006       NB = 40
000007    50 READ 1000, HED
000015       IF (HED(1) .EQ. END)  GO TO 9000
000017       READ 1010, NUMNP, NUMEL, NUMMAT, NUMPC, ACELX,ACELY,NP,NRES,NSHELL
000045       PRINT 2000,HED,NUMNP,NUMEL,NUMMAT,NUMPC,ACELX,ACELY,NP,NSHELL
000073       PRINT 2030
000077       IF (NSHELL .EQ. 0)  NSHELL = 13

000101    56 DO 59 M=1,NUMMAT
000103       READ 1001,MTYPE,RO(MTYPE),(E(J,MTYPE), J=1,7)
000121       IF (MTYPE .GT. NSHELL)  GO TO 560
000125       PRINT 2011,MTYPE, RO(MTYPE),(E(J,MTYPE), J=1,4)
000143       GO TO 59
      C
000144   560 PRINT 2017, MTYPE, (E(J,MTYPE), J=1,5)
000161    59 CONTINUE
      C
C*****************************************************************
C     READ AND PRINT OF NODAL POINT DATA
C*****************************************************************
000164       PRINT    2004
000167       L = 1
000170    60 READ     1002, N,CODE(N),R(N),Z(N),UR(N),UZ(N)
000210       IF (N - L)  100, 90, 70
000213    70 ZX=N-L+1
000216       DR = (R(N) - R(L-1)) / ZX
000221       DZ = (Z(N) - Z(L-1)) / ZX
000225    80 CODE(L)=0.0
000227       R(L)=R(L-1)+DR
000231       Z(L)=Z(L-1)+DZ
000234       UR(L)=0.0
000235       UZ(L)=0.0
000236    90 PRINT 2002, L, CODE(L), R(L), Z(L), UR(L), UZ(L)
000256       IF (L .EQ. NUMNP)  GO TO 110
000260       L = L + 1
000261       IF (N - L)  60, 90, 80
000264   100 PRINT    2009, N
000272       LBAD = LBAD + 1
000274       GO TO 60
000274   110 CONTINUE
000274       N1=NUMNP+1
000276       DO 111 N=N1,900
000277       UR(N)=0.0
000300   111 UZ(N)=0.0
      C*****************************************************************
      C      READ AND PRINT OF ELEMENT PROPERTIES
      C     DETERMINE BAND WIDTH
      C*****************************************************************
000303       PRINT    2001
000306       MBAND = 0
000307       N = 1
000310   130 READ     1003, M,(IX(M,I),I=1,5)

000326       DO 131  I=1,3
000330       I1 = I + 1
000332       DO 131  L = I1,4
000334       KK = IABS(IX(M,I) - IX(M,L))
000343       IF (KK .GE. NB)  GO TO 179
000346   131 IF (KK .GT. MBAND)  MBAND = KK

000355       IF (M - N)  180, 170, 150
000360   150 IX(N,1)=IX(N-1,1)+1
000363       IX(N,2)=IX(N-1,2)+1
000365       IX(N,3)=IX(N-1,3)+1
000367       IX(N,4)=IX(N-1,4)+1
000371       IX(N,5)=IX(N-1,5)
000372   170 PRINT    2003, N,(IX(N,I),I=1,5)
000410       IF (N .EQ. NUMEL)  GO TO 190
000412       N = N + 1
000413       IF (M - N)  130, 170, 150

000416   179 N = N + 1
000420   180 PRINT 2018, M, KK, N
000432       LBAD = LBAD + 1
000434       GO TO 130

000434   190 CONTINUE
000434       MBAND = 2 * MBAND + 2
000436       PRINT 2012,MBAND
C*****************************************************************
C     READ AND PRINT OF PRESSURE BOUNDARY CONDITIONS
C*****************************************************************
000444       IF (NUMPC) 290,310,290
000445   290 PRINT    2005
000451       DO 300 L=1,NUMPC
000453       READ 1004, IBC(L),JBC(L),PR(L)
```

```
000464      300 PRINT    2007, IBC(L),JBC(L),PR(L)
000501      310 CONTINUE
            C*************************************************************************
            C     READ INITIAL STRESSES FOR THE PROBLEM, PRINT AS PART OF FIRST STEP
            C *************************************************************************
000501            DO 32 N=1,NUMEL
000503            DO 32 I=1,3
000504       32 RESID(N,I)=0.0

000514            IF(NRES.EQ.0) GO TO 45
000515            L = 1
000516       47 READ 1007,N,(PRNSTR(N,I),I=1,3)
000534            THETA = PRNSTR(N,3) * 0.01745329
000537            RESID(N,1)= (PRNSTR(N,1)+PRNSTR(N,2))/2.+((PRNSTR(N,1)-PRNSTR(N,2)
                 1)/2.)*COS(2.*THETA)
000553            RESID(N,2)= (PRNSTR(N,1)+PRNSTR(N,2))/2.-((PRNSTR(N,1)-PRNSTR(N,2)
                 1)/2.)*COS(2.*THETA)
000570            RESID(N,3)= ((PRNSTR(N,1)-PRNSTR(N,2))/2.)*SIN(2.*THETA)
000602            IF(N-L) 40,41,42
000604       42 DO 46 I=1,3
000606       46 RESID(L,I)=RESID(L-1,I)
000617       41 IF (L .EQ. NUMEL)  GO TO 45
000621            L = L + 1
000622            IF (N - L)  47, 41, 42
000625       40 PRINT 1008,N
000633            LBAD = LBAD + 1
000635            GO TO 47
000635       45 CONTINUE

            C*************************************************************************
            C     SOLVE NON-LINEAR STRUCTURE BY SUCCESSIVE APPROXIMATIONS
            C*************************************************************************

000635            DO 360 N=1,NUMEL
000637            MTAG(N)=1
000641       360 CONTINUE

            C     ANGLE = 0 -- (1) = SIN**2, (2) = COS**2, (3) = SIN*COS

000643            EPS(1) = 0.0
000644            EPS(2) = 1.0
000645            EPS(3) = 0.0

000646            DO 500 NNN=1,NP

000647            IF(NRES.EQ. 0) GO TO 351
000650            PRINT 1006
000653            PRINT 1007, (K,(RESID(K,I),I=1,3),K=1,NUMEL)
000675       351 CONTINUE
            C
            C     FORM STIFFNESS MATRIX
            C
000675            CALL STIFF
000676            IF (LBAD .NE. 0)  GO TO 9950
            C
            C     SOLVE FOR DISPLACEMENTS
            C
000677            CALL BANSOL
            C
000700            PRINT  2006, (N,B(2*N-1),B(2*N),N=1,NUMNP)
            C
            C     COMPUTE STRESSES
            C
000720            CALL STRESS
000721            CALL JTSTR
            C
000722       500 CONTINUE

            C*************************************************************************
000725            GO TO 50
            C*************************************************************************

000725       1000 FORMAT (8A10)
000725       1001 FORMAT (I5,8F9.0)
000725       1002 FORMAT (I5,F5.0,5F10.0)
000725       1003 FORMAT (615)
000725       1004 FORMAT (2I5,F10.0)
000725       1006 FORMAT (37H1      I N I T I A L   S T R E S S E S/8HOELEMENT3X,7HXS
                 1TRESS8X,7HYSTRESS7X,8HXYSTRESS)
000725       1007 FORMAT (I5,3F15.4)
000725       1008 FORMAT(* RESIDUAL STRESS INPUT ERROR, N=*I4)
000725       1010 FORMAT (4I5,2F10.2,4I5)
000725       2000 FORMAT (1H1/2CX,8A10/
                 1 30HO NUMBER OF NODAL POINTS------ I3 /
                 2 30HO NUMBER OF ELEMENTS---------- I3 /
                 3 30HO NUMBER OF DIFF. MATERIALS--- I3 /
                 4 30HO NUMBER OF PRESSURE CARDS---- I3 /
                 5 30HO X-ACCELERATION-------------- E12.4/
                 6 30HO Y-ACCELERATION-------------- E12.4/
                 8 30HO NUMBER OF APPROXIMATIONS---- I3/
                 9 30HO HIGHEST NO SOLID MATERIAL--- I3 )
000725       2001 FORMAT (49H1ELEMENT NO.      I     J     K     L    MATERIAL  )
000725       2002 FORMAT (I12,F12.2,2F12.3,2E24.7)
000725       2003 FORMAT (1113,4I6,1112)
000725       2004 FORMAT (1C8H1NODAL POINT        TYPE  X-ORDINATE  Y-ORDINATE  X LO
                 1AD OR DISPLACEMENT  Y LOAD OR DISPLACEMENT                )
000725       2005 FORMAT (29HOPRESSURE BOUNDARY CONDITIONS/ 24H     I     J    PRESS
                 1URE )
000725       2006 FORMAT (12H1N.P. NUMBER 13X 2HUX 18X 2HUY / (1I12,2E20.7))
000725       2007 FORMAT (2I6,F12.3)
000725       2009 FORMAT (26HONODAL POINT CARD ERROR N= I5)
000725       2011 FORMAT  (15HOMATERIAL NO. =I3,16H  MASS DENSITY =E12.4/63HO  TENSI
                 1LE STRGTH   COMP MODULUS   POISSON RATIO   TENS MODULUS/7E15.4)
000725       2012 FORMAT (/6HMBAND= I5 /)
000725       2017 FORMAT (1H 10X,15HMATERIAL NUMBERI5/1H+6X,2HKN13X,2HKT14X,1HC13X,3
                 1HPHI8X,12HMAX. CLOSURE/5E15.4)
000725       2018 FORMAT (16H ELEMENT CARD NOI6,5X,4HKK =I4,5X,8HNEXT N =I6)
000725       2019 FORMAT (23H NUMBER OF ERRORS FOUND14)
000725       2030 FORMAT (/*0PLANE STRAIN ANALYSIS OF JOINTED STRUCTURES*)
            C
000725       8950 PRINT 2019, LBAD
000733       9000 RETURN
```

```
      SUBROUTINE STIFF
C
      COMMON // B(80), B2(90), A(80,80), A2(80,80), MBAND, ND2,
     1          NUMBLK, MBMAX, NB
      COMMON /STF/ NUMNP, NUMPC, IBC(200), JBC(200), PR(200),
     1             UR(900), UZ(900)
      COMMON /OTHER/ N, IX(800,5), EPS(3),  MTAG(800), RESID(800,3),
     1               NUMEL, NRES, NSHELL, R(900), Z(900), CODE(900),
     2               RSTRS(4), LBAD, NEC, ACELX, ACELY, VOL, E(8,12),
     3               RO(12), S(10,10), P(10), NP, NNN
      COMMON /SCRATCH/ LM(4), XTRA(152)
      EQUIVALENCE (ND, MBMAX)
C
C*****************************************************************
C     INITIALIZATION
C*****************************************************************
      REWIND 9
      NUMBLK=0
C
      DO 50 N=1,ND
      B(N)=0.0
      B2(N) = 0.0
      DO 50 M=1,ND
      A2(M,N) = 0.0
   50 A(M,N) = 0.0
C*****************************************************************
C     FORM STIFFNESS MATRIX IN BLOCKS
C*****************************************************************
   60 NUMBLK=NUMBLK+1
      NH=NB*(NUMBLK+1)
      NM=NH-NB
      NL=NM-NB+1
      KSHIFT=2*NL-2
C
      DO 210 N=1,NUMEL
C
      IF (IX(N,5)) 210,210,65
   65 DO 80 I=1,4
      IF (IX(N,I)-NL) 80,70,70
   70 IF (IX(N,I)-NM) 90,90,80
   80 CONTINUE
      GO TO 210
C
   90 IF(IX(N,5).LE.NSHELL) GO TO 92
      CALL JTSTIF
      IF (VOL .GT. 0.0)  GO TO 165
      LBAD = LBAD + 1
      GO TO 209
   92 CALL QUAD
      IF (VOL .LE. 0.0)  GO TO 209
C
  144 IF(IX(N,3)-IX(N,4)) 145,165,145
  145 DO 150 II=1,9
      CC=S(II,10)/S(10,10)
      P(II)=P(II)-CC*P(10)
      DO 150 JJ=1,9
  150 S(II,JJ)=S(II,JJ)-CC*S(10,JJ)
C
      DO 160 II=1,8
      CC=S(II,9)/S(9,9)
      P(II)=P(II)-CC*P(9)
      DO 160 JJ=1,8
  160 S(II,JJ)=S(II,JJ)-CC*S(9,JJ)
C
C          ADD ELEMENT STIFFNESS TO TOTAL STIFFNESS
C
  165 DO 166 I=1,4
  166 LM(I)=2*IX(N,I)-2
C
      DO 200 I=1,4
      DO 200 K=1,2
      II=LM(I)+K-KSHIFT
      KK=2*I-2+K
      B(II)=B(II)+P(KK)
      DO 200 J=1,4
      DO 200 L=1,2
      JJ=LM(J)+L-II+1-KSHIFT
      LL=2*J-2+L
      IF (JJ .LE. 0)  GO TO 200
      A(JJ,II) = A(JJ,II) + S(KK,LL)
  200 CONTINUE
C
  209 IX(N,5) = -IX(N,5)
  210 CONTINUE
      IF (LBAD .NE. 0)  GO TO 405
C
C     ADD CONCENTRATED FORCES WITHIN BLOCK
C
      DO 250 N=NL,NM
      K=2*N-KSHIFT
      B(K)=B(K)+UZ(N)
  250 B(K-1)=B(K-1)+UR(N)
C
C     BOUNDARY CONDITIONS
C
C       1. PRESSURE B.C.
C
      IF (NUMPC) 260,310,260
  260 DO 300 L=1,NUMPC
      I=IBC(L)
      J=JBC(L)
      PP=PR(L)/2.
      DZ=(Z(I)-Z(J))*PP
      DR=(R(J)-R(I))*PP
  264 II=2*I-KSHIFT
      JJ=2*J-KSHIFT
      IF (II) 280,280,265
  265 IF (II-ND) 270,270,280
  270 SINA=0.0
      COSA=1.0
      IF (CODE(I)) 271,272,272
```

```
000331     271 SINA=SIN(CODE(I))
000335         COSA=COS(CODE(I))
000340     272 B(II-1)=B(II-1)+(COSA*DZ+SINA*DR)
000346         B(II)=B(II)-(SINA*DZ-COSA*DR)
000353     280 IF (JJ) 300,300,285
000355     285 IF (JJ-ND) 290,290,300
000360     290 SINA=0.0
000361         COSA=1.0
000363         IF (CODE(J)) 291,292,292
000365     291 SINA=SIN(CODE(J))
000371         COSA=COS(CODE(J))
000374     292 B(JJ-1)=B(JJ-1)+(COSA*DZ+SINA*DR)
000402         B(JJ)=B(JJ)-(SINA*DZ-COSA*DR)
000407     300 CONTINUE
           C
           C       2. DISPLACEMENT B.C.
           C
000412     310 DO 400 M=NL,NH
000414         IF (M .GT. NUMNP)  GO TO 401
000417         N=2*M-1-KSHIFT
000421         IF (CODE(M))  390, 400, 316
000423     316 IF (CODE(M) .EQ. 2.0)  GO TO 390
000426         CALL MODIFY (N, UR(M))
000431         IF (CODE(M) .EQ. 1.0)  GO TO 400
000434     390 N = N + 1
000436         CALL MODIFY (N, UZ(M))
000441     400 CONTINUE
000444     401 CONTINUE
           C
           C      WRITE BLOCK OF EQUATIONS ON TAPE AND SHIFT UP LOWER BLOCK
           C
000444         WRITE (9) B, A
           C
000453     405 IF (NM .GE. NUMNP)  GO TO 480
000456         IF (LBAD .NE. 0)  GO TO 60
000457         DO 420 N=1,ND
000460         B(N) = B2(N)
000463         B2(N) = 0.0
000464         DO 420 M=1,ND
000466         A(M,N) = A2(M,N)
000474     420 A2(M,N) = 0.0
000502         GO TO 60
           C
000503     480 CONTINUE
           C
000503     500 RETURN
           C
000504         END
*FOLLOWING VARIABLES EQUIVALENCED BUT NOT REFERENCED
MBMAX
```

```
               SUBROUTINE MODIFY (N, U)
           C
000005         COMMON // B(160), A(80,160), MBAND, ND2, NUMBLK, MBMAX, MB
           C
000005         DO 250 M=2,MBAND
000006         K=N-M+1
000010         IF (K .LE. 0)  GO TO 235
000012         IF (A(M,K) .EQ. 0.0)  GO TO 235
000015         B(K) = B(K) - A(M,K) * U
000023         A(M,K) = 0.0
000026     235 K=N+M-1
000031         IF (K .GT. ND2)  GO TO 250
000034         IF (A(M,N) .EQ. 0.0)  GO TO 250
000037         B(K) = B(K) - A(M,N) * U
000045         A(M,N) = 0.0
000050     250 CONTINUE
000053         A(1,N) = 1.0
000057         B(N)=U
000061         RETURN
           C
000061         END
```

```
      SUBROUTINE QUAD
C
      COMMON /OTHER/ N, IX(800,5), FPS(3),   MTAG(800), RESID(800,3),
     1               NUMEL, NRES, NSHELL, R(900), Z(900), CODE(900),
     2               RSTRS(4), LBAD, NEC, ACELX, ACELY, VOL, E(6,12),
     3               RO(12), S(10,10), P(10), NP, NNN
      COMMON /SCRATCH/ EE(4), H(3,4), XTRA(140)
      COMMON /ARG/ ANGLE(4), RRR(5), ZZZ(5), XI, HH(6,10), C(4,4), MTYPE
      EQUIVALENCE (S2,EPS(1)), (C2,EPS(2)), (SC, EPS(3))
      DIMENSION  D(3,4)
      DATA  D(1,1) /100./
C
      I=IX(N,1)
      J=IX(N,2)
      K=IX(N,3)
      L=IX(N,4)
      MTYPE=IX(N,5)
C
C  FORM STRESS-STRAIN RELATIONSHIP FOR PLANE STRAIN
C
      DO 105 KK=1,4
  105 EE(KK)=E(KK+1,MTYPE)
C
      IF (MTAG(N)-2) 82,84,83
   82 EE(3)=EE(1)
      GO TO 84
   83 EE(1)=EE(3)
C
   84 EE(1)=EE(1)/(1.-EE(2)**2)
      EE(3)=EE(3)/(1.-EE(2)**2)
      EE(2)=EE(2)/(1.-EE(2))
      XX=EE(1)/EE(3)
      COMM=EE(1)/(XX-EE(2)**2)
      C(1,1)=COMM*XX
      C(1,2)=COMM*EE(2)
      C(1,3)=0.0
      C(2,1)=C(1,2)
      C(2,2)=COMM
      C(2,3)=0.0
      C(3,1)=0.0
      C(3,2)=0.0
      C(3,3)=.5*EE(1)/(XX+EE(2))
      IF (D(1,1) .NE. 100.)  GO TO 85
C
      D(1,1)=S2
      D(1,2)=C2
      D(1,3)=0.0
      D(1,4)=-SC
      D(2,1)=C2
      D(2,2)=S2
      D(2,3)=0.0
      D(2,4)=SC
      D(3,1)=2.*SC
      D(3,2)=-D(3,1)
      D(3,3)=0.0
      D(3,4)=-C2+S2
C
   85 DO 88 II=1,3
      DO 88 JJ=1,4
      H(II,JJ)=0.0
      DO 88 KK=1,3
   88 H(II,JJ)=H(II,JJ) +C(II,KK)*D(KK,JJ)
C
      DO 89 II=1,4
      DO 89 JJ=1,4
      C(II,JJ)=0.0
      DO 89 KK=1,3
   89 C(II,JJ)=C(II,JJ)+D(KK,II)*H(KK,JJ)
C
C     REPLACE RESIDUAL STRESSES FOR NTH ELEMENT BY RSTRS(IJ)
C
      IF(NRES.EQ.0) GO TO 112
      DO 111 IJ=1,3
  111 RSTRS(IJ)=RESID(N,IJ)
      GO TO 114
  112 DO 113 IJ=1,3
  113 RSTRS(IJ)=0.
  114 RSTRS(4)=RSTRS(3)

C*****************************************************************
C          FORM QUADRILATERAL STIFFNESS MATRIX
C*****************************************************************

      DO 94 M=1,4
      MM=IX(N,M)
   93 RRR(M)=R(MM)
   94 ZZZ(M)=Z(MM)
C
      DO 100 II=1,10
      P(II)=0.0
      DO 95 JJ=1,6
   95 HH(JJ,II)=0.0
      DO 100 JJ=1,10
  100 S(II,JJ)=0.0
      DO 119 II=1,4
      JJ=IX(N,II)
  119 ANGLE(II)=CODE(JJ)/57.3
C
C     FORM BAR STIFFNESS
C
      IF (IX(N,2)-IX(N,3)) 250,240,250
  240 DR=R(J)-R(I)
      DZ=Z(J)-Z(I)
      XL=SQRT(DR**2+DZ**2)
      RRR(5)=(R(I)+R(J))/2.-2.*EE(4)*DZ/XL
      ZZZ(5)=(Z(I)+Z(J))/2.+2.*EE(4)*DR/XL
      CALL TRISTF(1,2,5)
      GO TO 130
  250 CONTINUE
C
      IF (K-L) 125,120,125
```

```
000323     120 CALL TRISTF(1,2,3)
000326         RRR(5)=(RRR(1)+RRR(2)+RRR(3))/3.0
000332         ZZZ(5)=(ZZZ(1)+ZZZ(2)+ZZZ(3))/3.0
000336         VOL = XI
000340         IF (VOL .GT. 0.0)  GO TO 130
               C     ERROR RETURN
000342     122 LBAD = LBAD + 1
000344         GO TO 130

000344     125 VOL=0.0
000345         RRR(5)=(R(I)+R(J)+R(K)+R(L))/4.0
000356         ZZZ(5)=(Z(I)+Z(J)+Z(K)+Z(L))/4.0
000367         CALL TRISTF(4,1,5)
000372         CALL TRISTF(1,2,5)
000375         CALL TRISTF(2,3,5)
000400         CALL TRISTF(3,4,5)
000403         IF (VOL .LE. 0.0)  GO TO 122
               C
000405     145 DO 140 II=1,6
000407         DO 140 JJ=1,10
000410     140 HH(II,JJ)=HH(II,JJ)/4.0
               C
000421     130 RETURN
               C
000422         END
```

```
               SUBROUTINE TRISTF(II,JJ,KK)
               C
000006         COMMON /OTHER/ N, IX(800,5), EPS(3),   MTAG(800), RESID(900,3),
              1               NUMEL, NRES, NSHELL, R(900), Z(900), CODE(900),
              2               RSTRS(4), LBAD, NFC, ACELX, ACELY, VOL, E(8,12),
              3               RO(12), S(10,10), P(10), NP, NNN
000006         COMMON /SCRATCH/ F(6,10), H(6,10),  D(6,6)
000006         COMMON /ARG/ ANGLE(4), RRR(5), ZZZ(5), XI, HH(6,10), C(4,4), MTYPE
000006         DIMENSION  RR(4), ZZ(4), DD(3,3), LM(3)
               C
               C     1. INITIALIZATION
               C
000006         LM(1)=II
000007         LM(2)=JJ
000010         LM(3)=KK
               C
000011         RR(1)=RRR(II)
000013         RR(2)=RRR(JJ)
000015         RR(3)=RRR(KK)
000017         RR(4)=RRR(II)
000021         ZZ(1)=ZZZ(II)
000023         ZZ(2)=ZZZ(JJ)
000025         ZZ(3)=ZZZ(KK)
000027         ZZ(4)=ZZZ(II)
               C
000031      85 DO 100 I=1,6
000033         DO 90 J=1,10
000034         F(I,J)=0.0
000040      90 H(I,J)=0.0
000044         DO 100 J=1,6
000046     100 D(I,J)=0.0
               C
               C          FORM INTEGRAL(G)T*(C)*(G)
               C
000056         COMM=RR(2)*(ZZ(3)-ZZ(1))+RR(1)*(ZZ(2)-ZZ(3))+RR(3)*(ZZ(1)-ZZ(2))
000070         XI = COMM / 2.0
000072         IF (XI .GT. 0.0)  GO TO 102
000074         PRINT 1000, II,JJ,KK, N
000107    1000 FORMAT (32H ZERO OR NEGATIVE AREA, TRIANGLE3I6,5X,7HELEMENTI5)
000107         RETURN
000116     102 VOL = VOL + XI
               C
000112         D(2,2)=XI    *C(1,1)
000114         D(2,6) = XI * C(1,2)
000116         D(3,3)=XI    *C(4,4)
000120         D(3,5)=XI    *C(4,4)
000121         D(5,5)=XI    *C(4,4)
000122         D(6,6)=XI    *C(2,2)
               C
000124     108 DO 110  I=1,5
000130         K = I + 1
000132         DO 110  J = K,6
000134     110 D(J,I)=D(I,J)
               C
               C          FORM  COEFFICIENT-DISPLACEMENT TRANSFORMATION MATRIX
```

```
      C
000150      DD(1,1)=(RR(2)*ZZ(3)-RR(3)*ZZ(2))/COMM
000154      DD(1,2)=(RR(3)*ZZ(1)-RR(1)*ZZ(3))/COMM
000160      DD(1,3)=(RR(1)*ZZ(2)-RR(2)*ZZ(1))/COMM
000164      DD(2,1)=(ZZ(2)-ZZ(3))/COMM
000166      DD(2,2)=(ZZ(3)-ZZ(1))/COMM
000170      DD(2,3)=(ZZ(1)-ZZ(2))/COMM
000172      DD(3,1)=(RR(3)-RR(2))/COMM
000175      DD(3,2)=(RR(1)-RR(3))/COMM
000177      DD(3,3)=(RR(2)-RR(1))/COMM
      C
000201      DO 120 I=1,3
000202      J=2*LM(I)-1
000205      H(1,J)=DD(1,I)
000212      H(2,J)=DD(2,I)
000217      H(3,J)=DD(3,I)
000224      H(4,J+1)=DD(1,I)
000231      H(5,J+1)=DD(2,I)
000235    120 H(6,J+1)=DD(3,I)
      C
      C     ROTATE UNKNOWNS IF REQUIRED
      C
000242      DO 125 J=1,2
000244      I=LM(J)
000246      IF (ANGLE(I)) 122,125,125
000251    122 SINA=SIN(ANGLE(I))
000255      COSA=COS(ANGLE(I))
000261      IJ=2*I
000262      DO 124 K=1,6
000266      TEM=H(K,IJ-1)
000272      H(K,IJ-1)=TEM*COSA+H(K,IJ)*SINA
000301    124 H(K,IJ)= -TEM*SINA+H(K,IJ)*COSA
000310    125 CONTINUE
      C
      C          FORM ELEMENT STIFFNESS MATRIX (H)T*(D)*(H)
      C
000312      DO 130 J=1,10
000314      DO 130 K=1,6
000315      IF (H(K,J)) 128,130,128
000321    128 DO 129 I=1,6
000323    129 F(I,J)=F(I,J)+D(I,K)*H(K,J)
000341    130 CONTINUE
      C
000345      DO 140 I=1,10
000347      DO 140 K=1,6
000350      IF (H(K,I)) 138,140,138
000354    138 DO 139 J=1,10
000356    139 S(I,J)=S(I,J)+H(K,I)*F(K,J)
000374    140 CONTINUE
      C
      C       FORM RESIDUAL LOAD MATRIX
      C
000400    150 DO 160 I=1,10
000402    160 P(I) = P(I) - XI *(RSTRS(1)*H(2,I) + RSTRS(2)*H(6,I)
     1                + RSTRS(3)*(H(3,I) + H(5,I)))
      C
      C     ACCELERATION LOADS
      C
000436      COMM = RO(MTYPE) * XI / 3.0
000442      DO 170 I=1,3
000443      J=2*LM(I)-1
000446      P(J) = P(J)-ACELX*COMM
000452    170 P(J+1) = P(J+1) - ACELY*COMM
      C
      C     FORM STRAIN TRANSFORMATION MATRIX
      C
000457    400 DO 410 I=1,6
000461      DO 410 J=1,10
000462    410 HH(I,J)=HH(I,J)+H(I,J)
      C
000475      RETURN
      C
000476      END
```

```
      SUBROUTINE JTSTIF

02    COMMON /JNT/ KN(800), KS(800)
02    COMMON /OTHER/ N, IX(800,5), EPS(3),   MTAG(800), RESID(800,3),
     1               NUMEL, NRES, NSHELL, R(900), Z(900), CODE(900),
     2               RSTRS(4), EBAD, NEC, ACELX, ACELY, VOL, E(8,12),
     3               RO(12), S(10,10), P(10), NP, NNN
02    COMMON /SCRATCH/ TR(2,2), PPP(8), XTRA(144).
02    DIMENSION  D(4,4), ESTIF(10,10)
02    EQUIVALENCE (L,VOL), (S(1,1), ESTIF(1,1))
02    REAL KS,KN,L
02    DATA D/2.,1.,-1.,-2.,1.,2.,-2.,-1.,-1.,-2.,2.,1.,-2.,-1.,1.,2./

02    II=IX(N,1)
05    JJ= IX(N,2)
06    DR=R(JJ)-R(II)
12    DZ=Z(JJ)-Z(II)
15    L=SQRT(DR*DR+DZ*DZ)
22    IF(L.EQ.0.) GO TO 201
23    MAT=IX(N,5)
C**   MATERIAL PROPERTIES
25    IF(NNN.GT.1) GO TO 50
30    KN(N)=E(1,MAT)
34    KS(N)=E(2,MAT)
37   50 COMS=KS(N)*L/6.
43    COMN=KN(N)*L/6.
C          INITIALIZE
46    DO 100 II=1,8
47    P(II)=0.0
51    DO 100 JJ=1,8
52   100 ESTIF(II,JJ)=0.0

C*****************************************************************
C       DEVELOP RESIDUAL STRESS CONTRIBUTIONS TO THE LOAD VECTOR

C THE FOLLOWING SIGN CONVENTION IS ADOPTED.THE NORMAL STRESS IS POSITIVE WHEN
C DIRECTED OUTWARDS THE ELEMENT ON THE FACE (II,JJ).THE SHEAR STRESS IS POSITIVE
C WHEN DIRECTED FROM II TO JJ AND KK TO LL INSIDE THE ELEMENT.
C BESIDES,AND FOR EXAMPLE,S2 IS THE SQUARE OF THE COSINE OF THE ANGLE BETWEEN
C THE GLOBAL X DIRECTION AND THE LOCAL NORMAL STRESS DIRECTION.
C *****************************************************************

63    TR(1,1)=DR/L
65    TR(1,2)=DZ/L
66    SC = TR(1,1) * TR(1,2)
70    S2 = TR(1,2)  ** 2
71    C2 = TR(1,1) ** 2
72   111 RSTRS(1)=RESID(N,1)*S2 + RESID(N,2)*C2+2*RESID(N,3)*SC
02    RSTRS(2)=(RESID(N,2)-RESID(N,1))*SC +(RESID(N,3)*(S2-C2))

12    EL2 = L / 2.0
14    DO 160 I=1,4
15    J=2*I-1
17    PPP(J) = RSTRS(1) * EL2
22    J=2*I
000123   160 PPP(J) = RSTRS(2) * EL2
000127       DO 161 I=1,4
000131   161 PPP(I)=-PPP(I)
000135       DO 200 II=1,4
000136       IS=2*II-1
000140       IN=2*II
000141       DO 200 JJ=1,4
000143       JS = 2*JJ-1
000145       JN = 2*JJ
000146       ESTIF(IS,JS) = COMS * D(II,JJ)
000155   200 ESTIF(IN,JN) = COMN * D(II,JJ)

         C   ROTATE TO GLOBAL COORDINATES
000171       TR(2,1) = -TR(1,2)
000172       TR(2,2) = TR(1,1)
000174       IF(TR(1,1).EQ.1.) GO TO 405
000176       DO 400 NN=1,4
000177       DO 410 II=1,8
000200       JJ= 2*NN-1
000202       TEMP = ESTIF(II,JJ)
000206       DO 410 KK=1,2
000207       ESTIF(II,JJ)=TEMP*TR(1,KK)+ESTIF(II,2*NN)*TR(2,KK)
000224   410 JJ=JJ+1
000232       DO 420 II=1,8
000233       JJ=2*NN-1
000235       TEMP =ESTIF(JJ,II)
000241       DO 420 KK=1,2
000242       ESTIF(JJ,II)=TR(1,KK)*TEMP+TR(2,KK)*ESTIF(2*NN,II)
000257   420 JJ=JJ+1
000264   400 CONTINUE
000266   405 CONTINUE
000266       DO 401 I=1,4
000270       J=2*I-1
000272       II=2*I
000273       P(J)=PPP(J)*TR(1,2)+PPP(II)*TR(2,2)
000302   401 P(II)=-PPP(J)*TR(2,2)+PPP(II)*TR(1,2)
000312       RETURN

000313   201 PRINT 2090, N
000321       RETURN

000322  2090 FORMAT(14H BAD JOINT,N= I3/)
000322       END
*FOLLOWING VARIABLES EQUIVALENCED BUT NOT REFERENCED
VOL
```

```
      SUBROUTINE BANSOL
C
000002      COMMON // B(80), B2(80), A(80,8C), A2(80,80), MBAND, NO2,
     1          NUMBLK, MBMAX, NBB
000002      EQUIVALENCE (NN,MBMAX), (MM,MBAND)
C
C
000002      REWIND 8
000004      REWIND 9
000006      NB=0
000007      GO TO 150
C*****************************************************************
C     REDUCE EQUATIONS BY BLOCKS
C*****************************************************************
C
C     1. SHIFT BLOCK OF EQUATIONS
C
00001C    100 NB=NB+1
000012      DO 125 N=1,NN
XXXX24      CALL SLEW
XXXX27      CALL XLOC
000017      DO 125 M=1,MM
000021      A(M,N) = A2(M,N)
000027    125 A2(M,N) = 0.0
C
C     2. READ NEXT BLOCK OF EQUATIONS INTO CORE
C
000036      IF (NUMBLK-NB) 150,200,150
000040    150 READ (9)  B2, A2
000047      IF (NB) 200,100,200
C
C     3. REDUCE BLOCK OF EQUATIONS
C
000050    200 DO 300 N=1,NN
000052      IF (A(1,N) .EQ. 0.0)  GO TO 300
000055      B(N) = B(N) / A(1,N)
000062      DO 275 L=2,MM
000063      IF (A(L,N) .EQ. 0.0)  GO TO 275
000067      C = A(L,N) / A(1,N)
000075      I=N+L-1
000077      J=0
000100      DO 250 K=L,MM
000101      J=J+1
000103    250 A(J,I) = A(J,I) - C * A(K,N)
000115      B(I) = B(I) - A(L,N) * B(N)
000125      A(L,N) = C
000136    275 CONTINUE
000133    300 CONTINUE
C
C     WRITE BLOCK OF REDUCED EQUATIONS ON TAPE 8
C
000136      IF (NUMBLK-NB) 375,400,375
000140    375 WRITE (8)  B, A
000147      GO TO 100
C*****************************************************************
C     BACK-SUBSTITUTION
C*****************************************************************
000150    400 DO 450 M=1,NN
000152      N=NN+1-M
000155      DO 425 K=2,MM
000156      L=N+K-1
000161    425 B(N) = B(N) - A(K,N) * B(L)
000172      B2(N) = B(N)
000175    450 A2(NB,N) = B(N)
000204      NB=NB-1
000205      IF (NB) 475,500,475
000206    475 BACKSPACE 8
00021C      READ (8) B, A
000217      BACKSPACE 8
000221      GO TO 400
C*****************************************************************
C     ORDER UNKNOWNS IN B ARRAY
C*****************************************************************
000222    500 K=0
000223      DO 600 NB=1,NUMBLK
000225      DO 600 N=1,NN
000226      K=K+1
000230    600 B(K) = A2(NB,N)
000241      RETURN
C
C
000242      END
*FOLLOWING VARIABLES EQUIVALENCED BUT NOT REFERENCED
MBMAX
MBAND
```

```
      SUBROUTINE STRESS
C
      COMMON // B(1601), A(80,160), MBAND, ND2, NUMBLK, MBMAX, NB
      COMMON /OTHER/ N, IX(800,5), EPS(3),   MTAG(800), RESID(800,3),
     1               NUMEL, NRES, NSHELL, R(900), Z(900), CODE(900),
     2               RSTRS(4), LOAD, NEC, ACELX, ACELY, VOL, E(8,12),
     3               RO(12), S(10,10), P(10), NP, NNN
      COMMON /SCRATCH/ TP(6), SIG(10), RR(4), XTRA(136)
      COMMON /ARG/ ANGLE(4), RRR(5), ZZZ(5), XI, HH(6,10), C(4,4), MTYPE
C*****************************************************************
C     COMPUTE ELEMENT STRESSES
C*****************************************************************
      MPRINT =0
C
      DO 300   N=1,NUMEL
C
      IX(N,5)=IABS(IX(N,5))
      IF (IX(N,5) .GT. NSHELL)  GO TO 300
C
      CALL QUAD
C
      DO 120 I=1,4
      II=2*I
      JJ=2*IX(N,I)
      P(II-1)=B(JJ-1)
  120 P(II)=B(JJ)
C
      DO 150 I=1,2
      RR(I)=P(I+8)
      DO 150 K=1,8
  150 RR(I)=RR(I)-S(I+8,K)*P(K)
C
      COMM=S(9,9)*S(10,10)-S(9,10)*S(10,9)
      IF (COMM) 155,160,155
  155 P(9)=(S(10,10)*RR(1)-S(9,10)*RR(2))/COMM
      P(10)=(-S(10,9)*RR(1)+S(9,9)*RR(2))/COMM
C
  160 DO 170 I=1,6
      TP(I)=0.0
      DO 170 K=1,10
  170 TP(I)=TP(I)+HH(I,K)*P(K)
C
C
      RR(1)=TP(2)
      RR(2)=TP(6)
      RR(3)=0.0
      RR(4)=TP(3)+TP(5)
C
  176 DO 180 I=1,4
      SIG(I)=RSTRS(I)
      RSTRS(I)=0.
      DO 180 K=1,4
  180 SIG(I)=SIG(I)+C(I,K)*RR(K)
      SIG(3)=SIG(4)
C
C*****************************************************************
C     OUTPUT STRESSES
C*****************************************************************
C
C     CALCULATE PRINCIPAL STRESSES
C
      CC=(SIG(1)+SIG(2))/2.0
      BB=(SIG(1)-SIG(2))/2.0
      CR=SQRT(BB**2+SIG(3)**2)
      SIG(4)=CC+CR
      SIG(5)=CC-CR
      SIG(6) = 0.0
      IF (BB .NE. 0.0)  SIG(6) = 28.698 * ATAN2(SIG(3),BB)
      MTAG(N)=1
      IF(SIG(4).LE.0.) GO TO 263
      MTAG(N)=2
      IF(SIG(5).LE.0.) GO TO 263
      MTAG(N)=3
  263 CONTINUE

      IF (MPRINT) 110,105,110
  105 PRINT 2000
      MPRINT=50
  110 MPRINT=MPRINT-1
C
      PRINT 2001, N,RRR(5),ZZZ(5), (SIG(I),I=1,6)
  300 CONTINUE
C
  320 RETURN
C
 2000 FORMAT (7H1EL.NO.   7X  1HX 7X 1HY 4X 8HX-STRESS 4X 8HY-STRESS 3X
     19HXY-STRESS 2X 10HMAX-STRESS 2X 10HMIN-STRESS 7H  ANGLE)
 2001 FORMAT(I7,2F8.2,1P5E12.4,0PF7.2)
      END
```

```
      SUBROUTINE JTSTR
      COMMON // B(160), A(80,160), MBAND, ND2, NUMBLK, MBMAX, NB
      COMMON /OTHER/ N, IX(800,5), EPS(3),   MTAG(800), RESID(800,3),
     1               NUMEL, NRES, NSHELL, R(900), Z(900), CODE(900),
     2               RSTRS(4), LBAD, NEC, ACELX, ACELY, VOL, E(8,12),
     3               RD(12), S(10,10), P(10), NP, NNN
      COMMON /SCRATCH/ V(4), U(4), XTRA(148)
      COMMON /JNT/ KN(800), KS(800)
      REAL L,KN,KS

      PRINT 1001
C
C  ESTABLISH DISPLACEMENT ALONG AND NORMAL TO JOINT
C
      DO 500 N=1,NUMEL
      MAT = IX(N,5)
      IF(MAT.LE.NSHELL) GO TO 500
      I=IX(N,1)
      J= IX(N,2)
      DR=R(J)-R(I)
      DZ=Z(J)-Z(I)
      RR = 0.5 * (R(J) + R(I))
      ZZ = 0.5 * (Z(J) + Z(I))
      L=SQRT(DR*DR+DZ*DZ)
      DR=DR/L
      DZ=DZ/L
      DO 100 II=1,4
      K=IX(N,II)
      V(II)=-B(2*K-1)*DZ+B(2*K)*DR
  100 U(II)=B(2*K-1)*DR+B(2*K)*DZ

C  COMPUTE EFFECTIVE STRAIN
C EPSN POSITIVE MEANS JOINT IS OPEN
C EPST POSITIVE MEANS (KK,LL) MOVES ALONG U+ MORE THAN (II,JJ)

  200 EPST=0.5*(U(4)-U(1)+U(3)-U(2))
      EPSN=0.5*(V(4)-V(1)+V(3)-V(2))

C  COMPUTE NORMAL AND SHEAR FORCE PER UNIT LENGTH AND CALCULATE STRENGTH
C INITIAL STRESSES INPUT ARE ALWAYS COMPRESSIVE (NEGATIVE)

      C2=DR**2
      S2=DZ**2
      SC=DR*DZ
      FNRES=RESID(N,1)*S2+RESID(N,2)*C2+RESID(N,3)*2.*SC
      FTRES= -RESID(N,1)*SC+RESID(N,2)*SC+RESID(N,3)*(S2-C2)
      FN=KN(N)*EPSN+FNRES
      IF(FN.LE.0.) GO TO 201
      KN(N)=ABS(FNRES/EPSN)
      GO TO 202
  201 IF(EPSN.GE.0.) GO TO 202
      IF(E(5,MAT).EQ.0.) GO TO 204
      IF(EPSN.GT.E(5,MAT)) GO TO 202
C
C E(5,MAT) SHOULD BE INPUT AS A NEGATIVE QUANTITY
C
      KN(N)=KN(N)*EPSN/E(5,MAT)
      GO TO 202
  204 KN(N) = KN(N) * 1.0E10
  202 FT=KS(N)*EPST+FTRES
      IF(FN.GE.0.) GO TO 205
      IF (EPST.EQ.0.) GO TO 210
      STREN = E(3,MAT) + ABS(FN) * TAN(E(4,MAT)*0.01745329)
      IF (ABS(FT).LT.STREN) GO TO 210
      IF(EPST.LT.0.) GO TO 203
      KS(N)=(STREN-FTRES)/EPST
      GO TO 210
  203 KS(N)=(-STREN-FTRES)/EPST
      GO TO 210
  205 KS(N)=1.

  210 PRINT 1000, N, RR, ZZ, FN, FT, EPSN, EPST
  500 CONTINUE
      RETURN

 1001 FORMAT(1H1,7HELEMENT,3X,1HX,5X,1HY,4X,4X,13HNORMAL STRESS,4X,
     1  12X,17HTANGENTIAL STRESS,  4X,12HNORMAL DISPL,4X 2X,16HTANGENTIAL DISPL
     2ISPL/1HC  )
 1000 FORMAT (I5,2F8.2,4E20.5)

      END
```

APPENDIX B — "NO TENSION" PROGRAM LISTING

```
      PROGRAM MAIN(INPUT,OUTPUT, PUNCH,TAPE9,TAPE90,TAPE91)
C ***************************************************************************
C     PLANE STRAIN STRUCTURES WITH RESIDUAL STRESS LOADING,  NO TENSION SOLUTION
C     ONLY TENSION REINPUT AFTER FIRST ITERATION
C ***************************************************************************
C
33    COMMON /STF/ NUMNP, NUMPC, IBC(200), JBC(200), PR(200),
     1             UR(900), UZ(900)
33    COMMON /MATRX/B(160), A(60,160), MBAND, ND2, NUMBLK, MBMAX, NB,
     1      BTOT(1800)
33    COMMON /   / N, IX(800,5), EPS(800), MTAG(800), RESID(800,3),
     1       NUMEL, NRES, R(900), Z(900), CODE(900), RSTRS(4), LBAD,
     2         NEC, ACELX, ACELY, VOL, E(8,12), RO(12), S(10,10), P(10),
     3  NSTOP,NNN, HED(8), MTYPE, XTRA(147)
33    COMMON /STRS/ FRAC, NUMMAT, SIGY(800,5), TMAX, IMAX, NELFOR(15),
     1              FACTOR(15), NP
33    COMMON /RECALC/ NCALC, STR(800,3), NC, NCHNG(50), CHNG(50,3)
33    DATA  MBMAX/80/, ND2/160/, END/3HEND/ , NB/40/
C
C*****************************************************************************
C     READ AND PRINT OF CONTROL INFORMATION AND MATERIAL PROPERTIES
C*****************************************************************************
03    LBAD = 0
04  50 READ 1000, HED
12    IF (HED(1) .EQ. END)  GO TO 9000
C     FINAL CARD IN DECK MUST READ END
14    READ 1009, NUMNP, NUMEL, NUMMAT, NUMPC, ACELX, ACELY, NP, NRES,
     1 FRAC
42    PRINT 2000,HED,NUMNP,NUMEL,NUMMAT,NUMPC,ACELX,ACELY,NP
C
66    DO 59 M=1,NUMMAT
70    READ 1001,MTYPE,RO(MTYPE), (E(J,MTYPE),J=1,7)
06    PRINT 2011,MTYPE, RO(MTYPE)
16    PRINT 2010, (E(J,MTYPE),J=1,7)
31  59 CONTINUE
C
C*****************************************************************************
C     READ AND PRINT OF NODAL POINT DATA
C*****************************************************************************
34    PRINT 2004
37    L=1
40  60 READ 1002,N,CODE(N),R(N),Z(N),UR(N),UZ(N)
60    IF (N-L) 100,90,70
63  70 ZX=N-L+1
66    DR=(R(N)-R(L-1))/ZX
71    DZ=(Z(N)-Z(L-1))/ZX
75  80 CODE(L)=0.0
77    R(L)=R(L-1)+DR
01    Z(L)=Z(L-1)+DZ
04    UR(L)=0.0
05    UZ(L)=0.0
06  90 PRINT 2002,L,CODE(L),R(L),Z(L),UR(L),UZ(L)
26    IF (L.EQ.NUMNP) GO TO 110
30    L=L+1
31    IF (N-L) 60,90,80
000234  100 PRINT 2009,N
000242      LBAD=LBAD+1
000244      GO TO 60
000244  110 CONTINUE

000244      N1=NUMNP+1
000246      DO 112 N=N1,900
000247      UR(N)=0.0
000250      UZ(N)=0.0
000251  112 CONTINUE

000253      NC = 0
000254      NSTOP=1

C     STORE INPUT WHICH IS TO BE REUSED AT LAST ITERATION BUT NOT
C     BETWEEN FIRST AND LAST

000255      DO 111 I=1,NUMNP
000256      IF (CODE(I).LE.3.) GO TO 111
000261      NC = NC + 1
000262      NCHNG(NC) = I
000264      CHNG(NC,1) = CODE(I)
000266      CHNG(NC,2) = UR(I)
000267      CHNG(NC,3) = UZ(I)
000271  111 CONTINUE
000274      IF (NC .GT. 0)  NSTOP = 2
000276      NCALC = 1
C*****************************************************************************
C       READ AND PRINT OF ELEMENT PROPERTIES
C     DETERMINE BAND WIDTH
C*****************************************************************************
000277      PRINT    2001
000303      MBAND = 0
000304      N = 1
000305  130 READ    1003, M,(IX(M,I),I=1,5)

C     CHECK BAND WIDTH FOR EACH PAIR AND EACH CARD ONLY ONCE

000323      DO 131  I=1,3
000325      J = I+1
000327      DO 131  L=J,4
000331      KK=IABS(IX(M,I)-IX(M,L))
000340      IF (KK .GE. NB)  GO TO 179
000343  131 IF (KK .GT. MBAND)  MBAND = KK

000352      IF (M-N) 180,170,150
000355  150 IX(N,1)=IX(N-1,1)+1
000360      IX(N,2)=IX(N-1,2)+1
000362      IX(N,3)=IX(N-1,3)+1
000364      IX(N,4)=IX(N-1,4)+1
000366      IX(N,5)=IX(N-1,5)
000367  170 PRINT    2003, N,(IX(N,I),I=1,5)
000405      IF (N .EQ. NUMEL)  GO TO 190
000407      N = N + 1
000410      IF (M - N)  130, 170, 150
```

```
000413     179 N = N + 1
000415     180 PRINT 2018, M, KK, N
000427         LBAD = LBAD + 1
000431         GO TO 130

000431     190 CONTINUE
000431         MBAND = 2*MBAND + 2
000433         PRINT 2012,MBAND
           C*****************************************************************
           C      READ AND PRINT OF PRESSURE BOUNDARY CONDITIONS
           C*****************************************************************
000441         IF (NUMPC) 290,310,290
000442     290 PRINT     2005
000446         DO 300 L=1,NUMPC
000450         READ 1004, IBC(L),JBC(L),PR(L)
000461     300 PRINT     2007, IBC(L),JBC(L),PR(L)
000476     310 CONTINUE
           C*****************************************************************
           C      READ INITIAL STRESSES - PRINT AS PART OF FIRST TIME STEP
           C      ********************************************************
000476         DO 32 N=1,NUMEL
000500         DO 32 I=1,3
000501      32 RESID(N,I)=0.0

000511         IF(NRES.EQ.0) GO TO 45
000512         L = 1
000513      47 READ 1007, N, (RESID(N,I),I=1,3)
000531         IF(N-L) 40,41,42
000534      42 DO 46 I=1,3
000536      46 RESID(L,I)=RESID(L-1,I)
000547      41 IF ( L .EQ. NUMEL)  GO TO 45
000551         L = L + 1
000552         IF (N - L)  47, 41, 42
000555      40 PRINT 1008,N
000563         LBAD = LBAD + 1
000565         GO TO 47
000565      45 CONTINUE

           C NO RESIDUAL STRESSES INPUT IN SIMULATED VOIDS

000565         DO 43 N=1,NUMEL
000567         DO 43 I=1,3
000570         IF (IX(N,5).EQ.NUMMAT) RESID(N,I) =0.0
000575      43 CONTINUE

           C      SAVE INITIAL STRESSES FOR RECALCULATION

000602         DO 51 N =1,NUMEL
000603         DO 51 I =1,3
000604      51 STR(N,I)=RESID(N,I)

           C*****************************************************************
           C      READ AREA FACTORS FOR CONSTANT DISPLACEMENT CASE
           C  TMAX IS THE TENSILE STRENGTH OF THE MEDIUM. ALWAYS INPUT AS POSITIVE
           C *****************************************************************

000617         READ 1100,IMAX,TMAX
000627         IF(IMAX.EQ.0) GO TO 1111
000630         READ 1003, (NELFOR(I), I=1,IMAX)
000643         READ 3002, (FACTOR(I), I=1,IMAX)

000656    1111 DO 350 N=1,NUMEL
000660         EPS(N) = 0.0
000661     350 MTAG(N)=1
           C
000665         DO 352  I=1,NUMEL
000666         DO 352 N =1,5
000667     352 SIGT(I,N) = 0.0
000677         PRESSUR = 0.0
           C*****************************************************************
           C      SOLVE NON-LINEAR STRUCTURE BY SUCCESSIVE APPROXIMATIONS
           C*****************************************************************

000700         DO 500 NNN=1,NP
000701         CALL SECOND(T4)
           C
000702         IF(NRES.EQ. 0) GO TO 351
000703         PRINT 1006
000707         PRINT 1007, (K,(RESID(K,I),I=1,3),K=1,NUMEL)
000731     351 CONTINUE
           C
           C      FORM STIFFNESS MATRIX
           C
000731         CALL SECOND(T1)
000733         CALL STIFF
000734         IF (LBAD .NE. 0)  GO TO 8950
000735         CALL SECOND (T2)
           C
           C      SOLVE FOR DISPLACEMENTS
           C
000737         CALL BANSOL (NNN, NSTOP, NCALC)
000742         CALL SECOND(T3)
           C
           C      CURRENT DISPLACEMENTS - DUE TO B.C. 1 AND REINPUT RESID
000744         PRINT 2006, (N,B(2*N-1),B(2*N),CODE(N),BTOT(2*N-1),BTOT(2*N),N=1,
               1 NUMNP)
           C
           C      COMPUTE STRESSES
000774         CALL STRESS
           C
000775         T1 = T2 - T1
000777         T2 = T3 - T2
001001         CALL SECOND(T5)
001002         T3 = T5 - T4
001004         PRINT 2020, T1, T2, T3
001016     500 CONTINUE

           C*****************************************************************
001021         GO TO 50
           C*****************************************************************

001021    1000 FORMAT (8A10)
```

```
001021     1001 FORMAT (I5,8F9.0)
001021     1002 FORMAT (I5,F5.0,5F10.0)
001021     1003 FORMAT(15I5)
001021     1004 FORMAT (2I5,F10.0)
001021     1006 FORMAT (37H1     I N I T I A L   S T R E S S E S//8H ELEMENT,3X,7H
          1KSTRESS8X,7HYSTRESS7X,8HXYSTRESS)
001021     1007 FORMAT (I5,3E15.4)
001021     1008 FORMAT(* RESIDUAL STRESS INPUT ERROR, N=*I4)
001021     1009 FORMAT (4I5,2F10.2,2I5,F5.2)
001021     1100 FORMAT(I5,E10.2)
001021     2000 FORMAT (1H1 8A10/
          1 30HO NUMBER OF NODAL POINTS------ I3 /
          2 30HO NUMBER OF ELEMENTS---------- I3 /
          3 30HO NUMBER OF DIFF. MATERIALS--- I3 /
          4 30HO NUMBER OF PRESSURE CARDS---- I3 /
          5 30HO X-ACCELERATION-------------- E12.4/
          6 30HO Y-ACCELERATION-------------- E12.4/
          8 30HO NUMBER OF APPROXIMATIONS---- I3)
001021     2001 FORMAT (49H1ELEMENT NO.      I     J     K     L     MATERIAL  )
001021     2002 FORMAT (I12,F12.2,2F12.3,2E24.7)
001021     2003 FORMAT (1I13,4I6,1I12)
001021     2004 FORMAT (106H1NODAL POINT        TYPE  X-ORDINATE  Y-ORDINATE  X LO
          1AD OR DISPLACEMENT  Y LOAD OR DISPLACEMENT               )
001021     2005 FORMAT (29HOPRESSURE BOUNDARY CONDITIONS/ 24H     I     J    PRESS
          1URE )
001021     2006 FORMAT(12H1N.P. NUMBER18X,2HUX18X,2HUY16X,4HCODE12X,8HUX CUMUL12X,
          1 8HUY CUMUL/(I12,1P2E20.7,0PF20.0,1P2E20.7))
001021     2007 FORMAT (2I6,F12.3)
001021     2009 FORMAT (26HONODAL POINT CARD ERROR N= I5)
001021     2010 FORMAT (14HO  TEMPERATURE11X,4HE(C)10X,2HNU15X,4HE(T)/(F15.2,6E15.
          15))
001021     2011 FORMAT (*0MATERIAL NO. =*I3, *  MASS DENSITY =* E12.4)
001021     2012 FORMAT (/6HMBAND= I5 /)
001021     2018 FORMAT (16H ELEMENT CARD NOI6,5X,4HKK =I4,5X,8HNEXT N =I6)
001021     2019 FORMAT (41H NUMBER OF ERRORS FOUND - INPUT AND AREAS14)
001021     2020 FORMAT (13HOTIMING-STIFFF8.3,5X,6HBANSOLF8.3,5X,9HITERATIONF8.3)
001021     3002 FORMAT (10F7.4)
           C
           C     PROGRAM WILL CONTINUE THROUGH ALL AREA CHECKING BEFORE STOPPING

001021     8950 PRINT 2019, LBAD
001027     9000 RETURN
001031          END
```

```
           SUBROUTINE STIFF
           C     CALCULATION OF STIFFNESS MATRIX FOR FIRST TIME STEP ONLY
           C     CALCULATION OF B ARRAY FOR EACH TIME STEP
           C
000002          COMMON /STF/ NUMNP, NUMPC, IBC(200), JBC(200), PR(200),
                1            UR(900), UZ(900)
000002          COMMON /MATRX/ B(80), B2(80), A(80,80), A2(80,80), MBAND,
                1              ND2, NUMBLK, MBMAX, NB, BTOT(1800)
000002          COMMON /   / N, IX(800,5), EPS(800), MTAG(800), RESID(800,3),
                1       NUMEL, NRES, R(900), Z(900), CODE(900), RST2S(4), LBAD,
                2         NEC, ACELX, ACELY, VOL, E(8,12), RO(12), S(10,10), P(10),
                3  NSTOP,NNN, LM(4), XTRA(152)
000002          COMMON /PRECALC/ NCALC, STP(800,3), NC, NCHNG(50), CHNG(50,3)
000002          EQUIVALENCE (ND,MBMAX)
           C
           C*****************************************************************
           C     INITIALIZATION
           C*****************************************************************
000002          PRINT 2010
000006          REWIND 9
000010          REWIND 90
000012          NUMBLK=0
000013          REWIND 91
000015          NEC = 0
000016          DO 49  N=1,ND
000020       49 B2(N) = 0.0
000024          IF (NCALC .EQ. 0)  GO TO 60
           C
000025          ASSIGN 170 TO NEXT
000026          DO 50 N=1,ND2
000030          DO 50 M=1,ND
000031       50 A(M,N)=0.0
           C*****************************************************************
           C     FORM STIFFNESS MATRIX IN BLOCKS
           C*****************************************************************
000042       60 NUMBLK=NUMBLK+1
000044          NH=NB*(NUMBLK+1)
000047          NM=NH-NB
000050          NL=NM-NB+1
000052          KSHIFT=2*NL-2
000054          IF (LBAD .NE. 0)  GO TO 3002
           C
           C     ADD CONCENTRATED FORCES WITHIN BLOCK
           C
000055          DO 250 N=NL,NM
000056          K=2*N-KSHIFT
000060          B(K) = UZ(N) + B2(K)
000065          B2(K) = 0.0
000066          B(K-1) = UR(N) + B2(K-1)
000072      250 B2(K-1) = 0.0
000076          IF (NCALC .EQ. 0)  GO TO 3002
           C
           C     BOUNDARY CONDITIONS
           C
           C       1. PRESSURE B.C.
```

```
      C
000077        IF (NUMPC) 260,310,260
000100    260 DO 300 L=1,NUMPC
000102        I=IBC(L)
000104        J=JBC(L)
000106        PP=PR(L)/2.
000111        DZ=(Z(I)-Z(J))*PP
000116        DR=(R(J)-R(I))*PP
000122    264 II=2*I-KSHIFT
000124        JJ=2*J-KSHIFT
000126        IF (II) 280,280,265
000130    265 IF (II-ND) 270,270,280
000133    270 SINA=0.0
000134        COSA=1.0
000136        IF (CODE(I)) 271,272,272
000140    271 SINA=SIN(CODE(I))
000144        COSA=COS(CODE(I))
000147    272 B(II-1)=B(II-1)+(COSA*DZ+SINA*DR)
000155        B(II)=B(II)-(SINA*DZ-COSA*DR)
000162    280 IF (JJ) 300,300,285
000164    285 IF (JJ-ND) 290,290,300
000167    290 SINA=0.0
000170        COSA=1.0
000172        IF (CODE(J)) 291,292,292
000174    291 SINA=SIN(CODE(J))
000200        COSA=COS(CODE(J))
000203    292 B(JJ-1)=B(JJ-1)+(COSA*DZ+SINA*DR)
000211        B(JJ)=B(JJ)-(SINA*DZ-COSA*DR)
000216    300 CONTINUE
000221    310 CONTINUE

000221   3002 DO 210 N=1,NUMEL
      C
000223        IF (IX(N,5)) 210,210,65
000225     65 DO 80 I=1,4
000227        IF (IX(N,I)-NL) 80,70,70
000234     70 IF (IX(N,I)-NM) 90,90,80
000242     80 CONTINUE
000244        GO TO 210
      C
000245     90 IF (NCALC .EQ. 0)  GO TO 95
000246        NEC1 = NEC
000250        CALL QUAD
000251        IF (VOL .LE. 0.0)  GO TO 209
000253        NEC = NEC1
000254        GO TO 99
000255     95 READ (91) I, S
000264     99 CALL REDC (1,NCALC)
      C
000266    144 IF(IX(N,3)-IX(N,4)) 145,165,145
000271    145 DO 151 II=1,9
000273        CC=S(II,10)/S(10,10)
000275        P(II)=P(II)-CC*P(10)
000301        IF (NCALC .EQ. 0)  GO TO 151
000302        DO 150 JJ=1,9
000304    150 S(II,JJ)=S(II,JJ)-CC*S(10,JJ)
000317    151 CONTINUE
      C
000321        DO 161 II=1,8
000323        CC=S(II,9)/S(9,9)
000325        P(II)=P(II)-CC*P(9)
000331        IF (NCALC .EQ. 0)  GO TO 161
000332        DO 160 JJ=1,8
000334    160 S(II,JJ)=S(II,JJ)-CC*S(9,JJ)
000347    161 CONTINUE
      C
      C          ADD ELEMENT STIFFNESS TO TOTAL STIFFNESS
      C
000351    165 DO 166 I=1,4
000353    166 LM(I)=2*IX(N,I)-2
      C
000364        DO 200 I=1,4
000365        DO 200 K=1,2
000366        II=LM(I)+K-KSHIFT
000372        KK=2*I-2+K
000374        B(II)=B(II)+P(KK)
000400        GO TO NEXT, (199,170)

000404    170 DO 196  J=1,4
000406        DO 196 L=1,2
000407        JJ=LM(J)+L-II+1-KSHIFT
000415        LL=2*J-2+L
000417        IF (JJ .LE. 0)  GO TO 196
000421    195 A(JJ,II) = A(JJ,II) + S(KK,LL)
000431    196 CONTINUE
000435    199 CONTINUE
000435    200 CONTINUE

000441    209 IX(N,5)=-IX(N,5)
000443    210 CONTINUE
000446        IF (LBAD .NE. 0)  GO TO 405
000447        IF (NNN .EQ. 1)  WRITE (90) A,A2
000460        IF (NCALC .EQ. 0)  READ (90) A, A2
      C
      C       2. DISPLACEMENT B.C.
      C     NEW CODES -- IF WANT CODE SET TO 3 FOR NNN GT 1 PUNCH IT AS
      C     10, 20, OR 30 INSTEAD OF 1, 2 OR 3
      C
000470        DO 400 M=NL,NH
000472        IF (M .GT. NUMNP)  GO TO 401
000475        IF (CODE(M) .LE. 0.0)  GO TO 400
000477    315 N = 2*M - 1 - KSHIFT
000502        IF (CODE(M) .EQ. 2. .OR. CODE(M) .EQ. 20.)  GO TO 390
000513        CALL MODIFY (A, B, ND2, MBAND, N, UR(M))
000520        IF (CODE(M) .EQ. 1. .OR. CODE(M) .EQ. 10.)  GO TO 400
000531    390 N = N + 1
000533        CALL MODIFY (A, B, ND2, MBAND, N, UZ(M))
000540    400 CONTINUE
000543    401 CONTINUE
      C
      C     REDUCE BLOCK OF EQUATIONS AND SHIFT UP LOWER BLOCK
      C
```

```
000543          WRITE (9) B
000550          IF (NNN .LE. NSTOP .OR. NCALC .EQ. 1)  WRITE (9) A
          C
          C     CHECK FOR LAST BLOCK
          C
000566      405 IF (NM .GE. NUMNP)  GO TO 480
000571          IF (LBAD .NE. 0)  GO TO 60
000572          IF (NCALC .EQ. 0)  GO TO 60
000573          DO 420 N=1,ND
000574          DO 420 M=1,ND
000575          A(M,N) = A2(M,N)
000603      420 A2(M,N) = 0.0
000611          GO TO 60
000612      480 CONTINUE
000612          ASSIGN 199 TO NEXT
          C
          C
000613          IF(NNN.GT.1) GO TO 500
          C     CLEAR DISPLACEMENTS FOR SUBSEQUENT STEPS
000617          IF (NC .EQ. 0)  GO TO 500
000620          DO 490  I = 1,NC
000621          M = NCHNG(I)
000623          CODE(M) = 3.
000626          UR(M) = 0.0
000627          UZ(M) = 0.0
000631      490 CONTINUE
000633      500 RETURN
          C
          C
000634     2010 FORMAT(1H1)
000634          END
*FOLLOWING VARIABLES EQUIVALENCED BUT NOT REFERENCED
MBMAX
```

```
          SUBROUTINE MODIFY(A,B,NEQ,MBAND,N,U)
          C
000011        DIMENSION  A(80,160), B(160)
          C
000011        DO 250 M=2,MBAND
000012        K=N-M+1
000014        IF (K .LE. 0)  GO TO 235
000016        IF (A(M,K) .EQ. 0.0)  GO TO 235
000021        B(K) = B(K) - A(M,K) * U
000026        A(M,K) = 0.0
000030    235 K=N+M-1
000033        IF (K .GT. NEQ)  GO TO 250
000036        IF (A(M,N) .EQ. 0.0)  GO TO 250
000041        B(K) = B(K) - A(M,N) * U
000047        A(M,N) = 0.0
000051    250 CONTINUE
000054        B(N)=U
000056        A(1,N) = 1.0
000061        RETURN
          C
000061        END
```

```
                SUBROUTINE QUAD
      C
000002          COMMON /    / N, IX(800,5), EPS(800), MTAG(800), RESID(800,3),
                1       NUMEL, NRES, R(900), Z(900), CODE(900), RSTRS(4), LBAD,
                2         NEC, ACELX, ACELY, VOL, E(8,12), RO(12), S(10,10), P(10),
                3  NSTOP,NNN, EE(4), H(3,4), D(3,4), XTRA(128)
000002          COMMON /ARG/ ANGLE(4), RRR(5), ZZZ(5), XI, HH(6,10), C(4,4),MTYPE
      C
000002          I=IX(N,1)
000005          J=IX(N,2)
000006          K=IX(N,3)
000010          L=IX(N,4)
000011          MTYPE=IX(N,5)
      C
      C FORM STRESS STRAIN RELATIONSHIP FOR PLANE STRAIN
      C
000013          DO 105 KK=1,4
000014        105 EE(KK)=E(KK+1,MTYPE)

      C  MTAG=1 MEANS THAT BOTH PRINCIPAL STRESSES ARE COMPRESSIVE
      C  MTAG=2 MEANS THAT ONLY THE MAJOR PRINCIPAL STRESS IS TENSILE
      C  MTAG=3 MEANS THAT BOTH PRINCIPAL STRESSES ARE TENSILE

000024          IF (MTAG(N)-2) 82,84,83
000027        82 EE(3)=EE(1)
000031           GO TO 84
000031        83 EE(1)=EE(3)
      C
000033        84 EE(1)=EE(1)/(1.-EE(2)**2)
000036           EE(3)=EE(3)/(1.-EE(2)**2)
000041           EE(2)=EE(2)/(1.-EE(2))
000042           XX=EE(1)/EE(3)
000044           COMM=EE(1)/(XX-EE(2)**2)
000046           C(1,1)=COMM*XX
000047           C(1,2)=COMM*EE(2)
000051           C(1,3)=0.0
000052           C(2,1)=C(1,2)
000053           C(2,2)=COMM
000054           C(2,3)=0.0
000055           C(3,1)=0.0
000056           C(3,2)=0.0
000057           C(3,3)=.5*EE(1)/(XX+EE(2))
      C
000062           SS=SIN(EPS(N))
000065           CC=COS(EPS(N))
000070           S2=SS*SS
000071           C2=CC*CC
000073           SC=SS*CC
      C
000074           D(1,1)=S2
000076           D(1,2)=C2
000077           D(1,3)=0.0
000100           D(1,4)=-SC
000101           D(2,1)=C2
000102           D(2,2)=S2
000103           D(2,3)=0.0
000104           D(2,4)=SC
000105           D(3,1)=2.*SC
000106           D(3,2)=-D(3,1)
000107           D(3,3)=0.0
000110           D(3,4)=-C2+S2
      C
000112           DO 88 II=1,3
000114           DO 88 JJ=1,4
000115           H(II,JJ)=0.0
000120           DO 88 KK=1,3
000122        88 H(II,JJ)=H(II,JJ) +C(II,KK)*D(KK,JJ)
      C
000143           DO 89 II=1,4
000144           DO 89 JJ=1,4
000145           C(II,JJ)=0.0
000150           DO 89 KK=1,3
000152        89 C(II,JJ)=C(II,JJ)+D(KK,II)*H(KK,JJ)
      C
      C          FORM QUADRILATERAL STIFFNESS MATRIX
      C
000172           DO 94 M=1,4
000173           MM=IX(N,M)
000177        93 RRR(M)=R(MM)
000203        94 ZZZ(M)=Z(MM)
      C
000207           DO 100 II=1,10
000211           P(II)=0.0
000213           DO 95 JJ=1,6
000214        95 HH(JJ,II)=0.0
000222           DO 100 JJ=1,10
000223       100 S(II,JJ)=0.0
000233           DO 119 II=1,4
000234           JJ=IX(N,II)
000240       119 ANGLE(II)=CODE(JJ)/57.3
      C
      C     FORM BAR STIFFNESS
      C
000245           IF (IX(N,2)-IX(N,3)) 250,240,250
000250       240 DR=R(J)-R(I)
000254           DZ=Z(J)-Z(I)
000257           XL=SQRT(DR**2+DZ**2)
000265           RRR(5)=(R(I)+R(J))/2.-2.*EE(4)*DZ/XL
000275           ZZZ(5)=(Z(I)+Z(J))/2.+2.*EE(4)*DR/XL
000305           CALL TRISTF(1,2,5)
000310           GO TO 130
000311       250 CONTINUE
      C
000311           IF (K-L) 125,120,125
000313       120 CALL TRISTF(1,2,3)
000316           RRR(5)=(RRR(1)+RRR(2)+RRR(3))/3.0
000322           ZZZ(5)=(ZZZ(1)+ZZZ(2)+ZZZ(3))/3.0
000326           VOL = XI
000330           IF (VOL.GT.0.) GO TO 130
      C     ERROR RETURN
000332       122 LBAD = LBAD + 1
```

```
000334          GO TO 135
000334      125 VOL=0.0
000335          RRR(5)=(R(I)+R(J)+R(K)+R(L))/4.0
000346          ZZZ(5)=(Z(I)+Z(J)+Z(K)+Z(L))/4.0
000357          CALL TRISTF(4,1,5)
000362          CALL TRISTF(1,2,5)
000365          CALL TRISTF(2,3,5)
000370          CALL TRISTF(3,4,5)
000373          IF (VOL .LE. 0.0)  GO TO 122
      C
000375          DO 140 II=1,6
000376          DO 140 JJ=1,10
000377      140 HH(II,JJ)=HH(II,JJ)/4.0
      C
000410      130 WRITE (91) N, S, HH, RRR(5), ZZZ(5), C, P
000431      135 RETURN
      C
000432          END
```

```
                SUBROUTINE TRISTF(II,JJ,KK)
      C
000006          COMMON /   / N, IX(800,5), EPS(800), MTAG(800), RESID(800,3),
                1       NUMEL, NRES, R(900), Z(900), CODE(900), RSTRS(4), LBAD,
                2         NEC, ACELX, ACELY, VOL, E(8,12), RO(12), S(10,10), P(10),
                3  NSTOP,NHN, F(6,10), H(6,10), D(6,6)
000006          COMMON /ARG/ ANGLE(4), RRR(5), ZZZ(5), XI, HH(6,10), C(4,4),MTYPE
000006          DIMENSION  RR(4), ZZ(4), DD(3,3), LM(3),HSAVE(3,10),HS(31)
000006          EQUIVALENCE (F(1,1), HS(1), HSAVE(1,1))
      C
      C         1. INITIALIZATION
      C
000006          LM(1)=II
000007          LM(2)=JJ
000010          LM(3)=KK
      C
000011          RR(1)=RRR(II)
000013          RR(2)=RRR(JJ)
000015          RR(3)=RRR(KK)
000017          RR(4)=RRR(II)
000021          ZZ(1)=ZZZ(II)
000023          ZZ(2)=ZZZ(JJ)
000025          ZZ(3)=ZZZ(KK)
000027          ZZ(4)=ZZZ(II)
      C
000031       85 DO 90  I=1,6
000033          DO 90 J=1,10
000034          F(I,J)=0.0
000040       90 H(I,J)=0.0
      C
000047          COMM=RR(2)*(ZZ(3)-ZZ(1))+RR(1)*(ZZ(2)-ZZ(3))+RR(3)*(ZZ(1)-ZZ(2))
000061          XI   =COMM/2.0
000063          IF (XI.GT.0.0) GO TO 102
000065          PRINT 1000, II, JJ, KK, N
000100          RETURN
000101      102 VOL=VOL+XI
      C
      C              FORM  COEFFICIENT-DISPLACEMENT TRANSFORMATION MATRIX
      C
000103          DD(1,1)=(RR(2)*ZZ(3)-RR(3)*ZZ(2))/COMM
000110          DD(1,2)=(RR(3)*ZZ(1)-RR(1)*ZZ(3))/COMM
000114          DD(1,3)=(RR(1)*ZZ(2)-RR(2)*ZZ(1))/COMM
000120          DD(2,1)=(ZZ(2)-ZZ(3))/COMM
000122          DD(2,2)=(ZZ(3)-ZZ(1))/COMM
000124          DD(2,3)=(ZZ(1)-ZZ(2))/COMM
000126          DD(3,1)=(RR(3)-RR(2))/COMM
000131          DD(3,2)=(RR(1)-RR(3))/COMM
000133          DD(3,3)=(RR(2)-RR(1))/COMM
      C
000135          DO 120 I=1,3
000140          J=2*LM(I)-1
000143          H(1,J)=DD(1,I)
000150          H(2,J)=DD(2,I)
000155          H(3,J)=DD(3,I)
000162          H(4,J+1)=DD(1,I)
```

```
000167          H(5,J+1)=DD(2,I)
000173        120 H(6,J+1)=DD(3,I)
              C
              C     ROTATE UNKNOWNS IF REQUIRED
              C
000200          DO 125 J=1,2
000202          I=LM(J)
000204          IF (ANGLE(I)) 122,125,125
000207        122 SINA=SIN(ANGLE(I))
000213          COSA=COS(ANGLE(I))
000217          IJ=2*I
000220          DO 124 K=1,6
000224          TEM=H(K,IJ-1)
000230          H(K,IJ-1)=TEM*COSA+H(K,IJ)*SINA
000237        124 H(K,IJ)= -TEM*SINA+H(K,IJ)*COSA
000246        125 CONTINUE
              C
              C     ACCELERATION LOADS
              C     CALCULATED ONLY FOR FIRST TIME STEP
              C
000250          COMM=RO(MTYPE)*XI    /3.0
000254          DO 170 I=1,3
000255          J=2*LM(I)-1
000260          P(J) = P(J)-ACELX*COMM
000264        170 P(J+1) = P(J+1) - ACELY*COMM
              C
000271          DO 100  I=1,6
000273          DO 100 J=1,6
000274        100 D(I,J)=0.0
              C
              C          FORM INTEGRAL(G)T*(C)*(G)
              C
000304          D(2,2)=XI    *C(1,1)
000306          D(2,6)=XI    *C(1,2)
000310          D(3,3)=XI    *C(4,4)
000312          D(3,5)=XI    *C(4,4)
000313          D(5,5)=XI    *C(4,4)
000314          D(6,6)=XI    *C(2,2)
              C
000316        108 DO 110 I=1,5
000320          K = I + 1
000322          DO 110  J=K,6
000324        110 D(J,I)=D(I,J)
              C
              C          FORM ELEMENT STIFFNESS MATRIX (H)T*(D)*(H)
              C
000340          DO 130 J=1,10
000341          DO 130 K=1,6
000342          IF (H(K,J)) 128,130,128
000346        128 DO 129 I=1,6
000350        129 F(I,J)=F(I,J)+D(I,K)*H(K,J)
000367        130 CONTINUE
              C
000373          DO 140 I=1,10
000375          DO 140 K=1,6
000376          IF (H(K,I)) 138,140,138
000402        138 DO 139 J=1,10
000404        139 S(I,J)=S(I,J)+H(K,I)*F(K,J)
000422        140 CONTINUE
              C
              C       FORM RESIDUAL LOAD MATRIX
              C
000426        150 DO 160 I=1,10
000430          HSAVE(1,I) = H(2,I)
000435          HSAVE(2,I) = H(6,I)
000443        160 HSAVE(3,I) = H(3,I) + H(5,I)
              C
              C     FORM STRAIN TRANSFORMATION MATRIX
              C
000454        400 DO 410 I=1,6
000456          DO 410 J=1,10
000457        410 HH(I,J)=HH(I,J)+H(I,J)
              C
000472          HS(31) = XI
000474          CALL ECRITE (HS, NEC, 31)
              C     ECRITE WRITES 31 WORDS FROM CORE BEGINNING WITH LOCATION HS
              C     ONTO EXTENDED CORE BEGINNING WITH LOCATION NEC
000476          NEC = NEC + 31
000500       1000 FORMAT (32H ZERO OR NEGATIVE AREA, TRIANGLE316,5X,7HELEMENT15)
000500          RETURN
              C
000500          END
```

```
      SUBROUTINE BANSOL (NNN, NSTOP, NCALC)
C
000006      COMMON /MATRX/ B(80), B2(80), A(80,80), A2(80,80), MBAND,
     1                ND2, NUMBLK, MBMAX, NC,BTOT(1800)
000006      EQUIVALENCE (NN, MBMAX)
000006      EQUIVALENCE (MM,MBAND)
C
000006      IF (NNN .LE. NSTOP .OR. NCALC .EQ. 1)  NTAPE = 9
000017   99 REWIND 9
000021      NB=0
000022      GO TO 150
C*********************************************************************
C     REDUCE EQUATIONS BY BLOCKS
C*********************************************************************
C
C     1. SHIFT BLOCK OF EQUATIONS
C
000023  100 NB=NB+1
000025      DO 125 N=1,NN
000026      B(N) = B2(N)
000031      B2(N) = 0.0
000032      DO 125 M=1,MM
000034      A(M,N) = A2(M,N)
000042  125 A2(M,N) = 0.0
C
C     2. READ NEXT BLOCK OF EQUATIONS INTO CORE
C
000051      IF (NUMBLK-NB) 150,200,150
000053  150 READ (9) B2
000060      READ (NTAPE) A2
000065      IF (NB) 200,100,200
C
C     3. REDUCE BLOCK OF EQUATIONS
C
000071  200 IF (NNN .GT. NSTOP .AND. NCALC .EQ. 0)  GO TO 2000
000100      DO 300 N=1,NN
000101      IF (A(1,N) .EQ. 0.0)  GO TO 300
000104      DO 275  L = 2,MBAND
000106      IF (A(L,N) .EQ. 0.0)  GO TO 275
000112      C = A(L,N) / A(1,N)
000120      I = N + L - 1
000122      J = 0
000123      DO 250  K = L,MBAND
000124      J = J + 1
000126  250 A(J,I) = A(J,I) - C * A(K,N)
000140      A(L,N) = C
000145  275 CONTINUE
000150  300 CONTINUE
000153      WRITE (90) A

000160 2000 DO 2300 N=1,NN
000164      IF (A(1,N) .EQ. 0.0)  GO TO 2300
000167      DO 2275  L=2,MBAND
000171      IF (A(L,N) .EQ. 0.0)  GO TO 2275
000175      I = N + L - 1
000177      B(I) = B(I) - A(L,N)*B(N)
000206 2275 CONTINUE
000211      B(N) = B(N) / A(1,N)
000216 2300 CONTINUE
C
C     WRITE BLOCK OF REDUCED EQUATIONS ON TAPE 91
C
C
000221      IF (NUMBLK-NB) 375,399,375
000223  375 WRITE (91) B
000230      GO TO 100
C*********************************************************************
C     BACK-SUBSTITUTION
C*********************************************************************
000233  399 BACKSPACE 90
000235      NTAPE = 90
000236  400 DO 450 M=1,NN
000240      N=NN+1-M
000243      DO 425 K=2,MM
000244      L=N+K-1
000247  425 B(N) = B(N) - A(K,N) * B(L)
000260      B2(N) = B(N)
000263  450 A2(NB,N) = B(N)
000272      NB=NB-1
000273      IF (NB) 475,500,475
000274  475 BACKSPACE 90
000276      BACKSPACE 91
000300      READ (90) A
000305      READ (91) B
000312      BACKSPACE 90
000314      BACKSPACE 91
000316      GO TO 400
C*********************************************************************
C     ORDER UNKNOWNS IN B ARRAY
C*********************************************************************
000321  500 K=0
000322      DO 600 NB=1,NUMBLK
000324      DO 600 N=1,NN
000325      K=K+1
000327      B(K) = A2(NB,N)
000334      IF (NCALC .EQ. 1)  BTOT(K) = 0.0
000337  600 BTOT(K)=BTOT(K)+B(K)
000350      RETURN
C
C
000350      END
*FOLLOWING VARIABLES EQUIVALENCED BUT NOT REFERENCED
MBMAX
```

```
                SUBROUTINE STRESS
      C
000002            COMMON /STF/ NUMNP, NUMPC, IBC(200), JBC(200), PR(200),
                 1           UR(900), UZ(900)
000002            COMMON /MATRX/B(160),A(80,80),RRR(800),ZZZ(800),MTY(4800)
                 1           ,MBAND, ND2, NUMBLK, MBMAX, NB,BTJT(1800)
000002            COMMON /   / N, IX(800,5), EPS(800), MTAG(900), RESID(800,3),
                 1       NUMEL, NRES, R(900), Z(900), CODE(900), RSTRS(4), LBAD,
                 2         NEC, ACELX, ACELY, VOL, E(8,12), RO(12), S(10,10), P(10),
                 3  NSTOP,NNN, TP(6), SIG(10), RR(4), HH(6,10),PRESSUP,MS(31),
                 4           C(4,4), XTRA(28)
000002            COMMON /STRS/ FRAC, NUMMAT, SIGT(800,5), TMAX, IMAX, NELFOR(15),
                 1           FACTOR(15), NP
000002            COMMON /RECALC/ NCALC, STR(800,3), NC, NCHNG(50), CHNG(50,3)
000002            DIMENSION  EMTY(800), TPR(8)
000002            EQUIVALENCE (MTY(1),00), EMTY(1)), (MTY(10), TPR(1))
                C*****************************************************************
                C     COMPUTE ELEMENT STRESSES
                C*****************************************************************
000002            REWIND 91
000004            NEC = 0
000005            PRESSUP = 0.0
000006            MPRINT=0
000007            TENMAX = 0.0
                C
000010            DO 300 M=1,NUMEL
000011            READ (91) N, S, HH, RRR(N), ZZZ(N), C, P
                C
000034            IX(N,5)=IABS(IX(N,5))
                C
000037            CALL REDO(9, NCALC)
                C
000041            DO 120 I=1,4
000043            II=2*I
000044            JJ=2*IX(N,I)
000050            P(II-1)=B(JJ-1)
000054          120 P(II)=B(JJ)
                C
000060            DO 150 I=1,2
000062            RR(I)=P(I+8)
000064            DO 150 K=1,8
000066          150 RR(I)=RR(I)-S(I+8,K)*P(K)
                C
000102            COMM=S(9,9)*S(10,10)-S(9,10)*S(10,9)
000105            IF (COMM) 155,160,155
000106          155 P(9)=(S(10,10)*RR(1)-S(9,10)*RR(2))/COMM
000113            P(10)=(-S(10,9)*RR(1)+S(9,9)*RR(2))/COMM
                C
000117          160 DO 170 I=1,6
000121            TP(I)=0.0
000123            DO 170 K=1,10
000124          170 TP(I)=TP(I)+HH(I,K)*P(K)
                C
                C
000140            RR(1)=TP(2)
000141            RR(2)=TP(6)
000143            RR(3)=0.0
000144            RR(4)=TP(3)+TP(5)
                C
000146          176 DO 180 I=1,4
000150            SIG(I)=RSTRS(I)
000153            DO 180 K=1,4
000154          180 SIG(I)=SIG(I)+C(I,K)*RR(K)
000170            SIG(3)=SIG(4)
                C
                C*****************************************************************
                C     OUTPUT STRESSES
                C*****************************************************************
                C
                C     CALCULATE PRINCIPAL STRESSES
                C
000171            CC=(SIG(1)+SIG(2))/2.0
000174            BB=(SIG(1)-SIG(2))/2.0
000176            CR=SQRT(BB**2+SIG(3)**2)
000203            SIG(4)=CC+CR
000205            SIG(5)=CC-CR
000206            IF(BB.NE.0.) GO TO 195
000207            EPSM = 77777.
000211            GO TO 196
000211          195 EPSM = ATAN2(SIG(3),BB) / 2.
000215          196 SIG(6)=57.296*EPSM
                C
000217            EMTY(N)=SIG(4)
000222            IF (SIG(4).LE.TENMAX) GO TO 200
000224            TENMAX=SIG(4)
000225            NTEN=N
000226          200 CONTINUE
                C
                C     CALCULATE TENSILE STRESSES TO BE REINPUT
                C
000226            S2 = SIN(EPSM) ** 2
000231            C2 = COS(EPSM) ** 2
000234            CS = SIN(EPSM) * COS(EPSM)
000242            TENS1 = 0.0
000243            TENS2 = 0.0
000244            MTAG(N)=1
000246            IF (SIG(4).LE.TMAX) GO TO 266
000251            MTAG(N)=2
000253            TENS1=SIG(4)
000254            IF (SIG(5).LE.TMAX) GO TO 266
000256            MTAG(N)=3
000260            TENS2=SIG(5)
000261          266 CONTINUE
000261            DO 270  I=1,5
000263          270 SIGT(N,I)=SIGT(N,I)+SIG(I)

000273            NRES = 1
000274            RESID(N,1) = TENS1*C2 + TENS2*S2
000301            RESID(N,2) = TENS1*S2 + TENS2*C2
000304            RESID(N,3)=(TENS2-TENS1)*CS
```

```
      C COMPUTE AVERAGE PRESSURE UNDER PLATE
000307          IF(IMAX.EQ.0) GO TO 402
000310          DO 401 I=1,IMAX
000312          IF(N.NE.NELFOF (I)) GO TO 401
000315          PRESSUR = PRESSUR + SIGT(N,I) * FACTOR(I)
000321          GO TO 402
000321        401 CONTINUE
000324        402 CONTINUE
      C
      C  PRINT OUT STRESSES
      C
000324          IF (MPRINT .GT. 0)  GO TO 110
000327        105 PRINT 2000
000333          MPRINT=50
000334        110 MPRINT=MPRINT-1
000336          PRINT 2001, N,RAD(N),ZZZ(N), (SIGT(N,I), I=1,5),SIG(6)
000363          DO 115 I=1,5
000365        115 IF(SIG(I).GT.TMAX)  SIGT(N,I)=SIGT(N,I)-SIG(I)
000377        300 CONTINUE
000402          IF(IMAX.EQ.0) GO TO 320
000403          PRINT 3003,PRESSUR
      C
      C ***********************************************************
      C  DETERMINE AND LOCATE HIGHEST TENSION .  SET TENSILE STRENGTH LIMIT
      C ALL ELEMENTS WHERE TENSION EXCEEDS LIMIT SET ARE GIVEN NEW MATERIAL
      C PROPERTIES BEFORE FINAL RUN
      C ***********************************************************
      C
000410        320 NCALC = 0
000411          IF (NP - NNN .NE. 1)  GO TO 350
000414          NCALC = 1
000415          TLIM = FRAC * TENMAX
000417          PRINT 2002, TENMAX, NTEN, TLIM
      C
000430          NQ = 0
000431          DO 330  N = 1,NUMEL
000433          DO 325  I = 1,3
000434        325 RESID(N,I) = STR(N,I)
000446          IF (EMTY(N) .LT. TLIM)  GO TO 330
000451          NQ = NQ + 1
000453          MTY(NQ) = N
000455          TPR(NQ) = EMTY(N) / TENMAX
000461          IF (NQ .LT. 8 .OR. N .NE. NUMEL)  GO TO 326
000470          PRINT 2003, (MTY(I), TPR(I), I=1,NQ)
000505        326 IX(N,5) = NUMMAT
000507        330 CONTINUE

000512          IF (NC .EQ. 0)  GO TO 350
000513          DO 340  I = 1,NC
000514          N = NCHNG(I)
000516          CODE(N) = CHNG(I,1)
000521          UR(N) = CHNG(I,2)
000523        340 UZ(N) = CHNG(I,3)
000527        350 RETURN
      C
      C***********************************************************************
      C
000530        2000 FORMAT (7H1EL.NO.    7X  1HX 7X 1HY 4X 8HX-STRESS 4X 8HY-STRESS 3X
          19HXY-STRESS 2X 10HMAX-STRESS 2X 10HMIN-STRESS 7H  ANGLE)
000530        2001 FORMAT(I7,2F8.2,1P5E12.4,0PF7.2)
000530        2002 FORMAT (1H1 10X,17HMAXIMUM TENSION =1PE10.3,11H AT ELEMENT IS,18H
          1TENSION LIMIT =E10.3//)
000530        2003 FORMAT (8(I7,F8.3))
000530        2017 FORMAT(I5,3E15.4)
000530        3003 FORMAT(///30H AVERAGE PRESSURE UNDER PLATE=,E10.3)
000530             END
```

```
      SUBROUTINE REDO (JUMP, NCALC)
C     FROM STIFF  JUMP = 1
C     FROM STRESS JUMP = 9  -  ONLY NEED P(9) AND P(10)

      COMMON /   / N, IX(800,5), EPS(800), NTAG(800), RESID(800,3),
     1      NUMEL, NPES, R(900), Z(900), CODE(900), RSTRS(4), LBAD,
     2        NEC, ACELX, ACELY, VOL, E(8,12), RO(12), S(10,10), P(10),
     3  NSTOP,NNN, TP(6), SIG(10), RR(4), HH(6,10),PRESSUR,HS(31),
     4             XTRA(44)
      DIMENSION  H(3,10)
      EQUIVALENCE (HS(1), H(1,1))

      IF (NCALC .EQ. 1)  GO TO 110
C      DO NOT CLEAR GRAVITY FOR  FULL CALCULATION
      DO 100 I=1,10
  100 P(I) = 0.0

  110 DO 111  IJ = 1,3
  111 RSTRS(IJ) = RESID(N,IJ)
      RSTRS(4) = RSTRS(3)

      IF (IX(N,2) .EQ. IX(N,3)) GO TO 240
      IF (IX(N,3) .EQ. IX(N,4))  GO TO 240
      II = 4
      GO TO 250
  240 II = 1

  250 DO 260  J=1,II
      CALL ECREAD (HS, NEC, 31)
      NEC = NEC + 31
      DO 260  I=JUMP,10
  260 P(I) = P(I) - HS(31)*(RSTRS(1)*H(1,I) + RSTRS(2)*H(2,I)
     1                     + RSTRS(3)*H(3,I))

      RETURN
      END
```

APPENDIX C USER'S MANUAL FOR "JOINT PERTURBATION" AND "NO TENSION" PROGRAMS

USER'S MANUAL FOR

JOINT PERTURBATION PROGRAM* AND NO TENSION PROGRAM**

COMPUTER PROGRAMS FOR ANALYSIS OF JOINTED ROCK SYSTEMS WITH INITIAL STRESSES - PLANE STRAIN OPTION

INPUT DATA

A. IDENTIFICATION CARD - (12A6)

COLUMNS 1 - 72 OF THIS CARD CONTAIN FORMATION TO BE PRINTED WITH RESULTS

B. CONTROL CARD - (4I5, 2F10.2, 3I5) OR (4I5, 2F10.2, 2I5, F5.2)

COLUMNS 1 - 5 NUMBER OF NODAL POINTS (900 MAXIMUM)

6 - 10 NUMBER OF ELEMENTS (800 MAXIMUM)

11 - 15 NUMBER OF DIFFERENT MATERIALS (12 MAXIMUM)

16 - 20 NUMBER OF BOUNDARY PRESSURE CARDS (200 MAXIMUM)

21 - 30 ACCELERATION IN X-DIRECTION

31 - 40 ACCELERATION IN Y-DIRECTION (GRAVITY IS INPUT AS POSITIVE)

41 - 45 NUMBER OF APPROXIMATIONS (NEVER LESS THAN 2 FOR JOINTED BODY) (NP)

46 - 50 RESIDUAL STRESS CODE (READS RESIDUAL STRESS IF NOT EQUAL TO 0) (NRES)

50 - 55 JOINT PERTURBATION. JOINT CUT-OFF NUMBER: ALL MATERIALS WITH HIGHER NUMBERS ARE JOINTS (NSHELL)

50 - 55 NO TENSION. PERCENTAGE OF INITIAL MAXIMUM TENSION USED TO DELINEATE CRACKED ZONE BEFORE FINAL RUN. EXAMPLE: FRAC = 0.05 MEANS THAT ELEMENTS WITH LESS THAN 5% OF ORIGINAL MAXIMUM TENSION ARE UNMODIFIED

C. MATERIAL PROPERTY CARDS*

THE FOLLOWING GROUP OF CARDS MUST BE SUPPLIED FOR EACH DIFFERENT SOLID MATERIAL AND JOINT MATERIAL, IF ANY.

SOLID MATERIALS

(I5, 7F9.2)

1 - 5 MATERIALS IDENTIFICATION (ANY NUMBER FROM 1 TO 12)

6 - 14 MASS DENSITY OF MATERIALS

$$\frac{\text{POUNDS/CU FT}}{\text{G FT/SEC}^2} = \text{POUNDS SEC}^2/\text{FT}^2$$

14 - 23 BLANK

*ADAPTED FROM PLANE STRESS PROGRAM BY E. L. WILSON, JULY 1965, AND JOINT STIFFNESS AND JOINT STRESS SUBROUTINES BY R. L. TAYLOR AND R. E. GOODMAN, JULY 1967. MODIFIED BY HEUZE AND GOODMAN, JUNE 1969.

**DEVELOPED BY HEUZÉ AND BORNSTEIN FROM 2D PROGRAM BY E. L. WILSON, 1965, AUGUST 1969.

*IF OPENINGS ARE SIMULATED BY A VERY SOFT MATERIAL (IN ADJUSTABLE MESHES), MAKE THIS MATERIAL NUMBER = NUMMAT. ALSO, IN THE FINAL RUN, THE "CRACKED" PORTION OF THE MEDIUM WILL BE GIVEN THE PROPERTIES OF MATERIAL NUMBER NUMMAT (THE HIGHEST NUMBER).

24 - 32 E COMPRESSION

33 - 41 ν

42 - 50 E TENSION

51 - 59 AREA (FOR BAR ELEMENTS ONLY)

60 - 68 INITIAL STRESS (FOR BAR ELEMENTS ONLY)

JOINT MATERIALS (JOINT PROGRAM ONLY)

COLUMNS 1 - 5 NUMBER OF JOINT MATERIAL

6 - 14 BLANK

15 - 23 NORMAL STIFFNESS, PSF/FT

24 - 32 TANGENTIAL STIFFNESS, PSF/FT

33 - 41 JOINT COHESION, PSF

42 - 50 JOINT FRICTION ANGLE, DEGREES

51 - 59 MAX CLOSURE OF JOINT: INPUT AS NEGATIVE QUANTITY. (RELATED TO THICKNESS OR APERTURE OF JOINT)

NOTE: IF JOINT IS NON-STIFF, THE VALUE OF STIFFNESS IS PROBABLY 1/10 - 1/100 OF THE STIFFNESS OF THE INTERVENING BLOCK, E.G., E_{BLOCK} = 1.0 X 10^8 PSF, BLOCK THICKNESS = 5.0 FT, THEN BLOCK STIFFNESS IS 2.0 x 10^7 PSF/FT AND A LOW JOINT STIFFNESS K_T = 10^6 PSF/FT.

D. NODAL POINT CARDS - (2I5, 4F10.0)

ONE CARD FOR EACH NODAL POINT WITH THE FOLLOWING INFORMATION. JOINT ELEMENTS ARE OBTAINED BY DOUBLE ROWS OF NODAL POINTS AT THE SAME COORDINATES.

COLUMNS 1 - 4 NODAL POINT NUMBER

6 - 10 NUMBER WHICH INDICATES IF DISPLACEMENTS OR FORCES ARE TO BE SPECIFIED *

11 - 20 X-ORDINATE

21 - 30 Y-ORDINATE

31 - 40 XR

41 - 50 XZ

NOTE: IF THE NUMBER IN COLUMN 10 IS

0 XR IS THE SPECIFIED X-LOAD AND XZ IS THE SPECIFIED Y-LOAD,

1 XR IS THE SPECIFIED X-DISPLACEMENT OF XZ IS THE SPECIFIED Y-LOAD,

2 XR IS THE SPECIFIED X-LOAD AND XZ IS THE SPECIFIED Y-DISPLACEMENT,

3 XR IS THE SPECIFIED X-DISPLACEMENT AND XZ IS THE SPECIFIED Y-DISPLACEMENT.

ALL LOADS ARE CONSIDERED TO BE TOTAL FORCES ACTING ON AN ELEMENT OF UNIT THICKNESS. NODAL POINT CARDS MUST BE IN NUMBERICAL SEQUENCE. IF CARDS ARE OMITTED, THE OMITTED NODAL POINTS ARE GENERATED AT EQUAL INTERVALS ALONG A STRAIGHT LINE BETWEEN THE DEFINED NODAL POINTS. THE BOUNDARY CODE (COLUMN 10), XR, AND XZ ARE SET EQUAL TO ZERO.

---

*IF THIS NUMBER IS 10, 20, OR 30, IT IS AS 1, 2, OR 3 FOR THE FIRST ITERATION AND RESET AT 3 FOR SUBSEQUENT ITERATIONS (NO TENSION ONLY).

E. ELEMENT CARDS - (6I5)

SOLID ELEMENTS

ONE CARD FOR EACH ELEMENT[1, 2]

COLUMNS 1 - 5 ELEMENT

6 - 10 NODAL POINT I

11 - 15 NODAL POINT J

16 - 20 NODAL POINT K

21 - 25 NODAL POINT L

26 - 30 MATERIAL IDENTIFICATION

ELEMENT CARDS MUST BE IN ELEMENT NUMBER SEQUENCE. IF ELEMENT CARDS ARE OMITTED, THE PROGRAM AUTOMATICALLY GENERATES THE OMITTED INFORMATION BY INCREMENTING BY ONE THE PRECEDING I, J, K, AND L. THE MATERIAL IDENTIFICATION CODE FOR THE GENERATED CARDS IS SET EQUAL TO THE VALUE OF THE LAST CARD. THE LAST ELEMENT CARD MUST ALWAYS BE SUPPLIED.

TRIANGULAR ELEMENTS ARE ALSO PERMISSIBLE: THEY ARE IDENTIFIED BY REPEATING THE LAST NODAL POINT NUMBER (I.E. I, J, K, K). ONE-DIMENSIONAL BAR ELEMENTS ARE IDENTIFIED BY A NODAL POINT NUMBERING SEQUENCE OF THE FORM I, J, J, I.

JOINT ELEMENTS

NODAL POINTS MUST BE NUMBERED I, J, K, L COUNTER CLOCKWISE PROCEEDING ALONG LENGTH OF JOINT FROM I TO J AND ALONG LENGTH FROM K TO L. NODAL POINT, PAIR I, K, (AND J, L) HAS DIFFERENT NUMBERS BUT IDENTICAL COORDINATES.

F. PRESSURE CARDS - (2I5, 1F10.0)

ONE CARD FOR EACH BOUNDARY ELEMENT WHICH IS SUBJECTED TO A NORMAL PRESSURE

COLUMNS 1 - 5 NODAL POINT I

6 - 10 NODAL POINT J

11 - 20 NORMAL PRESSURE

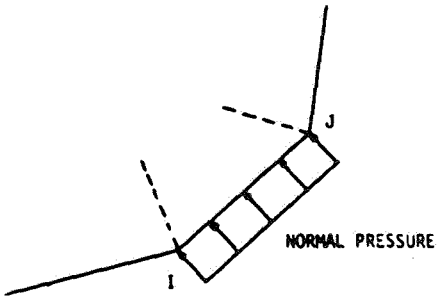

AS SHOWN ABOVE, THE BOUNDARY ELEMENT MUST BE ON THE LEFT AS ONE PROGRESSES FROM I TO J. SURFACE TENSILE FORCE IS INPUT AS A NEGATIVE PRESSURE. JOINTS CANNOT BE PLACED ON BOUNDARIES.

---

[1]FOR A RIGHT HAND COORDINATE SYSTEM, ORDER NODAL POINTS COUNTER CLOCKWISE AROUND

[2]MAXIMUM DIFFERENCE BETWEEN NODAL POINT I.D. MUST BE LESS THAN OR EQUAL TO 39.

G. RESIDUAL STRESS CARDS (I5, 3E15.4)

IF RESIDUAL STRESS CODE ON THE CONTROL CARD IS NOT EQUAL TO 0, ONE CARD FOR EACH ELEMENT MUST BE SUPPLIED WITH THE FOLLOWING INFORMATION:

COLUMNS	1 - 5	ELEMENT NUMBER
	6 - 20	X-STRESS
	21 - 35	Y-STRESS
	36 - 50	XY-STRESS

IF CARDS ARE OMITTED, THE STRESSES FOR THE OMITTED ELEMENTS ARE ASSUMED EQUAL TO THOSE SUPPLIED ON THE LAST CARD. IF ALL ELEMENTS HAVE THE SAME STRESSES, ONLY THE FIRST AND LAST ELEMENT STRESSES MAY BE SUPPLIED.

SIGN CONTENTION: TENSION POSITIVE.

H. TENSILE STRENGTH CARD (I5, E10.2) (NO TENSION ONLY)

COLUMNS	1 - 5	BLANK EXCEPT IN A BOREHOLE JACK PROBLEM WHERE IMAX IS THE NUMBER OF ELEMENTS UNDER A PRESSURE PLATE.
	6 - 15	TENSILE STRENGTH OF THE MEDIUM (TMAX). KEEP SMALL (FOR EXAMPLE 1% OF σ_T OF ROCK SUBSTANCE).

I. END CARD (3H)

THIS PROGRAM CAN RUN SEVERAL PROBLEMS IN A SEQUENCE. THE LAST CARD OF THE LAST DATA DECK MUST BE END PUNCHED IN COLUMNS 1 - 3.

OUTPUT INFORMATION

THE FOLLOWING INFORMATION IS DEVELOPED AND PRINTED BY THE PROGRAM:

1. REPRINTS OF INPUT DATA
2. NODAL POINT DISPLACEMENTS*
3. STRESSES AT THE CENTER OF EACH SOLID ELEMENT*
4. STRESSES AND RELATIVE DISPLACEMENTS (OF CENTER TOP AND BOTTOM) OF EACH JOINT ELEMENT*

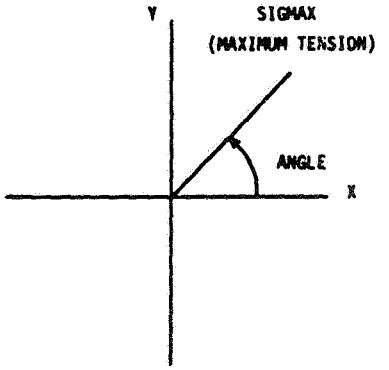

*2., 3., AND 4. ARE PRINTED AFTER EACH CYCLE.